Fall 2008

Mechanistic and Clinical Studies of Platelet Rich Plasma: A Simple Clinical Method for Enhancing Bone and Soft Tissue Healing

James L. Rutkowski

Follow this and additional works at: https://dsc.duq.edu/etd

MECHANISTIC AND CLINICAL STUDIES OF PLATELET RICH PLASMA:

A SIMPLE CLINICAL METHOD FOR ENHANCING BONE

AND SOFT TISSUE HEALING

A Dissertation

Submitted to the Graduate School

of Pharmaceutical Sciences

Duquesne University

In partial fulfillment of the requirements for

the degree of Doctor of Philosophy

By

James L. Rutkowski

December 2008

MECHANISTIC AND CLINICAL STUDIES OF PLATELET RICH PLASMA:

A SIMPLE CLINICAL METHOD FOR ENHANCING BONE

AND SOFT TISSUE HEALING

By

James L. Rutkowski

Approved: October 23, 2008

_____
David A. Johnson, Ph.D.
Dissertation Chairperson
Associate Professor of Pharmacology and
Duquesne University
Director of Graduate Studies
Graduate School Pharmaceutical Sciences
Duquesne University
Pittsburgh, PA

_____
Paula A. Witt-Enderby, Ph.D.
Professor of Pharmacology and Toxicology
Graduate School Pharmaceutical Sciences Toxicology
Pittsburgh, PA

_____
Vicki L. Davis, Ph.D.
Assistant Professor of Pharmacology
Graduate School Pharmaceutical Sciences
Duquesne University
Pittsburgh, PA

_____
C. Larry Bering, Ph.D.
Professor and Chair
Department of Chemistry and Biochemistry
Clarion University of Pennsylvania
Clarion, PA

_____
Douglas M. Smith, Ph.D.
Professor
Department of Biology
Clarion University of Pennsylvania
Clarion, PA

_____
Thomas J. Mattei, B.S., PharmD.
Associate Professor of Pharmacy Practice
Associate Dean for Professional Programs
Mylan School of Pharmacy
Duquesne University
Pittsburgh, PA

_____
J.Douglas Bricker, Ph.D.
Dean, Mylan School of Pharmacy and the
Graduate School Pharmaceutical Sciences
Duquesne University
Pittsburgh, PA

ABSTRACT

MECHANISTIC AND CLINICAL STUDIES OF PLATELET RICH PLASMA:

A SIMPLE CLINICAL METHOD FOR ENHANCING BONE

AND SOFT TISSUE HEALING

By

James L. Rutkowski

December 2008

Dissertation Supervised by David A. Johnson Ph.D.

Platelet rich plasma (PRP) is a methodology of using a patient's own platelets to enhance bone and soft tissue healing following oral surgical procedures. Whole blood is drawn from the patient by conventional phlebotomy techniques and then centrifuged with the formation of a distinct middle layer that contains platelets and white blood cells (WBCs). This layer of platelets and WBCs is then placed into the surgical site to enable faster and more predictable healing. This technique has also found use in general medical surgeries and is gaining in popularity.

Platelets contain growth factors and other cytokines that are beneficial for healing following surgical trauma. This project uses both *in vitro* and *in vivo* studies to provide the mechanistic basis for the continued and possible expanded clinical use of PRP.

A simple and inexpensive technique for acquiring PRP is examined and provides evidence that during the platelet harvesting steps the platelets are properly concentrated, not altered, and that growth factors (GFs) critical to bone formation are present.

A retrospective clinical trial provides data that illustrate a significant decrease ($p < .0001$) in the frequent complication of "dry socket" (alveolar osteitis, AO) formation following mandibular tooth extractions. The study reveals that not using PRP is a risk factor for AO formation.

The project also utilizes a molecular study utilizing human mesenchymal stem cells (hMSCs) to provide a mechanistic basis for bone formation following PRP use. Enhanced proliferation and inducement of differentiation of hMSCs were found to the possible explanations for the clinical successes reported with PRP use.

 A prospective clinical study provides radiographic evidence for increased radiographic opacity (indicating bone formation) during the initial two weeks following placement of PRP at the time of mandibular third molar removal.

This translational research offers scientific support for the use of PRP in osseous surgeries. The use of this simple and inexpensive PRP technique could help patients recover faster, with fewer complications and greater bone formation predictability following surgeries involving bone manipulation.

ACKNOWLEDGEMENTS

My wonderful family, who have put up with my consumption with work and Ph.D studies. Kasey, Jon, Adam, Molly, Jessi and my wife Debbie. I love you all so much and I thank you for your love, support and encouragement during a very busy time in our lives.

TABLE OF CONTENTS

LIST OF TABLES

LIST OF FIGURES

LIST OF ABBREVIATIONS

7TM   Seven Transmembrane Helix Receptor

ALP   Alkaline Phosphatase

AO   Alveolar Osteitis

ATP   Adenosine Triphosphate

ATPase   Adenosine Triphosphatase

BC   Buffy Coat

Bglap   Osteocalcin Gene- Bone gamma-Carboxyglutamate (gla) Protein

BMP   Bone Morphogenetic Protein

cAMP   Cyclic Adenosine Monophosphate

COX-2   Cyclooxygenase 2

cPRP   Concentrated Platelet Rich Plasma

CT   Computerized Tomography

DMEM   Dulbecco's Modified Eagle's Medium

DNA   Deoxyribonucleic Acid

EGF   Epidermal Growth Factor

EKG   Electrocardiogram

ELISA	Enzyme-Linked Immunosorbent Assay
FBS	Fetal Bovine Serum
FDA	Food and Drug Administration
fL	Femtoliter (10^{-12} L)
GAPDH	Glyceraldehyde Phosphate Dehydrogenase
GF	Growth Factor
GFs	Growth Factors
GH	Growth Hormone
GP	Glycoprotein
GPIIb	Glycoprotein IIb
HBSS	Hank's Balanced Salt Solution
hMSC	Human Mesenchymal Stem Cells
HTRPC1	human canonical transient potential-1
HU	Hounsfield Units
IBSP	Bone Sialoprotein
IL	Interleukin
ILGF	Insulin-Like Growth Factor

ITGA2B	Glycoprotein IIb
KGF	Keratinocyte Growth Factor
KVO	Vein Kept Open
LAP	Latency Associated Peptide
MMP	Matrix-Metalloproteinase
MPO	Myeloperoxidase
MTT	3-(4,5-Dimethylthiazol-2-yl)-2,5-Diphenyltetrazolium Bromide
NAD	Nicotinamide Adenine Dinucleotide
NFBD	Newly Formed Bone Density
NGF	Nerve Growth Factor
NSAID	Non-Steroidal Antinflammatory Drugs
OPG	Osteoprotogerin
PAI-1	Plasminogen activator Inhibitor-1
PC	Platelet Concentrates
PDGF	Platelet Derived Growth Factor
PE	Phosphatidylethanolamine
PF4	Platelet Factor 4

PGEL	Gelled Platelet Rich Plasma
PG	Prostaglandin
pNPP	*para*-Nitrophenyl Phosphate
PPP	Platelet Poor Plasma
PRF	Platelet Rich Fibrin
PRP	Platelet Rich Plasma
RBC	Red Blood Cells
RNA	Ribonucleic Acid
ROI	Regions of Interest
RT-PCR	Reverse Transcriptase Polymerase Chain Reaction
TBS	Tris Buffered Saline
TBST	Tris Buffered Saline- Tween 20
TGFβ	Transforming Growth Factor Beta
TNF	Tumor Necrosis Factor
TSP	Thrombospondin
TX	Thromboxane
VAS	Visual Analog Scale

VEGF   Vascular Endothelial Growth Factor

vWF   von Willebrand Factor

WBC   White Blood Cells

Introduction

Literature Review of Platelet Rich Plasma

Improved rate and predictability of healing is a goal for various medical and dental surgical procedures. It has become increasingly common in the clinical practice of dentistry to use autologous platelet-rich plasma (PRP) to facilitate soft and hard tissue healing following surgical procedures (1-8). PRP has been found to accelerate bone formation and induce healing in non-healing wounds (8-14). These referenced techniques involve expensive techniques that require 60 to 480 mL of whole blood to be drawn from the patient, however the method examined in this dissertation uses an inexpensive technique that requires only 5 to 10 mL of whole blood. PRP is a generic term that has some specific variations. These variations include: platelet concentrates (PC), concentrated platelet rich plasma (cPRP), gelled platelet rich plasma (PG), and the "buffy coat" (BC). The terms are often erroneously interchanged and many clinicians are unaware of the differences. Although one common aspect of all variations is a higher than normal baseline concentration of platelets (10, 15), there are subtle, but often clinically significant, differences between each of these blood products. The reason PRP (and its variants) is of interest is because platelets contain growth factors (GF), which are released upon activation. The literature pertaining to the role of growth factors in soft and hard tissue regeneration is abundant (8). PRP was approved for clinical use in 1998 (16). Since that time several PRP variants have been used. Review of the medical and dental literature supports (with some discrepancies) the use of

autologous PRP in clinical practice (16).   Clinical uses of PRP are as a healing adjuvant for soft tissue injuries, chronic diabetic foot ulcers, injuries to muscles, tendons or ligaments, distraction osteogenesis of extremities in patients with achondroplasia/hypchondroplasia, and for increased predictability following urologic, dental, ophthalmic, and plastic surgery procedures (17-31).

The studies of this dissertation examine a simple, cost-effective method of obtaining PRP. The studies provide evidence of suitable platelet concentration, platelet viability, growth factor content, positive effects on human mesenchymal stem cell (hMSC) proliferation, and positive effects on bone development in third molar tooth extraction sites, in addition to decreased alveolar osteitis (AO) following mandibular molar tooth removal in patients. In vitro molecular studies also suggest that this technique may have a positive effect on hMSC differentiation down the osteoblastic lineage. This project provides the necessary scientific basis to prove the efficacy of a simple BC method and therefore its suitability for use in a clinical setting.

A. Platelets

Histology

Platelets are anuclear, void of genomic DNA and discoid in shape (32). They are produced during hematopoiesis by budding off from megakaryocytes (33). Each megakaryoctye undergoes controlled cellular fragmentation that produces 5,000 to 10,000 platelets (34). Platelets are rapidly depleted and must be replaced every 7 to 10 days (15). Unless activated, platelets circulate normally in a resting state for approximately 7 to 9 days and are destroyed by the spleen and Kupffer cells in the liver. Platelets contain high concentrations of cytoskeleton, signaling, membrane-bound, protein-processing, and cytoskeletal regulatory proteins. These presynthesized proteins are made in the megakaryocytes and packaged into granules through vesicle-trafficking

processes. There are other proteins synthesized from platelet mRNA during platelet activation (35). Platelets contain RNA, mitochondria, a canalicular system (similar to an endoplasmic reticulum), and several different types of granules. There are three main storage compartments in platelets: lysosomes, dense granules, and α-granules. The lysosomes contain acid hydrolases; the dense granules contain ADP, ATP, serotonin, histamine and calcium; and the α-granules contain fibrinogen, factor V, vitronectin, thrombospondin, von Willebrand factor (vWF) and several growth factors. Platelets release the contents of intracellular granules in response to activation (15).

Morphology

Platelets appear in stained blood film as small, blue or colorless bodies with several purple-red granules (34). They average about 0.5 to 3 µm in diameter, although there is a wide variation in shape, from round to elongated, cigar-shaped forms (15, 36).

Platelet Count

Platelets are counted by enumerating particles in the unlysed whole blood sample within a specific volume window (e.g., 2-20 fL), where volume may be measured by electrical impedance or light scattering. Accurate platelet quantification is difficult and presents with variation because of their small size, predisposition to aggregation and potential overlap of platelets with more numerous red blood cells. Contemporary platelet quantifying instruments typically create a platelet volume histogram based upon the measured platelet size within the platelet volume window, and mathematically extrapolate the histogram to account for platelets whose size overlaps with debris of

small red cells. Platelet counts show substantial ethnic variation (37). The normal

platelet count is lower in individuals of African ethnic origin (38). See Table 1 for ethnic

difference in normal leukocyte and platelet count values

Gender	Men			Women		
Nationality	European Descent n=100	Afro-Caribbean n=51	African n=65	European Descent n=100	Afro-Caribbean n=51	African n=50
Leukocyte count*	5.7(3.6-9.2)	5.2(2.8-9.5)	4.5(2.8-7.2)	6.2(3.5-10.8)	5.7(3.3-9.9)	5.0(3.2-7.8)
Neutrophil count	3.2(1.7-6.1)	2.5(1.0-5.8)	2.0(0.9-4.2)	3.6(1.7-5.5)	3.0(1.4-6.5)	2.4(1.3-4.2)
Lymphocyte count	1.7(1.0-2.9)	1.9(1.0-3.6)	1.8(1.0-3.2)	1.8(1.0-3.5)	2.0(1.2-3.4)	2.0(1.1-3.6)
Monocyte count	0.34(0.18-0.62)	0.33(0.18-0.52)	0.29(0.15-0.58)	0.30(0.14-0.61)	0.31(0.16-0.59)	0.28(0.15-0.39)
Eosinophil count	0.12(0.03-0.48)	0.13(0.03-0.58)	0.12(0.02-0.79)	0.13(0.04-0.44)	0.10(0.03-0.33)	0.10(0.02-0.41)
Platelet count	218(143-332)	196(122-313)	183(115-290)	246(169-358)	236(149-374)	207(125-342)

Table 1. Ethnic Differences in Normal Leukocyte and Platelet Count Values

All counts expressed in thousands per μL. Geometric mean and 95% reference range are in parentheses (15).

Function

Platelets have two distinct physical states.
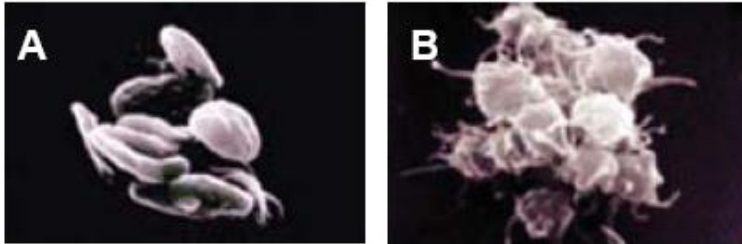
Figure 1. Two States of Platelets

Platelets in their resting form (A) and at the beginning of activation (B) (39).

At rest, the platelets circulate through the vasculature as small discs of reproducible structure having an elegant, actin-based cytoskeleton. In response to vascular damage or when blood flow ceases (becomes stagnant), the platelets enter a second stage where they rapidly convert into their active form with filopodia and lamellipodia that derive from a remodeled actin skeleton and a sophisticated assembly of new actin filaments (36). This change in physical state allows platelets to interact with each other and adhere to, the injured vessel, specifically with the subendothelium. This process is mediated by von Willebrand factor (vWF), collagen, fibrinogen, thrombospondin, and different platelet membrane glycoproteins (Figure 2) (15, 40).
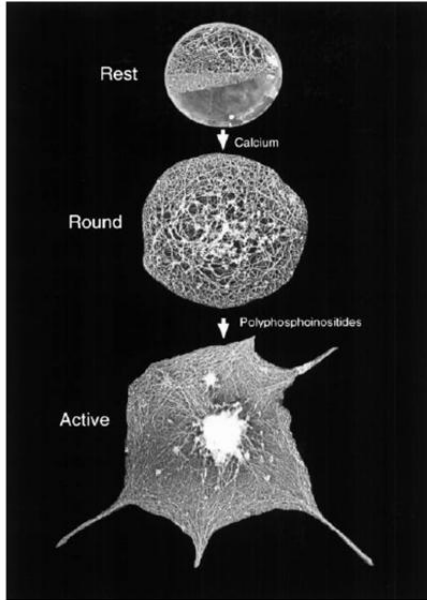
Figure 2. Platelet Shapes

Top-resting platelets shown as small discs. Middle - platelets increasing in size due to vascular damage. Bottom-active platelets showing filopodia (36).

Aggregation

As platelets change their shape, they begin to aggregate which results in a hemostatic plug (clot). Platelet aggregation is stimulated by thromboxane and α_2 adrenergic receptor-activation. Platelets adhere to each other via adhesion receptors or integrins and, in conjunction with fibrin, to endothelial cells in the wall of the blood vessel forming the hemostatic plug. Myosin and actin filaments within the platelets are stimulated to contract during aggregation, further reinforcing the plug. The most abundant platelet adhesion receptor is glycoprotein (GP)IIb/IIIa. This is a calcium-dependent receptor for fibrinogen, fibronectin, vitronectin, thrombospondin and vWF. Activation of the GPIIb/IIIa receptor facilitates the aggregation process, which helps generate thrombin.

Thrombin leads to the activation of other platelets. The GPIIb/IIIA receptor action is further augmented by other elements secreted by platelets, such as ADP, 5-HT, collagen, and thromboxane A_2. Two other receptors involved are GPIb-V-IX complex (VWF) and GHPVI (collagen) (40). Epinephrine is a weak platelet agonist (α_2 adrenergic receptor), but probably plays a significant role by enhancing the platelet's response to other agonists (15, 40).

Several inhibitory factors prevent excessive platelet aggregation. The endothelial cells synthesize three anti-aggregation products: PGI_2 (prostacyclin), PGD_2, and nitric oxide. Other important inhibitory factors include platelet-leukocyte interactions and the speed of blood flow (15, 40).

Platelet Activation

Activation follows the aggregation process and occurs when platelets experience several biochemical changes before secreting their active components. Platelets are activated when brought into contact with collagen, thrombin, fibronectin, laminin, thromboxane A2, epinephrine, ADP, a negatively charged surface (e.g. glass), and platelet-activating factors. If whole blood is collected in a glass tube, it must contain an anticoagulant (heparin or tri-sodium citrate) to prevent coagulation. Activation involves specific extracellular membrane receptors that transduce the signal via G-proteins or other mechanisms that induce intracellular signaling. Figure 3 illustrates the steps involved in platelet activation.
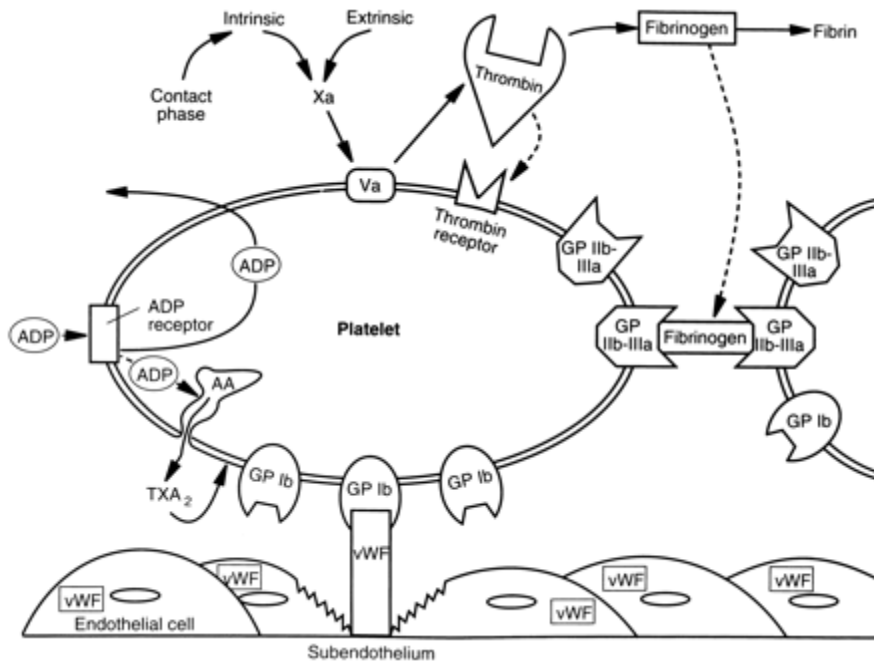
Figure 3. Schematic Representation of Platelet Activation by Extracellular Factors (40)

Several platelet membrane receptors bind with extracellular factors in response to platelet adhesion and aggregation, resulting in platelet activation. GPIb in the platelet membrane binds von Willebrand factor (vWF) and mediates adhesion. Not illustrated is a second site on vWF that binds to GPIIb/IIIa. GPIIB-IIIa in the membrane binds fibrinogen and mediates platelet-platelet interactions. ADP and thrombin receptors are illustrated to show the relationship between ADP stimulation and arachidonic acid pathway (AA), with release of thromboxane A_2 (TXA_2), which further stimulates aggregation. (40)

Upon activation, granules contained within the platelets release coagulation factors, platelet activating factors, adhesion molecules, cell-activating molecules, cytokines, integrins, inflammatory molecules, and GFs. The release process is mediated by molecular mechanisms homologous to other secretory cells, uniquely coupled to cell activation by intracellular signaling events (41). Platelets in the resting state do not expose negatively charged phospholipids on the surface. However binding to collagen initiates a sequence of biochemical reactions that results in the activation of the membrane protein scramblase. Scramblase transports negatively charged phospholipids from the inner leaflet of the membrane to the outer leaflet. The presence of negatively charged phospholipids allows the binding and the formation of a prothrombinase complex. These phospholipids provide a catalytic surface (with the charge provided by phosphatidylserine and phosphatidylethanolamine) for tenase and prothrombinase complexes. The tenase complex is formed by the activated forms of the blood coagulation factors, factor VIII and factor IX. It forms on a phospholipid surface in the presence of calcium and is responsible for the activation of factor X. Prothrombinase is the protein complex which consists of negatively charged phospholipid (phosphatidylserine), prothrombin, Factors Va and Xa. The prothrombinase complex converts the inactive protease prothrombin into thrombin, which has proteolytic activity to convert fibrinogen into fibrin.

Some of the substances released by platelets – in particular adenosine diphosphate, serotonin, and thromboxane, can act in an autocrine and paracrine manner to further

10

enhance platelet activation and aggregation (39). In addition, thrombin also stimulates platelet activation producing a positive feedback loop (41).

Role of Platelets in Inflammation

Platelets, the chief cellular effectors of hemostasis, are also deployed to sites of injury or infection to modulate inflammatory processes by interactions with leukocytes through the secretion of cytokines, chemokines and other inflammatory mediators (42-45).

Cytokines particularly involved with healing include: transforming growth factor-β1 (TGFβ1), platelet derived growth factors (PDGFs), and insulin-like growth factor (ILGF). These cytokines and others of significance will be discussed in detail in the discussion of α-granules.

Plasma Membrane

The platelet plasma membrane consists of a phospholipid bilayer in which cholesterol, glycolipids, and glycoproteins are embedded (46, 47). Platelets have more intramembranous particles embedded in the outer platelet membrane leaflet than in the inner leaflet. The greater number of particles in the outer membrane most likely reflects the many external receptors that mediate platelet interactions. The plasma membrane contains sodium- and calcium-adenosine triphosphatase (ATPase) pumps that control the platelet's intracellular ionic environment. It is estimated that slightly over half of platelet phospholipids are contained in the plasma membrane. When platelets are in the resting state, negatively charged phospholipids are almost exclusively present in the inner leaflet, whereas other phospholipids are more uniformly dispersed (48). When platelets are in the resting state the negatively charged phospholipids, including

phosphatidylserine, are capable of initiating several steps of the coagulation sequence. Therefore, the presence of phosphatidylserine in the inner leaflet of resting platelets sequesters them from circulating plasma coagulation factors thereby preventing inappropriate coagulation (49, 50). When agonists induce platelet activation, the aminophospholipids become exposed on the platelet surface or on the surface of microparticles associated with the activation cascade (49-52). The location of phospholipids in quiescent platelets is maintained by an ATP-dependent aminophospholipid translocase that actively moves phosphatidylserine and phosphatidylethanolamine (PE) from the outer leaflet to the inner leaflet (49, 53).

The asymmetry of the negatively charged phospholipids may also be maintained by interactions that occur with cytoskeletal or other cytoplasmic elements (49, 50, 54, 55).

Platelet Membrane Receptors

Platelet receptors, some of which are expressed only on activated platelets (41), are comprised of glycoproteins that receive signals from outside the platelet and transduce them to the interior. Receptors are also activated by signals orginating inside the platelet that affect surface domains. Membrane receptors determine the reactivity of the platelets with a wide range of agonists and adhesive proteins.

Platelet receptors are derived from several different receptor families including integrins, leucine-rich glycoproteins, immunoglobulin (Ig) cell adhesion molecules, selectins, quadraspanins, and seven transmembrane (7TM) domain receptors (15). A single member of the integrin family, αIIβ3, is thought to be exclusive to platelets, as is GPVI. The leucine-rich glycoproteins GPIb-IX and GPV appear to have a limited expression that includes platelets and cytokine-activated endothelial cells (56-58). The

αIIbβ3 integrin receptor mediates interactions between platelets and between proteins and platelets (15, 59).

 αIIbβ3 (GPIIb/IIIa; Fibrinogen Receptor; CD41/CD61) Receptor

The integrin αIIbβ3 (Figure 4) is among the most densely expressed adhesion/aggregation receptors present on any cell type, (15) and is necessary for platelet aggregation (59). It is a heterodimeric receptor composed of an alpha chain and a beta chain that binds fibrinogen, vWF, fibronectin, and vitronectin. Expression of the receptor is thought to be limited to cells of the megakaryoctye lineage (59-61). The genes for the αIIb (α chain) subunit are encoded by the gene designated ITGA2B. The β3 portion (β chain) is encoded from the ITGB3 gene (15, 34). The αIIb chain undergoes post-translational cleavage to yield disulfide-linked light and heavy chains that join with beta 3 to form the receptor.

The αIIbβ3 receptor not only plays a crucial role in coagulation, but is also significant in cell-surface mediated signaling, resulting in activation. Upon activation, these receptors are able to join the plasma membrane and undergo the release of the GFs contained within the α-granules (62-64). On quiescent platelets, αIIbβ3 has low affinity for fibrinogen. However when platelets are activated by ADP, epinephrine, thrombin, or other agonists, αIIbβ3 binds fibrinogen with higher affinity (65-67). Platelet activation induces changes in the αIIbβ3 integrin receptor that are responsible for the change in fibrinogen-binding affinity (68-70), although changes in the environment surrounding αIIbβ3 may also be involved. αIIbβ3 receptors in α-granules appear to cycle to and from

the plasma membrane (70). This recycling explains the capacity of αIIbβ3 to take up fibrinogen from plasma and transport it to α-granules, where it is concentrated (71, 72).

α2β1(GPIa-IIa; Collagen Receptor; CD49b/CD29) Receptor

Unlike the integrin αIIbβ3, α2β1 (Figure 4) is widely expressed in many cell types and can mediate adhesion to collagen (73-79). The GPVI receptor activates α2β1, as well as other integrins. α2β1 promotes firm adhesion of the platelet to collagen, stabilizes thrombus growth on collagen, and promotes procoagulant activity (15, 80, 81). It is linked to the membrane skeleton and is competent to mediate adhesion of resting platelets (15, 82). Interestingly, activation of α2β1 can initiate protein synthesis in platelets (15, 83).

Cytoskeletal Elements

A planar network of thin, elongated spectrin tetramers interconnected by the ends of actin filaments is present immediately below the plasma membrane of the platelet and the membranes of the open canalicular system (15). Filamin-A (actin-bonding protein) can interact with both the transmembrane glycoprotein (GPIbα) and the actin immediately below the plasma membrane. This interaction connects these components to the cytoskeleton protein spectrin (on the intracellular side of the plasma membrane) forming a scaffolding cytoskeleton that possibly stabilizes the membrane's discoid shape. In addition, the association of GPIbα with the membrane skeleton restricts the expansion of the spectrin network and probably helps to organize receptors into linear arrays on the platelet surface, thus enhancing receptor cooperation (84).
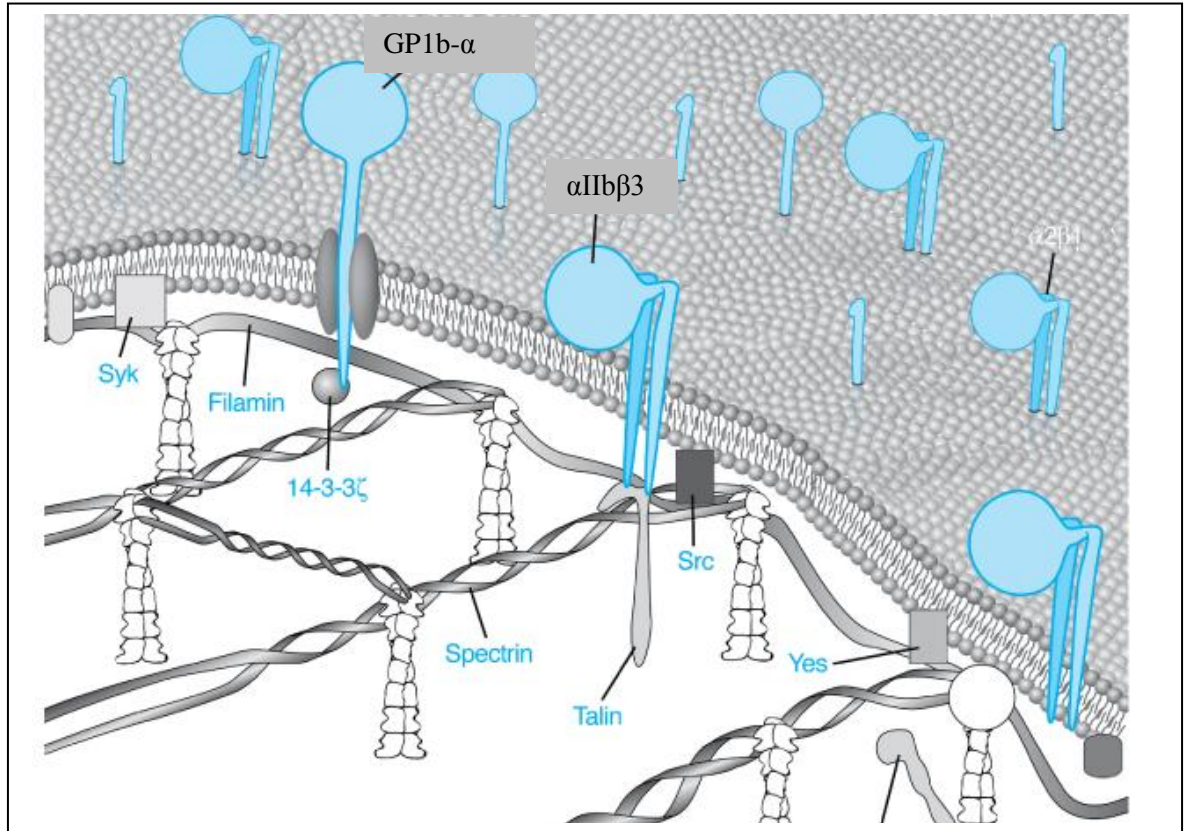
Figure 4: Platelet Membrane Transmembrane Glycoproteins

Depiction of selected platelet transmembrane glycoprotein connections to the cytoplasmic skeleton (15, 85).

Talin is another protein found in the membrane skeleton and is implicated in the control of αIIbβ3 activation by virtue of binding to the cytoplasm domains of αIIbβ3 (61, 84, 86-89). When platelets are activated, receptors αIIbβ3 and α2β1 may bind to the cytoskeleton as well. Therefore, the cytoskeleton may affect whether receptors are free to move in the plane of the membrane have a role in moving certain receptors from the surface to the interior of platelets and vice versa, via the canalicular system (84, 90).

Microtubules

The circumferential band of microtubules present underneath the plasma membrane in all probability plays a significant role in platelet formation from megakaryocytes and contributes to the platelet's discoid shape (15, 34, 91-93). Microtubules are hollow polarized polymers (25 nm diameter) that contain 13 protofilaments consisting of α, β, β-tubulin dimers (15, 34, 61, 84). Four tubulin isoforms (β_1, β_2, β_4, β_5) are found in platelets. β_1 is dominant and is megakaryoctye- and platelet-specific. Approximately 50 to 60 percent of platelet tubulin is utilized in microtubules, with an equilibrium maintained between polymerized and free tubulin subunits (34, 94). Motor proteins associated with the microtubules contribute to the development and function of platelets (15).

Organelles

Peroxisomes, mitochondria, lysosomes, dense bodies, exosomes, α-granules, and ribosomes (with mRNA) are all found in platelets. Alpha-granules and ribosomes are of particular importance to this project and are discussed below.

α-Granules

The majority of secretory substances found in platelets are localized in α-granules, numbering approximately 50 to 80 per platelet (15, 34, 95). The α-granules are approximately 200 nm in diameter and demonstrate internal variation in electron density, often with an eccentric area of accentuated electron density, termed a nucleoid, in which β-thromboglobulin, platelet factor 4 (PF4), and proteoglycans are concentrated (46). The

less dense electron areas include tubular elements in which vWF, multimerin, and factor

V are preferentially contained (96). Table 2 lists some of the most important proteins

relevant to this research that are present in α-granules.

Category	Term	Biological activities
Adhesive proteins	vWf + propeptide, Fg, Fn, Vn, TSP-1, laminin-8	Cell contact interactions, clotting, extracellular matrix composition
Clotting factors and associated proteins	Factor V/Va, factor XI, multimerin, gas6, protein S, high-molecular weight fibrinogen, antithrombin, tissue factor pathway inhibitor (TFPI)	Thrombin production and its regulation, angiogenesis
Fibrinolytic factors and associated proteins	Plasminogen, PAI-I, u-PA, osteonectin, α2-antiplasmin, histidine-rich glycoprotein, TAFI, α2-macroglobulin	Plasmin production and vascular remodeling
Proteases and anti-proteases	Tissue inhibitor of metalloprotease-4 (TIMP-4), metalloprotease-4, platelet inhibitor of FIX, protease nexin-2, C1 inhibitor, α1-antitripsin	Angiogenesis, vascular modeling, regulation of coagulation, regulation of cellular behavior
Growth factors, cytokines, and chemokines	PDGF, TGFβ1,and 2, EGF, IGF-1, VEGF (A and C), bFGF, and FGF-2, hepatocyte GF, RANTS, IL-8, MIP-1α, growth regulated oncogene-α, ENA-78, MCP-3, angiopoietin-1, Il-1β,IGF BP-3, neutrophil chemotactive protein	Chemotaxis, cell proliferation and differentiation, angiogenesis
Basic proteins and others	PF4, β-thromboglobulin, platelet basic protein, connective tissue activating peptide III, neutrophil activating peptide-2, endostatins	Regulation of angiogenesis, vascular modeling, cellular interactions
Anti-microbial proteins	Thrombocidins	Bactericidal and fungicidal properties
Others	Chondroitin 4-sulfate, albumin, immunoglobulins	Diverse
Membrane glycoproteins	αIIbβ3, αβ3, GPIb, PECAM-1, most plasma membrane constituents, receptors for primary agonists, CD40L,	Platelet aggregation and adhesion, endocytosis of proteins, inflammation, thrombin generation, platelet-

Category	Term	Biological activities
	tissue factor, P-selectin	leukocyte interactions

Table 2. Contents of the Platelet α-granules

Platelet α-granule contents by category (39, 97).

Small quantities of nearly all plasma proteins are nonspecifically taken up into α-granules. Platelet levels of these proteins are determined by their plasma concentrations (98, 99). This is especially significant for the α-granule pool of immunoglobulins (Ig), because the majority of total platelet Ig is affected by plasma Ig levels, rather than by changes in platelet surface Ig (15, 98, 99).

The concentrations of the platelet-specific proteins, PF4 and the β-thromboglobulin family members, in α-granules are on the order of 20,000 times higher than their plasma concentrations. These proteins also share amino acid sequence homology with each other and with other members of the "intercrine-cytokine" family of molecules. Once PF4 is released from platelets, it inhibits angiogenesis, perhaps through inhibition of endothelial cell proliferation (100).

The α-granules also contain platelet-derived growth factor (PDGF). PDGF is a disulfide-linked dimeric molecule of the tyrosine kinase receptor family (101). PDGF is mitogenic for smooth muscle cells (102). After PDGF was discovered in platelets and was given its name, other tissues were found to produce the same factor; thus, the name *platelet-derived* growth factor is misleading because its presence is not limited to

platelets. The PDGF in platelet α-granules contains a mixture of a homodimer PDGF-BB (30%) and a heterodimer PDGF-AB (70%). These two isoforms appear to have different functional activities (103). Platelet-derived growth factors PDGFs (PDGF-AA, PDGF-BB) are essential regulators for migration, proliferation and survival of mesenchymal cell lineages. (104-106) PDGF's function in regulating mesenchymal cell lineages is of great importance for bone development, remodeling (104, 107) and cicatrization (fibrous scar formation) (104, 108). PDGF may also be instrumental in normal cell proliferation and in the development of atherosclerosis, tumor growth, wound repair, and fibroproliferative responses (pulmonary and renal fibrosis) (109-111).

Vascular endothelial growth factor (VEGF), an important stimulator of angiogenesis, is also found in high concentrations in α-granules. VEGF is released after platelet stimulation during the hemostatic response to a bleeding wound (112-114). Platelets and megakaryocytes express the gene transcript for a VEGF receptor termed *KDR* (115). VEGF is the most prominent and ubiquitous of the known vascular growth promoters (116, 117). It is instrumental in the control of endothelial cell proliferation, migration, specialization, and survival (116, 118, 119). The singular presence of VEGF is enough to initiate angiogenesis and the availability of different isoforms VEGF makes it possible to direct and refine the development plan for tissue growth (46, 116, 120).

Insulin-like growth factors (ILGFs) I and II are positive regulators of proliferation and differentiation for most cell types, including tumor cells. ILGF also is important in the regulation of apoptosis regulation by inducing survival signals and inhibiting pro-

apoptotic stimuli (104, 121). ILGF is released during platelet degranulation and is also ubiquitous in circulating blood (104).

Platelet α-granules contain high concentrations of the growth factor TGF-β_1. TGF-β is a large superfamily with more than 30 members. TGF-β is of great importance for bone formation and is the isoform of greatest abundance not only in platelet α-granules, but is also, important for intercellular signaling (104, 122). *In vitro,* the effects of TGF-β are varied depending upon the concentration, the matrix environment and cell type. TGF-β_1 has been shown to stimulate the proliferation of osteoblasts as well as causing their inhibition (104, 123). Despite TGF-β_1's variable effects on proliferation, for the great majority of cell types, it represents the most powerful fibrosis inducing agent among all cytokines (104, 124). Therefore, TGF-β_1 can be considered an inflammation regulator because of its ability to induce fibrous wound healing leading to scar formation.

Depending on the cell type being affected, TGF-β1 can promote or inhibit the growth of cells (125). TGF-β1 can increase thrombopoietin production by bone marrow stromal cells. Thrombopoietin, in turn, induces megakaryoctye expression of TGF-β1 receptors. This enables TGF-β1 to arrest the maturation of megakaryoctye colony forming units (126). TGF-β1 also promotes synthesis of extracellular matrix proteins, plasminogen activator inhibitor-1 (PAI-1), and metalloproteinases. TGF-β_1 has been implicated in wound healing, malignancy, and tissue fibrosis (125). TGF-β1 acts as a chemoattractant for monocytes and fibroblasts, but inhibits the migration of endothelial cells. There are three isoforms-TGF-β_1, TGF-β_2, and TGF-β_3- with a wide tissue distribution, but platelets contain only TGF-β_1. TGF-β1 released from platelets can stimulate smooth muscle cells to express and release VEGF, thus supporting re-endothelialization after vascular injury

(127). TGF-β1 is released from platelets in an inactive (latent) form that is complexed

with a portion of the precursor protein (latency-associated peptide, LAP). A fraction of

LAP is covalently coupled to another protein latent TGF-β–binding protein (LTBP),

which localizes the complex to the extracellular matrix (128). Activation of latent TGF-

β1 is a multifaceted process that is thought to involve a conformational change in LAP

that unmasks the active site of TGF-β_1 (128). Activation of latent TGF-β1 can be

achieved by several different mechanisms, including acidification, proteolysis by

plasmin, interaction with the integrin αVβ6, or interaction with thrombospondin-1 (TSP-

1) or a small peptide derived from TSP-1. However, the physiologic activator(s) remains

unclear (15, 128-130). The ability of TSP-1 to activate TGF-β1 is of special interest

because both TGF-β1 and TSP-1 are present in α-granules. Only a small percentage of

the TGF-β1 released from platelets with thrombin stimulation becomes activated, but the

amount is sufficient to activate synthesis of plasminogen activator inhibitor-1(PAI-1)

(130-132). Active TGF-β1 can bind to three different cell surface proteins- a

proteoglycan (β-glycan), and two serine/threonine kinases (125, 133).

Epidermal growth factor (EGF) has also been observed in platelet α-granules, but the

kinetics of its release differs from that of other granule proteins (134).

Platelets also contain endothelial cell growth factor which stimulates endothelial cell

proliferation and angiogenesis (135). It is thought to be present in the cytoplasm of

platelets but not the α-granules. Therefore, it is released only at the time of platelet

disintegration--not stimulation.

Ribosomes and Messenger RNA

Platelets contain a relatively small number of ribosomes and remnants of a Golgi apparatus. Platelets also have a small amount of mRNA on platelet polysomes carried over from megakaryocytes but cannot synthesize mRNA due to the lack of a nucleus (136-138). Although mRNA is present in platelets where it corresponds with constitutively expressed factors, mRNA undergoes progressive decay due to the absence of any new gene transcription (138, 139). Platelets contain a plethora of mitochondria, with each containing multiple copies of its own genome that can be actively transcribed (138, 139). Regulated synthesis of new proteins by platelets has been reported upon thrombin activation as a result of redistribution of the eukaryotic initiation factor 4E. Signaling produced by ligand engagement of αIIbβ3 appears to be necessary to initiate the process of protein synthesis (83, 140, 141). One of the translated proteins is pro–IL-Iβ, which provides a link between thrombosis and inflammation (142). Signaling through α2β1 (GPIa-IIa) also can initiate platelet protein synthesis (83).

Membrane Systems

The open canalicular system is an intricate series of conduits that originate as indentations of the plasma membrane and course throughout the interior of the platelet (91, 143). Electron microscopy of sectioned platelets demonstrates that the open canalicular system is contiguous with the exterior of the platelet, even though elements of the open canalicular system may appear as closed vesicles or vacuoles (91, 143, 144). The open canalicular system serves several functions. It provides a point for entry of external elements into the interior of the platelet and a potential means for the release of

granule contents to the outside, eliminating the need for granule fusion with the plasma membrane itself (144, 145). This latter purpose is particularly significant because, under most circumstances, platelet granules move to the center of the platelet upon platelet activation, rather than to the periphery (91, 146). However, the degree to which α granule secretion occurs via the open canalicular system, versus direct fusion with the plasma membrane remains unclear (91, 147). The open canalicular system is contiguous with the platelet plasma membrane. Platelet spreading after adhesion requires a significant increase in the surface area of the plasma membrane. New membrane cannot be synthesized quickly enough to accommodate this phenomenon, therefore, the membrane of the open canalicular system contributes to the suface plasma membrane following platelet activation. The membrane of α-granules also may contribute, but only if the stimulus is sufficient to induce the fusion of these organelles with the plasma membrane (also known as release reaction). Lastly, the membrane of the open canalicular system may serve as a storage site for plasma membrane glycoproteins. For example, platelet activation by thrombin can lead to a predictable, selective loss of GPIb-IX from the membrane surface. Electron microscopy analysis indicates the GPIb-IX becomes sequestered into the open canalicular system (90, 148, 149). Plasmin may stimulate a similar event (90, 150). Platelet activation leads to an increase in surface αIIbβ3, and although much of this αIIbβ3 is thought to derive from α-granule, some may come from αIIbβ3 in the membranes of the open canalicular system (15, 90, 151).

Platelet Secretion

Granule secretion is thought to be mediated by a contractile mechanism involving actin and myosin, but the details remain obscure (152, 153). After an initial platelet

shape change, actin becomes centrally organized into thick filamentous masses, where it most likely associates with myosin filaments (96). The contractile reaction is initiated by an increase in cytosolic calcium, which results in the formation of a calcium–calmodulin complex that activates myosin light-chain kinase. Phosphatases and cyclic adenosine monophosphate (cAMP) kinase modulate the reaction. The centralization of organelles in a contractile ring correlates with secretion (15, 91). However, as stated earlier, it is unclear if platelets secrete the contents of their granules by fusion with the open canalicular system in the center of the platelet or by direct fusion with the plasma membrane (91, 147). A complex multistep model for granule secretion has been suggested in which granules tether and dock to the inner leaflet of the plasma membrane and then additional molecular interactions lead to fusion of the lipid bilayers (15, 34, 152, 154-163).

Platelet Growth Factors in Treating Wounds and Soft-Tissue Injuries

Platelets are not only critical for hemostasis, but also in promoting tissue repair, angiogenesis, and inflammation by releasing growth factors. Tissue repair begins with the formation of a clot and subsequent platelet activation and degranulation that releases inflammatory and mitogenic substances that are involved in all aspects of wound-healing (164). The released substances include growth factors (GFs) that are necessary for wound repair. These GFs are proteins that enhance tissue repair mechanisms including chemotaxis, cell proliferation, angiogenesis, extracellular matrix deposition, and remodeling (39, 165).

More than 60 biologically active substance groups are found in platelets that are involved in tissue-repair mechanisms such as chemotaxis, cell proliferation and differentiation, angiogenesis, intracellular matrix deposition, immune modulation, antimicrobial activity, and remodeling (39). Of all these substances, GFs are the most important (Table 3).

Growth Factor	Function
EGF (epidermal growth factor), β-Urogastron	• Stimulates the proliferation of epidermal and epithelial cells, fibroblasts, and embryonic cells • Chemoattractant for fibroblasts and epithelial cells • Stimulates re-epithelialization, augments angiogenesis • Influences the synthesis and turn-over of extracellular matrix
PDGF (platelet-derived growth factor)	• A and B isoforms are potent mitogens for fibroblasts, arterial smooth muscle cells, chondrocytes, and epithelial and endothelial cells • Potent chemoattractant for hematopoietic and mesenchymal cells, fibroblasts, and muscle cells, stimulates chemotaxis toward a gradient of PDGF • Activates TGF-β, stimulates neutrophils and macrophages, mitogenesis of fibroblasts and smooth muscle cells, collagen synthesis, collagenase activity, and angiogenesis
TGF-α (transforming growth factor alpha)	• Resembles EGF, binds to the same receptor • Stimulates mesenchymal, epithelia, and endothelial cell growth, endothelial chemotaxis, controls the epidermal development • Stimulate the proliferation of endothelial cells, more potent than EGF • Promotes the generation of osteoblasts, influencing them to lay down bone matrix during osteogenesis • Affects bone formation and remodeling

Growth Factor	Function
TGF-α (transforming growth factor alpha) (cont'd)	by inhibition of the synthesis of collagen and release of calcium
TGF-β1 (transforming growth factor beta)	• Stimulates fibroblast chemotaxis and proliferation and stimulates collagen synthesis • Decreases dermal scarring • Growth inhibitor for epithelial and endothelial cells, fibroblasts, neuronal cells, hematopoietic cell types, and keratinocytes • Antagonizes the biological activities of EGF, PDGF, aFGF and bFGF
KGF or FGF-7 (keratinocytes growth factor)	• Most potent GF for skin keratinocytes, playing a role in tissue repair following skin injuries • Promotes wound healing via proliferation, differentiation, angiogenesis, and cell migration • Mitogens for many epithelial cells but not for fibroblasts and endothelial cells
aFGF or FGF-1 (fibroblast growth factor; acidic)	• Participates in proliferation, differentiation, angiogenesis, and cell migration • A mitogens for skin-derived keratinocytes, dermal fibroblasts, and vascular endothelial cells
bFGF or FGF-2 (fibroblast growth factor; basic)	• Stimulate the growth of fibroblasts, myoblasts, osteoblasts, neuronal cells, endothelial cells, keratinocytes, and chondrocytes • Stimulates angiogenesis, endothelial cell proliferation, collagen synthesis, wound contraction, matrix synthesis, epithelialization, and KGF production

Growth Factor	Function
VEGF/VEP (vascular endothelial growth factor)	• Stimulates the proliferation of macrovascular endothelial cells • A strong angiogenic protein, induces neovascularization • Induces the synthesis of metalloproteinase, which degrades interstitial collagen type 1,2,and 3
CTGF (connective tissue growth factor)	• Induces the proliferation, migration, and tube formation of vascular endothelial cells and angiogenesis • A potent stimulator for the proliferation ad differentiation of osteoblasts, stimulates the matrix mineralization
GN-CSF or CSF-α (granulocyte/macrophage colony-stimulating factor)	• Stimulates proliferation and differentiation of osteoblasts • Synergizes with Epo in the proliferation of BM progenitor cells • Strong chemoattractant for neutrophils
IGF (insulin-like growth factor)	• Growth factor for normal fibroblasts, mitogenic *in vitro* for a number of mesodermal cell types • Promotes the synthesis of collagenase and prostaglandin E2 in fibroblasts • Stimulates collagen and matrix synthesis by bone cells, regulating the metabolism of joint cartilage
TNFα (tumor necrosis factor alpha)	• Growth factor for fibroblasts • Promotes angiogenesis
IL-1βI (interleukin-1β)	• Inhibits the growth of endothelial cells and hepatocytes • Activates osteoclasts, therefore suppresses the formation of new bone, but in low concentrations it promotes new bone growth

Growth Factor	Function
	• Enhances inflammatory reactions and collagenase activity
IL-8 (interleukin 8)	• Supports angiogenesis mitogenic for epidermal cells
NGF (nerve growth factor)	• Responsible for the survival and differentiation and the functional activities of sensory and sympathetic neurons in the peripheral nervous system. • Play an important role in the development and functional activities of cholinergic neurons in the central nervous system. • Induces the synthesis of specific transmitter like peptides in sensory neurons, including substance P

Table #3: Growth Factors Contained Within Platelets.

The growth factors of interest found in platelets and their function (166).

Leukocyte Cytokines of Interest

The various PRP techniques, with the exception of the leukocyte poor method, contain concentrated white blood cells (WBCs). The WBCs contain many cytokines that are instrumental in the inflammatory and healing processes. The BC method examined in this project includes WBCs and therefore has an effect on the various cells types involved in tissue injury and healing. The cytokines of relevance to bone formation are described below.

Interleukin-1

IL-1 is produced by activated macrophages and neutrophils. It is also produced by endothelial cells, fibroblasts, keratinocytes, and Langerhans cells. IL-1 is a significant mediator of inflammation (116, 167-169). It exists as 2 isoforms, α and β with IL-1β being the prevalent form. IL-1 synthesis is mediated by TNF-α, Interferons (IFN) α, β, and γ, and bacterial endotoxins (116). The principle action of IL-1 is to stimulate T-helper lymphocytes. TNF-α and IL-1β are also present in the platelets and their combination is known to activate osteoclasts and inhibit bone formation (116, 170).

Interleukin-6 (IL-6)

IL-6 is an inflammatory cytokine associated with the IL-1β/TNF-α pathway (116, 171). It is found in activated monocytes, macrophages, T and B lymphocytes, granulocytes, fibroblasts, endothelial cells, mastocytes, chondrocytes, and osteoblasts (116). IL-6 secretion is stimulated by IL-1, bacterial endotoxins, TNF-α, and PDGFs. It is also self-regulating in that it can stimulate or inhibit its own synthesis (116, 172). IL-6 increases the rate of antibody secretion by 120 to 400 times and *in vitro* is known to promote hematopoietic stem cell proliferation (116). IL-6 constitutes an important amplification pathway for signaling immune cells and therefore supports the reaction chains leading to inflammation, destruction, and remodeling of tissues (116, 173, 174).

Tumor Necrosis Factor-α (TNF-α)

TNF-α is released during the inflammatory response induced by bacterial endotoxins. Once stimulated by bacterial antigens, TNF-α is secreted by monocytes/macrophages, neutrophils, polymorphonuclear leukocytes, and T lymphocytes. The production of TNF-α is down-regulated by IL-6 and TGF-β (116, 175). TNF-α activates monocytes, stimulates the remodeling ability of fibroblasts, increases phagocytosis, neutrophil cytotoxicity and modulates the expression of key mediators such as IL-1 and IL-6 (116, 176, 177).

Interleukin-4 (IL-4)

IL-4 is produced principally by the subpopulation of activated T cells (TH2, CD4+), which also secrete IL-6 (116, 178). It supports proliferation and differentiation of the activated B cell, but its effects are completely dependent upon the cytokine environment (116, 179, 180). IL-4 supports the healing response by modulating inflammation. IL-4 increases fibrillary collagen synthesis by fibroblasts and inhibits stimulation of MMP-1 and MMP-3 by IL-1β (116, 181). It opposes transduction pathways mediated by IL-1β, such as stimulation of PGE2 synthesis (116, 182). When macrophages are treated with IL-4 there is diminished production of IL-1β, TNF-α, and prostaglandins in response to bacterial endotoxins or IFN-γ (116, 183, 184).

B. History of PRP Use

Autologous PRP was first developed in the early 1970s as a byproduct of multi-component apheresis. Various GFs from platelets had been discovered by that time, but the clinical use of PRP was rarely reported in the 1980s. Historically it was principally used in an activated gel state. PRP gel is made by the addition of thrombin and excess calcium, which promotes both platelet activation and the coagulation cascade, resulting in the formation of a thrombus-like gelatinous substance (platelet gel, PGEL). Activated platelets are trapped within the fibrin network, where they secrete bioactive substances that slowly diffuse into the surroundings tissues (39, 185-192). The use of thrombin has recently been questioned because of the possible auto-immune responses to bovine thrombin (193). PRP was introduced to the dental community by Whitman *et al.* who hypothesized that the activation of platelets and the subsequent release of GFs would enhance surgical wound healing (39, 194). Autologous PRP GFs had been proposed as a treatment option for enhancing wound healing of chronic cutaneous ulcers by promoting the formation of granulation tissue. This hypothesis was confirmed by a randomized prospective double-blind study which demonstrated improved wound healing compared to standard treatments (39, 195). Since the publication of the initial studies, the use of PRP by the medical and dental communities has increased, but has often been cost-prohibitive for individual practitioners. Anecdotally, it is now generally accepted that the best procedure for promoting wound healing by PRP is to prepare an autologous PRP or PRP platelet gel (PRP/PGEL) that contains relevant GFs and to administer it directly to the site of the surgical intervention or wounds (39, 196). The various methods for collection of PRP are discussed elsewhere in this manuscript.

Clinical Use of Platelet-Gel or PRP Growth Factors

PRP (and PRP/PG) use is widespread in dentistry and oral-maxillofacial surgery. It is routinely used in conjunction with dental implant placement and bone regeneration techniques (197, 198). It is also used in cardiovascular, renal, opthalmological, orthopedic, and plastic surgeries. Moreover, several wound clinics use PRP or recombinant GFs to promote healing for patients with chronic diabetic ulcerations and other slow healing wounds. Treatment of diabetic wounds with PRP was more effective in patients with deeper wounds than superficial lesions (39, 199). In a study of 54 diabetic patients with 86 wounds, treatment with PGEL significantly improved healing efficacy and reduced the incidence of amputations (39, 200). Surprisingly Crovetti et al. (201) found that patients experienced less pain when PGEL was applied to diabetic ulcers.

It has also been reported that the use of PRP in 14 patients with skin and soft-tissue losses caused by acute trauma or chronic pathology led to fewer infections and a shortened length of hospital stays (202). This finding highlights the significance of the WBCs contained in PRP and their possible role in decreasing or preventing infection. Man *et al*. (27) demonstrated decreased capillary bleeding in the surgical flaps of 20 patients undergoing various cosmetic surgical procedures (face lifts, breast size changes, or neck lifts.) PGEL or PRP is currently being used in the treatment of tendonitis, and tendon/muscle repairs (203). A study of 100 patients who received calcified autologous PRP matrix in the surgical treatment to reconstruct the anterior cruciate ligament had enhanced attachment of the new articular cartilage graft (204). PGEL used in the

treatment of chronic elbow tendonitis improved function and decreased pain when compared to conservative standardized physical therapy protocols (205).

Each of the above studies used variants of PRP that were prepared with expensive and time consuming techniques that limited the use and benefits of PRP use to larger sophisticated medical centers. This dissertation examines a less expensive and time efficient method of obtaining a variant of PRP so the benefits will be readily available for multiple procedures in smaller out-patient clinics.

Soft Tissue Wound Healing

Soft tissue-healing is a complex process that includes coagulation, inflammation, ground substance/matrix synthesis, angiogenesis, fibroplasias, epithelialization, wound contraction, and subsequent remodeling. The physiological process begins immediately upon tissue injury and includes four distinct, yet overlapping, phases: a) hemostasis, b) inflammation, c) proliferation, and d) remodeling (164).

Hemostasis Phase

Immediately following tissue injury that includes a vascular injury, intracellular calcium is released activating coagulation factor VII and inducing the extrinsic coagulation cascade. Concurrently with the coagulation cascade, the arachidonic acid pathways, and the release of GFs and cytokines work jointly to initiate and sustain the inflammatory phase including the sequencing of cells involved in the process. Locally, a reflex vasoconstriction occurs to facilitate hemostasis. Hemostasis is ultimately achieved

by the formation of a fibrin plug composed of a provisional wound matrix that functions as a lattice network upon which platelets aggregate (39, 164).

Inflammation Phase

During the early post-injury period platelets provide an abundance of GFs. These GFs act on inflammatory cells, fibroblasts, and endothelial cells to orchestrate wound healing including chemotaxis of neutrophils, monocytes, and fibroblasts into the wound (39, 164, 206, 207). In the first two days of healing, the inflammatory process is initiated by the migration of neutrophils. Neutrophils are responsible for debris scavenging, complement-mediated opsonization of bacteria, and bacteria destruction via myeloperoxidase (MPO)-driven oxidative burst mechanisms (i.e. superoxide and hydrogen peroxide formation) (39). Neutrophils destroy bacteria and decontaminate the wound by removing lymphocytes and macrophages (monocytes). The macrophages secrete multiple enzymes including collagenases, which lead to wound debridement. The macrophages also secrete additional GFs, which in turn stimulate fibroblasts to produce collagen and promote angiogenesis. This step marks the transition from the inflammatory phase to the proliferation phase of tissue reconstruction (39).

Proliferation Phase

The proliferative phase begins approximately 2 to 3 days after wounding. This phase begins with the arrival of fibroblasts into the wound site. Fibroblasts migrate from the wound margins by means of the fibrin-based interim matrix established during the inflammatory phase. During the first week of healing, fibroblasts are driven by a

macrophage-derived fraction, TGF-β, and PDGF to proliferate and synthesize

glycosaminoglycans and proteoglycans. The glycosaminoglycans and proteoglycans

become the foundation for a new extracellular matrix of granulation tissue and collagen.

(39, 164, 206) Angiogenesis and fibroplasias begin after day three, followed by the

initiation of collagen synthesis on days three to five (39, 208).

Remodeling Phase

During the remodeling phase, macrophage numbers diminish in the wound,

therefore fibroblasts become the primary source for TGF-β, PDGF, keratinocytes growth

factor (KGF) and IGF-1. Fibroblasts are the dominant cell type, reaching peak numbers

at 7 to 14 days. Once fibroblasts have secreted collagen molecules, fibroblasts then

gather them extracellularly to form collagen fibers. These collagen fibers then become

cross-linked and assembled into a bundle form. Collagen is the most important

component of acute wound connective tissue, and production continues for the next 6

weeks. Increasing amounts of wound collagen correlates with greater tissue tensile

strength (39, 206, 207). The increased tensile strength is the most significant step in

wound-healing, followed by epithelialization and finally wound remodeling (39).

During the wound-healing process, platelet GFs regulate the time-critical and

multifaceted mechanisms involved in cell-cell and cell-matrix interactions (39, 189, 206,

209). Therefore, the local application of PRP or PGEL to enhance repair of surgically

induced wounds has the benefit of providing numerous synergistically working

autologous GFs to induce proliferation of mesenchymal and other stem cells at the wound

site (39, 210, 211). Bone formation is covered in the section titled: Osteogenesis –

Developmental Pathways for Bone Formation.

 Platelet Concentrate Storage

Occasionally it is necessary to collect whole blood and process the PRP for use at a

later time point. This may be due to the complexity and extensive nature of the pending

surgery or that the patient may have difficult veins to access and the end-user facility may

not have the adequate personal to obtain the whole blood. In these situations, it becomes

necessary to store PRP for this future use. The storage of PRP for clinical use with

surgical procedures has only recently been studied. Liu *et al*. (212) in 2008 found that

levels of GFs in PRP that had been activated with calcium and thrombin and stored for 2

to 10 days resulted in TGF-β1 and PDGF-AB concentrations that decreased rapidly when

stored at various temperatures. When stored at -20°C and -70°C the levels declined but

were significantly higher than when stored at 4°C. Therefore if PRP is to be stored it

appears that lower temperatures (<-20°C) are preferred. The optimal storage conditions

for platelets differ from that of other blood cell types. The isolation of platelets from

other blood cells allows for the storage of the PC under optimal conditions. This

dissertation examines the effect of short-term storage (6 hours or less) at room

temperature. PRP is often collected prior to commencing the surgical procedure. The

time to final use of the PRP is dependent upon the time requirements for the intended

procedure. This may vary from as little as 15 minutes to more than 4 to 6 hours.

Therefore, it is important that clinicians have a guideline as to how long PRP (processed

by the investigated technique) and its constituents are stable for at room temperature after processing.

Platelet Collection for Surgical Site Application

Two major techniques are used to concentrate autologous platelets from whole blood in the medical or dental office setting. Each method has several variations, but they can be summarized as concentrated platelet-rich plasma (cPRP) and the buffy coat (BC) methods (34, 213). This dissertation investigates the BC method of acquiring PRP because it can be achieved in a time-efficient manner and with a standard clinical table top centrifuge that creates a force of 1150 x g.

Concentrated Platelet Rich Plasma (cPRP) Collection Technique

The cPRP technique has widespread popularity in the United States (15). The cPRP collection technique involves collecting whole blood that is anti-coagulated and is separated by centrifugation. The separation is based on the physical properties of cells (specific gravity, size, and deformability) in addition to the viscosity of the plasma (34). Steps for this technique are as follows:

1. Initially 20 - 450 mL of whole blood is subject to a low g force "soft" spin that allows for separation of the blood into 3 layers. The bottom of the tube contains red blood cells (RBCs-55% by volume), the middle contains platelet rich plasma (PRP-5% by volume) and the top contains platelet poor plasma (PPP-40% by volume). This low-speed centrifugation results in a PRP layer that contains the

majority of suspended platelets, 30 to 50% of the original total white blood cells, and some red blood cells.

The PPP and PRP layers are transferred to a satellite container and centrifuged at a higher g force referred to as a "hard" spin for a longer time period. This allows for platelets to be concentrated at the bottom of the tube and to subsequently obtain, once again, 3 distinct layers (some residual RBCs will be trapped at the bottom of this 2nd tube).
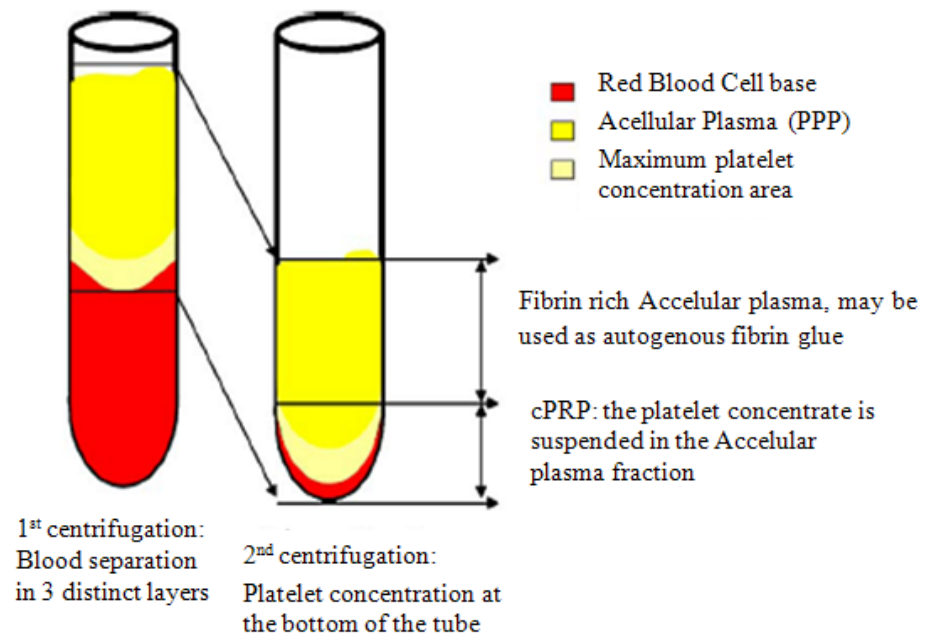
Figure 5: Schematic Showing Concentrated PRP Collection (214)**.**

2. It is recommended that the platelet pellet should be left undisturbed for 1 hour prior to the next step to minimize platelet aggregation and damage (215).

3. At this stage, it becomes easy to collect the PRP. The major portion (50 to 80%) of the supernatant serum is now removed. Enough serum is left behind to allow for suspension of the PRP and any remaining RBCs by gentle shaking. This now provides concentrated PRP (cPRP), which has a rosy aspect due to the presence of some RBCs.

4. Most techniques call for making a platelet gel (PGEL) from this suspension by the addition of calcium and bovine thrombin. This can be achieved with the use of a mixing syringe. Gelling of platelet concentrate will then occur quickly. Fibrinogen is also concentrated during the cPRP preparation, and its polymerization will constitute a fibrin matrix with hemostatic and adhesive properties.

This cPRP technique followed by gelling is a technology that is deemed new, but in reality is similar to conventional fibrin adhesives (214, 216-232). The potential for platelet cytokines and growth factors being released *en masse* during platelet activation with bovine thrombin appear to be dependent on the time of activation and the mechanical and biological properties of the final fibrin matrix (214, 233). Unfortunately, many studies indicate that the clinical effects of PGEL are very near those observed with conventional fibrin adhesives (204, 214, 216-232). Concentrated PRP gelling with bovine thrombin and calcium chloride begins during the final stages of coagulation and results in sudden fibrin polymerization. This mode of polymerization will considerably influence the mechanical and biological properties of the final fibrin matrix (214, 233). The fibrin network is a condensed tetra-molecular or bilateral junction with high thrombin concentrations that forms a rigid network not favorable to cytokine

enmeshment and cellular migration (Figure 6). Although PGEL should support cytokine

action, cytokines may be released too quickly to be incorporated into the fibrin.

Therefore, the released cytokines will be extrinsic, that is, trapped in the colloidal

suspension during the gelling process. Therefore, cytokine/fibrin synergies may be lost

because of rapid elimination (104). This could explain the modest clinical effects

observed with PGELs (214).
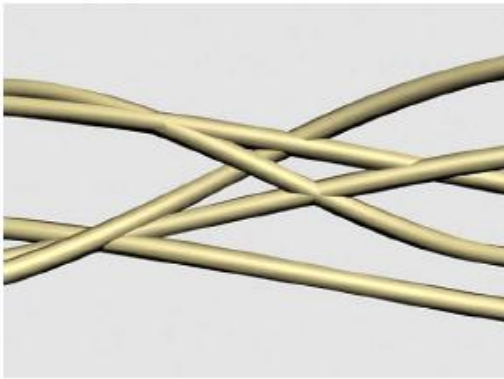
Figure 6. Rigid Fibrin Junctions

Theorectical computer model of rigid condensed tetramolecular or bilateral fibrin branch
junctions (214).

Buffy Coat Technique

The buffy coat technique is more common in Europe and is similar to the technique

studied in this project. Steps involved in the BC technique are as follows:

1. The desired quantity of whole blood is drawn and is centrifuged for 7 to 10

   minutes at 3000 x g. This creates a "buffy coat" (BC) of platelets and

   leukocytes. During high speed centrifugation WBCs initially sediment with

   RBCs while platelets remain in the plasma supernatant. Next the RBCs become

packed closely together and rapidly fall to the bottom of the collection vessel. This process forces WBCs upwards to the plasma interface. The platelets in the supernatant plasma then settle and accumulate on this interface. Interestingly, this settling of platelets on the red cell interface may explain the lesser degree of platelet activation when platelets are prepared in this manner as compared to the cPRP method (234). The BC consisting of platelets and WBCs is removed along with a small portion of the lower plasma layer and the upper red cell layer.

2. The BC is then centrifuged at low speed to separate the platelets from leukocytes and any remaining RBCs. Collection vessel systems that have a top/bottom separation partition facilitate separation by allowing the platelets in the BC to remain undisturbed in the initial separation bag (with plasma and RBCs removed from the top and bottom ports, respectively) (235).

3. The collection of platelets, now referred to as platelet rich plasma (PRP), is transferred to a delivery device for immediate use.

Platelet rich plasma acquired by other methods are referred to generically as PRP. In this dissertation, the technique under investigation is referred to as the "buffy coat" or BC method and steps 2 and 3 is not followed during platelet processing. Our technique also uses a g force of 1150 rather than 3000. Therefore, the "platelet rich plasma" of this investigated technique is actually a combination of platelet concentrates and WBCs.

The two PRP methods (cPRP and BC) used in dental/medical offices are summarized in the figures 7 and 8. PRP techniques that include the addition of exogenous bovine thrombin and excessive calcium are added at the completion of the "hard" centrifugation

seen in figure 7. One-third to one-half of the platelet poor plasma (PPP) is also added

back into the cPRP. The BC technique examined here is similar to that shown in figure

8, but does not include the "soft" centrifugation (2nd centrifugation).
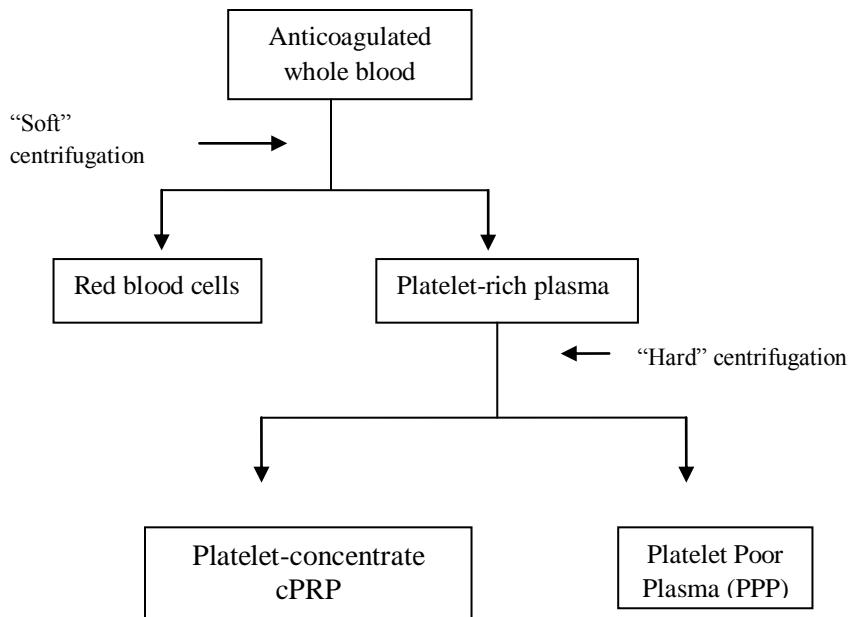
Figure 7: Preparation of cPRP

Concentrated Platelet-rich plasma (cPRP) preparation from anticoagulated whole blood
(34). To make gelled PRP at the completion of the above steps, one-third to one-half of
the platelet poor plasma (PPP) is added back into the cPRP, followed by the addition of
bovine thrombin and excess calcium.

```
                        ┌─────────────────┐
                        │  Anticoagulated │
                        │  whole blood    │
                        └─────────────────┘
                                 │
"Hard" centrifugation  ────────▶ │
            ┌────────────────────┼────────────────────┐
            ▼                    ▼                    ▼
      ┌──────────┐        ┌──────────────┐      ┌──────────────────┐
      │  Plasma  │        │ Buffy Coat   │      │ Red Blood Cells  │
      │          │        │    (BC)      │      │                  │
      └──────────┘        └──────────────┘      └──────────────────┘
                                 ┆
                                 ┆
                                 ┆ ◀── "Soft" centrifugation
                                 ┆
                                 ▼
                 ┌───────────────┴───────────────┐
                 ▼                               ▼
       ┌──────────────────────┐      ┌──────────────────────────┐
       │ Platelet concentrate │      │ White Blood Cells and     │
       │ – "Leukocyte poor or │      │ residual                  │
       │ depleted"            │      │                           │
       └──────────────────────┘      └──────────────────────────┘
```
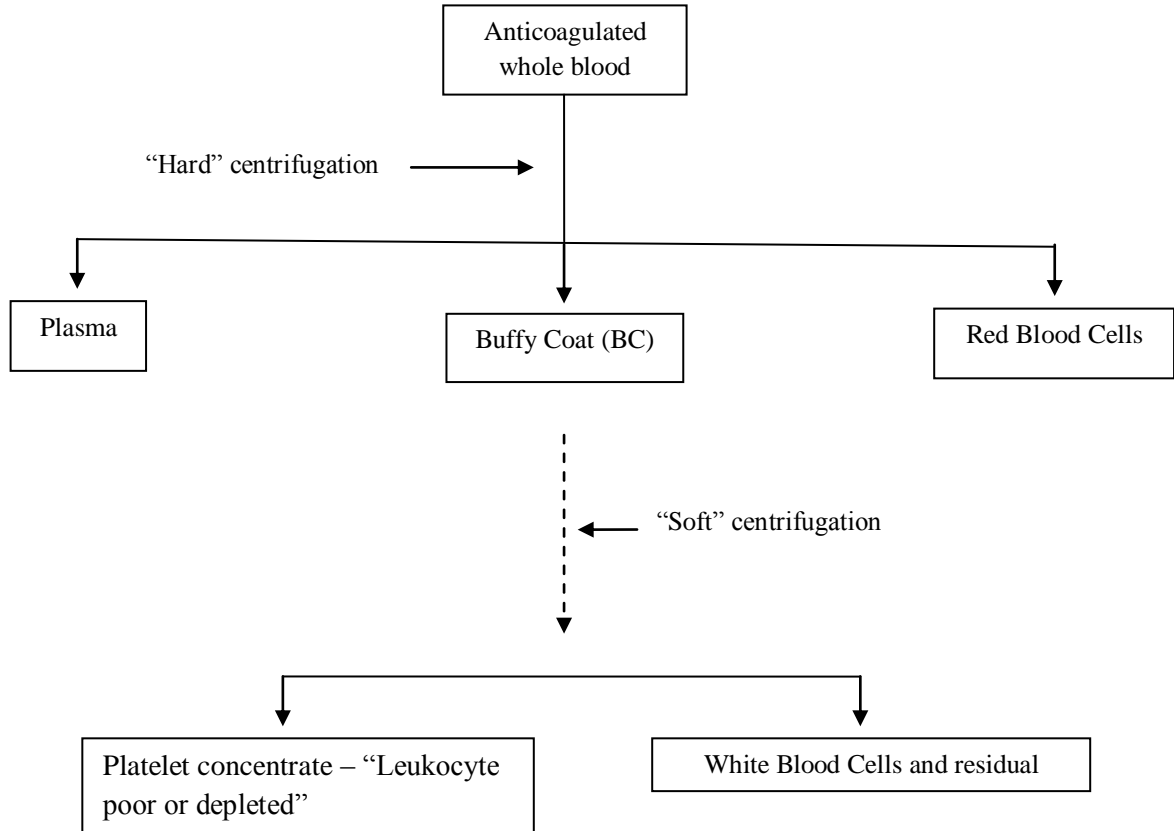
Figure 8: Preparation of Buffy Coat From Anticoagulated Whole Blood

Buffy coat (BC) preparation from anticoagulated whole blood (34). The technique investigated in this dissertation utilizes the "hard"centrifugation at 1150 x g and does not include the "soft" centrifugation (2nd centrifugation).

Concerns of Residual WBCs in Platelet Concentrates:

When platelets are obtained from one individual for transfusion into another

individual the presence of WBCs is of concern. WBCs from the donor can theoretically

induce the rare, incurable, and often-fatal degenerative neurological disorder Creutzfeld-Jacob disease. Another benefit of using leukocyte poor PRP is a decrease in the risk of common febrile non-hemolytic transfusion reactions such as cytomegalovirus (CMV) transmission, and HLA alloimmunization (34, 236, 237). These complications are only of concern if the recipient of the PRP differed from the donor. When the PRP donor and recipient is the same individual, the presence of WBCs in the PRP is of no concern.

Zimermann *et al.* (238) examined whether the presence of leukocytes had an effect on PDGF-AB, PDGF-BB, and TGF-β1 levels. The mean absolute levels of PDGF-AB and PDGF-BB showed differences between leukocyte rich and leukocyte poor preparations. Leukocyte rich PRP had significantly higher levels of PDGF-AB, PDGF-BB, and TGF- β1 than leukocyte poor PRP did (P < .05). Stepwise regression analysis revealed that platelet concentration was the most significant variable and the presence of monocytes was a significant co-variable for predicting the variance in PDGF-BB and TGF-β1 measurements (238).

Platelet Rich Fibrin (PRF): A Second –Generation Platelet Concentrate

A new family of platelet concentrates has recently been developed that is a cross between an autologous fibrin glue and classical platelet concentrates. This new biomaterial, referred to as platelet-rich fibrin (PRF), is similar to an autologous cicatricial matrix (214). Study 2 of this dissertation examined the effect of the BC method on dry socket formation following mandibular tooth extraction using a gelled BC technique that is similar to PDF. The BC had been prepared as described previously and followed by the addition ½ of the obtained PPP layer and 0.5 mL calcium chloride 10% and allowed

to set for 10 minutes. This resulted in a fibrin gelled clot similar to this PRF platelet concentrate described in this section. The gelled BC method collected the blood in a glass tube containing the anti-coagulant tri-sodium citrate and the PRF method uses a glass tube that does not contain an anti-coagulant.

Fibrin adhesives have been used for the past 30 years as adjuncts for regulating inflammation and increasing healing following surgical procedures (214, 239). Use of PRF has been limited due to the complexity of the production protocols for autologous adhesives and the risk of cross-infection from commercial adhesives.

Fibrinogen is present in platelet α-granules and is instrumental in platelet aggregation during hemostasis (214). Fibrinogen is the final substrate for all coagulation reactions and is cleaved by thrombin to yield insoluble fibrin. The result is a polymerized gel that constitutes the scar-like matrix for the injured site (214, 240-242). Just as in PGELs, combining the advantages of a fibrin adhesive with the advantages of concentrated platelets may have greater benefits to the healing process. However, since 1978 many of the commercial fibrin adhesives have been removed from the commercial market due to the risk of hepatitis. To avoid this complication Tayapongsak *et al*. (243) developed an autologous fibrin adhesive technique in 1994 (214, 243). Due to the time and expense commitment, this methodology never gained widespread acceptance for simple procedures but did find a place in cardiothoracic, vascular, and plastic surgeries (214, 243, 244). The possibility of obtaining autologous growth factors from PRP or BCs sparked interest in combining a fibrin adhesive with PRP treatment. The PRF protocol is similar to the BC technique examined in this dissertation.

PRF Protocol

Blood is drawn into 10 mL tubes without anticoagulant and then immediately centrifuged in a table top centrifuge at 3000 x rpm (approximately 400 x g) for 10 minutes. Since there is no anticoagulant present, platelet activation will begin once the blood comes in contact with the tube walls and subsequently initiate the coagulation cascade. Fibrinogen is initially concentrated in the top and middle portions of the tube, before circulating thrombin transforms it into fibrin. This leads to the development of a fibrin clot in the middle of the tube, just between the red blood cells at the bottom and the acellular plasma at the top of the tube. Platelets will theoretically be trapped in the fibrin clot (Figures 9 and 10) (214).
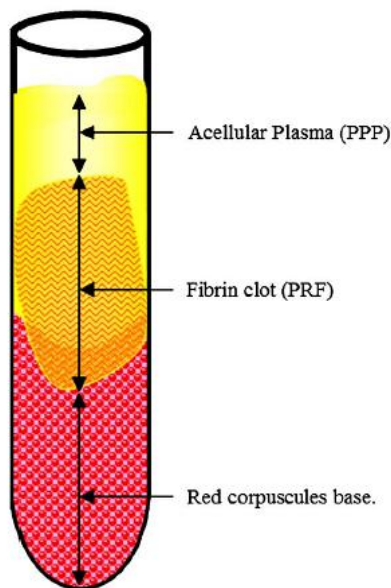
Figure 9. Centrifuged Whole Blood

Result of centrifugation of whole blood by PRF protocol. The fibrin clot is shown in the middle with the red blood cells below and the acellular plasma layer above (214).
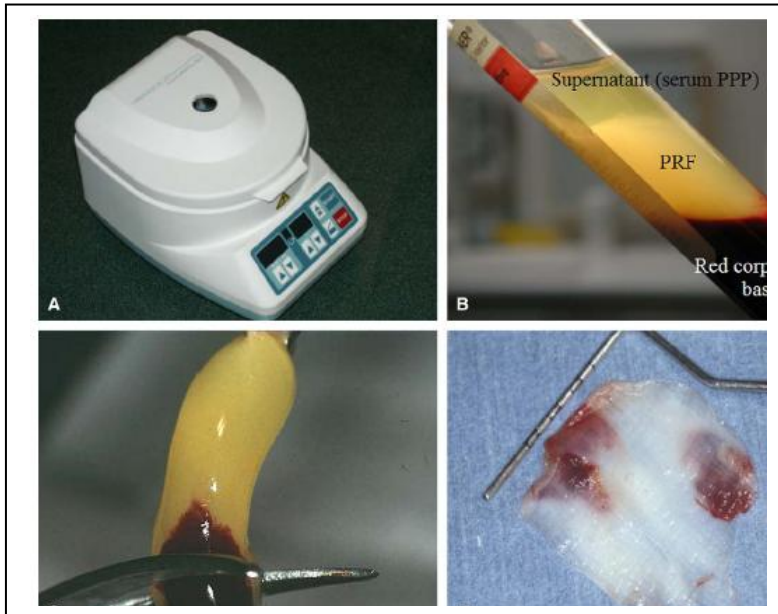
Figure 10. Protocol for Platelet Rich Fibrin Processing

A. Clinical centrifuge used for PRF protocol. B. Results of centrifugation showing fibrin clot as PRF. C. Removal of the clot from the tube. D. Resistant autologous fibrin membranes obtained by driving out the serum from the clot (214).

The success of the technique depends entirely upon promptly centrifuging the whole blood after collection. Without anticoagulant the collected whole blood begins to coagulate immediately upon coming in contact with the glass wall of the collection tube. It takes a minimum of a few minutes of centrifugation to concentrate fibrinogen in the middle and upper part of the tube. Efficient handling is essential to obtaining a clinically usable PRF clot. If the time required to collect blood and to begin centrifugation is prolonged, the fibrin will polymerize in a dispersed manner in the tube and only a small blood clot without consistency will be obtained (214).

PRF is different from PGELs in that it polymerizes naturally and slowly during centrifugation. Thrombin acts on fibrinogen to produce a fibrin mesh that has tri-molecular or equilateral fibrin junctions. These connected junctions allow the establishment of a fine and flexible fibrin network capable of supporting cytokine enmeshment and cellular migration. The trimolecular fibrin organization (Figure 11) gives greater elasticity to the fibrin matrix in comparison to PGELs tetra-molecular or bilateral fibrin architecture (Figure 6). This results in a flexible, elastic, and strong PRF membrane (214).
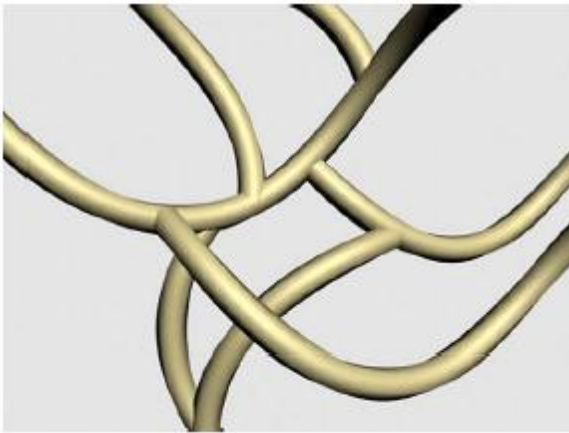
Figure 11. Flexible Fibrin Junctions

Theorectical computer model of flexible trimolecular or equilateral fibrin branch junctions (214).

It should also be noted that the PRF matrix enmeshes glycosaminoglycans (heparin and hyaluronic acid) from the blood and platelets. The fibrillary architecture of fibrin is followed, meaning that the glycanic links are incorporated within fibrin polymers.

Glycosaminoglycans have high affinity for small circulating peptides including platelet cytokines and therefore support cell migrations and the healing processes (104, 240).

This PRF technique has relevance to this dissertation, because Study 2 uses a gelled-BC methodology that is very similar to this technique. The findings of a flexible fibrin junction and the trapping of GFs in this matrix may explain why the results of Study 1 show stable or increasing levels of growth factors over bench set time after BC preparation.

Bovine Thrombin

Many clinicians believe that PRP must have the platelets activated for the growth factors to be released and made available for healing benefits to be achieved (7). The most common method to achieve this platelet activation is with the addition of bovine thrombin to the PRP. The BC PRP technique examined in this dissertation does not utilize bovine thrombin for platelet activation because it may not be necessary to exogenously activate the platelets. Activation will occur spontaneously due to the high calcium molar concentration that is available endogenously in plasma (approximately 2 mM) plus the many other activating agonists found at the site of injury such as collagen, thrombin, thromboxane A_2, ADP, serotonin, vasopressin, thrombospondin, von Willebrand factor, fibrinogen, PAF, immune complexes, and plasmin. (15).

Bovine thrombin is utilized in surgical procedures because of its biological ability to convert fibrinogen into fibrin. Thrombin is a naturally occurring enzyme that has been widely characterized for its roles in hemostasis, inflammation, and cell signaling (193). It has been purified from multiple sources and used as a clinical adjunct for topical hemostasis for more than 60 years in nearly all types of surgical procedures. Thrombin is used routinely in cardiovascular, orthopedic, neurologic, general, gynecologic, oral surgical and dental procedures. Thrombin is also used to aid in the thrombosis of vascular pseudo-aneurysms and for topical application at bleeding cannulation sites of dialysis access grafts (193, 245-247). A conservative estimate is that at least 1 million patients in the United States are treated with topical thrombin each year. Currently, the only FDA approved stand-alone hemostatic product is a derivative from bovine sources. Bovine-derived thrombin has potent biological activity that converts fibrinogen to fibrin, activates platelets, and induces vascular contraction. Thrombin can also induce a robust immune response in humans (193). There are several reports in the medical literature that document multiple clinical events following exposure to bovine thrombin in surgical settings (193, 248-261). These events included the development of antibodies against thrombin, prothrombin, factor V, and cardiolipin (193). In some cases, these antibodies cross-react with the analogous human coagulation proteins, specifically factor V, resulting in hypocoagulopathies (256, 262, 263). Bovine thrombin is extremely immunogenic in cardiac surgical patients, and greater than 90% of the patients who are exposed to bovine thrombin develop a significant immunologic response. It is of even greater concern that a significant number of these patients also develop cross-reacting antibodies to their own endogenous coagulation proteins with associated hematologic

abnormalities in more than 30% of these patients (193, 256). The process of breaching self-tolerance through molecular mimicry can lead to autoimmunity (264-268). It has been hypothesized by Lawson *et al.* (193) that the consequences of applying immunologically disparate, yet biologically active, thrombin at physiologically extreme concentrations (1000U/mL) into surgical sites may lead to direct immune recognition and other biologic cascades, resulting in deleterious complications.

Zimmermann *et al.* (238) compared the effect of the adding bovine thrombin and calcium gluconate 10% in a 1:1 mixture with PRP to untreated PRP. They found the addition of the thrombin/calcium did not have an effect on PDGF-AB or PDGF-BB levels when compared with untreated PRP samples. However, the addition of bovine thrombin and calcium gluconate did cause a significant decrease in TGF-β1 levels when compared with the untreated group (238). This finding might explain reports that PRP mixed with bovine thrombin and calcium do not improve bone healing, but do improve soft tissue healing (269). These reports may be explained by the following: PDGF-AB and PDGF-BB are significant to soft tissue healing and only contribute to bone formation when in the correct ratio with TGF-β1 levels. PDGF-AB and PDGF-BB concentrations are unaltered by the addition of bovine thrombin, therefore the soft tissue healing benefits would be present. However, the addition of bovine thrombin does decrease concentrations of TGF-β1. Therefore, one could expect that bone healing maybe diminished with the bovine thrombin formulation.

Most dental PRP procedures use a 1:10 (bovine thrombin/PRP) ratio (upwards of 1000+ units) for converting cPRP to PGEL. Because the use of bovine thrombin is

associated with a significant risk of immunologic side effects and a potential decreased

TGF-β1 levels, its use for the production of PGELs should be questioned. The BC PRP

technique examined in this dissertation does not utilize bovine thrombin and may offer an

alternative for clinicians. If this technique is able to provide the necessary growth factors

to facilitate healing, then the continual use of bovine thrombin with its potential

autoimmune responses and decreased TGF- β1levels can be avoided.

C. Cellular Aspects of Bone Formation

Genetic Markers of Osteoblast Differentiation

Osteoblasts synthesize the macromolecules responsible for forming and

mineralizing bone matrix including type I collagen, osteocalcin, osteonectin, osteopontin,

proteoglycans I and II, bone sialoprotein, matrix gla-protein, bone glycoprotein 75, and

other proteins including growth factors (270). Additionally, osteoblasts have high levels

of the membrane-bound enzyme alkaline phosphatase, which is important in matrix

mineralization, and receptors for tissue-specific hormones, such as parathyroid hormone,

cytokines and growth factors. These molecules act in concert to regulate bone growth,

cell differentiation and metabolism. Although these proteins are not exclusive to

osteoblasts, together they characterize bone phenotype (270).

The differentiation process of osteoblasts, originating from mesenchymal

precursors, involves a complex process of timely activation of specific transcription

factors that regulate the expression of certain genes. The genes *Runx2/Cbfa1* and *Osterix*

(*Osx*) are master controllers of the osteoblastic lineage, and the absence of any of these

genes results in a complete lack of a mineralized bone (271-274). The expression of these genes during osteoblast differentiation occurs in a stepwise fashion involving multiple regulatory factors. Type I collagen and alkaline phosphatase are expressed early during differentiation while osteopontin and osteocalcin appear later during differentiation (270). The gene for bone sialoprotein (IBSP) is expressed in newly formed osteoblasts (275). Osteocalcin gene expression follows the expression of IBSP (276). Osteoblasts pass through many phases in the differentiation process and the gene-expression profile varies widely depending upon the stage of differentiation. Therefore, changes in gene expression must be interpreted in a way that accounts for hMSC culture diversity with respect to the mixture of cells that may be in various stages of differentiation.

There are several osteoblastic cell culture models available to study the expression of osteoblast-related genes *in vitro*. These models include primary cultures from calvaria or trabecular, osteosarcoma-derived cell lines, and experimentally immortalized cells (270). The current investigation uses a line of commercially available human mesenchymal stem cells.

Osteocalcin Gene [BGLAP bone gamma-carboxyglutamate (gla) protein] [*Homo sapiens*]

This dissertation used the osteocalcin gene as a marker of hMSC differentiation into a mature osteoblast because it is known to be a late marker of this differentiation (276). Osteocalcin is bone γ-carboxyglutamic acid-containing protein thought to be produced exclusively by relatively mature osteoblasts (276, 277). Serum levels of

osteocalcin correlate well with histomorphometric parameters of bone formation. Osteocalcin controls hydroxyapatite crystal growth and signals osteoclast induced bone resorption. *In vitro* experiments demonstrate that osteocalcin is a chemoattractant for monocytes, which are osteoclast precursors (276-278). Osteocalcin gene expression has been used to study cell type-specific gene expression for osteoblasts (276, 279). This study uses the osteocalcin gene (*BGLAP-Homo sapiens*) as a marker of late osteoblast differentiation.

Bone Sialoprotein Gene (IBSP: integrin-binding sialoprotein (bone sialoprotein, bone sialoprotein II) [*Homo sapiens*]

This dissertation used the bone sialoprotein gene as a marker of hMSC differentiation down the osteoblast lineage because it is known to be a middle to late marker of this differentiation (280). Bone sialoprotein (IBSP) is a bone extracellular matrix glycoprotein that represents 8 to 12% of the total noncollagenous proteins associated with mineralized tissues (281-285). IBSP expression correlates with terminal osteoblastic differentiation and the onset of bone matrix mineralization. Expression of high levels of IBSP coincides with *de novo* bone formation. Bone formation results from IBSP's biophysical and chemical properties that include high binding affinity for calcium and for the ability to initiate hydroxyapatite formation (275, 281, 286-291). It is well accepted that IBSP plays a major role in bone formation and remodeling and is considered one of the primary markers of terminally differentiated osteoblasts (288). IBSP has cell attachment and cell signaling properties that are utilized in bone remodeling and may also play a role in various pathologies (288).

Bone sialoprotein mRNA is highly expressed in newly formed cuboidal osteoblastic cells that form bone matrix (287) and is readily detectable in osteoblasts of embryonic bone, indicating that IBSP is induced when osteoblasts are generated (275, 282). IBSP gene expression is up-regulated by hormones and cytokines that promote bone formation and down-regulated by factors that suppress bone formation (275).

There are few cell lines that constitutively synthesize IBSP. Rat osteosarcoma cell lines ROS17/2.8 and UMR 106-01 cells have recognized characteristics of osteoblasts and they both express IBSP. The high levels of IBSP mRNA and the absence of osteocalcin expression suggest that UMR 106-01 cells model newly formed osteoblasts, whereas the lower expression of IBSP and high osteocalcin in ROS cells model a more mature osteoblast phenotype (288, 292). The investigator examined both osteocalcin and IBSP gene expression in this study.

Glycoprotein IIb [ITGA2B integrin, alpha 2b (platelet glycoprotein IIb of IIb/IIIa complex, antigen CD41) [*Homo sapiens*]

The glycoprotein IIb gene (ITGA2B) was chosen as a marker of platelet presence and expression would hopefully diminish with time. The PRP treatments done in this dissertation were for a 24-hour period only and therefore should be removed with aspiration of the PRP medium after 24 hours and what did remain would be removed with successive growth medium changes. The ITGA2B gene encodes for the protein integrin α-chain 2b portion of the glycoprotein IIb/IIIa. This integrin α-chain 2b is part of a heterodimeric integral membrane protein receptor composed of an alpha chain and a beta chain. The α-chain 2b undergoes post-translational cleavage to yield disulfide-

linked light and heavy chains that join with beta 3 to form the fibronectin receptor expressed in platelets that plays a crucial role in coagulation. In addition to adhesion, the glycoprotein IIb/IIIa receptor is known to participate in cell-surface mediated signaling (293). The glycoprotein receptor and its expression are discussed in detail in the platelet membrane glycoprotein section of this paper.

In the mouse and murine embryo, Cd41 is the initial and most explicit surface marker that distinguishes cells that are committed to the hematopoietic lineage from endothelial and other mesodermal cell types (294-299). However, Cd41 is expressed only in nascent hematopoietic mouse stem cells (HMCs), whereas mature HMCs lose Cd41 expression, with the exception of megakaryocytes and platelets which maintain it (294, 300-302). In humans, ITGA2b gene expression is thought to be limited to megakaryocytes and platelets (293).

GAPDH (glyceraldehyde-3-phosphate dehydrogenase; G3PD; GAPD)

Glyceraldehyde-3-phosphate dehydrogenase was chosen as the "housekeeping" gene for this study because it is not regulated by PRP treatment. Glyceraldeye-3-phosphate dehydrogenase catalyzes an essential energy-yielding step in carbohydrate metabolism, the reversible oxidative phosphorylation of glyceraldehyde-3-phosphate in the presence of inorganic phosphate and nicotinamide adenine dinucleotide (NAD$^+$). GAPDH is a tetramer of four identical chains. GAPDH is expressed in hMSCs, differentiating osteoblasts, mature osteoblasts, leukocytes, and platelets (303-306).

Osteogenesis – Developmental Pathways for Bone Formation

Osteogenesis is the process of bone formation. Bone is an organ that is comprised of mineralized calcium phosphate matrix and a variety of cell types that provide structural support for the body and play a role in bone metabolism. Bone develops as osteoblasts - cells that produce and secrete mineralized matrix - mature and then differentiate into osteocytes or bone lining cells or undergo apoptosis. Maturation of osteoblasts is coupled with the breakdown of damaged bone by osteoclasts. Bone is therefore a continually remodeled structure. The site of remodeling is the mineralized matrix, which is also the location of the osteoclasts and osteoblasts.

Osteoclasts are large, multi-nucleated cells that are of hematopoietic origin, differentiating from the monocyte-macrophage lineage (307). These cells are responsible for bone resorption at sites within the osteiod of microdamage. The maturation and differentiation of osteoclasts is directly linked with that of osteoblasts, as a balance between bone resorption and matrix production must exist.

Osteoblasts develop from mesenchymal stem cells (MSCs) and are responsible for secreting the calcium phosphate matrix, or osteiod found in bone (308). There are four stages in the osteoblast life span (309, 310). The first stage is the preosteoblast, which is located within bone one or two cell layers apart from mature bone forming osteoblasts. For preosteoblasts to become active, they must locate to the bone surface. This is achieved by osteoclast-induced bone breakdown. Once in position, the preosteoblast begins to produce and secrete bone matrix proteins and is identified as an osteoblast. After an osteoblast has ceased synthesis and mineralization of new bone, it is fated to one of three states: osteocyte, bone-lining cell, or apoptosis. A small fraction of the osteoblasts are ultimately embedded in the mineralized matrix of the bone and termed

osteocytes. Osteocytes represent the final differentiation stage of the osteoblast lineage (309, 311). Osteocytes regulate bone turnover by detecting microdamage of the bone (309). Inactive bone surfaces are covered with post-proliferative osteoblastic cells known as bone-lining cells. It is thought that bone-lining cells are not involved in matrix formation, but play a role in initiating remodeling and other functions (312). Interestingly, the total population of osteocytes and bone-lining cells does not equal the total population of once active osteoblasts, thus suggesting that the third fate, apoptosis, may be of importance (309, 313-316).

Other cell types that develop from mesenchymal stem cells include chondrocytes and adipocytes (317). The osteogenic protein BMP-2 and the cytokine TGFβ1 are examples of regulatory molecules that help mediate the commitment of the progenitor cells to the osteoblast lineage (317). Osteoblasts are under the control of many factors including paracrine, autocrine, and endocrine compounds that influence cell replication, recruitment, and differentiation. These factors include bone morphogenetic proteins (318), cell growth factors and cytokines (IGF-I, TGF-β, others) (319), hormones (GH, insulin, glucocorticoids, 1,25 $(OH)_2$-vitamin D_3) (320), and biomechanical forces (321).

Genetic Aspects of Bone Development

Bone formation is directed by multiple genes (322). The transcriptional cascade that regulates osteoblastogenesis is initiated by developmental signals that recruit MSCs to organize embryonic bone via osteoblast differentiation (intramembranous bone), or MSC condensation into a cartilage template for endochondral bone formation (323). Primary intramembranous bone is formed from mesenchymal cells that develop directly into

osteoblasts and is responsible for the formation of the cranial vault, facial bones, and, in part, the clavicle and mandible (324, 325). Endochondral bone formation is responsible for the formation of the axial and appendicular skeleton (325, 326). Endochondral bone development is a complex process that involves a highly specific temporo-spatial pattern in which undifferentiated MSCs differentiate into chondrocytes, and then undergo well-ordered and controlled phases of proliferation, hypertrophic differentiation, death, blood vessel invasion, and finally replacement of cartilage with bone. Fibroblast growth factors (FGF) and parathyroid hormone/parathyroid related protein (PTH/PTHrP) are regulators of proliferation for expansion of progenitor cell populations and growth plate maturation during bone development (323, 324, 326). Secreted factors that have a significant impact on bone development include the BMP/TGFβ type factors.

Several members of the TGF-β superfamily, the bone morphogenetic proteins (BMP 2, 4, and 7) have potent osteogenic effects. It should be noted that PRP contains TGF-β1 and BMP2 (327). Graziani *et al.* (328) found that various concentrations of leucodepleted PRP activated with calcium gluconate and autologous thrombin had an effect on hMSC proliferation and osteoblast expression of, osteocalcin, and osteoprotegerin. In 2005, Kanno found that bovine thrombin activated PRP enhanced both osteoblast cell proliferation and differentiation (329). This dissertation differs from these two works because the BC PRP used in this technique was not activated with thrombin.

The mechanism for BMP signaling is through heteromeric formation of BMP transmembrane receptors that phosphorylate specific receptor Smad proteins resulting in translocation to the nucleus with DNA binding Smad4 (figure 12) (323, 330-332). While

BMP-Smad signaling is a major pathway for induction of osteoblast differentiation, it

should be noted that BMPs induce other kinase-dependent signaling pathways (e.g., p38,

MAPK, PKC, and JNK) that also contribute to Smad phosphorylation and mediate the

effects of BMP on bone formation (323, 333-340).
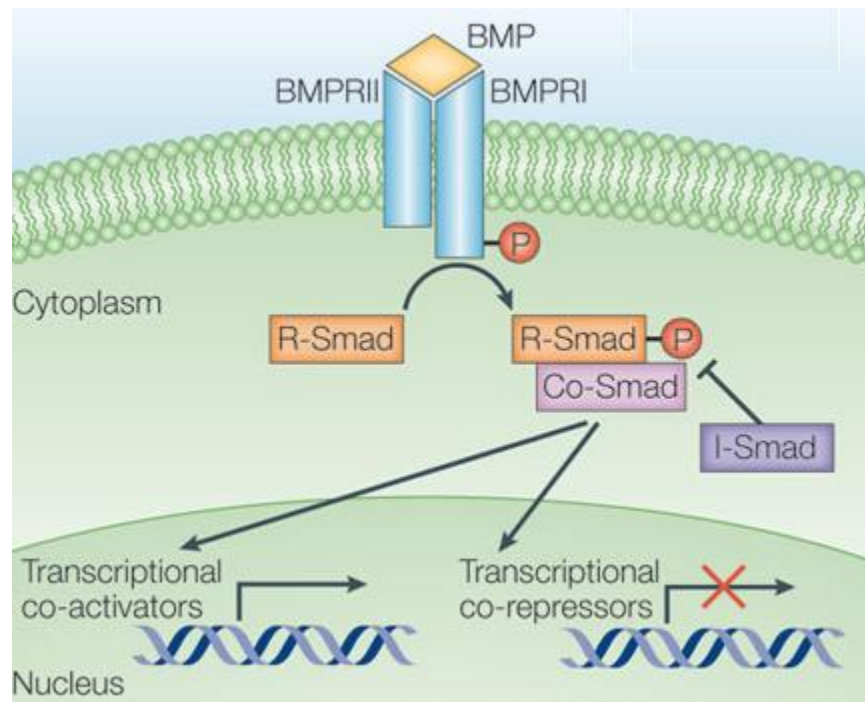
Figure 12. Bone Morphogenetic Protein Signaling Cascade

Bone morphogenetic protein (BMP) ligands bind to the BMP receptors BMPRI and
BMPRII. Once binding has occurred, BMPRI becomes phosphorylated and activated.
Phosphorylated BMPRI in-turn phosphorylates receptor-activated Smad proteins (R-
Smads), which combine with common mediator-Smad (co-Smad) and enter the nucleus.
Once in the nucleus they regulate gene expression by either transcriptional co-activators
or co-repressors (332).

Human Mesenchymal Stem Cells (hMSCs)

Human mesenchymal stem cells (hMSCs), also referred to as marrow stromal cells, mesenchymal progenitor cells, or colony forming-unit fibroblasts, are multipotent cells with a long columnar or fibroblastic appearance that are present in bone marrow. They can replicate as undifferentiated cells and then differentiate to lineages of mesenchymal tissues that include bone, nerve, cartilage, fat, tendon, muscle, and marrow stroma (341-344). Human MSCs' non-hematopoeitic adult stem cells have the capacity for renewal after trauma, disease, or aging and can be expanded *ex vivo* (341-344). Expanded culture populations of hMSCs are comprised primarily of a single phenotypic population (95% and 98% homogenous at passages 1 and 2 respectively) that can be differentiated with high fidelity into the various tissue cell types (341, 342). These cells can also be obtained via culture from other tissues, such as the periosteum, fat and skin (345).
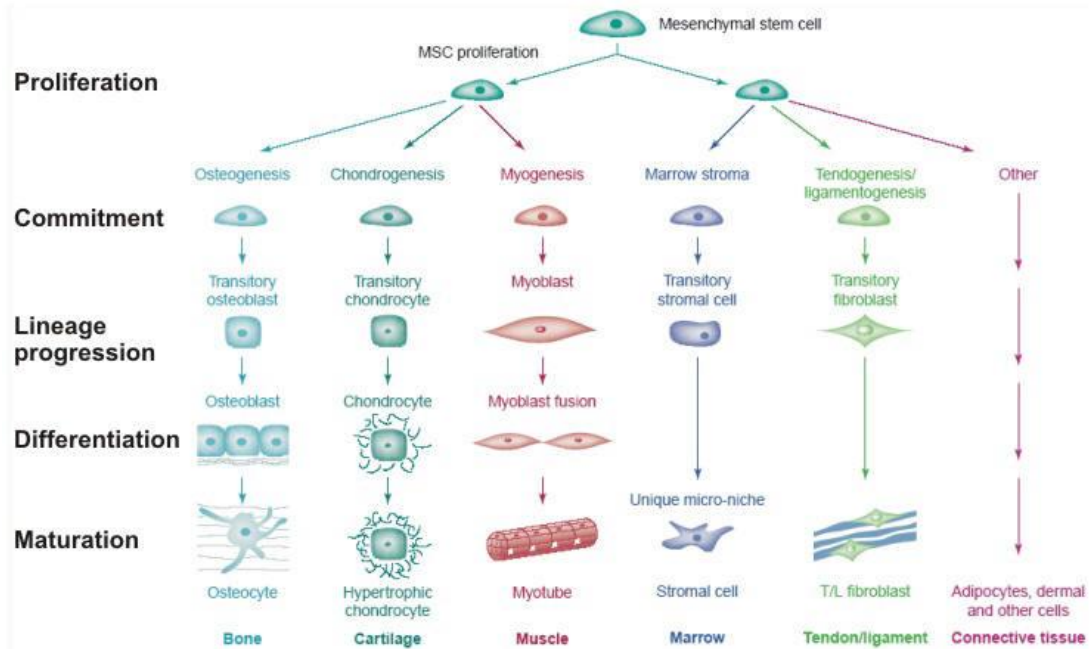
Figure 13. A hypothesized lineage progression for MSCs from Caplan *et al*. (346)

Typically, various supplements are added to stimulate the differentiation of MSCs into the various cell types. For osteogenic differentiation, the supplements ascorbate-2 phosphate, dexamethasone, and β-glycerophosphate are added to the cell culture medium (343). Following treatment, within 21 days the cultured cells form alkaline phosphatase (ALP)-positive granules. Osteoblast specific genes such as Runx2, bone morphogenic protein-2 (BMP-2), BMP-6, osteocalcin (BGLAP), bone sialoprotein (IBSP) and osteoprotegerin are expressed as the osteoblasts mature (309).

Pittenger (341) has extensively analyzed the expression of cell-surface receptors on hMSCs by reverse transcriptase-polymerase chain reaction (RT-PCR) analysis of mRNA and confirmed the results by fluorescent antibodies and flow cytometry (342). Table 4 provides examples of some hMSC surface markers.

hMSC Surface Markers	
Receptor Type	Receptors
Cytokine	IL-1R, IL-3R, IL-4R, IL-6R, IL-7R
Extracellular Matrix	ICAM-1, ICAM-2, VCAM-1, ALCAM, Endoglin, Hyaluonate , Integrins α1, α2, α3, αA, αV, β1, β2, β3, β4
Growth Factor	BFGFR, PDGFR
Others	Thy-1, IFNγR, TGFβR, TNFR

Table 4. Human Mesenchymal Stem Cell Surface Markers (342).

Dissertation Outline

This dissertation includes both *in vitro* and clinical studies. It is divided into 4 studies.

Study 1 is an in vitro study that validates the use of a simple clinical table top centrifuge that creates 1150 x g. Platelet and white blood cell concentrations with optimal centrifugation times are tested. Platelet morphology changes with centrifugation and bench set time are examined. The presence of key growth factors PDGF-BB, VEGF, EGF, and TGF-β1 are confirmed and the effect bench set time has on their presence is studied.

Study 2 examines the effect of a gelled BC has on the incidence of dry socket formation with mandibular molar tooth extractions. Individual patient factors for AO formation are considered and the effect PRP application has on each of them. Combination of factors is considered and the effect PRP had on these combinations.

Study 3 is an *in vitro* analysis of the effect BC PRP application has on hMSC proliferation and differentiation.

Study 4 is a blinded prospective clinical trial that examines the effect of BC PRP on bone density changes following the removal of bilateral mandibular 3rd molars.

Study I: Preparation and Characterization of PRP

A. Introduction

Review of the medical and dental literature supports the use of autologous PRP in clinical practice (347, 348). There are a number of procedures by which platelets can be concentrated to produce PRP in a clinical office setting by dental personnel for immediate post-operative use (7, 197). However, techniques that ensure the production of large quantities of autologous PRP can be time- and labor-intensive, and expensive. In contrast, techniques that produce small quantities of PRP can be time- and cost-efficient and easily accomplished by dental auxiliaries.

A variety of systems are available for use by dental practitioners that involve basic protocols for blood collection, platelet concentration via centrifugation, and delivery to the surgical site via a syringe. One such generic system utilizes a single speed (1150 x g) clinical centrifuge known as the Clinaseal Centrifuge™ (Salvin Dental Specialties, Charlotte, NC). Use of this type of clinical centrifuge is a simple and cost-effective method of concentrating platelets and the desired growth factors contained within them. While Eby reported an average platelet yield increase of 356% versus whole blood using this method (349), there is only limited analysis on the use of this centrifuge for concentrating intact platelets that also includes confirmation of the presence of GFs. If this research can provide scientific evidence that supports this technique as a method for enhancing soft and hard tissue healing and provide mechanistic reasoning for its success, then patients and clinicians will benefit.

In this section of the dissertation, results of our investigation into the use of the clinical centrifuge to obtain PRP are reported. Platelet and WBC enrichment as a function of centrifugation time are evaluated. Western blot analysis reveals that three key GFs are present after centrifugation for 10 minutes at 1150 x g. The effect of bench-setting time on PRP platelet enrichment, platelet microscopic morphology, and GF content (PDGF-BB, EGF, VEGF, NGF, and TGFβ1) using enzyme-linked immunosorbent assays (ELISAs) are also reported. Collection of this data and its analysis will answer the question if this technique can effectively concentrate platelets, WBCs, GFs, and does bench set time affect the concentration of GFs.

B. Materials and Methods

Collection of PRP

For platelet and WBC concentration studies seven different subjects (4 male, 3 female) were used and values were done in triplicate. For the GF studies there was an N of 3 with each sample run in triplicate. Whole blood was drawn using a 21 gauge 1.5 inch latex-free needle (EXELINT Int. Co., Los Angeles, CA), and 4.5 mL BD Vacutainer™ tubes containing 0.45 mL of the anticoagulant trisodium citrate (9:1) (Becton Dickinson & Co., Franklin Lakes, NJ) to prevent clotting of the blood in the Vacutainer™ tube. For each experiment, one Vacutainer™ tube was used to acquire baseline whole blood platelet and WBC values as a reference. Dependent upon the experiment, the required number of additional Vacutainer™ tubes were centrifuged for various times at 1150 x g to assess the optimal spin time for the recovery of platelets in PRP. After centrifugation, the tubes were removed and placed in a test tube rack on the bench for various time intervals to

ascertain whether bench set time affected the recovery of platelets in PRP. The red blood cell/plasma interface was allowed to set for 3 minutes. Pre-made labels were placed on the outside of the tube to reproducibly delineate the PRP layer to be harvested. Labels possessed a center dotted line positioned at the blood cell/plasma interface, a solid line 3 mm above the dotted line, and a second solid line 2 mm below the dotted line (Figure 14). Figure 13 displays the label used during the course of this study on a Vacutainer™ tube filled with water (for illustration purposes only).

Figure 14: Placement of Custom Label for Consistent Retrieval of PRP (Buffy Coat, BC).

The dotted line is placed at the interface of the RBCs and the PPP – between these two layers is the PRP layer. The PPP is removed down to the top solid line. The PRP layer is between the top solid line and the bottom solid line.
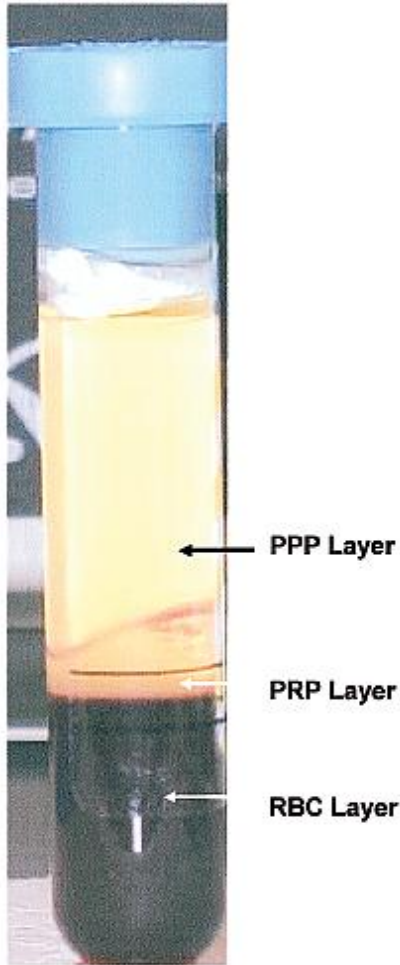
Figure 15. Anticoagulated Whole Blood After Centrifugation

Close-up of pelleted anticoagulated whole blood separated into the 3 layers. Note the placement of the label on the outside of the tube is dictated by matching the dotted line to the plasma/cell pellet interface.

The upper plasma layer (platelet poor plasma, PPP) was aspirated to the 3 mm mark (top solid line) using a sterile aluminum blunt end 20 gauge 1.5 inch needle (Monoject # 8881202363, TYCO Healthcare Group LP, Mansfield, MA) attached to a 3 mL B-D latex-free syringe (Becton Dickinson & Co., Franklin Lakes, NJ). The PRP was collected from between the upper 3 mm mark and the lower 2 mm mark using a beveled 20 gauge

1 inch B-D Precision Glide™ needle (Becton Dickinson & Co., Franklin Lakes, NJ) attached to a 3 mL B-D latex-free syringe.

Platelet Concentration Determination

Platelets were counted using a Cell Dyn 1600™ cell counter (Abbott Laboratories, Abbott Park, IL). Due to the viscosity of PRP it was necessary to dilute the PRP 1:10 with Streck Diluent™ (Streck Laboratories, Omaha, NE) prior to introducing the sample into the cell counter. The diluted sample was gently mixed by inversion to obtain a uniform suspension before aspiration and analysis using the cell counter.

Platelet Morphology in PRP

Smears of PRP were stained with Wright-Giemsa stain, and then examined by oil immersion brightfield microscopy at 1000X magnification using a Nikon Eclipse 600 microscope. Several fields were examined for each sample, and representative photomicrographs were obtained using the SPOT RT-Slider camera and SPOT Advanced Digital Image Analysis software (Fryer Co. Inc., Huntley IL).

Partial Purification of Platelets from PRP

In order to remove red blood cells from PRP, the Histopaque 1077 cell separation medium was used. Briefly, PRP was diluted ten-fold with Hank's Balanced Salt Solution (HBSS); Mediatech, Inc. Herndon, VA) and overlaid onto 5 mL Histopaque 1077 density gradient medium (Sigma-Aldrich St. Louis, MO). The overlaid PRP was then

centrifuged at 1150 x g for 20 minutes. The band containing platelets, lymphocytes and monocytes was aspirated using a sterile polypropylene pipet, then, diluted with HBSS, and centrifuged for 20 minutes at 1150 x g. Platelet-rich pellets were then resuspended and washed two times in HBSS for 5 minutes at 1150 x g and platelet counts performed as before. To lyse platelets, the washed pellets were suspended in 0.5% Triton X100, and gently rocked on an Ocelot shaking platform (Fisher Scientific, Pittsburgh PA) for 40-60 minutes. Lysis was verified by microscopic examination and by subjecting the lysate to centrifugation as before, with no visible pellet observed. The lysate was then used for analysis by immunoblotting to indicate the presence of specific growth factors (GFs), or by ELISA to quantify specific GFs.

Western Blotting

Pre-cast 5-20% polyacrylamide gradient gels (Jule Biotechnologies, Inc. Milford, CT) were loaded with either Kaleidoscope molecular weight standards (Bio-Rad, Chicago, IL), positive control purified human recombinant growth factors (US Biologicals, Swampscott, MA), or partially purified PRP platelet samples. The samples were subjected to electrophoresis for approximately 75 minutes at 150 v, 35 mA, and 8 watts. Transfer of proteins to nitrocellulose paper was performed at 100 v at 3°C for 1 hour. Blots were then placed in Tris-buffered saline (20mM Tris, 150 mM NaCl, TBS) with 0.5% v/v Tween 20 (TBST) and 3% BSA to block nonspecific binding for 8 hours or overnight. The blots were then removed and washed three times with TBST and placed in a sealed storage bag with the appropriate primary antibody (US Biologicals Swampscott, MA) at the manufacturer's specified concentration for Western blotting (20 ng/mL TGF-β1, 0.2 μg/mL PDGF, 0.2 μg/mL NGF) in TBST for 4 hours at 3°C. The

blots were removed and washed three times with TBST, then placed in anti-rabbit IgG alkaline phosphatase conjugate (US Biologicals, Swampscott, MA) as the secondary antibody for one hour. The blots were then removed, washed three times with distilled water, and placed in a solution of 5-bromo-4-chloro-3-indolyl phosphate nitro blue tetrazolium (Sigma Fast Tablets, Sigma Aldrich, St. Louis MO). Color development was allowed to proceed until positive control growth factor bands were readily apparent, then stopped by immersing the blot in distilled water. The blots were then photographed using a Sony Digital Mavica™ camera (Sony Corporation, NY, NY).

ELISAs

Enzyme-linked immunosorbent assays (ELISAs) were employed to determine the quantity of various growth factors. Lysed platelet samples were prepared for ELISA with Quantikine kits (R&D Systems Minneapolis, MN). The manufacturer's protocol was followed with the following modifications. To fully release TGFβ, it was necessary to use a 3-fold higher volume (600μL) of 1 N HCl with incubation of lysates at room temperature for the specified time. This change required that the lysate was subsequently neutralized using 600μL 1.2 N sodium hydroxide. It was also necessary to dilute samples 10-fold before adding to the anti-TFGβ1-coated wells because the residual 0.5% Triton X-100 used for lysis interfered with the ability of TGF-β1 to bind to the wells. PDGF-BB samples were diluted 5-fold to ensure that the absorbance was in the range of the standard curve. After color development, quantification was performed using a BIO-TEK Kinetic Microplate Reader Model EL312E (Winooski, VT).

Statistical Analysis

Statistical analysis was performed using one-way ANOVA with post-hoc Newman-Keuls analysis for the platelet and white blood cell concentrations, effect of bench set time on platelet concentration, and effect of bench set time on growth factor content per 10^5 platelets data. Analysis was performed using GraphPad Prism® 3.0 (La Jolla, CA) computer software.

C. Results

The first objective was to determine the optimum time of centrifugation in a table-top clinical centrifuge to obtain the most consistent and greatest enrichment of the PRP. The enrichment of platelets in PRP over whole blood using this centrifuge is displayed in Figure 16. A greater than 6-fold enrichment of platelet concentration was obtained consistently using a 6, 8, or 10-minute centrifugation time. Newman-Keuls analysis showed that compared to whole blood baseline platelet counts, a 2- and 20-minute centrifugation time did provided a significant increase ($p < .05$) in platelet concentration, but there was greater significance ($p < .001$) for 6, 8 and 10 minutes. There was no significant ($p > .05$) difference in platelet concentrations between 2- and 20-minute centrifugation times. Newman-Keuls analysis also found no significant difference ($p > .05$) in platelet concentrations between the 6, 8, and 10 minute centrifugation times. Centrifugation times greater than 20 minutes were not considered because these longer times would not be time efficient in the clinical setting and there was concern that too long a centrifugation time (> 20 minutes) might cause complicating factors such as damage to the platelets. The value of these findings is that centrifugation times between 6, 8, and 10 minutes do provide significant ($p < .001$) concentration increases in

comparison to whole blood, yet there is no significant difference ($p > .05$) in platelet

concentrations between 6-, 8-, and 10-minute centrifugation times. These data suggest

equivalent platelets would be harvested between 6- and 10-minute centrifugation times.
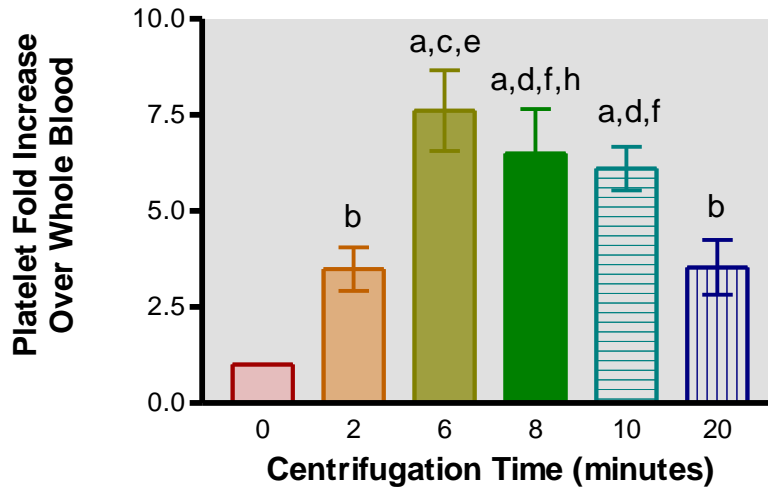
Figure 16. Platelet Concentration Fold Increase

Over Whole Blood By Centrifugation Time

   The effect of various centrifugation times on platelet concentration in comparison to
whole blood that had not been centrifuged (0 minutes). Each bar represents the ± S.E.M.
of 7 different specimens performed in triplicate. All data were analyzed with a one way
ANOVA followed by a Newman-Keuls post-hoc test where significance was defined as p
$< .05$, where a = $p < .001$when 6, 8, and 10 centrifugation times compared with 0
centrifugation time (whole blood); b = $p < .05$ when 2 and 20 centrifugation times
compared with 0 centrifugation time; c = $p < .01$ when 6 minute centrifugation time
compared with 2 minutes; d = $p < .05$ when 8 and 10 minute centrifugation times
compared with 2 minutes; e = $p < .001$when 6 minutes is compared with 20 minutes; f =
$p < .05$ when 8 and 10 minutes are compared with 20 minutes. The importance of these
findings is that centrifugation times between 6, 8, and 10 minutes do provide significant
($p < .001$) concentration increases in comparison to whole blood, yet there is not a
significant difference ($p > .05$) between 6, 8, and 10 minutes.

In the second study, WBC counts for various centrifugation times were determined. As seen in Figure 17, there was a slight increase in WBC counts even with a 2 minute centrifugation but the concentration continued to rise, peaking at 10 minutes before declining. One-way ANOVA with a Newman-Keuls post-hoc statistical analysis verifies that there is a significant difference ($p < .001$) in WBC concentrations when 2 through 20 minute centrifugation times are compared with whole blood that has not been centrifuged (0 time). Newman Keuls post-hoc analysis did not reveal a significant difference ($p > .05$) between any of the centrifugation times (2- through 20-minutes).

When considering that platelets contain the wanted GFs and WBCs contain macrophages plus factors such as thrombin that are involved in clotting, the 10-minute centrifugation time was chosen as the optimal time and used for the duration of the study.
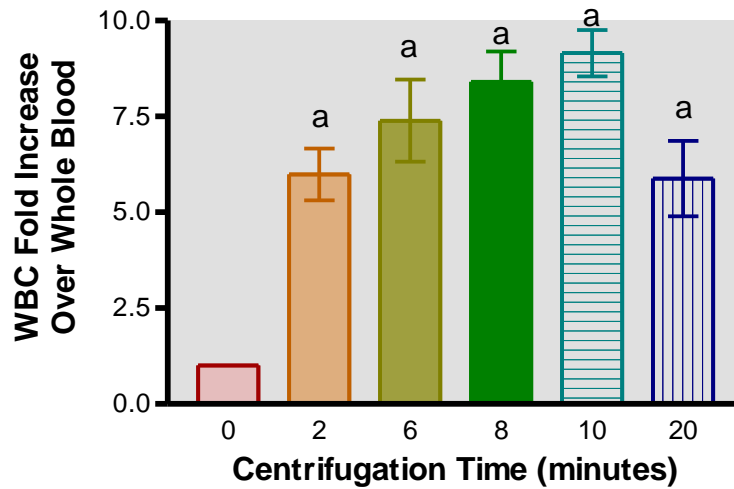
Figure 17. White Blood Cell Fold Increase Over

Whole Blood by Centrifugation Time

The effect of various centrifugation times on white blood cell (WBC) concentration in comparison to whole blood that had not been centrifuged (0 minutes). Each bar represents the ± S.E.M. of 7 different specimens performed in triplicate. All data were analyzed with a one way ANOVA followed by a Newman-Keuls post-hoc test where significance was defined as $p < .05$, where a $= p < .001$ when $2 - 20$ centrifugation times are compared with 0 centrifugation time (whole blood). There was no significant difference in WBC concentration when 2-20 minute centrifugation times are compared with each other. The importance of these findings is that centrifugation times between 2 and 20 minutes do provide significant ($p < .001$) concentration increases in comparison to whole blood, yet there is not a significant ($p > .05$) change in WBC concentrations with centrifugation times from 2-20 minutes.

The final objective of this investigation was to determine whether bench set time (time between centrifugation of the whole blood and application in the patient) at room temperature affected the recovery and enrichment of platelets in PRP. Figure 18 shows that after a 10-minute centrifugation, the enrichment did not vary as a function of bench set time for up to 6 hours. One-way ANOVA with a Newman-Keuls post-hoc test

showed that the fold enrichment of platelets vs. baseline platelet count of whole blood

was statistically significant ($p < .001$) for all times examined. When comparing all bench

set times (0 through 360 minutes) with each other there was not a significant difference

($p > .05$) in platelet enrichment as bench set time progressed. This confirmed that PRP

still contained platelets even if the blood was collected up to 6 hours prior to application.
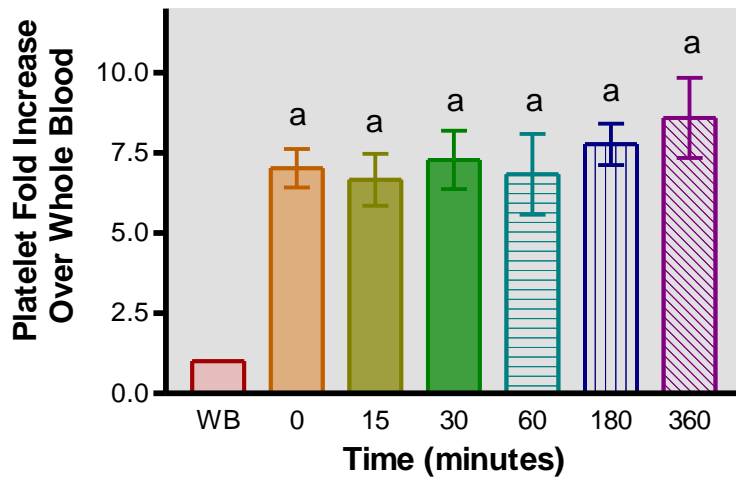
Figure 18. Platelet Fold Increase of Centrifuged Blood

Over Whole Blood with Bench Set Time

The effect of various bench set times at room temperature on platelet concentration when
compared to whole blood that had not been centrifuged or experienced bench set time.
Bench set time began after the whole blood was centrifuged and before removal of the
PRP layer. At completion of the prescribed bench set time the PRP layer was removed
and analyzed.   Each bar represents the $\pm$ S.E.M. of 7 different specimens performed in
triplicate. All data were analyzed with a one way ANOVA followed by a Newman-Keuls
post-hoc test where significance was defined as $p < .05$, where a $= p < .001$ when $0 - 360$
minute bench set times are compared with whole blood that did not experience bench set
time. There was no significant difference between the 0 to 360 minute bench set times.
The importance of these findings is that bench set times of centrifuged whole blood
between 0 and 360 minutes did maintain significant ($p < .001$) platelet concentration
increases in comparison to whole blood, yet there is not a significant ($p > .05$) change in
platelet concentrations with bench set time up to 360 minutes.

While the number and concentration of platelets did not appear to change as a function of bench set time, platelets in the PRP may change in other ways and, thereby, become less active in promoting healing. The fourth objective was to determine whether the morphology of platelets changed as a function of bench set time. Figure 18A shows the components of a typical stained whole blood smear. Figure 18B-F shows the changes that occurred in platelet morphology from 0-6 hours bench set time. From 0-2 hours, platelets appeared to be normal, much as they appear in whole blood: discoid and lightly stained with the blue Giemsa dye. The platelets displayed little to no aggregation. However, after 2 hours of bench set time, platelets began to appear smaller, and more densely stained, forming small clusters. These effects were more dramatically evident by 6 hours, indicating a change in their morphology as a function of bench set time.
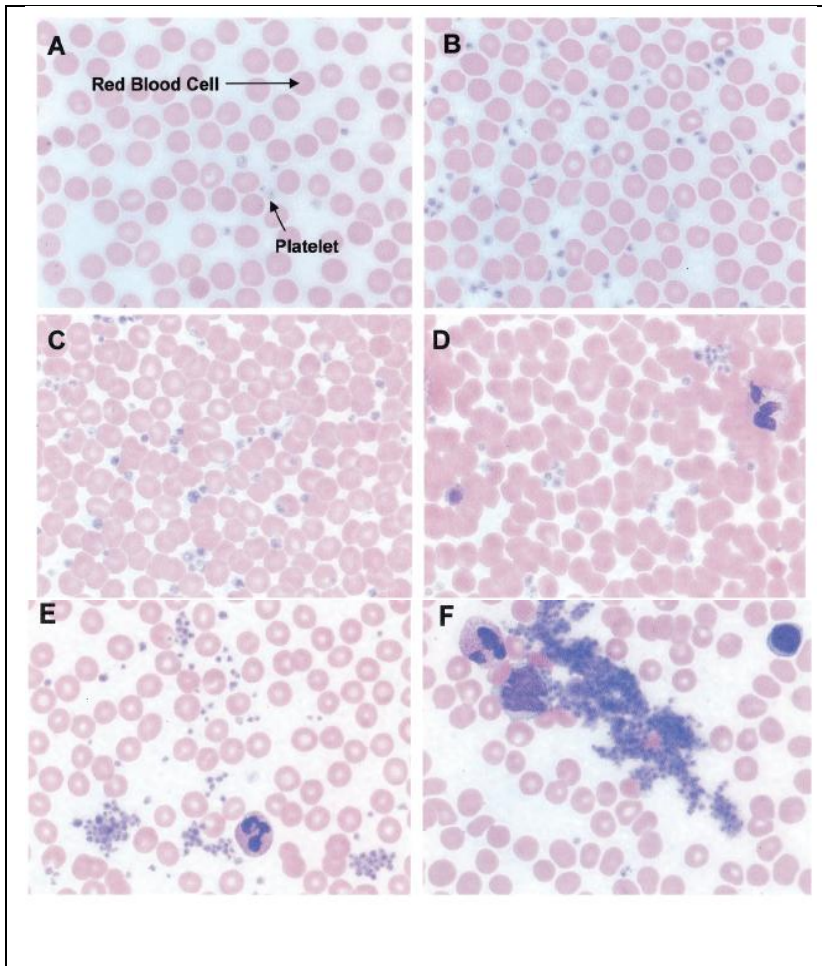
Figure 19. PRP Platelet Morphology with Bench Time.

The morphology of platelets in platelet-rich plasma (PRP) changed as a function of bench set time. Centrifuged blood was allowed to set on the bench for up to 6 hours, and then PRP was harvested at various times. Samples were smeared, stained with Wright-Giemsa, and viewed/photographed using brightfield microscopy. All fields are x1000 magnification. (A) Whole blood; note that very few platelets were present relative to the number of red blood cells (RBCs). (B) A 0-time bench set time; note that the platelets are higher in number relative to the RBCs, indicating that platelets have been enriched using the procedures described previously. Also note that the platelets possess a normal morphology (discoid, light blue staining, with little to no adherence to one another (aggregation). (C) A 30-minute bench set time: concentrated platelets continue to appear intact and healthy. (D) A 1-hour bench set time; platelets begin to aggregate but they are still ovoid and lightly stained. (E) A 2-hour bench set time; platelets form larger aggregates and have begun to lose ovoid shape developing bleb-like structures on the plasma membranes. (F) A 6-hour bench set time; note the aggregation that occurred with prolonged bench set time and more than 100 platelets per aggregate. Platelets appear shrunken and distorted, suggesting aggregation, possible activation and a loss of functional capacity.

PRP's effectiveness in wound healing and other responses is thought to be due to the presence of GFs present in the platelets. Western blots shown in Figure 19 demonstrated that the PRP obtained using the above protocol contains growth factors, including PDGF-BB, TGF-β_1, and NGF.
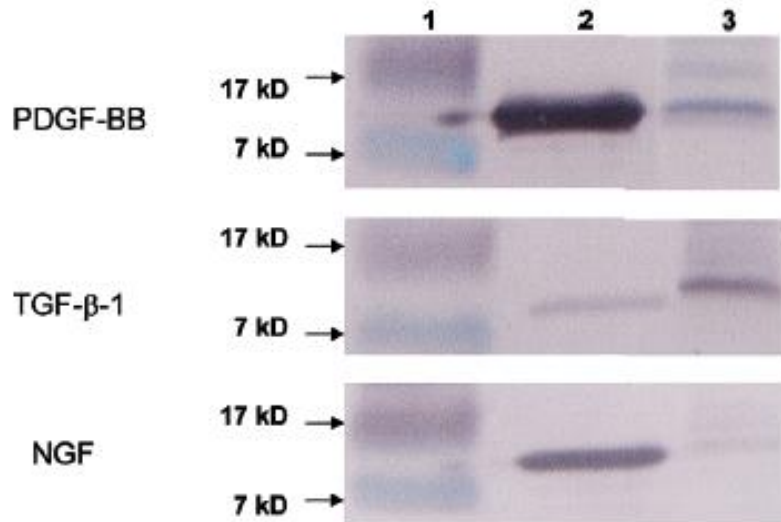
Figure 20. Platelets in Platelet-Rich Plasma (PRP) Prepared using the Clinaseal Centrifuge[TM] Method Contained Intact Growth Factors.

Western blotting was used to qualitatively assess whether platelets in PRP prepared using the methods described contained platelet-derived growth factor-BB (PDGF-BB), transforming growth factor-$\beta1$ (TGF$\beta1$), or nerve growth factor (NGF). Lane 1: molecular weight markers that flank the growth factor protein bands of interest. Lane 2: purified recombinant human growth factors that serve as positive controls. Lane 3: lysates from 5-7 X 10^6 partially purified platelets contained within the PRP. Note the presence of bands in Lane 3 that correspond in migration and immunoreactivity to the standard growth factors in Lane 2. Also note that the bands in Lanes 2 and 3 migrate to the known molecular weight range for each growth factor monomer (PDGF-BB = 15kD, TGF-$\beta1$ = 12. kD, nerve growth factor =14 kD).

Since GFs are small proteins (5-30 kDaltons) and their structure and activity may be sensitive to hydrolytic or proteolytic degradation over time, the next objective was to investigate whether the platelet morphological changes that occurred with increasing bench set time were accompanied by changes in GF content of the PRP. ELISAs were used to measure the content of TGF-β_1, EGF, VEGF, and PDGF-BB in PRP as a function of bench set time. Table 5 shows that levels of these GFs were comparable to the levels reported by others who used more complicated techniques for preparation of the PRP (238, 350, 351). While there was some variation observed in the data collected, the effect of bench set time did not have a significant effect ($p > .05$) on the concentration of select growth factors found in the platelets. These findings suggest that platelets, even when they undergo morphological changes and possible activation, retained significant growth factor concentrations over time.

Bench Set Time (hours)			
	0	3	6
Growth Factor Content* (pg/10^5 platelets)	Mean (SE)	Mean (SE)	Mean (SE)
PDGF-BB	2.877 (±0.6492)	2.135 (±0.8093)	2.432 (±0.8932)
EGF	0.1865 (±0.1440)	0.2826 (±0.2085)	0.2930 (±0.2659)
TGFβ1	5.257 (±0.5959)	4.043 (±0.6095)	4.525 (±1.024)
VEGF	2.474 (±0.5702)	3.052 (±0.5845)	3.202 (±0.9860)
OPG	BDL	BDL	BDL

Table 5: Growth Factor Content of Platelets with Bench Set Time

Growth factor content pg per 10^5 platelets after 10-minute centrifugation time at 1150 x g force as measured by enzyme linked absorbant assay (ELISA). All samples were run in triplicate. PDGF-BB N=4, EGF N=3, TGF-β1 N=4, VEGF N=3, OPG N=3. BDL = below detectable limits. All data were analyzed with a one-way ANOVA followed by a Newman-Keuls post-hoc test where significance was defined as $p < .05$. There was not a significant change in GF content over a 6-hour bench set time when compared with a 0 bench set time ($p > .05$)

D. Discussion

The goal of this study was to determine whether a simplified, inexpensive procedure to obtain platelet-rich plasma (PRP) by the buffy coat (BC) method would yield intact platelets and GFs in concentrations similar to those reported in the literature to facilitate clinical healing.

The investigation showed that platelet recovery and enrichment in PRP prepared using a clinical centrifuge creating 1150 x g force was optimal, consistent and significant ($p < .001$) between 6 and 10 minutes of centrifugation (Figure 16). This is of importance to the clinician because if time were limited in the clinical setting, then a centrifugation time of 6 minutes will provide optimal platelet concentrations. WBC concentration was also significantly ($p < .001$) increased with a 10-minute centrifugation time using the clinical centrifuge. It was also shown that platelet recovery and enrichment did not change significantly after centrifugation for up to six hours of bench set time at room temperature (Figure 18). Thus, this method of PRP preparation provides platelet concentrations and recoveries that match or exceed the PRP preparations obtained through more expensive and elaborate methods (178, 238).

However, it was found that platelet morphology did change over a period of six hours bench set time (Figure 18). Even with two hours of bench set time, platelets in PRP began to appear less normal and as an example, small aggregates formed indicative of platelet activation and possible growth factor release. In western blots, at 0 hour bench set time, detectable levels of the growth factors PDGF-BB, TGF-β1, and NGF were present

in partially purified platelets using this BC method of PRP preparation. PDGF-BB, EGF, TGFβ1, and VEGF levels did not significantly change over 6 hours of bench set time (Table 5).

There are a variety of explanations for why the time between blood draw and PRP harvest might exceed two hours. One obvious reason is that different methods of PRP collection vary in the length of time required to obtain the PRP for use; another is that if the blood is drawn from the patient upon arrival at the practice, some simple dental surgical procedures may require less than 30 minutes until PRP application while other more complex surgeries may require more than 3-4 hours. In practice, it is easiest to draw blood from the patient initially, centrifuge the Vacutainer™ immediately after draw, but then harvest the PRP layer just prior to administration. The centrifuged blood therefore will vary in the length of time it remains on the bench top prior to collection of PRP and use. The results suggest that bench set time does not influence the activity of PRP and therefore its effectiveness in promoting bone formation and wound healing, despite there being platelet morphology changes.

It is known that TGF-β1 stimulates osteogenesis (7, 352, 353), therefore the loss of the bioactivity of TGF-β1 in PRP preparations may account for the disparity among clinicians concerning the effectiveness of PRP. The current results suggest that TGF-β1concentration in PRP prepared by the BC method is not affected by bench set times of up to 6 hours.

A decrease in TGF-β_1 concentration in PRP prepared with bovine thrombin and excess calcium has been noted (238). The loss of this factor over time with when bovine

thrombin is added could be due to three factors including: 1) natural hydrolysis, 2) degradation by proteases, or 3) specific irreversible binding by molecules that may be present in the PRP. TGF-β1 is normally found in a latent form within platelets. When TGF-β1 is in the latent form it is either bound to latency associated peptide (LAP) or latent TGF-β binding protein (LTBP) and release from these proteins is required before it can bind to receptors on target stem cells and trigger the formation of osteoblasts and ultimately new bone tissue (354). If TGF-β1 were released from LAP or LTBP before reaching its receptor, it could be rapidly degraded by hydrolysis (354, 355). Therefore, hydrolysis is one explanation for the loss of TGF-β1 over time in the bovine thrombin induced PGEL (gelled PRP).

Another explanation for the potential loss of TGF-β1 with these other methods is via the action of proteases. If thrombin and Ca^{2+} are used in conjunction with PRP, the clotting cascade and platelets will become activated resulting in the secretion of a variety of granule components and growth factors. Two types of proteases found within platelet granules are matrix-metalloproteinase-2 (MMP-2) and thrombospondins-1 and -2 (TSP2, TSP2). One effect of these proteases is the release of TGF-β1 from its bound form rendering it active (355, 356). MMP-2 is found as a constituent of PRP, but MMP-2 must be activated in order to proteolytically cleave its substrates (357). Activation of MMP-2 depends upon other enzymes (MMP-14, -16) that are found in monocytes, also present in PRP preparations. Monocytes may be triggered to release MMP-2 activating proteases by platelet factors released during the clotting cascade initiated by thrombin and Ca^{2+} (355). Interestingly, monocytes and neutrophils, also found in PRP, contain TSP1 and 2, protease 3, and cathepsin G that may be released during the clotting cascade.

These proteases could act in concert with active MMP-2 to release TGF-β1 resulting in its rapid degradation (358). Zimmermann *et al.* (359) found that when thrombin and calcium were added to platelets prepared by plateletpheresis and leukaphoresis under various conditions and bench set times, the concentration of TGF-β1 decreased by approximately 60-65%. This study found that by not activating the platelets, TGF-β1 concentrations did not significantly change over six hours. Since the PRP in this current study was not used in conjunction with thrombin and Ca^{2+} hydrolysis of TGF-β1 via a protease cascade may not have occurred, this may explain why higher levels of TGF-β1 were detected when using the current protocol compared with the others (238, 269).

Recent evidence suggests another route whereby osteogenic TGF-β1 can be lost from PRP preparations. Alpha-2-macroglobulin (α2M) a protein that can bind active TGF-β1 is found in high concentrations (2-4 mg/mL) in PPP. Initially, active TGF-β1 non-covalently associates with α2M but this loose association leads to the formation of a covalent bond between the molecules (356). Once the TGFβ1/α2M complex is irreversibly formed, TGF-β1 becomes inactive, and incapable of binding to receptors. Therefore, the less PPP is present in PRP preparations, the greater the free TGF-β1 is available to bind to receptors triggering osteogenesis.

Growth factor levels in this PRP preparation were generally higher than those reported by other researchers (238). These findings may result from diluting the 0.5% Triton X-100 (TX-100) platelet lysates prior to adding the samples to the ELISA plate. Preliminary experiments showed that concentrations greater than 0.05% TX-100 interfered with stoichiometric measurement of this growth factor using the manufacturer's protocol. Diluting the TX-100 lysates allowed for lower binding interference by this detergent and

allowed the maximal TGF-β1 signal from the samples during ELISA analysis. Also, the ELISA kit for TGF-β1 analysis employed a monoclonal capturing antibody, whereas other researchers used kits employing Type II TGF-β1 receptor or polyclonal anti-TGF-β1 capturing antibodies to detect the growth factor. These differences may also account for the higher TGF-β1 yields in our study.

Because there are many methods to prepare PRP, and since forming a PRP gel by inducing clot formation with Ca^{2+} and thrombin appears to decrease the amount of TGF-β1 in PRP preparations, the clinical effects of PRP application with and without thrombin and Ca^{2+} over time need to be investigated. Future plans include experiments assessing the neutralizing activity of α2M by combining PRP with PPP in various quantities to examine whether immunoprecipitation of α2M from PPP allows higher levels of TGF-β1 to persist in PRP. Future studies will also address the *in vitro* efficacy of PRP on mesenchymal stem cell differentiation into osteoblasts.

E. Conclusion

This simple and inexpensive procedure for obtaining PRP by the BC method effectively recovers and concentrates platelets after a 10 minute centrifugation time at 1150 x g. Moreover, this technique did not alter platelet morphology during preparation of the BC. Platelet morphology did change after 2 hours of bench set time, but the concentration of GFs (PDGF-BB, EGF, TGF-β_1, and VEGF) contained within the platelets was not altered significantly with bench set time. Therefore, the efficacy of this preparation condition will be assessed in Study III (*in vitro*) and Study IV (prospective clinical study).

Study II: The Effect of PRP on the Frequency of Alveolar Osteitis Following Mandibular Tooth Extraction

A. Introduction

Alveolar osteitis (AO) is a complication that occurs with variable frequency (0.49% – 68.1%) following the removal of permanent teeth (360-368). AO is characterized by severe throbbing pain that begins within 3 to 5 post-operative days and is usually refractory to NSAIDs and/or narcotic analgesics (369, 370). The clinical presentation of AO demonstrates a partial or total disintegration of the intra-alveolar sanguine clot, resulting in a denuded bony crypt with surrounding debris (371, 372). Suppuration is not evident but the patient usually complains of an acute throbbing pain emanating from the extraction site, frequently radiating to the ipsilateral ear and side of the head. Although rare, AO can affect the jugulodigastric lymph glands on the affected side as well.

A definitive etiology for AO has not been universally accepted, but is commonly thought to include clot fibrinolysis as a result of bacterial invasion (373). Smoking, female gender, oral contraceptive use, surgical trauma, operator experience level, poor oral hygiene, gingivitis, periodontitis, and pericornitis have all been reported in the literature to be associated with AO formation (374-382). Increased age and systemic conditions such as diabetes and immunosuppression have also been associated with a greater incidence of AO (383).

Treatment for AO is typically preventative in nature, and is based on two theories of etiology: 1) control of fibrinolysis at the time of extraction and during healing and 2) control of bacterial populations (371, 384). Due to potential adverse reactions to antifibrinolytic agents, most treatment has been directed towards control of bacterial colonization.

More recently, platelet rich plasma (PRP) has been used to facilitate healing in various oral surgical procedures such as soft and hard tissue grafting (7). PRP has been placed in the sockets of lower wisdom teeth to decrease the incidence of AO (385). This section of the dissertation reports on retrospective studies of the effect of PRP on AO incidence and its relationship with other patient factors.

Platelet-rich plasma was employed as a gelled autologous fibrin clot to enhance post-operative healing in conjunction with the removal of teeth. Anecdotal clinical observations suggest a decrease in the incidence and severity of AO, compared to the previous techniques used for tooth removal. The purpose of this study was to examine the effect of PRP on the incidence of AO following mandibular molar tooth removal. The study examined the incidence of AO formation and its correlation with immediate placement of platelet rich plasma gel in the extraction alveolus socket. In addition to the efficacy of PRP in patients without independent risk factors for AO, the effectiveness of PRP in patients with potential risk factors was examined. Factors considered included:

- gender

- age

- smoking status

- systemic antibiotic therapy

- concurrent use of other oral medications

- oral contraceptive use

- presence of oral clenching/grinding habits (bruxism)

- tooth eruptive state

- tooth position, and

- concurrent restorative treatments provided at the time of surgery

B. Materials and Methods

Patient Information

This study was reviewed and approved by the Investigational Review Board for the Protection of Human Subjects in research of Duquesne University. Data were obtained by retrospective chart reviews of 904 mandibular molar extraction sites from 499 patients. A total of 506 patients had been treated, but 7 patients (all non-PRP treatment) were excluded because of missing data on one or more variables. All molar tooth positions and eruptive states (erupted, partially erupted, and complete bone impaction) were included in the study. Tooth removals done without PRP were performed between June 1996 and December 2000. Tooth removals done with PRP were performed between

January 2001 and August 2003. Demographics for the data collection set are presented in Table 6.

Demographic	Treatment		Total
	No-PRP	PRP	
Race:			
African-American	7 (2.6%)	4 (1.8%)	11
Asian	0 (0%)	1 (0.4%)	1
Caucasian	265 (97.4%)	222 (97.8%)	487
Age Groups:			
15-20	161 (59.2%)	146 (64.3%)	307
21-30	47 (17.3%)	47 (20.7%)	94
31-40	22 (8.0%)	9 (4.0%)	31
41-50	18 (6.6%)	10 (4.4%)	28
51-60	12 (4.4%)	10 (4.4%)	22
61-70	7 (2.6%)	4 (1.8%)	11
71-80	4 (1.5%)	1 (0.4%)	5
80+	1 (0.4%)	0 (0.0%)	1

Table 6. Demographic Profile of Data Collection

Demographic profile of database used in study by race and age of participants.

Protocol for Obtaining and Applying PRP

The procedure used is similar to that described in the Materials and Methods section of the Procedure portion of the Preparation and Characterization of PRP study but with 2 differences: 1) whole blood was drawn through a catheter, and 2) the PRP was gelled by the addition of a calcium chloride/platelet poor plasma (PPP) mixture. The reasons for

these variations is that whole blood obtained through the catheter eliminated an additional venipuncture site for the patient and at the time of this study the clinician performing the surgery preferred to use a gelled form of the BC as it was easier to place in the extraction site. Steps were performed using aseptic techniques and sterile materials.

Statistical Analysis

Statistical investigation for AO formation by treatment group was chi square analysis. When analyzing the effect of individual patient factors bivariate tests for independence of categorical data were performed and when analyzing the combination of factors multivariate analysis with multiple logistic regressions were performed using SPSS software (SPSS Inc., Chicago, IL). Values of $p < 0.05$ were considered significant. The Mantel-Haenszel test for equality of population odds ratios was used to investigate interaction effects among factors.

C. Results

The results of this study will provide information that will be of value to clinicians by revealing the patient factors that have an increased incidence of AO associated with them and the effect PRP administration has on decreasing that incidence. The 904 extraction sites were assumed to be independent from one another. The test for equality of proportions revealed a significantly greater proportion of AO cases occurring among the non-treated sites (n=491) compared with sites in the PRP treatment group (n=413); (p = .00043). The odds ratio (OR) was 2.81 (95% CI, 1.54 to 5.10), indicating an almost threefold increase in the odds of AO occurring in the control sites compared to the PRP-treatment group. Figure 20 illustrates the difference in AO formation for non-PRP

treatment sites and sites receiving PRP treatment at the time of surgery. Table 7 lists a

comparison of non-PRP treatment and PRP treatment for the various patient factors.
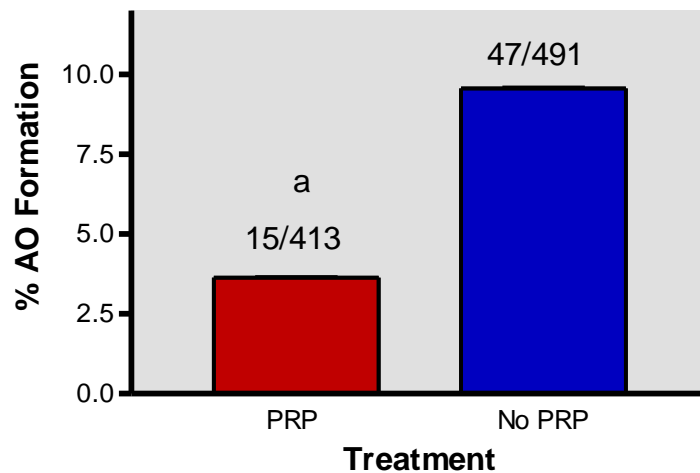
Figure 21. Percent AO Formation by Treatment Group

Alveolar Osteitis (AO) formation in extraction sites with or without PRP treatment. All
data were analyzed with a chi square analysis with SPSS software. Significance was
defined as $p < .05$, where [a]$p < .001$.

	Non-PRP Treated Sites			PRP Treated Sites			Change in % Occurrence of AO with PRP	% ↓ in AO with PRP
Patient Factor	# of AO formations/ total population	% AO formation	95 % Confidence Interval	# of AO formations/ total population	% AO formation	95% Confidence Interval	(%)	(%)
Sex (d) Male	21/231	9.10	5.4-12.8	4/191	2.10	0.1-4.1	7.00	76.90
Female	26/260	10.00	6.4-13.6	11/222	4.95	2.1-7.8	5.05	50.50
Age (d) **<40 yrs**	42/436	9.63	6.9-12.4	14/380	3.68	1.8-5.6	5.95	61.79
≥40yrs	5/55	9.09	1.5-16.7	1/33	3.03	-2.8-8.9	6.06	66.67
1st molar (d)	0/23	0.00	0.0	0/8	0.00	0.0	NC	NC
2nd molar (d)	1/22	4.55	-4.2-13.3	0/12	0.00	0.0	4.55	100.00
3rd molar (d)	46/446	10.31	7.5-13.1	15/393	3.82	1.9-5.7	6.49	62.95
Erupted (d)	6/93	6.45	1.5-11.74	1/55	1.82	-1.7-5.4	4.63	71.78
Partially impacted (d)	6/130	4.62	1.0-8.2	4/100	4.00	0.2-7.8	0.62	13.42

	Non-PRP Treated Sites			PRP Treated Sites			Change in % Occurrence of AO with PRP	% ↓ in AO with PRP
Patient Factor	# of AO formations/ total population	% AO formation	95 % Confidence Interval	# of AO formations/ total population	% AO formation	95% Confidence Interval	(%)	(%)
Full impaction (c)	35/268	13.06	9.0- 17.1	10/258	3.88	1.6- 6.5	9.18	70.29
Bruxism (a)	24/105	22.86	14.8- 30.9	6/41	14.63	3.8- 25.4	8.23	36.00
Prophylactic antibiotics (d)	6/60	10.00	2.4- 17.6	1/40	2.50	-2.3- 7.3	7.50	75.00
Oral Contraceptives (b)	8/45	17.78	6.6- 29.0	5/49	10.20	1.7- 18.7	7.58	42.63
Other meds (d)	7/88	7.95	2.3- 13.6	3/95	3.16	-0.4- 6.7	4.79	60.25
Tobacco Smoking (d)	10/59	16.95	7.4- 26.5	0/37	0.00	0.0	16.95	100.00
Other operative procedures (d)	7/48	14.58	4.6- 24.6	1/12	8.33	-7.3- 24.0	6.25	42.87

Table 7. Comparison of Non-PRP Treatment and PRP Treatment for Each Patient Factor

Table 7 lists all 10 patient factors considered in this study along with the corresponding proportions experiencing AO for both PRP and non-PRP treated sites. All data were analyzed with a chi square analysis with SPSS software. Significance was defined as $p <$ .05, where [a]$p < .001$; [b]$p < .01$; [c]$p < .05$; [c]$p > .05$. PRP treatment decreased AO incidence for all subpopulations in which AO occurred. When examining individual risk factors for AO formation, significance was found with only 4 factors. Three are listed in this table

bruxism, oral contraceptive use, and complete impaction. The fourth significant factor was not using PRP (Figure 21 and 22). AO formation was not observed with first molar extraction sites and was seen in only one second molar extraction site (which did not receive PRP treatment). The remaining 61 sites that developed AO formation were all third molar extraction sites. Note that bruxism and oral contraceptive use display the greatest likelihood of AO formation for both PRP and non-PRP groups.

Multiple logistic regression (multivariate) analysis revealed four significant risk factors for AO: complete impaction, oral contraceptive use, bruxism, and failure to use PRP. Figure 22 lists the expected probability of AO formation for each of these significant risk factors alone and in combination. The individuals most at risk for AO were those presenting with a combination of complete impaction, use of oral contraceptives, bruxism, and no treatment with PRP. With each risk factor combination, the use of PRP significantly reduced the probability of AO by approximately one half ($p < .05$, Figure 22). Multiple logistic regression analysis revealed that when PRP was not administered the other examined factors (gender, age, tooth position, smoking status, prophylactic antibiotic use, other operative procedures performed at the same appointment, and concurrent use of other medications) were not associated with an increase or decrease in the probability of AO.

Analysis of potential interactions between the use of PRP and identified risk factors were examined using the Mantel-Haenzel test for OR equality. The results revealed no significant interactions between PRP and other risk factors for AO. Thus, the effectiveness of PRP in reducing the incidence of AO is not dependent upon the presence or absence of other risk factors for this complication.

D. Discussion

Multivariate analyses revealed that PRP significantly reduced the incidence of AO, with the odds of AO formation 2.37 times higher for extraction sites without PRP treatment (95% CI, 1.3 to 4.4). In addition to the absence of PRP administration, this multivariate analysis revealed exactly three other significant risk factors for AO: bruxism, oral contraceptive use, and complete impaction. Figure 22 shows the expected AO probabilities for patients presenting with any combination of these four significant risk factors. Notice that when PRP is administered, the AO probability is reduced by roughly ½ for patients in any partition. Therefore, we can conclude that the administration of PRP following mandibular tooth extraction is beneficial in decreasing the incidence of AO. PRP use should be considered by the clinician especially for patients who have an impaction, take oral contraceptives, or brux (grind) their teeth, however all patients having a mandibular tooth removed would benefit from the application of PRP.

AO Formation for Combinations of Variables Found to be Significant Risk Factors

Partition (risk factor combination)	Complete Impaction	Oral Contraceptives	Bruxism	Non PRP treated % AO probability	PRP treated % AO probability
A	NO	No	No	3	1.3
B	Yes	No	No	6.2	2.70
C	No	Yes	No	8.7	3.8
D	No	No	Yes	15.2	7.0
E	Yes	Yes	No	16.9	7.9
F	Yes	No	Yes	27.8	14.0
G	No	Yes	Yes	35.6	18.9
H	Yes	Yes	Yes	54.3	33.4
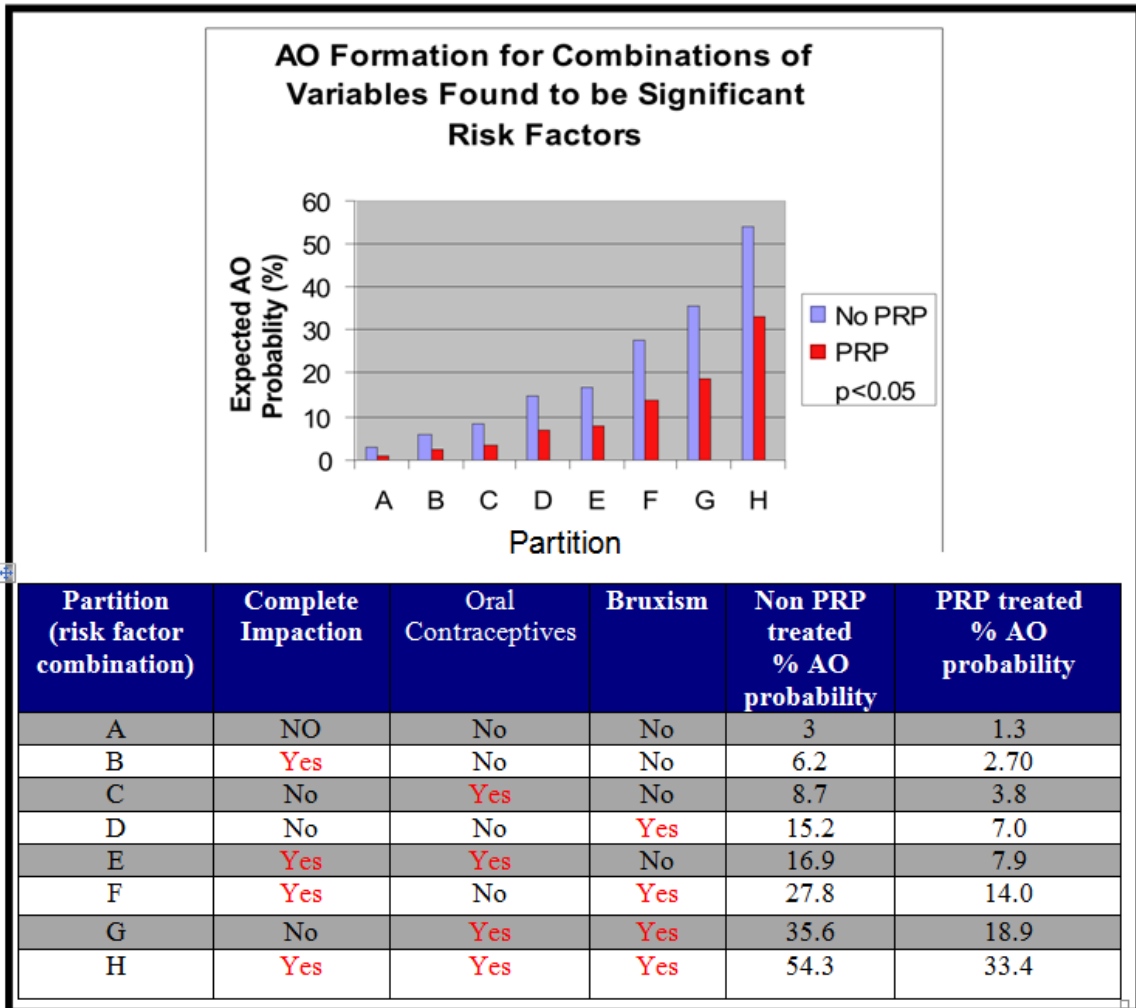
Figure 22. Alveolar Osteitis (AO) Formation by Partition

Alveolar osteitis (AO) formation for various partitions found to be significant risk factors (multivariate analysis). Statistical significance: $p < .05$ for all of the above combination of variables. PRP indicates platelet-rich plasma. Complete impaction N=526 (no PRP N=268; PRP N=258), oral contraceptive use N=94 (no PRP N=45; PRP N=49), bruxism N=146 (no PRP=105; PRP=41), Non-PRP N=491; PRP N=413). Partition A: N=904; Partition B: N=526; Partition C: N=94; Partition D: N=146; Partition E: 620; Partition F: N=672; Partition G: N=240; Partition H: N=766.

Furthermore, this analysis did not find an association between smoking status and the occurrence of AO ($p = 0.3$). However, this study did not take into account smoking

99

quantity. Moreover, smoking status is subject to a possible response bias. It was

interesting that none of the smoking PRP-treated patients (n=37) experienced AO.

Sorensen et al., (386) showed that smoking induced significant reductions in cutaneous

and subcutaneous tissue blood flow ($p < .001$), oxygen tension ($p < .05$), and aerobe

metabolism ($p < .01$). Sufficient oxygen supply is fundamental for normal healing, and

tissue hypoxia has been shown to impair the reparative processes of wound healing (387),

decrease the neutrophil defense against pathogens (388, 389), and increase the incidence

of wound infection (390) These factors have been implicated in AO formation (391-

393). Nicotine, a component of cigarette smoke, is known to increases tissue oxygen

(386) and induce angiogenesis (394). The increased oxygen and angiogenesis induced by

nicotine in combination with the growth factors in PRP may explain the 100% remission

in AO formation found with the application of PRP in cigarette smokers.

   Patients taking oral contraceptives also had a significant increase ($p < .05$)   in AO

formation. The particular oral contraceptive taken by each of the patients was not

recorded, but a similarity for each of these agents is an estrogen component. A possible

reason for the significant increase in AO formation for patients taking oral contraceptives

is that estrogen is known to induce fibrinolysis (395). Fibrinolysis is thought to be a

mechanism for AO formation (373). A feasible explanation for how PRP reduces the

incidence in AO formation for these patients is the induced angiogenesis and soft tissue

formation by VEGF, PDGF-AB, and PDGFD-BB growth factors found in the platelets of

PRP.

   The participants in this study were, overall, young (15 to ≤ 30 years of age, 80.5%)

and white. However, statistical analysis did reveal that the effectiveness of PRP in

reducing the occurrence of AO was significant and independent of all confounding factors, including age. Patients younger than 40 years of age and those older than 40 years of age both had AO formation reduced by approximately two thirds. Race was not considered a variable in the study because of the small number of nonwhite participants.

Placing PRP in surgical sites, particularly in the elderly and/or medically compromised patient, is a rational approach to treatment. This is supported by the *in vitro* work of Cei *et al*, who found that, irrespective of age, bone marrow stromal cells responded similarly to platelet-released supernatant and bone morphogenetic protein 6, both of which are found within PRP (396). Moreover, it is known that TGF-β1 enhances mineralization on dental implant materials in osteoblast cultures from elderly human subjects (397).

Mesenchymal stem cells decrease in number early during aging in humans (398). The stem cells can differentiate into osteoblasts when stimulated by the proper growth factors contained within platelets. However, the bone marrow microenvironment changes with maturity and may possibly be unfavorable for mesenchymal stem cell (MSC) proliferation or may favor MSC maturation toward a different cell lineage such as adipocytes (399-401). Adipogenesis can be inhibited by TGF-β1, which again is contained in PRP (402). Therefore, gelled PRP (PGEL) techniques that utilize bovine thrombin and have decreased TGF- β1 levels (238) could induce hMSCs to go down the adipogenic pathway and not the osteogenic pathway. This may be an additional reason for clinicians not witnessing the anticipated bone formation with bovine thrombin PGEL techniques. Ultimately, since stem cell numbers decrease with age but still retain their

juvenile potential, it is reasonable to suggest that PRP, with increased concentrations of growth factors, would be beneficial in treating elderly patients.

Many practitioners prescribe systemic antibiotics to prevent dry socket, but this study found no significant effect of prophylactic antibiotics on the incidence of AO. This result supports the position that using prophylactic antibiotics to prevent AO is without benefit, unless the patient has a systemic pathology that indicates the need for pre-medication with antibiotics. This study did not examine the effect of localized intra-alveolar post-extraction antibiotic administration. Sanchis *et al*, found that intra-alveolar placement of tetracycline did not affect the incidence of dry socket (403).

The beneficial effects of PRP for decreasing the incidence of AO may be related to a number of signaling proteins found in the platelets, including multiple growth factors such as insulin-like growth factor, vascular endothelial growth factor, epidermal growth factor, nerve growth factor, transforming growth factors β1 and β2 (TGF-β1,-β2), platelet-derived growth factors, and cytokines such as angiopoietin-2, and interleukin-1 (404, 405). These factors stimulate cell mitosis and differentiation (406), increase collagen production, recruit leukocytes and other cells to the surgical site, and initiate vascular in-growth. Growth factors promote both soft and hard tissue healing and angiogenesis. In addition, platelets promote clot formation, which is beneficial in healing. Aside from platelets, PRP also contains white blood cells that can inhibit bacterial growth. Therefore, PRP application mitigates the currently accepted causes of AO by facilitation of clot and soft tissue formation and inhibition of bacterial colonization.

E. Conclusion

This study found a substantial reduction in the incidence of AO following treatment of the extraction site with PRP. The results of this study also demonstrated that complete impaction, oral contraceptive use, and especially bruxism are associated with significant increases in AO incidence and PRP significantly ($p < .05$) reduced its incidence. This is the first time that a simple and cost-effective technique has been reported that provides a viable methodology by which dental practitioners can decrease the incidence of AO formation in patients. This study supports the use of PRP in mandibular extraction sites as a method for reducing patient postoperative discomfort and the need for multiple postoperative visits that can be associated with AO.

Study III: Effect of Platelet Rich Plasma on Human Mesenchymal Stem Cell Growth, Differentiation, and Gene Expression

A. Introduction

Use of autologous PRP in tooth extractions decreases the incidence of AO (8) and this benefit may be achieved by facilitating clot formation and decreasing the incidence of infection. Clinicians have anecdotally found that the use of PRP also seems to stimulate bone (re)modeling and jawbone density in dental patients prepared for tooth replacement with a dental implant. Alveolar bone development is fundamental to restoring dental patients to full function and, therefore is of great interest to clinicians. One way that PRP might trigger bone formation in these patients is to stimulate the proliferation and subsequent differentiation of resident hMSCs into osteoblasts.

The most conspicuous function of the osteoblast is the formation of bone. Clinically, bone formation is a multistep process that begins with the chemotaxis and attachment of hMSCs (407). Following this initial step, the initiation of bone induction is primarily regulated by bone morphogenetic proteins, PDGF, TGFβ1, ILGF, and FGF which are all found in platelets of PRP (407). During phases of active bone formation, osteoblasts synthesize bone matrix and prime it for subsequent mineralization. Active osteoblasts *in vivo* are plump, cuboidal cells rich in organelles involved in the synthesis and secretion of bone matrix proteins. Osteoblasts are polarized, allowing for the secretion of matrix onto the underlying bony substratum, which results in bone growth by

apposition. Some osteoblasts become trapped in matrix during bone formation and are entombed in lacunae. These cells are referred to as osteocytes and remain in the bone matrix in a state of low metabolic activity. At the completion of bone formation, those osteoblasts that avoid entombment in lacunae, lose their important matrix synthesis function and become bone-lining cells. In mature bone, these bone-lining cells cover most of the bone surfaces. Osteocytes and bone-lining cells should not be thought of as senescent, because they play a major role in the regulation of bone modeling and remodeling in addition to aiding in calcium homeostasis (408).

Bone development is dependent upon the proliferation of hMSCs and the controlled differentiation of those cells into osteoblasts. Therefore, hMSCs were chosen for this study because they are known to contribute to bone regeneration (341, 409). They are also essential for the growth and differentiation of primitive hemopoietic cells within the bone marrow microenvironment (341, 409-411) and are significant to bone development and remodeling. Human MSCs are primary cells that can be successfully cultured through approximately eight passages (412). Techniques are now available to isolate hMSCs and control their expansion *in vitro* under controlled culture conditions without change of phenotype or loss of function (409).

The effect of PRP on hMSCs is of interest because it provides a mechanism for explaining the clinical effects observed in the previous retrospective study. By studying the effects of PRP on hMSCs, clinicians may gain greater understanding of the mechanisms for PRP actions and apply the improved knowledge base to further improve clinical treatments. Studies have demonstrated the feasibility of transplanting hMSCs clinically to provide crucial new cellular therapy. The hMSCs are harvested and cultured

from normal human bone marrow obtained primarily from the posterior iliac crest of the pelvis (341, 413) and the tibial and femoral marrow compartments (414, 415). These cells are used in regenerative medicine, immune modulation, and tissue engineering.

Since PRP is thought to induce earlier and enhanced bone formation in the jaw, then the question arises to "Whether PRP induces earlier and enhanced proliferation of hMSCs as well as inducing their subsequent differentiation into osteoblasts?". It is known that hMSC cultured in growth medium will proliferate (grow in number) (341). This study examines if hMSC in growth medium with PRP exposure induces earlier and enhanced proliferation of hMSCs when compared to growth medium alone. Knowing if PRP does increase proliferation of hMSCs at an earlier time point would provide a partial mechanistic explanation for what is observed clinically in Studies II and IV of this dissertation. PRP proliferation effects were assessed by three accepted methods: cell counts, MTT assay, and total RNA analysis (416-418). We also examined if hMSCs in osteogenic differentiation medium with PRP exposure induced differentiation into osteoblasts at an earlier time point when compared to the osteogenic differentiation medium alone. The PRP differentiation effects were assessed by two known and accepted methods: alkaline phosphatase assay and examination of key gene expression by real time RT-PCR that confirm differentiation down the osteoblastic (osteogenic) pathway (419-422). This molecular study may improve mechanistic understanding of how PRP improves the bone modeling and remodeling *in vivo*.

Materials and Methods

Collection of PRP

PRP was collected as described in the Preparation and Characterization of PRP section (page 68), except that all Vacutainer™ tubes were centrifuged for 10 minutes at 1150 x g, and the PRP was used in these studies between a minimum of 3 minutes and a maximum of 30 minutes after collection from the Vacutainer™ tubes. Three to thirty minutes is the most typical time that elapses between completion of centrifugation and PRP application in clinical practice. The protocol for PRP collection in the Preparation and Characterization of PRP study is also the same protocol that is used in the prospective clinical study, therefore that protocol is used in this study. A new blood draw was performed for each cell culture flask. All PRP was collected from the same individual.

Cell Culture

Human mesenchymal stem cells were purchased from Lonza Biosciences (Walkersville, MD). Cell purity had been tested by the supplier with flow cytometry and for their ability to differentiate into osteogenic, chondrogenic and adipogenic lineages. As per the manufacturer's specification, these stem cells were positive for CD105, CD166, CD29, and CD44 expression and were negative for CD14, CD34 and CD45 expression. Upon arrival, cells were initially seeded at a density of approximately 7500 cells/cm^2 in a T-75 flask. Human mesenchymal stem cells when assessed by proliferative ability, morphological appearance, and surface antigen, gene and protein expression have been found to maintain a stable phenotype through the first 6-8 passages of culture (423).

Di Girolamo et al. found that early passages of hMSCs would most likely be the most useful in identifying samples that would provide the consistent and appropriate cell characterization (413). Therefore, for the experiments in this dissertation cells passaged 3 to 4 times were chosen. For each experiment, cells were seeded at an initial density of 2500 cells/cm^2 inT-25 flasks. Cells were cultured in growth medium alone [comprised of Dulbecco's Modified Eagle's Medium (DMEM) (Invitrogen, Carlsbad, CA) supplemented with 10% fetal bovine serum, 2mM L-Glutamine, and 0.5% gentamicin (10mg/mL)] and incubated at 37°C in a 5% CO_2 atmosphere for 24 hours. This initial 24-hour incubation was performed so the cells could attach to the flask. After the 24-hour attachment period all medium was removed and replaced with the appropriate medium for each experimental group. Cells displayed the typical morphology of growing MSCs in that they were long, columnar, and spindle-shaped (413, 424) following this initial attachment period. Growth medium was refreshed every third day. Differentiation studies relied on the use of supplemented DMEM medium containing 100 nM dexamethasone, 0.2 mM ascorbic acid, and 10 mM β-glycerophosphate (osteogenic medium) (425-427). Osteogenic medium will be referred to as differentiation medium in this manuscript. All differentiation medium supplements were purchased through Sigma (Sigma Aldrich, St Louis, MO). Cells cultured in differentiation medium displayed the typical characteristics associated with osteoblastic differentiation, i.e., they became flattened or broadened in appearance with a much more prominent cytoplasm that eventually became hardened or dense in appearance after thirty days in culture (424). Differentiation medium was refreshed every third day. For PRP treatment, PRP (375 μL) was collected as discussed above and added to the flasks containing 10 mL growth or

differentiation medium for 24 hours and incubated at 37°C in a 5% CO_2 atmosphere, after which all medium was aspirated and replaced with fresh growth or differentiation medium as per experimental group. Adding 375 μL of PRP to each flask containing 10mL of medium resulted in a 3.75% v/v concentration. PRP treatment for 24 hours was chosen because we felt it was more clinically relevant. When placing the BC PRP at the surgical site, it is uncertain how long it is retained in place, but it is known that when platelets are present in a blood clot, retraction is thought to occur within hours and extrudes a very large fraction of serum and its contents (15). Therefore, it seems reasonable that a 24-hour PRP treatment would be similar to what is occurring in the body at the surgical site. It should be noted that once the PRP was placed in the culture flask it would form a clot signifying platelet aggregation and activation. Upon aggregation and activation, granules within the platelets release their contents (cytokines, and GFs) (41).

For proliferation studies, cultures of hMSCs were passaged in growth medium until a sufficient number of flasks were obtained. Cells were then seeded in T-25 flasks at a density of 2500 cells/cm^2 in growth medium. Cells were incubated for 24 hours at 37°C in a 5% CO_2 atmosphere to allow cells to attach to the flask. After this initial 24 hour period, all medium was removed and replaced with: either growth medium or growth medium with 3.75% (v/v) PRP. All media were changed after the initial 24 hours. Samples cultured in growth + PRP were incubated thereafter in growth medium (no PRP). Media were changed every 3 days thereafter and cells were incubated for various times.

Human MSCs for differentiation studies were cultured as per the following protocols. For qualitative alkaline phosphatase assays, the cells were seeded on collagen-coated coverslips (Biocoat® Franklin Lakes NJ) at 2000 cells/cm^2 and were placed into each well. Three mL of growth medium were placed into the wells for 24 hours, after which all media were changed and replaced with either growth medium only, growth medium plus PRP 112 μL (3.75% v/v), differentiation medium only, or differentiation medium plus PRP 112 μL (3.75% v/v). After 24 hours, all medium were removed growth medium and growth medium + PRP groups had their medium replaced with growth medium (no PRP), and the differentiation and differentiation + PRP groups had their medium replaced with differentiation medium (no PRP) for 5 and 15 days. From this time forward, none of the cells for the experiment were exposed to PRP. All media were changed every 3 days.

 For total RNA and real time reverse-transcriptase polymerase chain reaction (real time RT-PCR) studies, the cells were cultured in their respective test group medium for the initial 24 hours to allow cell attachment to the flasks then 3.75% v/v PRP was added to flasks that were to receive the PRP treatment. Following this 24-hour exposure, all media were removed from the flasks and replaced with their respective media without PRP for 5, 10, or 21 days. All media were changed every 3 days.

Cell Counts

Cell counts were performed to evaluate the proliferation effects of a 24-hour exposure of PRP on hMSCs growth medium in comparison to growth medium alone. Changes in cell morphology, an indication of differentiation, were also noted. Cell counts were done

in three microscopic fields for days 1, 3, 4, 5, 7, 10, and 12 using a grid. Days 1, 4, 5, and 7 were examined in triplicate, while days 3, 10, and 12 were analyzed in duplicate.

MTT Assay

The (3-(4,5-Dimethylthiazol-2-yl)-2,5-diphenyltetrazolium bromide (MTT) assay (R&D Systems, Minneapolis, MN) was carried out as indicated by the manufacturer's instructions. The MTT colorimetric assay is well accepted as a measure of hMSC proliferation (419) and therefore, chosen for this study. This is a colorimetric assay that determines the ability of viable cells to convert a soluble tetrazolium salt- [3-(4,5-dimethylthiazol-2-yl)-2,5-diphenyltetrazolium bromide] (MTT)- into an insoluble formazan precipitate. Tetrazolium salts accept electrons from substrates such as NADH or NAPDH. Specifically, MTT is reduced at the ubiquinone and cytochrome bc_1 sites of the mitochondrial electron transport system. Figure 23 summarizes the reaction that transforms the yellow soluble salts to purple or dark blue-colored formazan crystals that can be dissolved in an organic solvent and concentration can be spectrophotometrically determined (412).
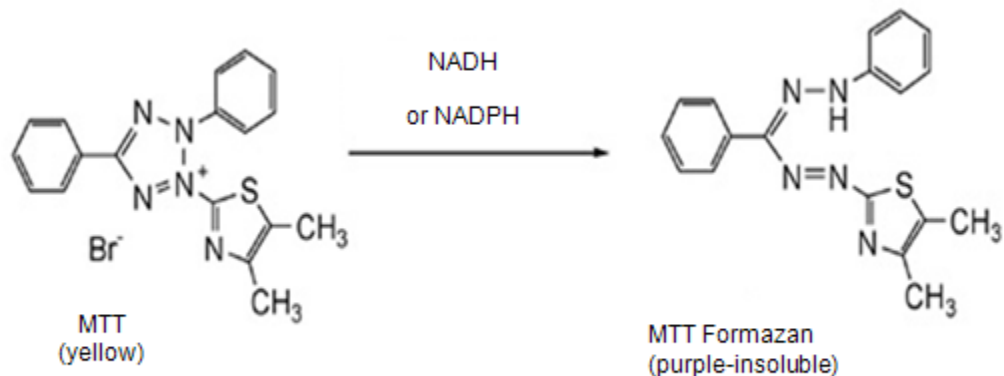
Figure 23. Conversion of Soluble MTT Salt to Insoluble MTT Formazan Crystals (428)

Briefly, cells were trypsinized from the flask and placed in a sterile 15 mL conical tube. The cells were re-suspended in two volumes of media. From this, 200 µL of cell suspension were added to each of the wells, five wells in total. Negative controls were used- three in total- and controls for PRP were used. This plate was placed in a 37° C incubator at 5% CO_2 overnight to allow the cells to reattach. The following day, 10 µL of the MTT reagent were added to each of the wells and placed in the incubator for 3 hours, until a purple, punctuate precipitate was visible under magnification. When this condition was visible, 100 µL of detergent were added to each of the wells and the plates incubated at room temperature for 4 hours. When the crystals had dissolved, the plate was quantified using a BIO-TEK Kinetic Microplate Reader Model EL312E (Winooski, VT) at 570 nm.

RNA Preparation

Total RNA formation can be collected in preparation for use in the subsequent RT-PCR experiments. Changes in total RNA production over baseline can be measured and are reflective of metabolic changes in the hMSC's functions of proliferation and differentiation(422).   All cells were cultured in their respective media and grown to a 50% confluent monolayer. The PRP treatment was applied and flasks were placed back in the incubator for 24 hours. Following the 24-hour incubation, all cell flask media were aspirated and replaced with new media that was without PRP. At this point all cells, including PRP treated cells, were grown in their respective medium without PRP for the set time of 5, 10, and 21 days. All media changes were completed every third day after this point. The groups examined were (1) growth medium, (2) differentiation medium, (3) growth medium + PRP treatment for 24 hours followed by growth medium only, and (4) differentiation medium + PRP treatment for 24 hours followed by differentiation medium only.

The procedure for the isolation of RNA and reagent preparation was done as specified by manufacturer's (Qiagen, Valencia, CA) instructions. Briefly, all media from the cell culture flasks were completely aspirated and 650 μL of lysis Buffer RTL^{TM} were added directly to the flask. This flask was then placed on a rotator and periodically visualized until no cell structures were evident. At this point, the flasks were shaken and the homogenized cell lysate was placed into a gDNA spin column and spun at 8000 x g for 15 seconds. The spin column was discarded and one volume of 70% ethanol was added to the flow through and mixed by pipetting. From this, 700 μL were taken and placed into an RNeasy$^®$ spin column and centrifuged at 8000 x g for 15 seconds and the flow

through was discarded. Seven hundred µL of Buffer RW1^{TM} were added to the spin

column and spun at 8000 x g for 15 seconds and the flow through was discarded. Five

hundred µL of Buffer RPE^{TM} were added to the spin column and spun at 8000 x g for 15

seconds and the flow through was discarded. Five hundred µL of Buffer RPE^{TM} were

again added to the spin column and spun at 8000 x g for two minutes. The RNeasy$^®$ spin

column was placed in a new 1.5 ml collection tube and 100 µL of 37°C RNase-free water

were added to the column and spun for one minute at 8000 x g to elute the RNA. Total

RNA was measured with spectrophotometry at 260nm and quality assessed with 280 nm.

Quantitative Alkaline Phosphatase Assay

The alkaline phosphatase (ALP) assay was chosen as one method to determine

hMSC differentiation. Alkaline phosphatase expression is an early marker of osteoblast

differentiation (429). ALP catalyzes the hydrolysis of phosphate esters found in

nucleotides, proteins, and alkaloids resulting in the formation of an organic moeity and

inorganic phosphate (430). It is known that ALP activity increases during bone

development (431). For this project ALP activity is detected by using *p*-nitrophenyl

phosphate (*p*NPP) as an effective chromogenic substrate for alkaline phosphatase. This

assay is highly sensitive with a detection limit that is less than 3 ng with a wide linear

range (432). The assay measures ALP activity as it hydrolyzes *p*NPP into a yellow

colored product (*p*-nitrophenol) with a reaction rate that is directly proportional to the

enzyme activity.

$$\text{\textit{p}-nitrophenyl phosphate} \xrightarrow{\text{ALP}} \text{\textit{p}-nitrophenol (yellow) + phosphate}$$
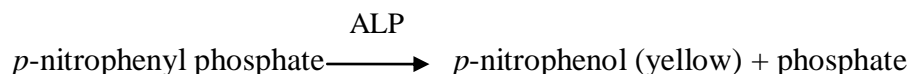
Alkaline Phosphatase (ALP) assays (Anaspec, San Jose, CA) were performed as per manufacturer's directions. Briefly, the *p*-nitrophenyl phosphate (pNPP) reaction mixture was diluted 1:100 with dH_2O. The ALP dilution buffer was prepared by diluting the 10X lysis buffer with dH_2O and adding 1% bovine serum albumin to yield a 1X working solution. The ALP standard was diluted 1:25 with dilution buffer. Diminishing serial dilutions were prepared, with final concentrations ranging from 0.2 to 0 ng/μL. To each of the wells, 50μL of samples and 50 μL of the serial dilution were added. The plate was mixed by gentle shaking for 30 seconds. The plate was incubated at room temperature for 30 minutes immediately followed by quantification using a BIO-TEK Kinetic Microplate Reader Model EL312E (Winooski, VT) at 405nm.

RT-PCR

Real-time RT-PCR has become the preferred method for quantifying changes in gene expression (433). This project examined two genes (bone sialoprotein and osteocalcin) that represent hMSC differentiation into osteoblasts. The bone sialoprotein gene (IBSP) was chosen because it is expressed at 14 days when cells are grown in differentiation medium (434). IBSP expression occurs prior to the mineralization phase and represents a functioning osteoblast (287, 435). The osteocalcin gene (BGLAP) expression is a definitive marker for functioning osteoblasts grown in differentiation medium at 21 days (276, 277, 279, 434). Two other genes were chosen as control markers. The housekeeper gene studied was glyceraldehyde-3 phosphate dehydrogenase (GAPDH) (303-306). The glycoprotein-IIb(GPIIb) gene was chosen because it is expressed in developing

megakaryocytes and is thought to be found only in platelets and therefore should not be expressed in the non-PRP treatment groups (294, 300-302). Glycoprotein-IIb gene expression was examined to assure that all platelet influence was removed following the medium change after the 24-hour PRP treatment.

The genes of interest were selected based upon their appearance in platelets and differentiating mesenchymal stem cells (MSCs) (into osteoblasts). The gene for glyceraldehyde-3 phosphate dehydrogenase (GAPDH) is a well-characterized housekeeper gene for differentiating MSCs. The gene for bone sialoprotein was chosen because it is expressed during the differentiation of MSCs, prior to the mineralization phase, but represents a mature functioning osteoblast. The gene BGLAP (osteocalcin) was chosen because it is definitive marker for functioning osteoblasts at 21 days in differentiation medium. The gene for glycoprotein-IIb (GPIIb) was chosen because it is expressed in developing megakaryocytes and found in platelets. Table 8 lists the forward and reverse primer sequences used for this study.

Gene	Forward Primer	Reverse Primer
Glyceraldehyde-3 phosphate dehydrogenase (GAPDH)	5'GAGTCAACGGATTTGGTCGT	CATTGATGACAAGCTTCCCG
Bone sialoprotein (IBSP)	5'CTATGGAGAGGACGCCACGCCTG	CATAGCCATCGTAGCCTTGTCCT
Osteocalcin(BGLAP)	5' TACCTGTATCAATGGCTGGG	ATGTGGTCAGCCAACTCGT
Glycoprotein-IIb (GPIIb)	5'GTCAGCTGGAGCGACGTCA	CTGAATGCCCAAAATACGACG

Table 8 Primer Sequences for Genes of Interest

Official abbreviations for the genes are listed in parenthesis in the first column.

The real time RT-PCR reaction protocol was completed in a Bio-Rad Chromo4 Real Time Detection System using the iScript One-Step RT-PCR Kit (Bio-Rad, Hercules, CA). Each reaction mixture contained 100 nM RNA. The 50 μL reaction mixture was placed in the thermal cycler and incubated at 55°C for 10 minutes, 5 minutes at 95°C for cDNA synthesis and reverse transcriptase inactivation. The PCR cycling was completed after 45 cycles; 10 seconds at 95°C, 30 seconds at 57°C. A melt curve analysis was completed; 1 minute at 95°C, 1 minute at 55°C, and 10 seconds at 55°C for 80 cycles, increasing 0.5°C each cycle. Data were analyzed using MC Opticon® software.

Statistical Analysis

Statistical analysis was performed using GraphPad Prism® 3.02. Cell count analyses and MTT analysis were performed using a two-way ANOVA with Newman Keuls post-hoc tests and unpaired two tailed t tests for comparison of growth ± PRP at specific time points or between time points for a specific medium. Total RNA and ALP were analyzed using one-way ANOVA with Newman Keuls post-hoc tests. Newman Keuls was chosen because it will compare between each of the groups. Real time RT-PCR data was analyzed by a two-tailed paired t test when two sample data sets were analyzed and a One-way ANOVA with Newman Keuls post-hoc tests were used when more than two sample data sets were being analyzed.

A. Results

Experimental Rationale:

For proliferation studies, cells cultured in growth medium and growth medium + PRP were compared. Cells are expected to proliferate when cultured in growth medium with a limited number of cells undergoing differentiation as the cells reach 100% confluence (341). When culturing hMSCs in growth medium ± PRP exposure for 24 hours, the effect of PRP on proliferation should be discerned. By culturing cells in growth medium only, it is possible to determine the rate of cell proliferation and if there is spontaneous differentiation. If differentiation is occurring in growth medium alone, differentiation studies will determine the time point that it does occur in growth medium alone. Cells cultured in growth medium will be compared to cells cultured in growth +

PRP. If PRP does induce differentiation, it should be observed at an earlier time point or at an increased level than differentiation seen in growth medium alone.

For differentiation studies, cells were cultured in growth medium, growth medium + PRP, differentiation medium, and differentiation medium + PRP. Culturing cells in differentiation medium is a control for known differentiation markers to confirm that osteoblastic differentiation is occurring (419-422). Culturing hMSCs in differentiation medium + PRP should determined if PRP has an effect on the normal differentiation process. PRP may be found to have one of three effects on the normal differentiation process, PRP may either 1) delay or inhibit normal differentiation 2) enhance differentiation, that is induce differentiation at an earlier time point, or 3) have no effect on the normal differentiation process.
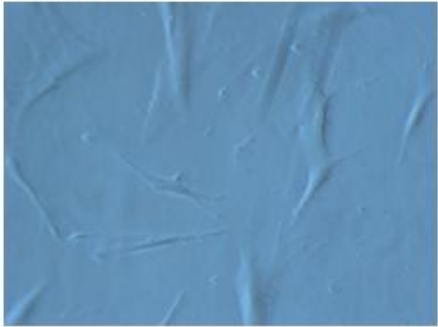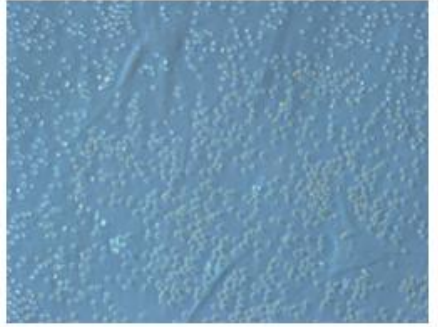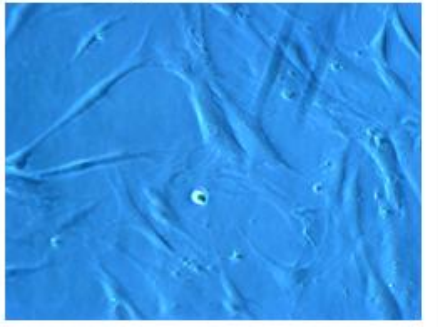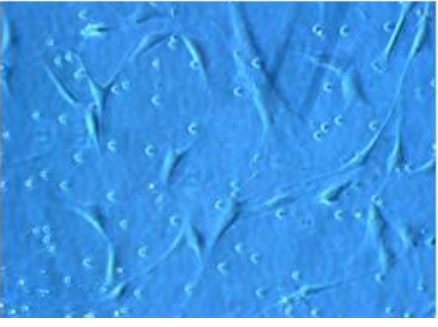
It should also be noted that the effects observed in each of these studies is the result of a 24-hour buffy coat (BC) PRP exposure. Buffy coat PRP contains concentrated platelets and WBCs therefore; the effects seen are the result of platelets, WBCs, and their contents.
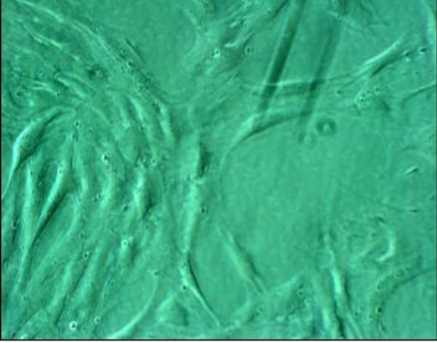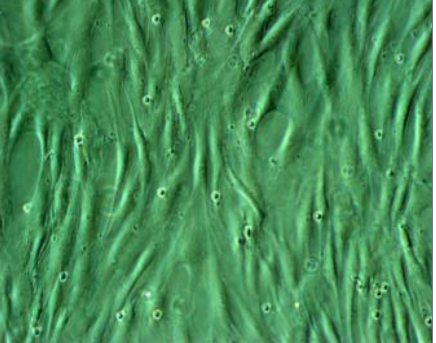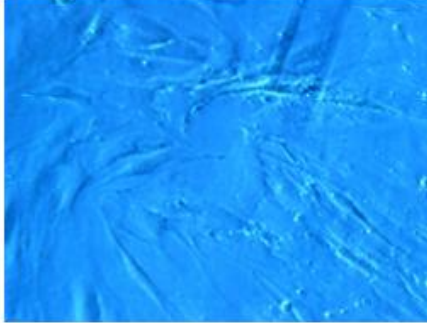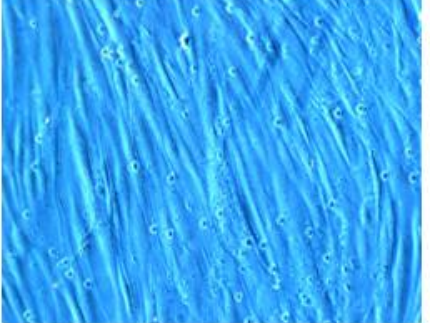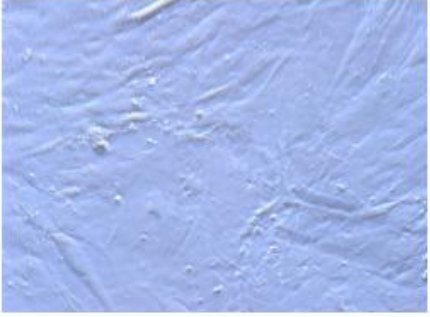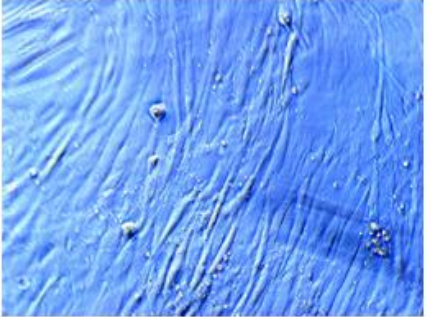
Proliferation Studies

Cell Microphotographs

To assess proliferation effects of PRP, hMSCs were cultured in either growth medium alone or growth medium with PRP. Cell counts were performed at 1, 3, 4, 5, 7, 10, and 12 days. Observations from representative photomicrographs are presented in Figure 24. Photomicrographs were done independently of the cell counts (Figure 25).

The growth medium control group represents the normal and expected growth patterns for cultured hMSCs *in vitro*. After a 24-hour PRP exposure, cells demonstrated an increase in cell number when compared to cells not exposed to PRP. Some variation exists between the photomicrographs and the cell counts because they were done independently of each other. It should be remembered that PRP contains concentrated platelets and WBCs. When observing the photomicrographs, PRP related cells (platelets and WBCs) can be observed in the growth + PRP (24-hour exposure) groups up to and including Day 5. The number of Platelets and WBCs decreases from Day 1 to Day 5 because of medium change after PRP exposure for the initial 24 hours and then again on Day 4. Medium was changed every 3 days thereafter.

Day	Growth Medium	Growth Medium + PRP (24 hr. exposure)
1		
3		

Day	Growth Medium	Growth Medium + PRP (24 hr. exposure)
4		
5		
7		
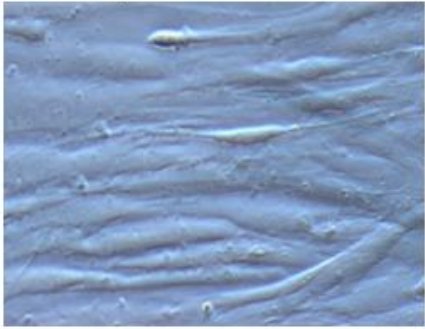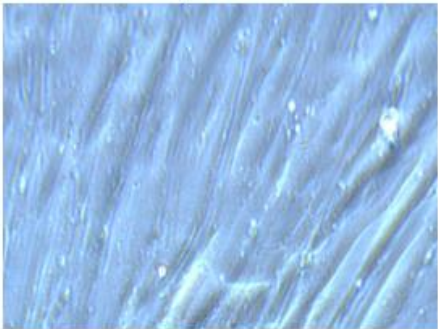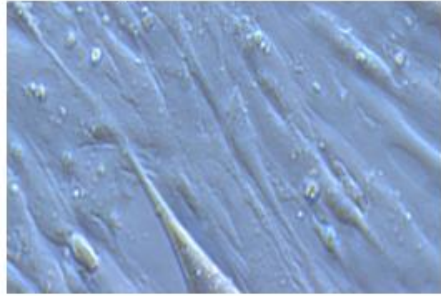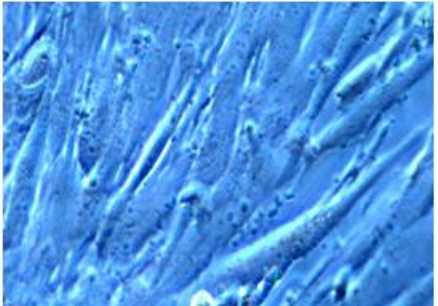
Day	Growth Medium	Growth Medium + PRP (24 hr. exposure)
10		
12		

Figure 24. Photomicrographs of Cell Cultures at Various Time Points

Representative photomicrographs of cell cultures: Cells were seeded 3×10^3 cells/cm^2 in a T-25 flask containing 10 mL of growth medium and allowed to attach to the cell flask for 24 hours. Following this 24-hour attachment period, 375 µL or PRP was added to the PRP treatment groups. Day 1 represents the cell proliferation after 24 hours of either growth medium alone or growth + PRP treatment. Several PRP related cells (platelets and WBCs) can be observed as small round dots in the Day 1 growth + PRP group photomicrograph. All media were removed and Day 1 photomicrographs taken. Subsequent microphotographs show the growth of cells in control (growth medium) and growth medium + PRP treatment for 24 hours. After this 24-hour PRP treatment, all media were removed from all flasks and replaced with growth media only. Media were changed every 3 days and replaced with growth media only. Day 3 photomicrographs demonstrate that both groups had achieved approximately 15% confluence and there are still several WBCs present in the growth + PRP treated group. On day 4, cells cultured in

growth medium had reached 25% confluence; growth + PRP had reached 80% confluence with no morphological changes and several WBCs are present. On day 5, growth group demonstrated no change in confluence, but the growth + PRP group increased to 100% confluence with noticeable changes in morphology. Fewer WBCs are present because this group had gone through two media changes. Day 7 growth group reached 40% confluence and the growth + PRP group demonstrated further morphological changes with a slight decrease in number. It is difficult to determine if any WBCs are still present in the growth + PRP treated group because of the large number of hMSCs present and morphological changes (cells spreading out and potentially overlapping). On day 10, the growth group had increased to 45% confluence with the growth + PRP group demonstrating greater morphological changes (cells are larger, layered, decreased number and crowding each other out). At Day 10 and beyond, it is difficult to determine the presence of WBCs in the growth + PRP treatment group. By day 12, the growth group reached 55% confluence with no changes in morphology, yet the PRP treated group demonstrated considerable morphological change and a continual decrease in cell number. Photomicrographs have varying colors due to the use of different cameras at different time points.

Cell Counts

Human mesenchymal stem cells were counted using phase contrast microscopy at these specified time points. Several fields were counted and photomicrographs were obtained. It should be noted that PRP contains concentrated platelets and WBCs. Therefore, the effects seen here are from PRP and all of its contents, not just the platelets, or the growth factors contained within them, although platelets and WBCs were not included in cell counts. Cell counts will be correlated with two other proliferation studies: MTT assay and total RNA expression.
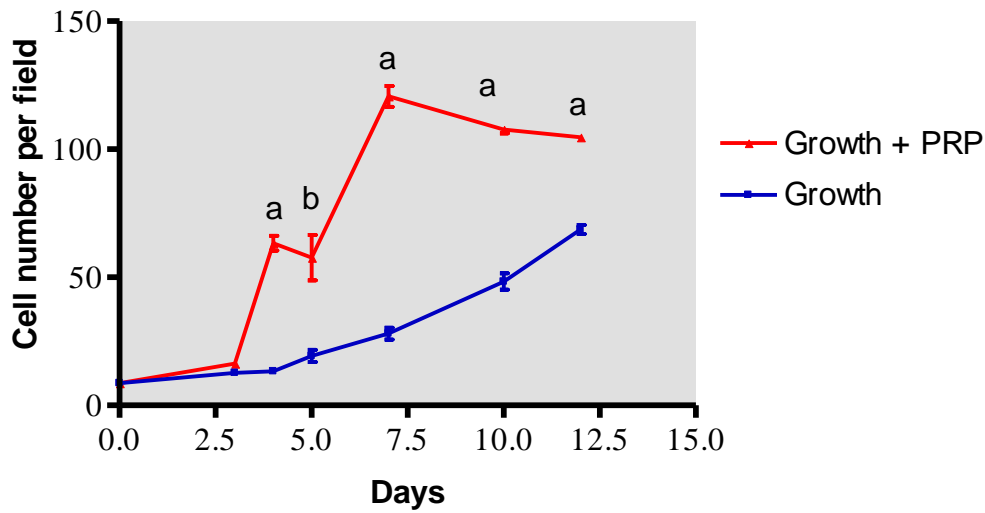
Cell Counts

Figure 25. Proliferation Confirmation with Cell Counts

hMSC counts per field after exposure to either growth medium (control) or growth medium with an initial 24-hour exposure to PRP (growth + PRP). Days 1,4,5,and 7 - N=3; Days 3, 10, and 12 - N=2. Cells were seeded at a density of 3×10^3 cells/cm^2 in a T-25 flask (represents a 1 to 6 split of an 80% confluent T-25 flask. All cell in this study were 3rd or 4th passage. Each bar represents the ± S.E.M. of 2 or 3 different tests performed in triplicate. All data for individual specific time points were analyzed with a two-tailed paired t test where significance was defined as $p < .05$, where a = $p < .01$ for Days 4, 7, 10, and 12 and b = $p < .05$ for Day 5. Examination of the actual cell counts at each individual time point (Days 1, 3, 4, 5,7, 10, and 12) with a two-tailed paired t test the PRP treatment had a significant effect ($p < .01$) on cell number for days 4, 7, 10 and 12 in comparison to cells that did not receive the 24-hour PRP treatment. There was also a significant increase on cell number with the 24-hour PRP treatment on day 5 ($p < .05$). Two-way ANOVA revealed that for the entire 12-day time, PRP treatment had a significant effect (F=583.1, $p < .0001$) on cell proliferation; total 12 day time elapsed also have a significant effect (F=206.2, $p < .0001$) on proliferation; PRP treatment and time elapsed were related to each other (F=53.68, $p < .0001$). Therefore, not only does PRP treatment affect cell proliferation, but also time elapsed from the start of the experiment has a significant effect on proliferation.

124

MTT Analysis

The MTT analysis was used as a measure of cell proliferation. The MTT assay monitors changes in mitochondrial activity, whereby increases in mitochondrial activity are associated with increased numbers of cells. Figure 26 illustrates increased mitochondrial activity with PRP-treated cells up to Day 5, after which the control cells demonstrated greater activity. Again, it should be noted that PRP contains concentrated platelets and WBCs. Therefore, the effects observed are from PRP and all of its contents, not just platelets, or the growth factors contained within them. Platelets and WBCs contain mitochondrial reductase that may be presenting a confounding factor for interpretation of the MTT data (15). There was significantly less activity in the PRP-treated cells in comparison to the non PRP-treated cells on Days 6 and 10, which corresponds to the decrease in platelet and WBC numbers observed in the photomicrographs (Figure 24). The mitochondrial reductase from the platelets and WBCs would reduce the soluble tetrazolium salt (MTT) into an insoluble formazan precipitate and therefore, prevented a portion of the MTT from entering the hMSCs. This decreased uptake of the soluble tetrazolium salt would mute the actual mitochondrial reductase activity of the hMSCs. There may have been more hMSCs, but there was insufficient concentration of the tetrazolium salt to record the true viability (number) of hMSCs. Figure 26 illustrates that MTT absorbance is significantly greater in the PRP-treated cells for the first 5 days (except Day 2), but these values may be artificially low in comparison to what should have been observed. Even though muted, significantly greater MTT activity was seen with PRP-treated cells in comparison to non-PRP-treated cells. This corresponds with the initial 5day significant increase in cell number observed

with growth + PRP (Figure 25). The finding of less MTT activity for PRP-treated cells in comparison to non PRP-treated cells after Day 5 is not surprising when compared with the cell count data (Figure 25), where the non PRP-treated cells continued to proliferate and the PRP-treated cells had reached a post-mitotic state. It would appear that after Day 5 the PRP-treated cells are not proliferating at the same rate as the non PRP-treated cells, possibly because the cells are beginning to become differentiated, and thus post mitotic. This indicates that the PRP exposure had a significant effect on proliferation in comparison to non PRP-treated cells for the initial 5 days, but when considering the entire10-day time, the effect of PRP treatment was lost over the time. Interestingly, the MTT activity did continue to increase for both non PRP-treated cells and PRP-treated cells. The significant increase in MTT activity between days 6 and 10 for non PRP-treated cells is due to continued proliferation as which correlates with cell count data (Figure 25). A possible explanation for the significant increase in MTT activity between days 6 and 10 for PRP-treated cells may be due to the decreased number of platelets and WBCs in the flask due to successive media changes that facilitate removal of any PRP residual PRP cells after the initial 24-hour PRP exposure. There is the possibly a portion of the tetrazolium salts may have been reduced prematurely by the mitochondrial reductase present in residual platelets or WBCs mixed in with the hMSCs or osteoblasts particularly at the earlier time points, therefore, producing an artificially low MTT absorbance for the initial 5 days. If a portion of the tetrazolium salts had been reduced by platelet or WBC mitochondrial reductase the full amount of MTT would not have been available for hMSCs uptake, therefore providing an artificially low MTT absorbance value for the initial 5 days. There may be other explanations for the increase in MTT

126

absorbance observed at Day 10. The Day 10 MTT reported value may be the more

accurate representation of total number of viable hMSCs that received PRP exposure,

than are earlier time point values. From this data, it is now known that a different

methodology to confirm cell viability is necessary for future experiments involving PRP

treated cells.
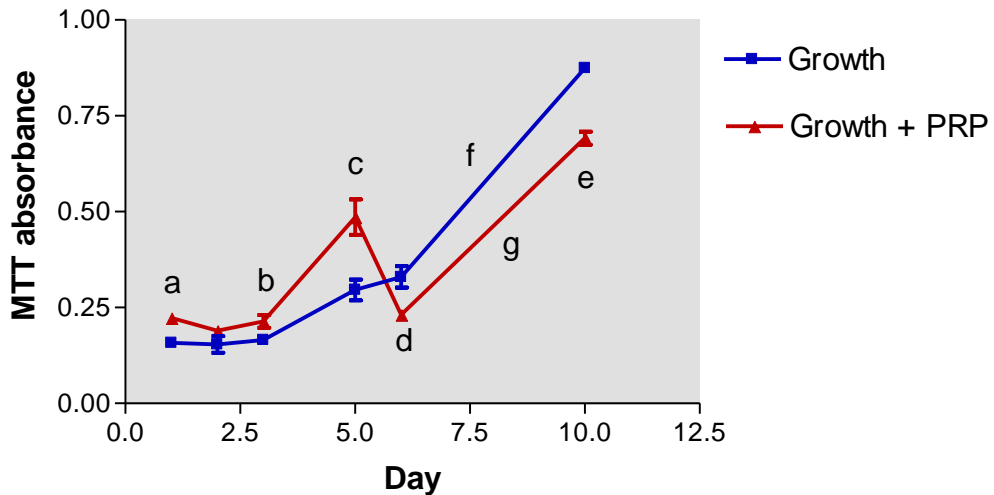
Figure 26. MTT Measured Cell Proliferation Effects of

Growth and Growth + PRP Media

Mitochondrial reductase activity in cells cultured in growth medium and cells
cultured in growth medium with an initial 24-hour PRP exposure. All cells in this study
were 3rd or 4th passage. Each bar represents the ± S.E.M. for N=3 with tests performed in
triplicate. All data for individual specific time points were analyzed with a two-tailed
paired t test where significance was defined as $p < .05$. Where a = p < .0001, PRP-treated
cells had significantly greater activity on day one ($p < .001$) when compared with cells
not receiving the 24-hour PRP treatment. For b = $p < .05$, PRP-treated cells had
significantly greater activity on day three when compared with cells not receiving the 24-
hour PRP treatment. Where c = $p < .01$, PRP-treated cells had significantly greater
activity on day five when compared with cells not receiving the 24-hour PRP treatment.
Where d = $p < .01$, non PRP-treated cells had significantly greater activity on day six
when compared with cells receiving the 24-hour PRP treatment. For e = $p < .0001$, non
PRP-treated cells had significantly greater activity on day ten when compared with cells

receiving the 24-hour PRP treatment. Where f = p < .0001 as an unpaired two-tailed t test found a significant difference between Day 6 and Day 10 MTT activity for cells not treated with PRP. For g = p < .0001 as an unpaired two tailed t test found a significant difference between Day 6 and Day 10 MTT activity for cells receiving the 24-hour PRP treatment. Two-way ANOVA analysis for the initial 5 days revealed that both treatment (F = 832.48, p < .0001) and time (F = 48.33, p < .0001) were significant. The interaction between treatment and time was significant (F = 5.686, $p < .05$). However, there was significantly less MTT activity in the PRP-treated cells on Days 6 and 10 when compared to non-PRP treated cells. For the entire 10 day period treatment was not significant (F = 0.7060, $p > .05$), and time was significant (F = 278.9. $p < .0001$). The interaction between treatment and time was significant (F = 21.68, $p < .0001$). This indicates that the PRP exposure had a significant effect on MTT activity for the initial 5 days, but when confluence was reached due to contact inhibition, continued benefits of PRP-treatment in comparison to non-PRP treated cells was not evident.

Total RNA Production

Another indicator of cell proliferation that was examined is global (total) RNA

production on Days 5, 10 and 21. *De novo* biosynthesis of pyrimidine nucleotides is an

indicator of DNA synthesis, metabolic activity, and cell proliferation (419, 421, 422).

Total RNA evaluation results are shown in Figure 27 A-C.
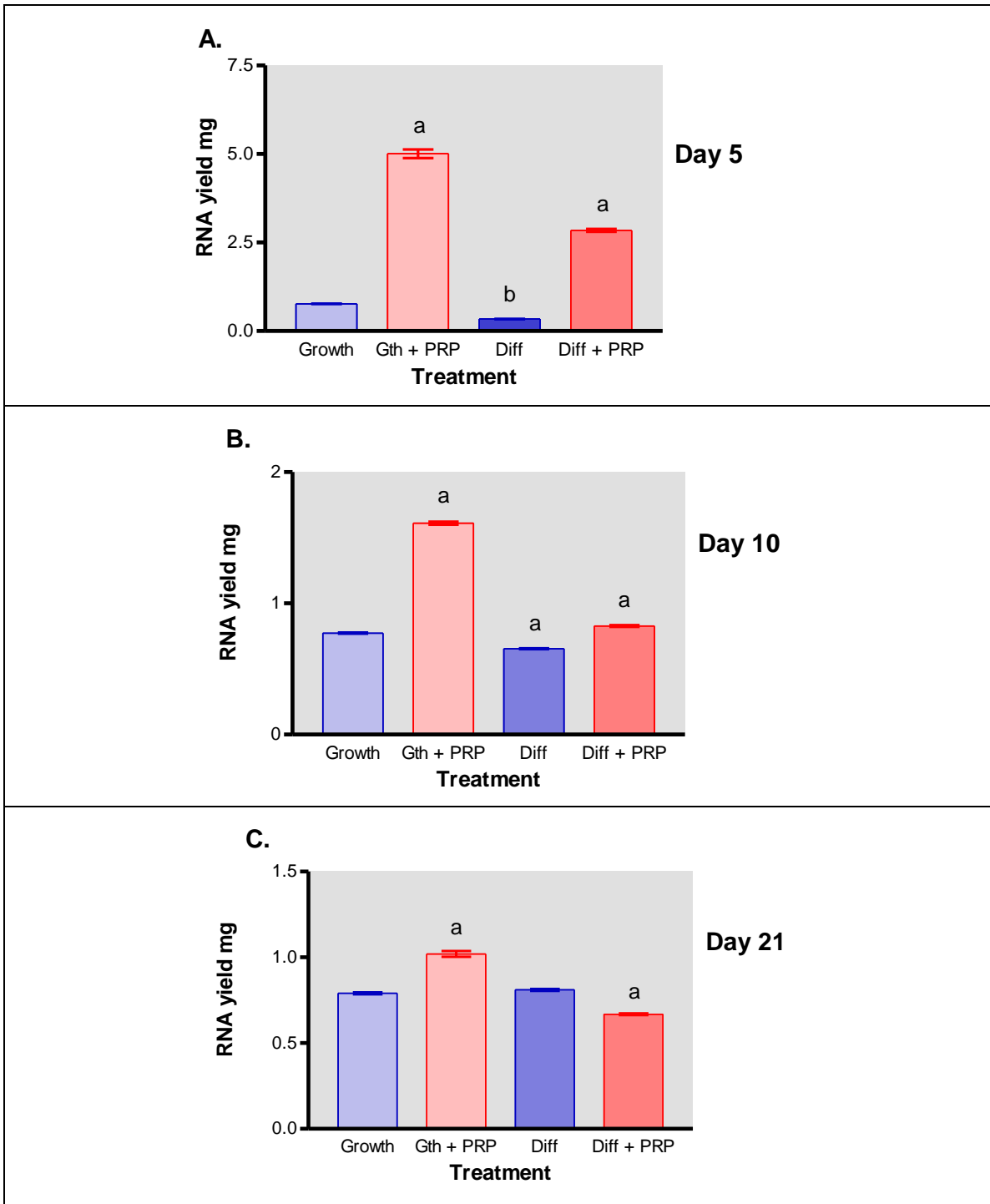
Figure 27. Total RNA Yield Days 5, 10, and 21

RNA yield measured with spectrophotometry at 260:280 ratio demonstrated all RNA preparations were of good quality. All cells in this study were 3rd or 4th passage. Each bar represents the ± S.E.M. for N=3 with tests performed in triplicate. All data were analyzed with a one-way ANOVA with a Newman Keuls post-hoc test where significance was defined as $p < .05$, where a $= p < .001$; b$= p < .01$. Newman Keuls analysis represents the comparison between each of the groups. Growth + PRP and Diff (differentiation) + PRP represent a 24-hour exposure of 3.75% v/v PRP followed by growth or differentiation medium only. All media was changed every 3 days. Note: Y-axis scale changes between A-C for illustrative purposes. For Day 5 (A) where a $= p < .001$ analysis revealed a significant difference between all groups; where b$= p < .01$ there was a significant difference between cells cultured in growth medium and cells cultured in differentiation medium. Growth + PRP and differentiation + PRP groups showed the greatest yield of total RNA. For Day 10 (B) where a $= p < .001$ analyses showed a significant difference between all groups with the PRP treated groups having the greatest RNA yield. The RNA yield for these two groups is approximately 1/3 of that seen on Day 5. For Day 21 (C) where a $= p < .001$ there is a significant difference between all groups except for cells cultured in growth and differentiation media where there was no significant difference. Total RNA yield for the growth and differentiation media groups remained similar to those of Days 5 and 10. PRP-treated groups maintain a signficant increase in RNA yield over the growth and differentitation media groups. The difference between the PRP-treated groups is also significant with the Growth + PRP yielding the most RNA. The total RNA yield for the Growth + PRP group is again highest, but the level is only 2/3 that of Day 10 and only 1/5 that of Day 5. This again demonstrates that PRP treatment does have some effect on total RNA yield, but the effect diminishes with time. This effect may be due to continual removal of residual platelets and WBCs with media changes every 3 days.

For Day 5 (Figure 27 A), one-way ANOVA with a post-hoc Newman Keuls analysis revealed a significant difference between all the groups. The growth + PRP group had the greatest global RNA yield - approximately 5 times that of control and twice that of differentiation + PRP. Cells cultured in differentiation medium demonstrated the lowest level of RNA production at day 5. This is expected because in differentiation medium the total number of cells does not increase significantly. Figure 27 A clearly shows the PRP-induced positive effect on RNA yield on Day 5. These results correlate with the MTT data and cell count data offering additional support for the early positive proliferative effects of PRP on hMSCs. This day 5 specific time point is also the time

when PRP-treated cells reached 100% confluence. Cell counts for the PRP-treated group increased by 3.2 fold at day 5 and MTT data had a 2-fold increase, yet the total RNA yield was increased by 5-fold. This large discrepancy in cell count and total RNA values may not represent only an increase in hMSC cell number as PRP contains platelets and WBCs that may be contributing to the RNA levels.

Figure 27 B illustrates the continual PRP-increase in total RNA as seen at day 10. RNA yield in the PRP-treated groups was again significant ($p < .001$) when compared to the non-treated groups. The Growth + PRP group had approximately twice the RNA level compared to the other 3 groups. It is also noteworthy that the RNA levels from the PRP-treated groups is about 1/3 that of Day 5 values, possibly due to the reduction in platelets and WBCs remaining in the culture. RNA yield levels for the non-PRP treated groups remained similar to those on Day 5 despite an increase in cell number.

 Day 21 (Figure 27 C), illustrates that the PRP-treated groups still maintain a signficant ($p < .001$) increase in RNA yield over the growth and differentitation media groups. The difference between the PRP-treated groups is also significant ($p < .001$) with the Growth + PRP yielding the most RNA. The non-treated groups have maintained approximately the same level of RNA production as found on Days 5 and 10, despite increases in cell number (Figure 25). The total RNA yield for the Growth + PRP group is again highest, but the level is only 2/3 that of Day 10 and only 1/5 that of Day 5. This again demonstrates that PRP treatment does have some effect on total RNA yield, but the effect diminishes with time.   This effect may be due to continual removal of residual platelets and WBCs with media changes every 3 days.

Differentiation Studies

Differentiation of hMSCs into osteoblasts was measured by the alkaline phosphatase assay (ALP) and examination of expression of specific mRNAs markers that would signify osteoblast formation. It should be remembered that these studies were performed by the application of 375 µL of BC-PRP for 24 hours following an initial cell attachment to the flask in either growth or differentiation medium. Therefore, the effects seen are for PRP and its constituents, platelets and WBCs and the cytokines and GFs contained within them. For growth medium, it is expected that ALP levels would remain unchanged between Day 5 and 15 because differentiation is not expected. For differentiation medium, it is anticipated that there will be a significant increase in ALP in comparison to growth medium alone. If PRP does induce differentiation, it would be expected to increase ALP expression on either Day 5 or 15 for cells cultured with growth + PRP or differentiation + PRP media.

The rationale for using growth ± PRP is to determine if PRP can induce differentiation without the aid of ingredients of differentiation medium, which is known to induce differentiation. Differentiation ± PRP is examined to determine if PRP alters or impedes the differentiation that is normally seen with differentiation medium. The *in vivo* environment more closely resembles the environment of differentiation medium than it does growth medium.

When hMSCs differentiate into bone-forming osteoblasts, the intracellular levels of ALP increase (436). Aubin et al. (431) found that as hMSCs became committed to mature osteoblasts that these cells became characterized by loss of proliferative capacity

and sequential increased markers of expression, specifically, alkaline phosphatase, followed by bone sialoprotein, and osteocalcin. This enzyme is used to dephosphorylate target proteins at specific sites that induce cellular consequences leading to cellular differentiation (437). Cells (Figure 28) were incubated in growth medium with and without PRP, and in differentiation medium with or without PRP as described previously. PRP treatments occurred in the first 24 hours. ALP was quantified by standard assays as described in the Materials and Methods section on page 114. ALP evaluation was performed with N=2 among small coefficients of variation. Since ALP expression was not normalized with cell number or total protein and there were, varying cell numbers present depending upon the culture medium of the treatment group, the ALP increases may reflect increased cell number. For Day 5, the growth medium cells had achieved a 45% confluence, differentiation medium cells had a 20% confluence, differentiation + PRP medium cells had a 55% confluence, and growth + PRP had achieved a 100% confluence. At Day 15, growth and growth + PRP media cells had reached 100% confluence, differentiation medium cells were at 85%, and differentiation + PRP medium cells had reached 90% confluence. Future examination of ALP levels will use equivalent cell number or normalize to protein to allow direct comparison to all the groups and different time points. Different time points will be examined because PRP may shift differentiation of hMSCs either earlier or later than what is normally observed.

ALP results are reported in Figure 28. It should be noted that with the small sample size (N=2) and lack of normalization for cell number statistical analysis cannot be performed on these data (Figure 28 A, B).
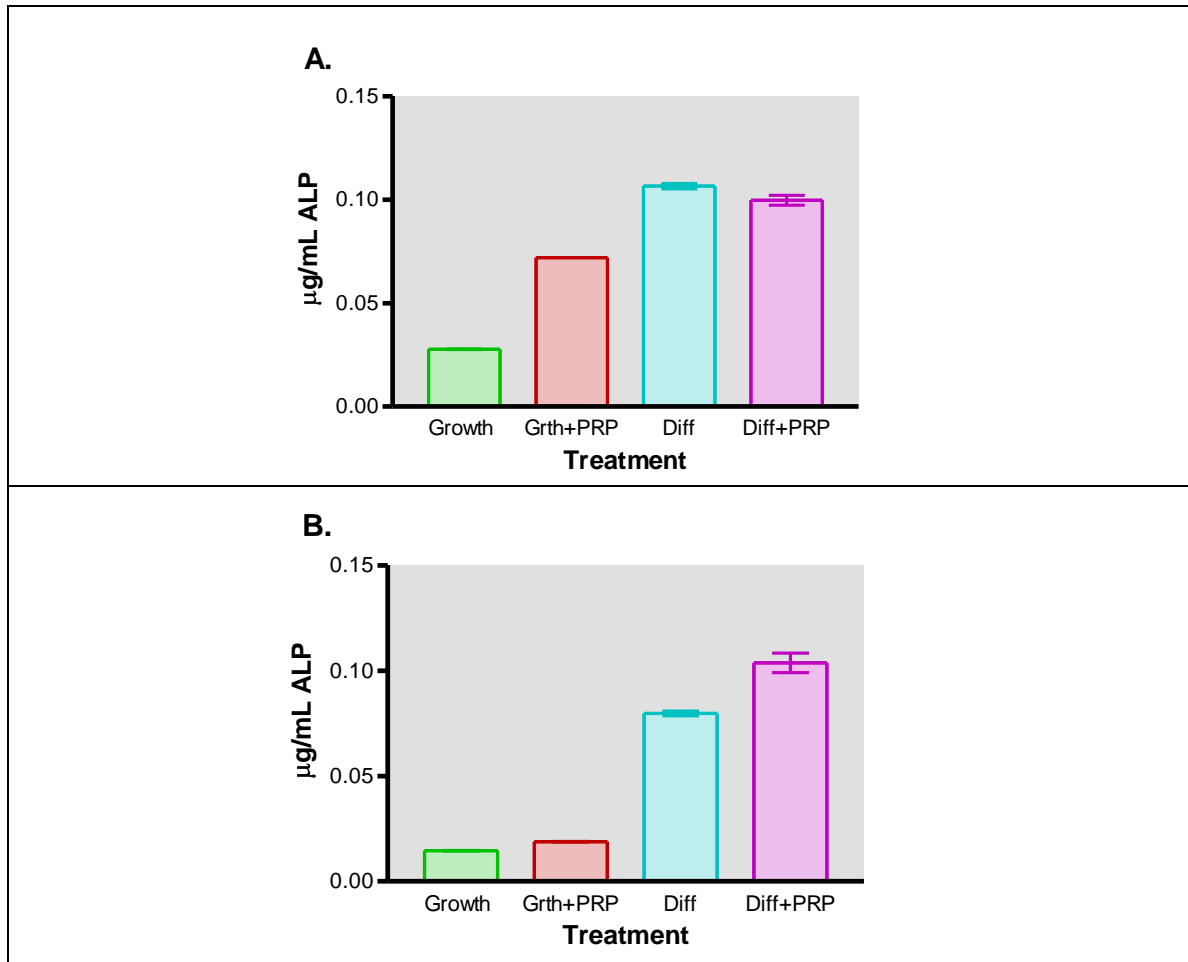
Figure 28. Alkaline Phosphatase Activity on Days 5 and 15

Alkaline Phosphatase activity (μg/mL) was quantified using spectrophotometry at 405nm for days 5 (A) and 15 (B) in the various media. Cells were seeded on collagen-coated coverslips (Biocoat® Franklin Lakes NJ) at 2000 cells/cm^2. All cells in this study were 3rd or 4th passage. Growth + PRP and Diff (differentiation) + PRP represent a 24-hour exposure of 3.75% v/v PRP followed by growth or differentiation medium only. All media was changed every 3 days. Each bar represents the ± S.E.M. for N=2 with tests performed in triplicate. Statistical analysis cannot be performed because of the small sample size. ALP expression is not normalized to cell number or total protein. At Day 5 (A), there is a baseline level of ALP in growth medium. In differentiation ± PRP medium, the levels increased 4-fold when compared to growth medium. Additionally, growth + PRP-treated cultures reveal a 3-fold increase at Day 5 when compared to growth medium alone. This suggests that at Day 5 PRP can induce differentiation in growth medium that does not contain the differentiation inducing factors dexamethasone, ascorbic acid, and β-glycerophosphate found in differentiation medium. All cell

treatment groups began with the same number of cells, but as time progressed each of the flasks experienced proliferation of cells at individual rates depending on the medium. Panel B illustrates ALP levels in cultures at day 15. Differentiation medium increased ALP 3-fold over the growth groups and differentiation medium + PRP induced a 4-fold increase ALP over the cells receiving growth medium with or without PRP at Day 15. It should be noted that the ALP levels in differentiation medium alone at Day 5 are higher than that seen on Day 5 for cells cultured in growth medium + PRP, however, ALP expression for differentiation medium on Day 15 is similar to that seen on Day 5 for growth + PRP medium. This suggests that a shift in the time of differentiation may be occurring with PRP treatment.

Figure 28 A illustrates, as expected, that there is only a baseline level of ALP in control cells (growth medium) at day 5. In differentiation medium, the levels increased 4-fold with or without PRP. However, PRP-treated cultures in growth medium also show a 3-fold increase in ALP at 5 days. There is a substantial difference between differentiation medium and differentiation + PRP medium at Day 5. This suggests that at Day 5 PRP can induce differentiation in growth medium that does not contain the differentiation-inducing factors that differentiation medium contains (dexamethasone, ascorbic acid, and β-glycerophosphate), therefore PRP contents (platelets and/or WBCs) contain the factors necessary for the early steps of differentiation. However, the increase in ALP levels for PRP-treated cells in growth medium is substantially less than that observed with differentiation or differentiation media. Differentiation + PRP treatment had substantially less ALP expression than differentiation medium alone, suggesting the PRP may delay differentiation.

Figure 28 B illustrates ALP levels in cell cultures at day 15. It should again be noted that the ALP levels in differentiation medium alone at Day 5 are higher than that seen on Day 5 for cells cultured in growth medium with PRP, however, ALP expression for differentiation medium on Day 15 is similar to that seen on Day 5 for growth + PRP

medium. In a study by Jaiswal *et al.* (438) using the same differentiation media, ALP activity was present on Day 4, doubled on Day 8, peaked at day 11, and then decreased as bone sialoprotein and osteocalcin mRNA markers were expressed. Therefore, it appears that in differentiation medium alone the Day 5 ALP levels may be earlier than ALP's normal expression peak and the Day 15 ALP levels may be beyond the peak and decreasing. Since, in the differentiation + PRP medium ALP activity is less than differentiation medium at Day 5, but more than differentiation medium at Day 15, this suggests that PRP does not stop the differentiation process. However, it may delay differentiation due to the initial 5 day proliferation period that is seen in cell count (Figure 25), MTT activity (Figure 26) and total RNA yield (Figure 27). The differentiation process appears to be delayed until the proliferation is complete. This suggestion is supported by Parsons *et al.* (439) who found that platelet rich concentrate, when added to the culture medium as a clot, induced an earlier onset of proliferation followed by a sustained increase in the key osteogenic transcription actor *RUNX2*.

Figure 29 reflects graphs that correct for the differences in cell density for the various treatment groups as Days 5 and 15. These data demonstrate that ALP activity is highest in the differentiation medium on Day 5, which correlates with previous reports (438). PRP addition to differentiation medium reduced ALP activity, possibly due to an initial period of proliferation preceeding differentiation. Differentiation + PRP is higher than growth medium alone suggesting some level of differentiation has begun. On Day 15, differentiation + PRP is similar to differentiation alone, suggestin that both treatments are past the peak times for ALP activity (438). Additional time points are also required to assess whether PRP addition to differentiation medium modifies the differentiation

capacity of the cultured hMSC cells. However, since cell density was estimated based on visual inspection and adjustments to ALP activity based on cell density may not be equivalent at varing levels of confluence, these trends will need to be confirmed in future studies by quantifying cell number.
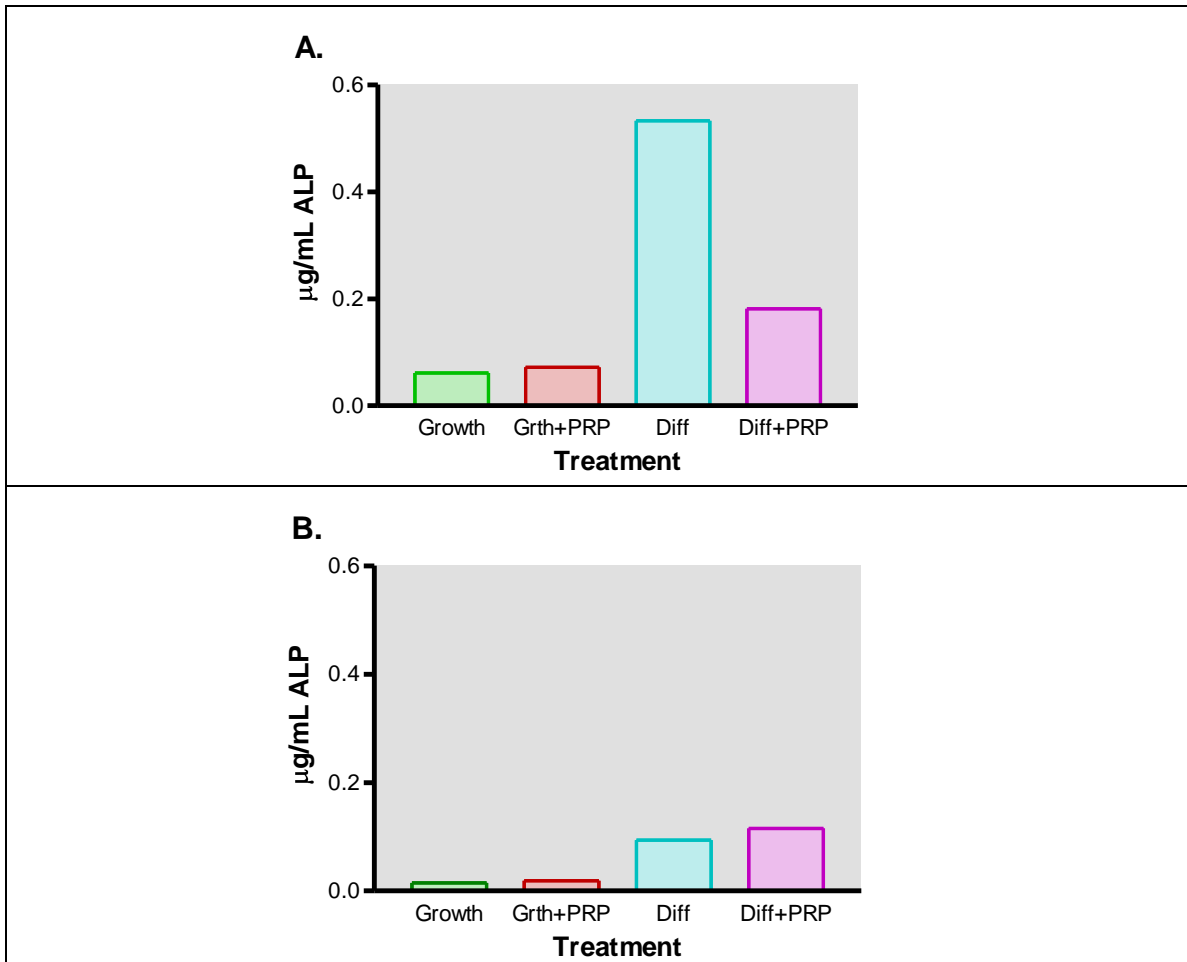
Figure 29. Alkaline Phosphatase Activity Corrected for Cell Density on Days 5 and 15

Alkaline Phosphatase (ALP) expression observed in Figure 28 is corrected for cell density variations between media at Day 5 (A) and Day 15 (B). Calculations were made by taking the actual ALP expression and multiplying it by the recorded cell density

(percentage confluence) for each medium at the respective time points. These values are then represented by the bars. This data cannot be analyzed for statistical significance because the data is corrected by individual interpretations of confluence and not actual cell counts and the small sample size. Panel A illustrates that as expected differentiation medium has the greatest ALP expression and growth medium has the least. It also appears that differentiation + PRP medium decreased the expression of ALP when compared to differentiation medium at Day 5, but at Day 15, differentiation and differentiation + PRP are similar. Differentiation medium has ALP expression similar to that observed with growth + PRP at Day 5 (A). Base on the time points examined this data suggests that PRP may not have the necessary factors to induce differentiation in growth media. When PRP is added to differentiation medium, differentiation still occurs, but it is suppressed at Day 5. It is difficult to say if differentiation is suppressed or if differentiation is shifted to an earlier or later time point. Most likely it would be to a later time point because it enhances proliferation at the earlier time point. Differentiation follows proliferation.

PRP contains the factors necessary to increase proliferation in growth medium (Figures 25-27). PRP may not induce differentiation in growth medium; however, because of the small sample size (N=2) and cell number was not normalized for the ALP assay, these data cannot be analyzed for statistical significance. Therefore, no definitive conclusions about PRP's effects on differentiation are possible from the current study. However, after normalizing ALP activity by correcting for cell density (Figure 29) there does not appear to be enhanced ALP activity in growth + PRP medium when compared to growth medium alone at either Days 5 or 15. Other time points may reveal different hypothesis, but at Day 5 and 15 enhanced ALP activity with PRP treatment in growth medium does not appear to occur. The decreased ALP activity with differentiation + PRP medium when compared to differentiation medium alone at Day 5 suggests that PRP may affect the differentiation process when differentiation signals are present. At Day 15, differentiation + PRP medium ALP activity is similar to that observed with differentiation medium. Therefore, at this one specific time point (Day 15) it appears that PRP did not affect differentiation. However, it cannot be clearly stated if differentiation + PRP medium reached the same peak of ALP activity at any time when compared to

differentiation medium. In addition, this study we cannot conclude when the peak in ALP activity with differentiation medium occurred. From this data, it can be suggested that PRP does not stop differentiation. However, it does not effectively address to what degree it affects differentiation. These data suggest that it may either delay and decrease differentiation, but this does not match what is seen clinically. Clincally early bone development occurs; therefore, in the *in vivo* environment it does not appear to substantially alter the differentiation process in a negative manner. Perhaps, the differentiation process is delayed until after proliferation has ended. Future studies to examine the effect of PRP on the early differentiation marker ALP will include a larger sample size and normalization with either cell number or protein levels and additional time points to determine if a shift in the differentiation process does occur.

Real time RT-PCR

Finally, differentiation was examined by looking at expression of key genes that are known to be switched on during osteogenesis. These genes are bone sialoprotein (IBSP) and osteocalcin (BGLAP). As a baseline control, expression of the housekeeper gene for glyceraldehyde-3 phosphate dehydrogenase (GAPDH) was monitored. The glycoprotein IIb gene (ITGA2B) was chosen because it is expected to be expressed in platelets specifically and would serve as a method of monitoring platelet mRNA contribution (59, 60, 294, 300). It was predicted that with a 24-hour PRP exposure and successive medium changes that all platelets would be removed and, therefore, ITGA2B expression would be non-existent after Day 5. Unexpectedly, ITGA2B was found expressed in all of the treatment groups, not just those that had been exposed to PRP (Table 8).

Real-time RT-PCR experiments were done in triplicate with 3 readings taken for each sample. For normalizing the tested osteoblast markers, a housekeeper gene, GAPDH, was also monitored. Gene expression was measured as a threshold cycle (C_T) value.

The analysis revealed that the housekeeper gene (GAPDH) was expressed 2-3 cycles sooner at the 5- and 10-day time points in the cells that had been exposed to PRP versus cells that had not received PRP treatment (Table 9). For accurate normalization, GAPDH expression should be consistent across all groups. In the PRP-treated groups, GAPDH expression is likely higher due to the presence of WBCs and other cellular constituents present in PRP. Therefore, C_T values for the PRP treated groups at Days 5 and 10 may not reflect effects observed only in hMSCs. However, GAPDH mRNA expression (C_T values) at Day 21were consistent between all groups (growth, growth + PRP, differentiation, and differentiation + PRP) and therefore analysis could be performed for all groups at this specific time point. At Days 5 and 10, GAPDH C_T values were consistent for the non-PRP groups; therefore, analysis could be performed for these groups on Days 5 and 10, unlike the PRP treated groups. Examining the C_T values for the non-PRP-treated groups at these time points provides confirmation that these genes are expressed as expected and therefore, confirms that differentiation medium does induce differentiation and growth medium alone results in little expression of these osteoblast markers.

Gene	Treatment	Day 5	Day 10	Day 21
GAPDH	Growth [a]	15.35	17.71	19.92
	Growth + PRP [b]	12.11	14.91	21.13
	Differentiation [a]	14.94	16.67	21.51
	Differentiation + PRP [b]	12.17	15.57	22.54
IBSP	Growth	16.19	15.94	14.77
	Growth + PRP	16.44	15.85	14.91
	Differentiation	16.24	15.70	14.66
	Differentiation + PRP	17.34	15.46	14.92
Bglap	Growth	25.07	24.02	24.30
	Growth + PRP	24.54	23.43	25.03
	Differentiation	25.51	23.87	24.90
	Differentiation + PRP	23.78	23.40	24.60
ITGA2B	Growth	30.37	29.39	29.18
	Growth + PRP	30.29	28.87	29.07
	Differentiation	30.72	28.79	28.83
	Differentiation + PRP	30.69	28.68	29.15

Table 9. C_T Values for Genes of Interest

C_T values for the genes of interest with the various treatment conditions. It should be noted that the lower the C_T value the greater the expression of the gene(s) and conversely, the higher the C_T value the lower the expression of the gene(s). The target genes (IBSP, BGLAP) and the platelet gene (ITGA2B) from the various treatment groups were normalized to the housekeeping gene found in the same RT preparation for which the target gene was evaluated. Note [a] consistency of C_T values for GAPDH on Days 5 and 10 (groups not exposed to PRP). Note [b] consistency of C_T value for GAPDH on Days 5 and 10 (groups were exposed to PRP). Note that C_T values for other genes in all treatment groups were consistent within each time point (meaning gene expression began at similar cycles of the real time RT-PCR process).

The question of whether differentiation occurred was addressed by the expression of the IBSP (bone sialoprotein) and BGLAP (osteocalcin) mRNAs for cells cultured in differentiation media as measured by real time RT-PCR. The IBSP gene expression has been reported to increase during middle to late stages of differentiation (14-21 days) and occurs prior to BGLAP gene mRNA expression at 21-28 days for hMSCs cultured in differentiation medium (275, 282, 287, 288).   Table 10 examines the expression of IBSP and BGLAP mRNAs on Days 10 and 21 relative to Day 5 for growth and differentiation media.

The relative quantification (fold changes) in expression for the genes of interest ($\Delta\Delta C_T$) for Days 10 and 21 relative to Day 5 in its medium were calculated and summarized in Table 10. The relative quantification calculation was performed by examining the gene of interest's ΔC_T expression for Day 10 or 21 in medium of interest (growth or differentiation media) and comparing this value to Day 5 (control) ΔC_T expression for the gene of interest in the same medium. $\Delta\Delta C_T$ values were calculated by subtracting the target gene's ΔC_T from the medium of interest (growth or differentiation) on Day 5 (control) from the ΔC_T value for the target gene in the medium of interest on Day 10 or 21. The final calculation (fold increase in expression) involved raising the efficiency value (2) to the negative $\Delta\Delta C_T$ value for the target gene. Calculations were done by raising the efficiency (e) of the gene to the negative power of the average target gene ΔC_T minus the average control gene ΔC_T for medium of interest (growth or differentiation medium). The formula used is: $e^{-(\text{target } \Delta C_T - \text{control } \Delta C_T)}$. An efficiency of "2" was used for all calculations. Table 10 lists the relative fold changes for IBSP and BGLAP gene expression on Days 10 and 21 compared with Day 5 for medium of interest

(growth medium or differentiation). These data are of importance because they confirm

that differentiation medium is inducing the hMSCs to induce the expression of

differentiation markers. Therefore, suggesting that osteogenic differentiation is taking

place.

Gene	Treatment	Day 5	Day 10	Day 21
IBSP	Growth	1	8.09	84.16
	Differentiation	1	1.74	413.96
BGLAP	Growth	1	12.91	49.12
	Differentiation	1	3.39	188.92

Table 10. Relative Quantification of Gene Expression for Days 10 and 21 When Compared with Day 5 for Growth and Differentiation media Using the Comparative C_T Method

The relative quantification of IBSP and BGLAP gene expression over time is shown for growth and differentiation media. There are 3 C_T readings for each sample. N=3 and each sample was run in triplicate. The average C_T was calculated for each day followed by averaging the three daily averages together. Method of calculation is presented in the text.   IBSP and BGLAP gene expression for Days 10 and 21 relative to Day 5 for growth and differentiation media illustrate that the relative IBSP gene expression at Day 21in differentiation medium is 413.96 times that of Day 1. This is expected because the IBSP mRNA is expressed at 14 to 21 days after initiation of the differentiation process. IBSP mRNA gene expression also precedes the expression of the BGLAP mRNA that is normally expressed at 21 to 28 days. BGLAP mRNA gene expression at Day 21 is 188.92 times that of Day 1. For both of these genes the mRNA gene expression of Day 21 exceeds that of Days 1 and 10 by several fold; therefore suggesting that these hMSCs are differentiation process of becoming osteoblasts.

Bone sialoprotein gene (IBSP) mRNA Δ C_T values for growth and differentiation

media are illustrated in Figure 30 A-C. Δ C_T values relate to the cycle at which the gene

is expressed after normalization to the housekeeper (GAPDH) for each sample. Because

these are ΔC_T values, the more positive or higher the values (bars) represent less

expression of the mRNA for that particular gene. Therefore, the lower, or more negative,

the ΔC_T values, the greater the gene mRNA expression. To find the relative expression of

the gene between treatment groups versus the control, one must examine the $\Delta\Delta C_T$ value.

To determine the $\Delta\Delta C_T$ value, the average ΔC_T values for the gene of interest in the

medium of interest is compared to the average ΔC_T values for the same gene in the

control (growth) medium. $\Delta\Delta C_T$ values are calculated by raising the efficiency of the

primer to the negative power of the growth medium target genes average ΔC_T value

minus the target gene average ΔC_T value for the medium of interest. The fold changes

between treatment groups for each time point are represented in Table 11. As sample

variation for calculating statistical significance is determined from the ΔC_T, these values

and not the $\Delta\Delta C_T$ or fold changes are graphed in Figures 30-32.
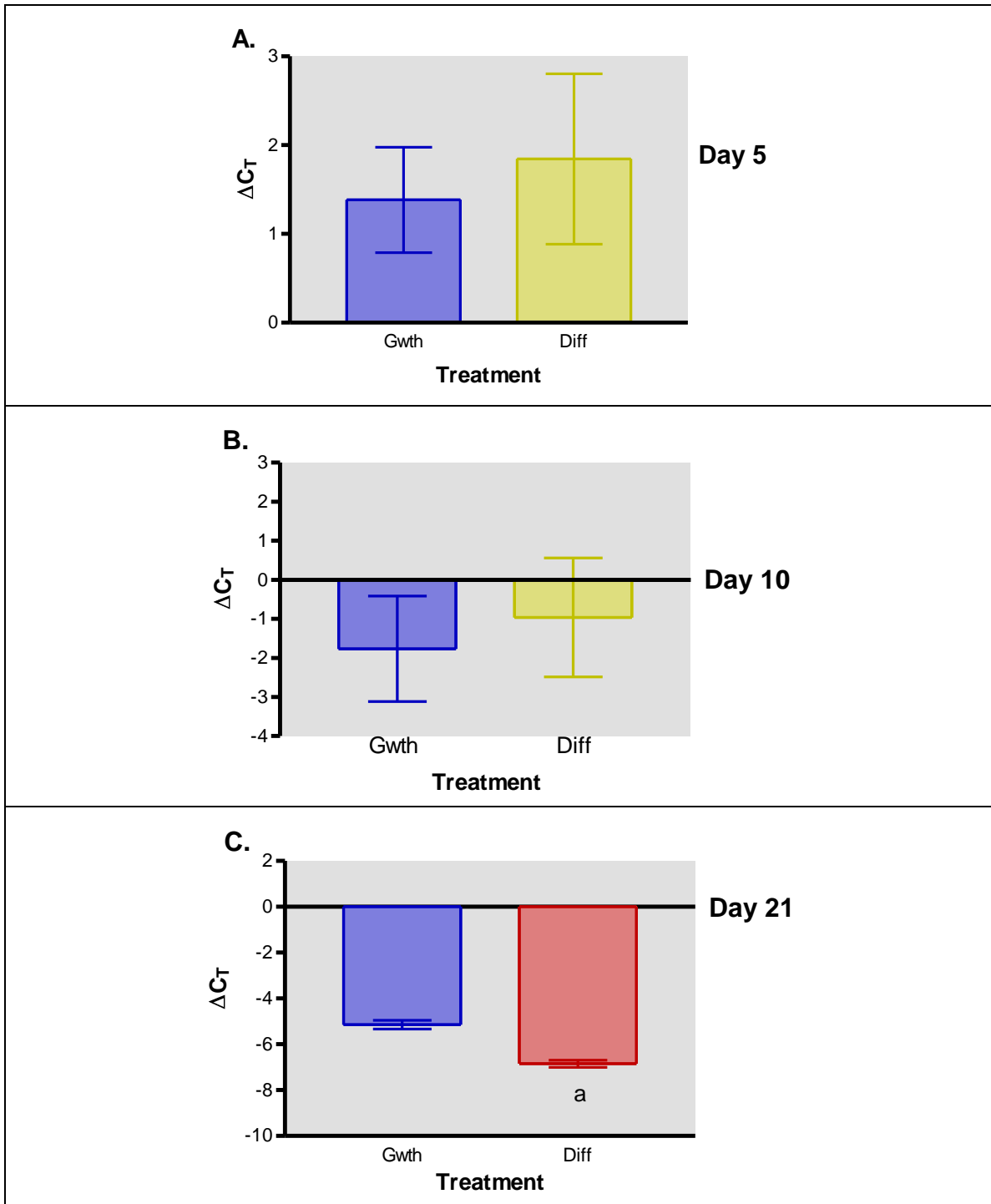
Figure 30. Bone Sialoprotein gene (IBSP) ΔC_T mRNA Expression for Days 5, 10, and 21 in Growth and Differentiation Media

Bone Sialoprotein gene (IBSP) ΔC_T expression as determined by real time RT-PCR reactions. It should be noted that the lower the C_T value the greater the expression of the gene(s) and conversely, the higher the C_T value the lower the expression of the gene(s). The target gene (IBSP) from growth and differentiation media were normalized to the housekeeper gene found in the same RT preparation for which the target gene was evaluated. All cells in this study were 3rd or 4th passage. Panels A, B, and C report only cells cultured in growth and differentiation media due to the interference of the WBCs with the PRP treated cells. All media was changed every 3 days. Each bar represents the ± S.E.M. for N=3 with tests performed in triplicate. All data for Panels A, B, and C were analyzed with a two-tailed unpaired t test where significance was defined as $p < .05$. Panels A-C shows the relative changes (ΔC_T) in IBSP expression at days 5, 10, and 21 in growth and differentiation media. There was no significant difference ($p > .05$) in IBSP gene expression at the Days 5 or 10, but there was significantly increased ($p < .01$) IBSP gene expression on Day 21.

PRP-induced expression of IBSP at Day 5 was low and not significantly different between the growth and differentiation media (Figure 30 A). The fold change for IBSP with differentiation medium was 0.73 times (Table 11) that of IBSP expression in growth medium. It was expected that IBSP expression in differentiation medium would not be significantly different from growth medium on Day 5 because IBSP is known to have middle to late expression during the differentiation process. Day 10 IBSP expression was not significantly different ($p > .05$) for differentiation medium when compared to growth medium. The fold increase for IBSP on Day 10 with differentiation treatment was 0.57 times (Table 11) that of IBSP expression observed in growth medium. Again, this was expected for Day 10 IBSP expression. For Day 21, there is a significant increase in IBSP gene expression in differentiation medium when compared to growth medium. IBSP mRNA expression for differentiation medium was 3.26 times (Table 11) that of growth medium.

Osteocalcin gene (BGLAP) mRNA expression for growth medium and differentiation medium is illustrated in Figure 31 Panels A-C.
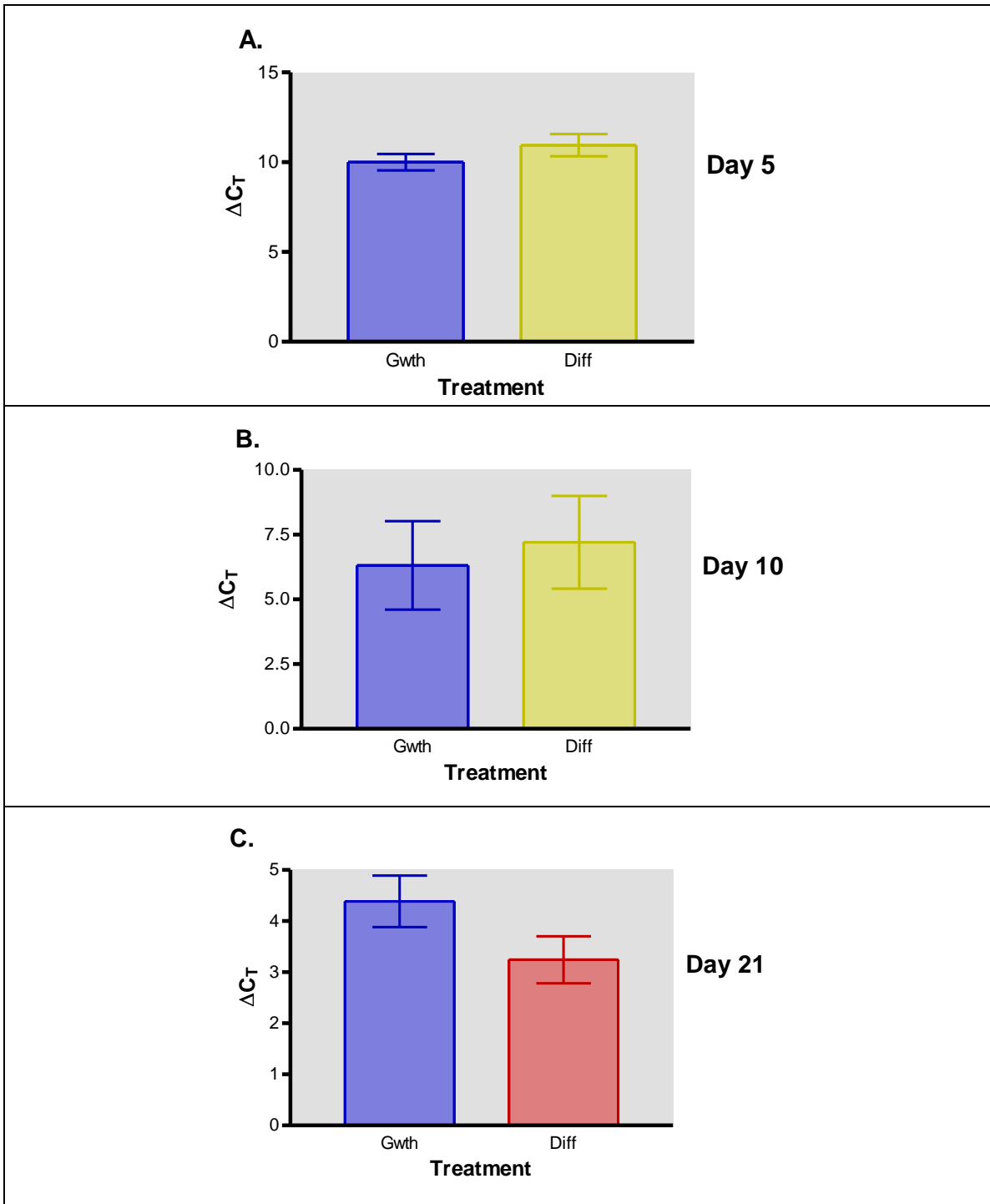
Figure 31. Osteocalcin (BGLAP) ΔC_T mRNA Expression for Days 5, 10, and 21 in Growth and Differentiation Media

Osteocalcin (BGLAP) ΔC_T expression as determined by real time RT-PCR reactions. It should be noted that the lower the C_T value the greater the expression of the gene(s) and conversely, the higher the Ct value the lower the expression of the gene(s). The target gene (BGLAP) from growth and differentiation media were normalized to the housekeeping gene found in the same RT preparation for which the target gene was evaluated. All cells in this study were 3rd or 4th passage. Osteocalcin (BGLAP) ΔC_T expression as determined was real time RT-PCR reactions. All cells in this study were 3rd or 4th passage. Panels A, B, and C report only cells cultured in growth and differentiation media due to the interference of the WBCs with the PRP-treated cells. . All media was changed every 3 days. Each bar represents the ± S.E.M. for N=3 with tests performed in triplicate. All data for Panels A, B, and C were analyzed with a two-tailed unpaired t test where significance was defined as $p < .05$. Panel A shows the relative changes (ΔC_T) in BGLAP expression at day 5. There was no significant difference ($p > .05$) in BGLAP expression between the differentiation and growth medium group ΔC_T values. Expression of BGLAP as measured by ΔC_T for either group at Day 5 was low with the fold change for IBSP with differentiation medium 0.55 times (Table 11) that of BGLAP expression in growth medium. Day 10 BGLAP expression as measured by ΔC_T and analyzed with a two-tailed unpaired t test was not significantly different ($p > .05$) for differentiation medium when compared to growth medium. The BGLAP fold increase for Day 10 with differentiation treatment was 0.54 times (Table 11) that of BGLAP expression observed in growth medium. For Day 21, there is no significant difference between any of the ΔC_T values when comparing differentiation medium to growth medium. Differentiation medium BGLAP gene expression was 2.00 times (Table 11) that of growth medium expression.

Figure 31 A-C illustrates the relative changes in BGLAP gene expression in growth

medium and differentiation medium at days 5, 10, and 21. When using a two-tailed

unpaired t test, there was no significant difference found in BGLAP gene expression at

days 5, 10, or 21 when comparing differentiation medium to growth medium. It was

expected that there would not be a significant difference between differentiation and

growth media at days 5 and 10, because BGLAP gene expression occurs late in the

differentiation cycle (21-28 days). On Day 21, there was a 2-fold increase in BGLAP

expression in differentiation medium when compared to growth medium (Table 11) as

expected for this late stage differentiation marker.
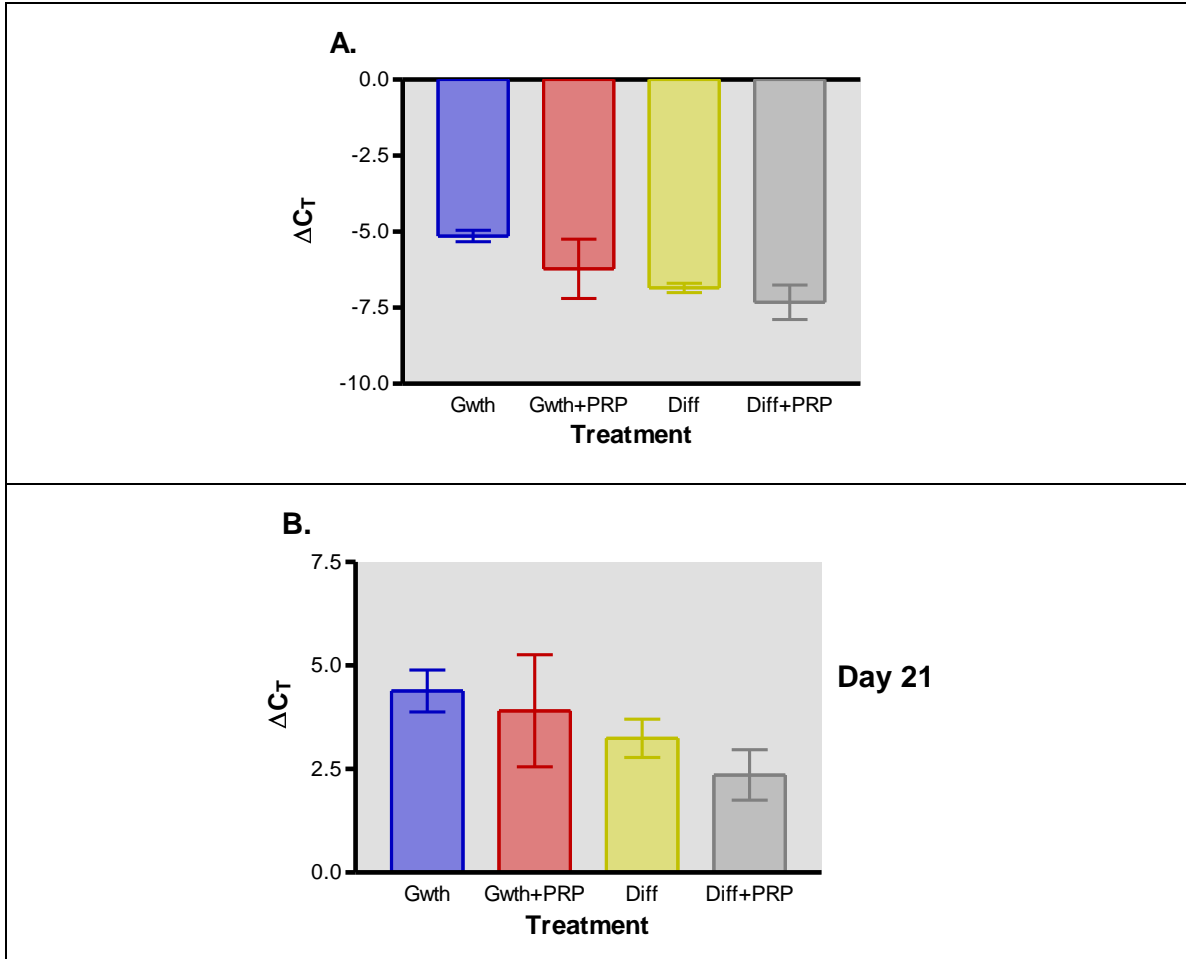
Figure 32. Bone Sialoprotein (IBSP) and Osteocalcin (BGLAP)

ΔC_T mRNA Expression for Day 21 in Growth ± PRP and

Differentiation ± PRP Media

Bone sialoprotein (IBSP) and osteocalcin (BGLAP) ΔC_T expression as determined by real time RT-PCR reactions. It should be noted that the lower the C_T value the greater the expression of the gene(s) and conversely, the higher the C_T value the lower the expression of the gene(s). The target genes (IBSP and BGLAP) from growth ± PRP and differentiation ± PRP media were normalized to the housekeeping gene found in the same RT preparation for which the target gene was evaluated. All cells in this study were 3rd or 4th passage. IBSP and BGLAP ΔC_T expression were determined by real time RT-PCR reactions. All cells in this study were 3rd or 4th passage. Panels A and B report both genes in all media because the interference of the WBCs with the PRP-treated cells

appears to be removed by Day 21. All media was changed every 3 days. Each bar represents the $\pm$ S.E.M. for N=3 with tests performed in triplicate. All data for Panels A and B were analyzed with a two-tailed unpaired t test where significance was defined as p < .05. Panel A shows the relative changes (ΔC_T) in IBSP expression. There was no significant difference (p > .05) in IBSP expression between the differentiation $\pm$ PRP and growth medium $\pm$ PRP groups ΔC_T values. The fold change for IBSP at Day 21 with differentiation + PRP medium was 4.52 times (Table 11) that of IBSP expression in growth medium (control). The fold change for IBSP at Day 21 with differentiation medium was 3.56 times (Table 11) that of IBSP expression in growth medium (control). Panel B represents Day 21 BGLAP expression as measured by ΔC_T and analyzed with a two-tailed unpaired t test. There was not significantly different (p > .05) between any of the media groups. The BGLAP fold increase for Day 21 with differentiation + PRP medium was 4.08 times (Table 11) that of BGLAP expression observed in growth medium. Differentiation medium BGLAP gene expression was 2.00 times (Table 11) that of growth medium expression.

The relative quantification (fold changes) in expression for the genes of interest ($\Delta\Delta C_T$) was calculated and summarized in Table 11. $\Delta\Delta C_T$ values were calculated by subtracting target gene's ΔC_T from the medium and day of interest from the ΔC_T value for the target gene in growth medium (control) on the day of interest. The final calculation (fold increase in expression) involved raising the efficiency value (2) to the negative $\Delta\Delta C_T$ value for the target gene. Table 11 lists the relative fold changes for each treatment compared with growth medium for each gene and time point.

Gene	Treatment	Day 5	Day 10	Day 21
IBSP	Growth	1	1	1
	Gwth + PRP	n/a	n/a	2.11
	Differentiation	0.73	0.57	3.26
	Diff + PRP	n/a	n/a	4.52
BGLAP	Growth	1	1	1
	Gwth + PRP	n/a	n/a	1.39
	Differentiation	0.55	0.54	2.00
	Diff + PRP	n/a	n/a	4.08
ITGA2B	Growth	1	1	1
	Gwth + PRP	n/a	n/a	2.50
	Differentiation	0.59	0.73	3.85
	Diff + PRP	n/a	n/a	5.12

Table 11. Relative Quantification Using the Comparative C_T

Method

The relative quantification calculation for all four genes in the medium of interest relative to growth medium (control) are presented. There are 3 C_T readings for each sample. N=3 and each sample was run in triplicate. The average C_T was calculated for each day followed by averaging the three daily averages together. Standard Error of Measures is reported in Figures 30 and 31. Delta C_Ts were calculated by subtracting the housekeeping gene average C_T value for the gene of interest in growth medium from the target gene average C_T value for the treatment of interest. Delta-delta C_T values were calculated by subtracting the growth medium target genes Delta C_T value from the delta C_T value for the target gene in the medium of interest. The final calculation (fold increase in expression) involved raising the efficiency value (2) to the negative delta-delta C_T value for the target gene. Note: n/a= not available, this data was not able to be calculated because the housekeeper gene (GAPDH) was not consistent across these groups at Days 5 and 10 due to a possible WBC interference for PRP treated groups at Days 5 and 10.

There was no relative increase in IBSP (bone sialoprotein) or BGLAP (osteocalcin) expression compared to growth medium for Days 5 or 10 with non-PRP treatments (PRP treatments not reported). By Day 21, IBSP expression had a 2.11 fold increase for the growth + PRP medium, 3.26 fold increase for the differentiation medium and a 4.52 fold increase for the differentiation + PRP medium. The results were similar for Bglap expression with the growth + PRP having the lowest fold increase (1.39), followed by differentiation (2.00) and differentiation + PRP again having the greatest fold increase (4.08). However, additional studies will be required to establish if these PRP-induced increases are significant.

The ITGA2B expression showed the same trend as the IBSP and BGLAP genes. Differentiation + PRP medium at Day 21 had the greatest fold increase (5.12). The expression of the ITGA2B gene mRNA in the non PRP treated groups at all time points and its expression in the PRP treated groups at Day 21 was unexpected as ITGA2B gene was reported to be expressed only in megakaryocytes and platelets (294, 300-302).

D. Discussion

Based on the premise that PRP will enhance bone formation by stimulating proliferation of hMSCs (and not interfere with hMSCs differentiation into osteoblasts) via platelet activation, it is important to consider whether the platelets are activated in the *in vitro* conditions. Platelets have several methods of activation *in vivo*, but a concern when working with platelets *in vitro* is, will the platelets be activated? When platelets become stagnant, the platelets enter a second stage where they rapidly convert into their active form with filopodia and lamellipodia that derive from a remodeled actin skeleton

and a sophisticated assembly of new actin filaments (36). This change in physical state allows platelets to interact with each other and adhere to each other. Platelet aggregation or coagulation occurs when platelets adhere to each other by adhesion receptors, with glycoprotein IIb/IIIa being the most abundant adhesion receptor (15, 59). Once the glycoprotein IIb/IIIa receptor is activated, it initiates cell-surface signaling, resulting in activation of the platelet (15). Upon activation, platelets release the contents of their α-granules. Alpha granules contain coagulation factors, platelet activating factors, adhesion molecules, cell-activating molecules, cytokines, integrins, inflammatory molecules, and growth factors. Therefore, it is believed that the platelets are activated *in vitro*.

Another concern is that PRP is processed from whole blood that is collected in BD Vacutainer™ tubes that contain the anticoagulant trisodium citrate (9:1). The reason for concern is that trisodium citrate may block the coagulation (aggregation) and subsequent platelet activation. However, in the BC PRP preparation process the whole blood in the Vacutainer™ tube undergoes centrifugation at 1150 x g for 10 minutes. The trisodium citrate is present in an ionic state in the whole blood and would rise to the supernatant (PPP) portion of the tube with centrifugation. Therefore, the trisodium citrate would be removed from the BC PRP. This is confirmed by the findings of the Study I: Preparation and Characterization of PRP (page 67). With bench set time, it became evident that platelets were aggregating (Figure 18) and therefore activation would follow. Additionally, when the BC PRP was applied to the culture flask the BC PRP would form a clot, again signifying aggregation and subsequent platelet activation and release of the α-granule contents.

The results of each of the proliferation studies (cell growth photomicrographs/ cell counts, MTT analysis, and total RNA) appear to correspond with each other. It is readily apparent that 24-hour PRP exposure does have an early effect on proliferation and that effect is seen most dramatically within 5 days and then appears to taper off after that time point. The reason for the decline in proliferation response at this time point may not be due to a loss of proliferative effects of PRP, but may be due to PRP promoting osteoblast differentiation into a post mitotic phenotype. At the time of PRP removal, it was noted there were actually fewer cells present than had been seeded. It appeared that some cells had been lost with the PRP removal. Cells normally attach to the flask within 24 hours of placement. PRP administration occurred after this initial 24-hour attachment period. The cytokines in PRP are known to be chemotactic to hMSCs and therefore, a portion of the cells may have detached from the flask and attracted to the PRP. The PRP that was aspirated was placed in a new T-25 flask and cells were found to be growing in these flasks over the subsequent days (data not reported). This observation further enforces the proliferative effects of PRP. This finding warrants additional investigation in future studies. The cell count study is the only proliferation study done in this study that is not confounded by the constituents of PRP and therefore the most reliable. The MTT assay may be compromised due to the mitochondrial reductase found in the residual platelets and WBCs and total RNA yield may be challenged by the presence of WBC RNA.

The MTT results correlate with those of Lucarrelli *et al.* (106). Lucarrelli found the PRP-induced increase in MTT values was PRP dose dependent. Stromal stem cells were exposed to thrombin plus calcium gluconate-activated PRP for 3, 6, and 9 days in a 1% or 10% concentration. Their experimental design differs from our work in that our exposure

was for 24 hours only and in a 3.75% v/v concentration. Lucarrelli *et al.* found that at day 3 (10% concentration) there was a 1.5-fold increase in MTT absorbance. In our study, there was a 1.34-fold increase. The difference between the two studies is that platelets in our study were not subjected to exogenous thrombin and calcium gluconate and we had 1/3 the concentration with 1/3 of the PRP exposure time. Many clinicians feel that PRP must be activated and in a gel form for PRP benefits to be realized and that is the thought behind using bovine thrombin and calcium gluconate. However, the BC PRP technique had a positive effect on proliferation without the addition of bovine thrombin and calcium gluconate. Future work should include examining similar concentrations of thrombin/calcium gluconate-activated PRP vs. our buffy coat PRP technique. With continuous exposure, Lucarrelli *et al.* found the same fold increase present at days 6 and 9. Their 1% concentration had a modest 1.1-fold increase at day 6.

In another study, Graziani *et al.* (328) examined leucodepleted thrombin/calcium gluconate-activated PRP (via negative-charged Pall™ filter) at various concentrations. Concentrations for the Graziani study were determined by recording baseline platelet values and then measuring the platelet count in the PRP samples. These samples were then diluted to give a range of 100% (PRP1x), 250% (PRP 2.5x), 350% (PRP 3.5x), and 550% (PRP 5.5x - undiluted) PRP concentrations over baseline values. PRP exposure was for either 24 or 72 hours. MTT measurements were taken for each of these time points. At the 24-hour time point, the maximal MTT absorbance occurred with the PRP 1x concentration and higher concentrations of PRP resulted in decrease proliferation. However, at the 72-hour mark, the PRP 2.5x had the highest MTT absorbance with a 70% increase in cell number compared to the negative control. Interestingly, in the

leucodepleted thrombin/calcium gluconate-activated PRP studies, none of the PRP-treated groups surpassed the control group, which was growth medium (328). In contrast, in our study, the PRP treated group surpassed growth medium until Day 6. The main difference in the techniques was the activation of the platelets with thrombin and calcium gluconate and that their preparation was leucodepleted and therefore may not have the degree of interference from the WBCs that our MTT assays do. Platelets were continuously applied in the Graziani study, therefore the platelets may have compromised their data also. This brings into question if leucodepleted thrombin/calcium gluconate-activated PRP retains the same proliferative qualities as PRP containing WBCs and not activated with bovine thrombin/calcium gluconate. Future work should include comparing various concentrations of leucodepleted thrombin/calcium gluconate-activated PRP with our buffy coat PRP technique.

At day 5, growth + PRP treated groups demonstrated a total RNA increase of 6.5-fold over growth medium alone (Figure 27). This represents a much greater increase than is seen with cell counts (3.2 fold increase) (Figure 25) or MTT assay (2-fold increase) (Figure 26). At day 5, total RNA expression is twice that of the cell count increase. Part of this excessive total RNA increase may be due to the 24- hour PRP exposure. PRP contains platelets and white blood cells (WBCs). Platelets contain mRNA carried over from megakaryocytes, but it cannot synthesize mRNA due to the lack of a nucleus and with time, mRNA undergoes progressive decay (136-139). Therefore, it is unlikely that platelet mRNA is responsible for the additional total RNA seen in Figure 27. WBCs contain ribosomal RNA (440) and this is most likely causing the excessive increase in total RNA at day 5. This marked increase in total RNA was present in both PRP treated

156

groups (growth + PRP and differentiation + PRP). The control groups (growth and differentiation media) did not display these large increases in total RNA. Differentiation medium alone had a significant ($p < .001$) decrease in expression of total RNA in comparison to growth medium. At Day 10, the total RNA difference between growth medium and growth + PRP treatment was much less. The growth medium total RNA was unchanged from day 5 and the differentiation medium total RNA had increased slightly. Interestingly, on day 10, the growth + PRP and the differentiation + PRP treatments had approximately 1/4 to 1/3 of the total RNA that these groups had on day 5. This drop in total RNA may not be due to a proliferation or differentiation effect, but rather the decreased presence of WBCs in the PRP. The PRP was removed after 24 hours, but WBCs can be adherent to the flask and therefore retained in the flask, even with successive medium changes every 3 days. The life expectancy of a WBC depends upon the cell type and can range from hours to weeks (441, 442). The decrease in WBCs either because of media changes every 3 days or apoptosis of existing WBCs could explain the drop in total RNA. Since the cell numbers increased by 3.2-fold with growth + PRP treatment over growth medium counts, we could take the total RNA value for the growth medium and multiply it by 3.2 to get the approximate total RNA value for the growth + PRP treatment effect. The difference would represent the WBC effect beyond the proliferative effect seen with the MTT assay (Figure 26). The potential WBC effect appears to be approximately 52% of the total effect seen with the growth + PRP treatment.
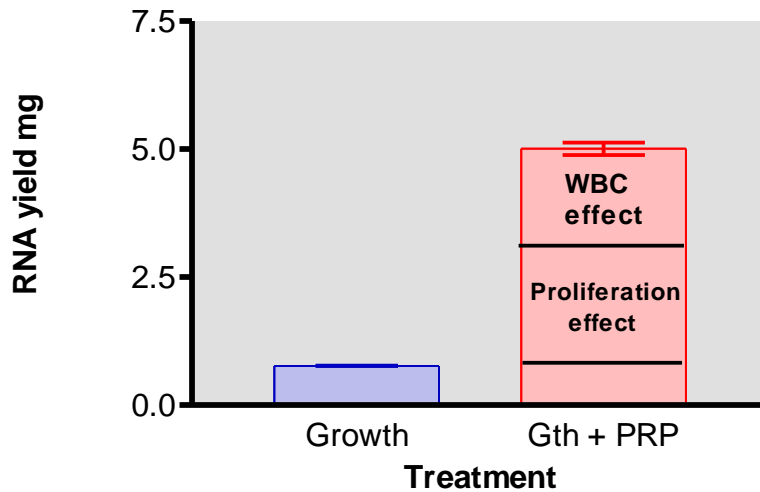
Figure 33. White Blood Cell Effect on Total RNA Yield - Day 5

Gth (growth) + PRP treatment bar is marked with the proposed effect WBCs may have upon the total RNA levels. Approximately 52% of the effect seen in this example may be due to ribosomal RNA from WBCs, 48% of the effect may be due to a true proliferative effect induced by PRP. Proliferative effect was measured by taking the growth medium total RNA production and multiplying it by 3.2, which represents the fold increase growth + PRP treatment cell counts were beyond growth medium alone cell counts.

 This potential WBC effect will be reviewed again with the real time RT-PCR discussion.

Despite this WBC effect, it appears that PRP has an enhancing effect on proliferation.

This finding is supported by the cell count and MTT data. At day 10, the RNA

expression for growth + PRP treatment had decreased by 67% of the day 5 level. This

may be due in part to the decrease in the number of WBCs. Even with this drop in

growth + PRP treatment total RNA, the total RNA level is still twice that of growth

medium alone. The effect of PRP on proliferation at day 10 is additive for growth

medium, but is sub-additive for differentiation medium. It is interesting to note that at day 10 the total RNA level for differentiation + PRP treatment had decreased by 70%, but still exceeded the differentiation or growth media. In this case, PRP is sub-additive for differentiation medium. It is obvious that the PRP effect is decreasing and the non-treatment groups are approaching the PRP treatment groups. At day 21, the growth + PRP treatment level had diminished by 80% of the total RNA occurring at day 5. Again, despite this continual drop, it still exceeded all other groups for RNA production by a significant amount (p <0 .001). At day 21, the differentiation only group had significantly exceeded the growth medium and differentiation + PRP treatment groups. This would occur because of the continual hMSC differentiation that is taking place in this medium. Notwithstanding the WBC effect, there is robust total RNA expression that may be due to the presence of TGF-β1 in PRP. TGF-β1 is known to control growth in hMSCs (443). By day 21 PRP is sub-additive for growth medium, but now interferes slightly with differentiation medium, which may be due to down-regulation of protein synthesis or differentiation signals.

Figure 34 A and B illustrate the total RNA yield for Days 5, 10, and 21 for growth medium and differentiation medium.
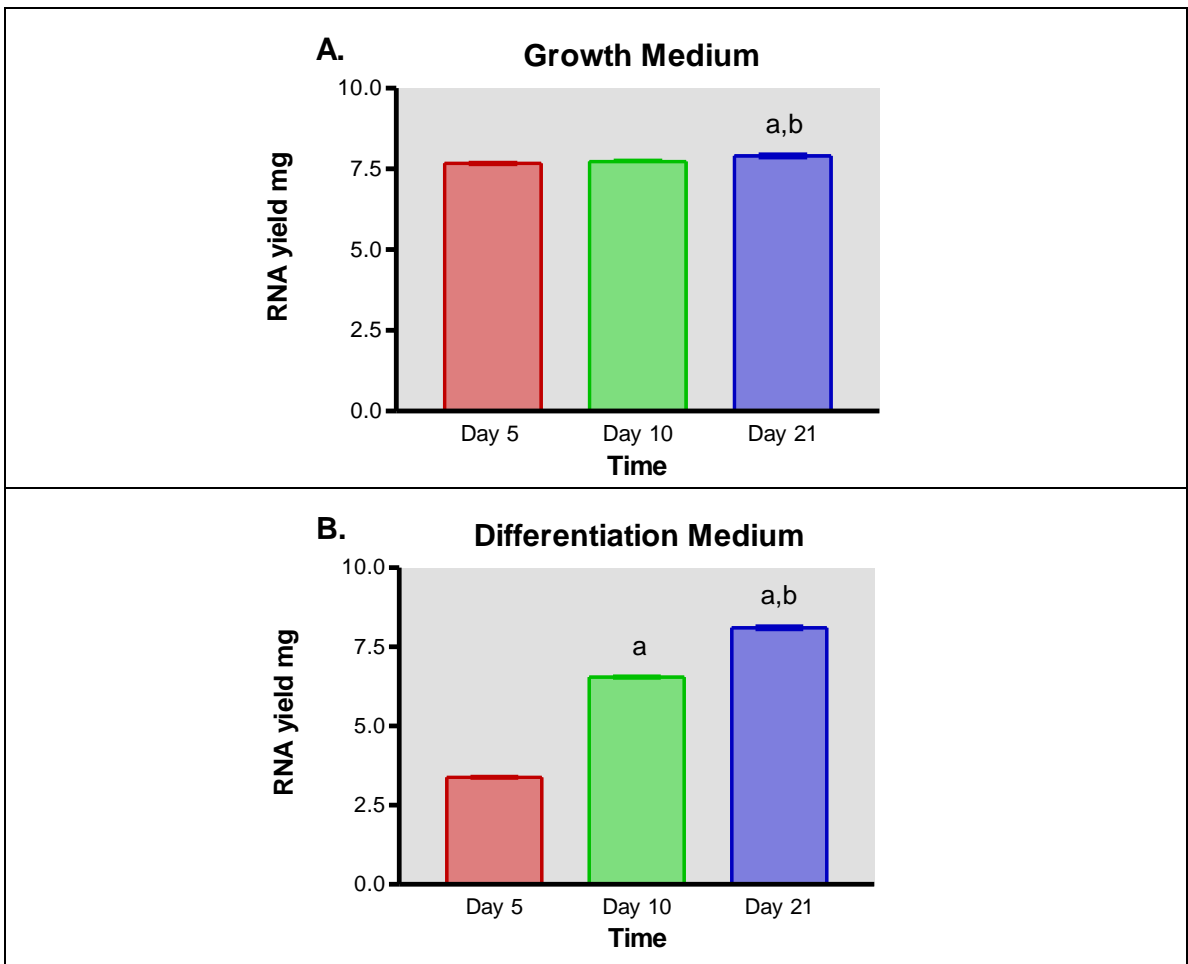
Figure 34 Total RNA Yield for Growth and Differentiation Media

Days 5, 10, 21

RNA yield measured with spectrophotometry at 260nm and quality assessed with 280 nm for growth medium (Panel A) and differentiation medium (Panel B) expressed as total RNA yield ng/µL. These graphs are extractions from Figure 27 with all conditions being the same. All data were analyzed with a one-way ANOVA with a Newman Keuls post-hoc test where significance was defined as $p < .05$, where a = $p < 0.05$ when compared to Day 5, b = $p < 0.05$ when compared to day 10. Newman Keuls analysis represents the comparison between each of the Days. Panel A (growth medium) analysis revealed that there was no significant difference ($p > .05$) in RNA yield between Days 5 and 10. Day 21 did have a significantly greater ($p < .01$) total RNA yield when compared to Days 5 or 10. Differentiation medium shown in Panel B did have a significant difference ($p < .001$) for each of the time points. Total RNA yield in differentiation medium continued to increase throughout the time span.

For growth medium there was no significant difference ($p > .05$) between Days 5 or 10 in total RNA yield, but there was a significant increase ($p < .01$) between Day 21 and these earlier time points. Neither of the other cell proliferation studies (cell count or MTT assay) was extended to Day 21. Cell count data (Figure 25) suggests that proliferation in growth media doubled between Days 5 and 10. MTT data (Figure 26) suggests that cell proliferation increased three fold in this time for cells cultured in growth medium. Therefore, total RNA may not be a good indicator of cell proliferation and the entire total RNA yield effect seen with growth + PRP medium and differentiation + PRP medium at Days 5 and 10 may be due to the WBCs.

In the future, proliferation studies should be performed with cell counts and the use of the CellTiter-Glo® Luminescent Cell Viability Assay that is a homogeneous method of determining the number of viable cells in culture based on quantification of ATP present (444, 445).

Total RNA levels will increase with differentiation as well as proliferation. For differentiation medium, there was a significant increase ($p < .001$) in RNA yield as time passed from Day 5 to 21. This most likely signifies that differentiation was taking place

to account for the increase in total RNA. Proliferation of hMSCs *in vivo* is of great importance clinically because there is an age-related decrease in hMSCs and the generation of osteoblasts. Additionally, the time for doubling of hMSC is increased by 1.7 fold for older patients (446). Therefore, these aging issues may compromise the healing response and PRP application may help negate these factors.

For the alkaline phosphatase assay our results (Figure 28) for differentiation medium without PRP correspond with those of Jaiswal *et al*. (438). Jaiswal *et al*. used the same differentiation media and found that on Day 4 ALP, expression was present and at day 8 ALP expression had doubled and peaked at day 11. However, over time there was a decrease in ALP activity beyond Day 12 that correlated with bone sialoprotein and osteocalcin mRNA expression and terminal osteogenic cell differentiation as hMSCs become osteocytes (438). Although our time points varied from Jaiswal *et al*., there was a greater ALP expression at Day 5 than at Day 15. For growth + PRP medium, ALP results suggest that PRP-treatment does induce this early differentiation marker in 5 days. A valid question is does the presence of WBCs affect these results. The WBCs may not be causing the increased ALP levels seen with the alkaline phosphatase assay, because there is not an additive effect with the differentiation + PRP treatment. There was an enhancing effect of PRP exposure to differentiation medium in the total RNA study for Days 5 and 10. This same effect was not observed with the ALP assay at Day 5. To answer the question if this 5-day ALP increase is truly due to platelets and not WBCs, the study would need to be repeated with a WBC-free PRP treatment in comparison to this BC method of PRP preparation. At Day 15, the differentiation + PRP treatment had significantly ($p < .001$) higher ALP expression than the other groups. At Day 15, PRP

162

may interfere with the normal effect of differentiation medium ALP production. Interestingly Day 15 differentiation medium ALP expression (average 0.07972 µg/mL ±SEM 0.0001383) was similar to that seen at Day 5 for growth + PRP medium (average 0.07194 µg/mL ±SEM 0.0006543). This may suggest that PRP treatment induces ALP formation, but at a lower level than does differentiation medium. At Day 5, differentiation medium ALP expression was substantially higher than that of growth + PRP medium. There was no sizeable difference between differentiation medium and differentiation + PRP induced expression of ALP. The reason that PRP treatment may not be as effective for inducing differentiation is that differentiation medium has signaling mechanisms (dexamethasone, β-glycerophosphate, and ascorbic acid) that are specific to differentiation, while PRP has signals that appear to enhance proliferation and differentiation. Owen et al. (447) found that a temporal relationship exists between proliferation and differentiation; therefore, maybe PRP-treatment must initially perform proliferation before progressing to differentiation. Since PRP-treatment induces proliferation initially, this may lead to a shift in the differentiation process to a different time point than what is normally observed. The Day 5 ALP activity for differentiation + PRP medium was less than that of differentiation medium alone; however, Day 21 ALP activity for differentiation + PRP medium was greater than that of differentiation medium alone. Also the growth + PRP medium had less ALP activity at Day 5 than differentiation medium, but the Day 15 differentiation medium ALP activity was similar to that of growth + PRP on Day 5. This suggests that PRP does have the following effects on differentiation: 1) it does not stop the differentiation process, 2) it may not have the factors necessary to induce differentiation in growth medium, and 3) it may

delay the differentiation process when the necessary differentiation signals are present to a later time point because of its initial influence on proliferation.

Further evaluation of the differentiation effect of PRP was performed by examining specific genes known to be markers of middle to late differentiation. Cells cultured in PRP treatment media had approximately a 3 cycle earlier expression of the GAPDH housekeeping gene at day 5 in comparison to cells cultured in media that did not have PRP exposure and each cycle represents a doubling in the expression of the gene of interest. At Day10, this difference had decreased to 1 or 2 cycles. The housekeeper gene is used as the internal standard and used to normalize and quantify target mRNA expression. The housekeeper expression should be stable within each cell regardless of the treatment (448, 449). These differences raised concerns about the validity of using this housekeeper for the study. The GAPDH expression was very consistent across all treatment groups with the day 21 samples. It was observed that the other osteoblast (IBSP) or platelet (BGLAP) specific genes were also consistent in their expression across all of the treatments. Therefore, the question is what was different about these PRP groups at the 5 and 10-day time points? As mentioned earlier in the introduction section, PRP contains platelets and WBCs. The possibility of platelets being the confounding factor was considered. Platelets were ruled out as the cause for the over expression of GAPDH in the 5- and 10-day samples because the ITGA2B gene that was thought to be expressed only in platelets did have consistent expression (albeit at low levels) in all treatment groups. WBCs express GAPDH that could be increasing the housekeeper gene expression. This housekeeper gene was selected because it had been reported as the housekeeper gene by Kanno *et al.* in a similar semiquantitative RT-PCR study examining

164

the differentiating effects of PRP (329). It was also thought that if the PRP were removed after 24 hours and new medium placed that the effects of PRP and its contents would be removed and therefore not a confounding factor for these studies.

At Day 21, IBSP expression (Table 11) was at a higher level than BGLAP expression for all media with differentiation + PRP having the greatest expression. It is expected that IBSP expression preceded BGLAP mRNA expression (276, 277, 279, 287). Gene expression for PRP treated groups is reported for the Day 21 samples because the housekeeper gene was stably expressed. This suggests that influence of the WBCs was gone by the Day 21 time point. Ingrwoth + PRP at Day 21, PRP may somewhat enhance differentiation of growth medium alone because, IBSP (2.11 fold) and BGLAP (1.39 fold) expression were higher than growth medium alone and approached that of differentiation medium. PRP exposure also demonstrated an enhancing effect on differentiation medium for IBSP (4.52 fold) and BGLAP (4.08 fold) expression at Day 21. Further studies will be required to confirm these proposed effects of PRP.

This dissertation is suggesting that BC PRP enhances hMSC proliferation and suggests that it may not stop their differentiation into osteoblasts. Proliferation seems to be occuring in a shorter time than what is normally observed *in vitro* with growth medium for proliferation. PRP does not appear to induce differentiation in growth medium, nor does it stop the differentiation process for cells cultured in differentiation medium. Parsons et al. (439) found that platelet rich concentrate, when added to the culture medium as a clot, PRC induced an earlier onset of proliferation and stimulated a transient enhancement of bone morphogenetic protein-2 mRNA that peaked after 12 hours and induced an earlier and a sustained increase in the key osteogenic transcription

actor *RUNX2*. After 3 days of treatment, PRC enhanced alkaline phosphatase activity

more than 2-fold compared to donor-matched serum, and at 23 days, the increase in

osteoblastic commitment translated to enhanced calcified matrix deposition. Our studies

found that cells cultured in growth + PRP medium had ALP activity increased by 2.5 fold

at Day 5 (Figure 28) when compared to growth medium alone, but when ALP activity

was corrected for cell density, there did not appear to be a difference in ALP activity

between cells cultured in growth or growth + PRP media. We also found that by Day 5,

cell counts (Figure 25) were 3.2 fold greater for cells cultured in growth + PRP in

comparison to cells cultured in growth medium alone. It is at Day 5 we also found that

the MTT assay showed a drop in MTT activity (Figure 26), signifying that proliferation

was ending. Therefore, it appears that proliferation discontinues and differentiation

begins immediately thereafter. A possible explanation for this may be found in the work

of Owen et al. (447). They found a relationship existed between fetal rat hMSC growth

and differentiation-related gene expression during the *in vitro* cultivation of osteoblasts.

They found a temporal, functional relationship between the decline in proliferative

activity and the subsequent induction of genes associated with osteoblast differentiation,

matrix maturation, and mineralization. Initially, proliferating cells express cell cycle and

cell growth regulated genes that lead to the production of a fibronectin/type I collagen

extracellular matrix. Immediately following a sequence of events occurs in which there

is an enhanced expression of ALP and later an increased expression of osteocalcin at the

onset of mineralization. Additionally, it was demonstrated that there is enhanced

expression of the osteoblast markers as a function of ascorbic acid-induced collagen

deposition. This suggests that the extracellular matrix contributes to both the shutdown of proliferation and the development of the post mitotic osteoblast phenotype.

E. Conclusion

This molecular-based study examining the effects of the buffy coat method of preparing PRP supports the hypothesis that PRP obtained by this simple and cost-effective method enhances proliferation. It also suggests that BC PRP does not interfere with hMSC differentiation down the osteogenic pathway. Proliferation was confirmed with cell count and MTT assays. Evidence of PRP not stopping the differentiation process was suggested by the unaltered ALP activity at Day 15 for differentain+ PRP medium when compared to differentiation medium . Additionally, evidence of differentiation was supported by the increased expression of the bone sialoprotein gene mRNA and the osteocalcin gene mRNA in differentiation +PRP medium. This study also supports the concept that PRP initially accelerates proliferation of hMSCs and it does not stop differentiation with the possibility of inducing differentiation at a late time point. PRP may induce a shift in the differentiation chronological framework. PRP causes the hMSCs to proliferate before differentiation into osteoblasts begins. These effects may promote bone healing and formation. This molecular study provides a mechanistic basis for the clinical use of PRP in osseous surgery.

Study IV: The Effect of PRP on Wound Healing

Following Tooth Extraction:

A Prospective Clinical Study

A. Introduction

Immediately following the removal of one or several teeth, a healing process begins that affects the eventual alveolar bone volume and architecture of the alveolar ridge. Proper and timely healing are essential in order to obtain the ideal functional reconstruction for the patient. Improper traumatic removal of a tooth or a poor healing response may lead to excessive bone loss delaying tooth replacement, may necessitate expensive and time-consuming alveolar bone reconstructive surgeries, or create a situation that is impossible to correct, leaving the patient severely compromised (450). If a cost-effective, simple technique were available that would decrease bone-healing time and increase the predictability of having a favorable result, patients and clinicians would benefit. The intent of this study was to determine whether the application of PRP to a tooth extraction site would facilitate healing.

Following tooth extraction, a cascade of inflammatory reactions begins immediately, and the extraction socket is temporarily closed by clotting blood. Epithelial tissue proliferation and migration start within the first week and the disrupted tissue integrity is quickly restored. Histological evidence of active bone formation in the bottom of the extraction socket is seen as early as 2 weeks following tooth removal. The socket is

filled with newly formed bone in about 6 months (451, 452). If the removed tooth is not replaced by an intraosseous fixture within 6 months of removal, the residual ridge alveolar bone undergoes a life-long catabolic remodeling (451).

Radiographic techniques have been used to document the gross morphologic changes of the alveolar processes after the loss of teeth (450, 453-455). A well-established method for the detection of subtle bone changes is the use of subtraction radiography. We used a variation of the technique reported by Hildebolt et al. in 1998 (456). To determine changes in alveolar bone radiodensity through time, homologous regions of interest (ROIs) were identified and compared (456, 457), with one image subtracted from the other, the difference representing the change in radiodensity (457-461). The regions of interest were interpreted using a computer program that examined the pixel number and converted to grayscale images. In this study, we used a combination of these techniques and normalized radiographs to an ROI (the adjacent tooth). The extraction sockets were evaluated by the same method and normalized to the ROI. The grayscale values of the baseline radiograph were subtracted from the grayscale value for the time point radiograph.

Macro-structural and micro-structural bone forming information can be acquired with advanced imaging techniques rather than with conventional radiography or standard bone densitometry (462). Computerized tomogram scanning technology (CT scan) provides a three-dimensional representation of the object in any geometry (463) which can provide information about bone healing and define the skeletal response to innovative therapies (462, 464-469). Investigators have employed quantitative CT scans to monitor fracture healing in experimental models and clinical studies (462, 464, 465). Since this

technology is expensive and requires more radiation exposure than digital radiography, it was used on only three patients in this study.

B. Materials and Methods

This study was reviewed and approved by the Investigational Review Board (IRB) for the Protection of Human Subjects at Duquesne University. Funding for this study was provided for by the American Academy of Implant Dentistry Research Foundation. The appendix contains forms relevant forms to IRB approval.

Patient Selection

All patients (N=6) selected were between ages 18-40 with a negative medical history and were non-smokers. Tooth extractions considered in the study were bilateral mandibular impacted third molars of equal eruptive states. Patients were informed individually of possible complications and signed study, surgical and IV sedation informed consent forms. Patients were remunerated $250.00 at the completion of the 25 week evaluation period.

PRP Collection

A venous puncture using a 21 gauge 1.5 inch latex-free needle(EXELINT Int. Co., Los Angeles, CA) with an attached vacutainer holder (EXELINT Int. Co., Los Angeles, CA) in the ante-cubital fossa, or the dorsal surface of the hand contra-lateral to the IV administration site was performed. Whole blood was drawn using two 4.5 mL BD Vacutainer™ tubes containing 0.45 mL of the anticoagulant tri-sodium citrate (9:1)

(Becton Dickinson & Co., Franklin Lakes, NJ). PRP was prepared as described previously in the Preparation and Characterization of PRP section (Study 1).

Third Molar Surgical Technique and PRP Placement

Intravenous access was obtained using a 22 gauge 1-inch Terumo Surflo™ intravenous catheter (Terumo Medical Corporation, Elkton, MD). The vein was kept open (KVO) with dextrose 5% in water (Baxter Healcare Corporation, Deerfield, IL). Patients were monitored via electrocardiogram (EKG), automatic blood pressure, and percent hemoglobin oxygen saturation with a Criticare Systems model 507 E (Criticare Systems, Inc. Waukesha WI) anesthesia monitor. All patients were sedated with a combination of intravenous midazolam HCl, diphenhydramine HCl, and fentanyl citrate (Ace Surgical, Brockton, MA) as needed to induce a state of conscious sedation. Once the patient was sedated, the blood draw was performed to acquire the PRP for use after the teeth were removed. Depending on allergies, patients were administered either cefazolin 2.0 gram (Baxter Healthcare Co, Deerfield, IL) or clindamycin 600 mg (Ace Surgical, Brockton, MA) immediately pre-operative via IV. Following sedation and administration of antibiotics, all patients were administered lidocaine HCl 2% with epinephrine 1:100,000 (Cook-Waite, Rochester, NY) bilaterally as follows: 1.8 mL (1 unit-dose carpule) as a Gow-Gates inferior alveolar block, 1 unit-dose carpule as a long buccal, buccal infiltration and lingual block. If anesthesia was deemed to be inadequate, additional carpules were administered as needed to a total maximum of 11 unit-dose carpules. Incisions were made in the envelope fashion. The posterior extension of the incision diverged laterally to avoid injury to the lingual nerve. The incision was brought anterior in the gingival sulcus to the mesial of the first molar (no vertical releasing

incision was made). The gingival soft-tissue was reflected exposing bone overlaying the

impacted tooth. Bone was removed by the use of a Elcomed 100 electric handpiece

(W&H Dentalwerk, Burmoos, GMbH, Austria) and a #8 round surgical burr (Henry

Schein Inc. Melville, NY). Teeth were sectioned as needed with a 45° High Impact

handpiece with a #700 Fisher burr (Henry Schein Inc., Melville, NY). The control

extraction site was treated immediately post-extraction as follows:

a. Placement of Gelfoam® (Pharmacia Corporation, Kalamazoo, MI) only (no PRP)

b. Primary closure was achieved with 3-O chromic gut suture material (Henry
   Schein Inc., Melville NY 11747 USA).

c. After removal of the tooth, a small periapical digital radiograph (Dentsply
   Gendex®, York, PA) was taken using an XCP-DS® mount to determine a
   baseline grayscale representing bone density at each extraction site.

The treated site was treated immediately post-extraction as follows:

a. Injection of 200 μL of PRP into the extraction site

b. Placement of Gelfoam®, moistened with 175 μL PRP

c. Primary closure was achieved with 3-O chromic gut suture material (Henry
   Schein Inc., Melville NY 11747 USA).

d. After removal of the tooth, a small periapical digital radiograph (Dentsply
   Gendex®, York, PA) was taken using an XCP-DS® mount to determine a
   baseline grayscale representing bone density at each extraction site.

To help prevent excessive post-operative inflammation, patients were administered

dexamethasone sodium phosphate (Ace Surgical, Brockton, MA) 8 mg IV pre-

operatively and methylprednisolone suspension Depo-medrol® (Pharmacia & Upjohn Co, New York, NY) suspension 40 mg IM immediately post-op. Patients were also administered ketorolac trimethamine 30 mg (Hospira, Lake Forest, IL) IV immediately post-op. Immediately post-operative bilateral Gow-Gates mandibular block injection using 1.8 mL of bupivacaine HCl 0.5% with 1:200,000 epinephrine (Hospira, Lake Forest, IL) was administered to prevent immediate post-op pain. Patients were advised to take ibuprofen 600 mg every 6 hours for 3 days and then every 6 hours as needed thereafter. They were advised to take acetaminophen 500 – 1000 mg every six hours if the ibuprofen did not control the pain. Patients were dismissed with a grade card for notations every 8-hours for 3 days, then notations every 12 hours for the following 6 days. Each surgical site was graded with a visual analogue scale (VAS) for:

1. Pain

2. Temperature (external feeling of warmth)

3. Facial swelling

4. Bleeding

5. Numbness or altered sensation of tongue, face, lip or chin.

The participants used the instrument in the appendix for post-operative evaluation from their perspective.

The patients returned post-operatively for observer evaluations plus digital radiographs using the same protocol for immediate post-operative radiographs. These evaluations were repeated at the following post-operative time points: 3 days plus weeks-

1, 2, 3, 4, 6, 8, 12, 16, 20, and 24. Blinded observers used a VAS to evaluate the

following:

1.   Dehiscence (surgical soft tissue opening)

2.   Bleeding

3.   Inflammation

4.   Facial edema

5.   Intra-oral edema

6.   Pain

Three of the patients had a mandibular computerized axial tomography (CT) scan

performed by a local hospital. Each of these three patients had one CT scan taken.

Patient-1 had theirs taken at 18 weeks post-operative, Patient-2 at 14 weeks post-

operative, and Patient-3 at 10.5 weeks post-operative. This allowed for verification of the

grayscale from digital radiography with the bone density Hounsfield units (HUs) of the

CT scan and percent bone fill of the extraction sites.

Radiographic Technique and Exposure

Radiographs were taken with a Trophy ETX Dental peri-apical X-ray machine

(Trophy Radiologie, Vincennes, Cedex, France). X-radiation settings were 70 KV, 8

mA, for 0.05 second exposure time. The digital x-ray sensor used was a Gendex GX-S

sensor (Gendex Dental System, Lake Zurich, IL). The radiograph sensor was held by a

Dentsply Sensor Holder XCP-DS® posterior holder and ring (Dentsply International

York, PA). Digital radiographs were formatted by VinWix Pro computer software

(Gendex Dental System, Lake Zurich, IL). Digital radiographs were used for two

reasons: 1) the technique allows for consistent radiographic opacity and evaluation, and

2) it exposes patients to only 25% of the radiation used with conventional radiography. A

correlation of bone density was confirmed during the study with a CT scan and computer

reformatting for bone density determination via HU for three patients. Because of the

need to evaluate the post-operative bone healing, participants were exposed to 22 digital

periapical radiographs.

CT Scan Technique and Exposure

Mandibles were scanned 1mm inferior to the mandible to the superior surface of the

mandibular teeth. CT specifics were as follows:

- Image size: 512 x 512 pixels

- Gantry tilt: 0.0 degrees

- Scanner slice thickness: 0.5 – 1.0 mm

- Scanner step increment: 0.5 – 1.0 mm

- Field of View: typically 150 – 180 mm

Images were taken in uncompressed DICOM 3.0 format. KV and MA were kept as low

as possible with a table pitch 1:1. CT scans were reformatted for quantitative

measurement using Logic VIPTM Data Conversion® software.

X-ray Analysis

Image J software (downloaded from http://rsb.info.nih.gov/ij/) was used for digital radiograph analysis. The radiographs were assessed by obtaining the average density of the third molar extraction socket sites. Three different readings were taken of each socket and averaged. This average was compared to the average of three density outlines of the adjacent tooth. When all radiographs for a patient were assessed in this manner, they were normalized to the original radiograph and the same untouched adjacent tooth. The baseline socket average was then subtracted from the normalized radiographic average for each of the tooth extraction sockets at the different time points. This accounted for minor radiographic exposure and technique variation with each time point. The final normalized socket value differences for each PRP treated and non-treated sites for the various time points were compared. Figure 35 illustrates the outline with ImageJ software for outline of adjacent tooth used for normalization of radiographs and the outline of the extraction socket.
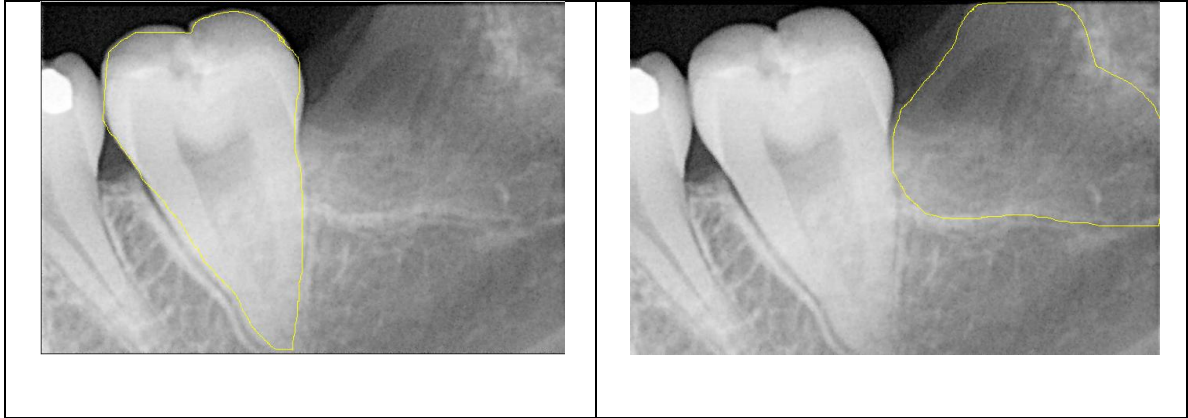
Figure 35. Example of ImageJ® Software Outline of Adjacent Tooth
and Extraction Socket

Example of ImageJ® software outline of adjacent tooth (left photo) used for
normalization with the baseline radiograph taken of the same site immediately following
tooth extraction and placement of the Gelfoam® (± PRP) and sutures. Right radiograph
illustrates outline of tooth extraction socket that is compared to the same region of
interest of the baseline radiograph. All radiographs were taken with the same exposure
parameters (KV, mA, and time) and similar angles and distance from x-ray source.

All radiographs were taken by a blinded certified X-ray dental assistant or hygienist.

Radiographs were taken immediately post-op and at the following time points after the

day of surgery: 3 days, 1 wk, 2 wks, 4 wks, 6 wks, 12 wks, 16 wks, 20 wks, and 24 wks.

Radiographs were evaluated by 3-blinded dental professionals.

CT Scan Analysis

CT scans were evaluated concerning percent bone fill, formed bone density, and total

socket formed bone density. CT scans were reformatted with Logic VIPTM Data

Conversion® software, which permitted quantitative measurements at 1mm increments of

the extraction socket. Percent bone fill was determined by measuring the quantity of bone that had formed in the socket at that time point and dividing this value by the entire socket depth and multiplying by 100% . Representative bone fill measurements for Patient-2 at 14 weeks are shown in Figure 36.
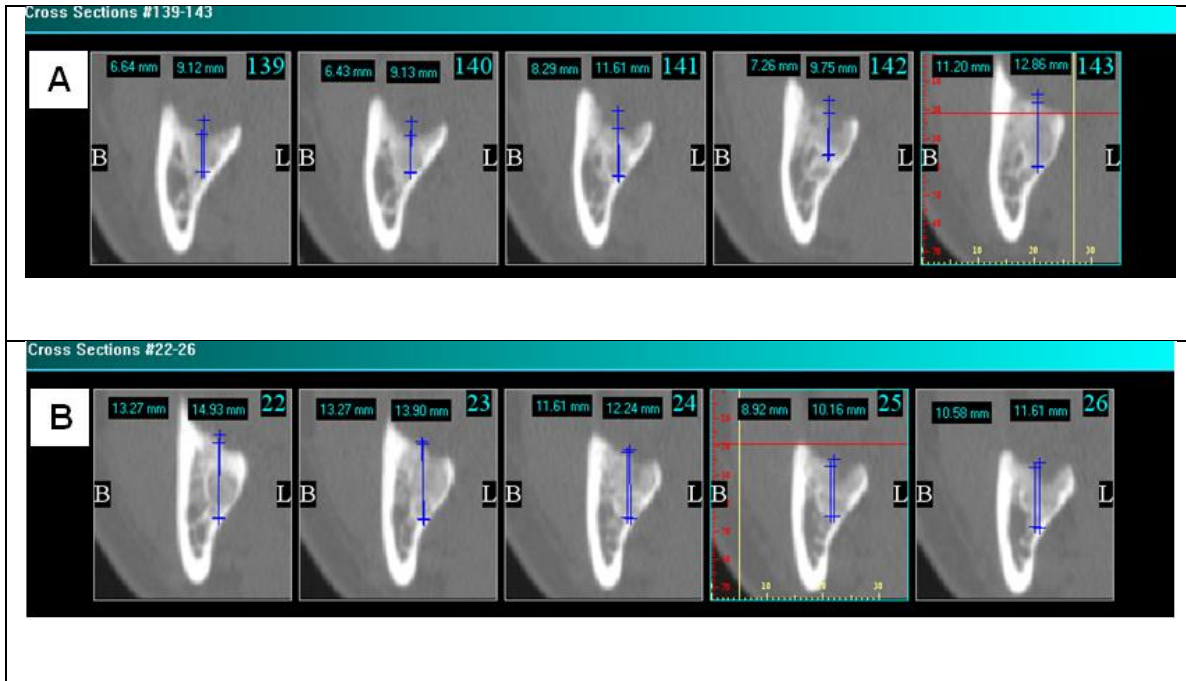
Figure 36. Example of CT Scan Evaluated Percent Bone Fill

Measurements (mm) for Extraction Sites

Representative CT scan projections of control and PRP-treatment extraction sites are illustrated by VIPTM Data Conversion® software for Patient-2 at 14 weeks. Each individual projection represents a 1 mm sagittal cross section slice of the extraction socket in a anterior to posterior direction. Measurements in millimeters (mm) are shown using the measuring tool provided by the software. Two measurements are taken, one that measures from the base of the extraction site to the superior aspect of actual formed bone (left number in each slice), the second is total socket depth and is measured from the base of the extraction socket to what would be the most superior aspect of the socket (right number in each slice). Dividing the actual bone formed bone by the total socket depth and multiplying this number by 100% provides the percent bone fill for the socket. All bone fill measurements for the multiple 1 mm slices of the respective extraction site were averaged together. Each CT scan was evaluated by 3-blinded observers. All three evaluator average readings were then analyzed by a two-tailed t test.

Newly formed bone density (NFBD) was measured in Hounsfield units (HU) by the use of an elliptical drawing tool provided with the software. Areas of new bone formation were outlined and quantified as HUs. Representative measurements of NFBD for Patient-2 at 14 weeks are illustrated in Figure 37.

Figure 37. Example of CT Scan Evaluated Newly Formed Bone Density (NFBD) in Hounsfield Units for Extraction Sites

Representative CT scan projections of control and PRP-treatment extraction sites are illustrated by VIPTM Data Conversion® software for Patient-2 at 14 weeks. Each individual projection represents a 1 mm sagital cross section slice of the extraction socket in a anterior to posterior direction. Measurements in Hounsfield units (Hus) are shown with the elliptical measurement tool provided by the software. The elliptical tool was used to outline actual bone that had formed in the extraction site as is referred to as newly formed bone. Each measurement provides an average HU that was recorded for each 1mm slice. Average HUs represent averaged bone density, therefore these values would represent the average newly formed bone density (NFBD) for that 1 mm slice. All HU measurements obtained for the multiple 1 mm slices of the respective extraction site were averaged together. Each CT scan was evaluated by 3-blinded observers. All three evaluator average readings were then analyzed by a two-tailed t test.

Total socket formed bone density (referred to as total formed bone density - TFBD) was a measurement of the HUs for the entire socket, regardless of the quantity of bone formed. Representative measurement of TFBD for Patient-2 at 14 weeks is shown in Figure 38. This measurement was done in a similar manner to NFBD (Figure 37) but the difference being that the entire height of the socket was considered, not just the areas that had actual bone formation. This measurement could more accurately represent the same areas measured by digital radiographs. Taking this measurement allowed for comparison of the two measurement tools.
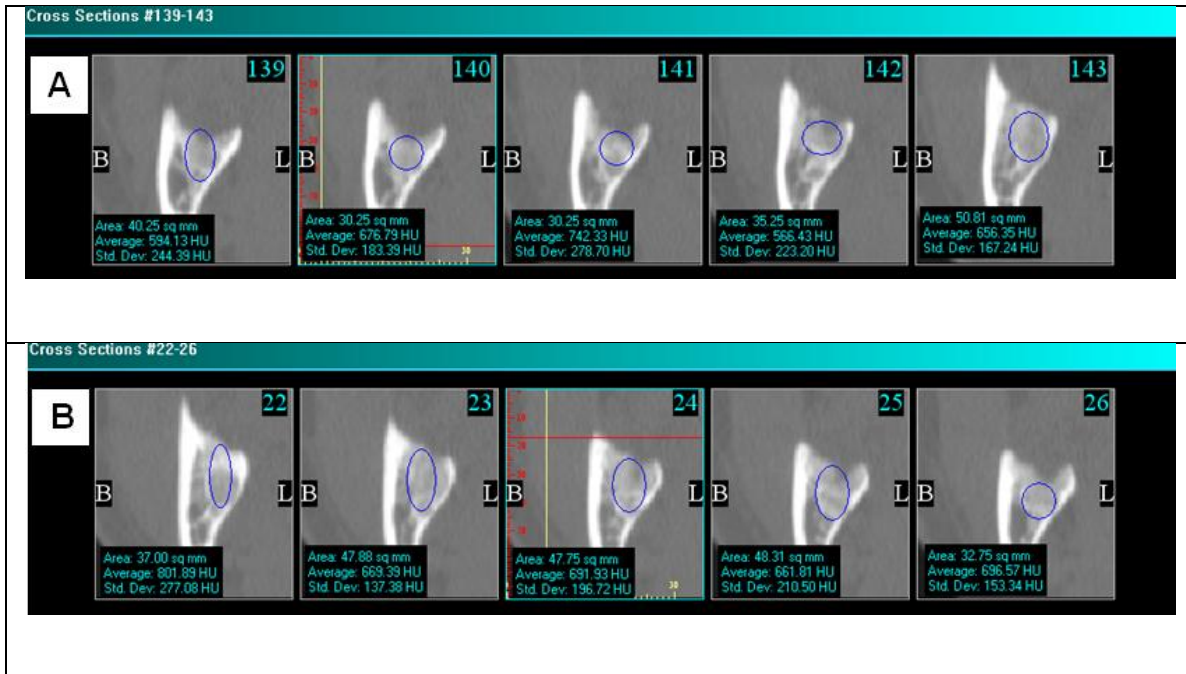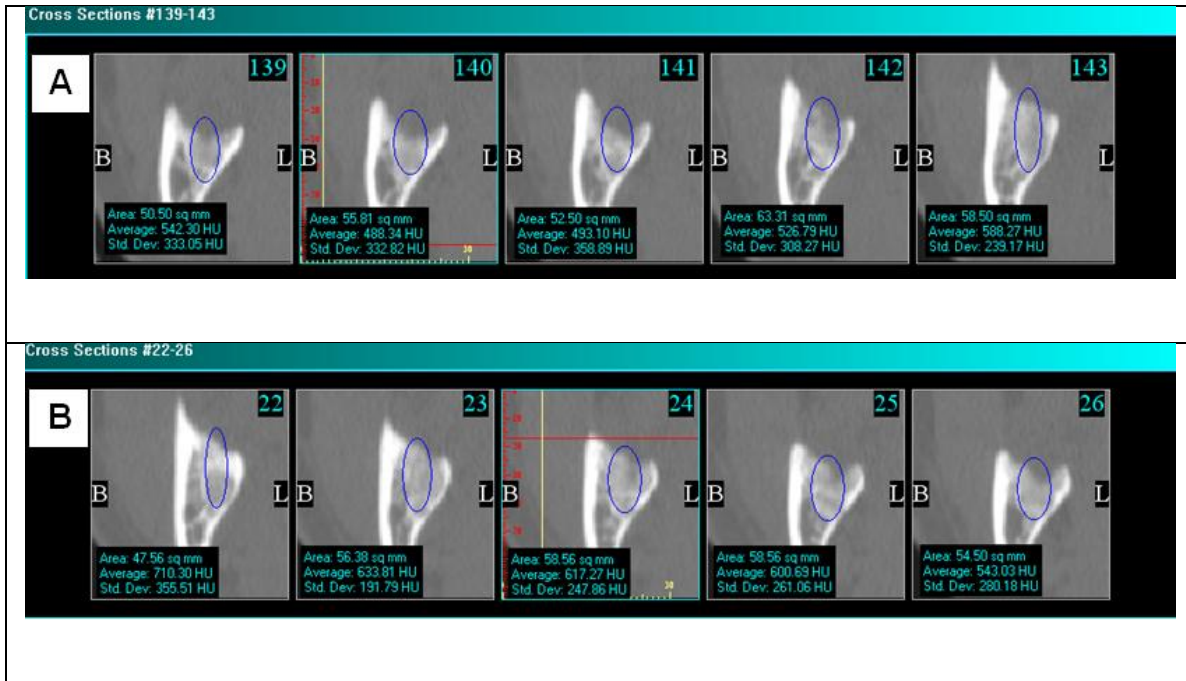
Figure 38. Example of CT Scan Evaluated Total Formed Bone Density (TFBD) in Hounsfield Units for Extraction Sites

Representative CT scan projections of control and PRP treatment extraction sites are illustrated by VIPTM Data Conversion® software for Patient-2 at 14 weeks. Each individual projection represents a 1 mm sagittal cross section slice of the extraction socket in an anterior to posterior direction. Measurements in Hounsfield units (HUs) are shown with the elliptical measurement tool provided by the software. The elliptical tool was used to outline the entire vertical height of the extraction site as is referred to as total bone formed. Each measurement provides an average HU that was recorded for each 1 mm slice. Average HUs represent averaged bone density, therefore these values would represent the average total formed bone density (TFBD) for that 1 mm slice. All HU measurements obtained for the multiple 1 mm slices of the respective extraction site were averaged together. Each CT scan was evaluated by 3-blinded observers. All three evaluator average readings were then analyzed by a two-tailed t test.

Patients 1 and 2 CT scans were measured in 1 mm cross section planes (anterior to posterior). The CT scan for patient three was measured in panoramic 1 mm sectional planes. The cross sectional planes were preferred, but the topography of the bone after

tooth removal for Patient-3 did not permit accurate quantitative measurements with those projections. CT scans were evaluated by 3-blinded evaluators working independently.

Statistical Analysis

Statistical analysis was performed using GraphPad Prism® 3.0 (GraphPad Software, Inc., La Jolla, CA). Two-way ANOVA analysis was performed for digital radiographs taken over a 0 to 2 weeks, 3 to 12 weeks, 3 to 25 weeks, and 0 to 25 weeks time-periods. Two-tailed paired t-tests were performed for individual time points with digital radiographs and CT scan analysis.

C. Results

Digital Radiographic Results:

Digital radiographs were used to evaluate changes in radiographic bone density for each extraction site. Three blinded dental professionals working independently evaluated all radiographs. All extractions were of bilateral mandibular third molars (wisdom teeth) that had similar eruptive states prior to removal. Each patient had one extraction site treated with PRP and the ipsilateral side did not receive PRP treatment. Three patients received PRP treatment on the right side and three received the PRP treatment on the left side. Treatment side was predetermined as follows. The first, third, and fifth patients would receive PRP treatment on the left side and the second, forth, and sixth patients would receive PRP treatment on the right side. This treatment decision was made prior to viewing patient radiographs and patient position in the sequence was based on their order of scheduling.

Radiographic analysis of the digital radiographs taken for the 6 patients over the 25 week time period show a significant (p < .0001) effect of localized PRP treatment on bone density. The data represent the percent change in radiographic density for each socket and each time point from its corresponding baseline value. Baseline values were determined as the radiographic density of extraction site immediately following tooth removal and placement of the Gelfoam® and sutures. Figure 39 illustrates the mean densities for all patients. The two-tailed paired t test was used to analyze each time point, while two-way ANOVA was used to analyze data representing the span of a time-period. The two-tailed paired t test showed that there was a significant increase in the radiographic bone density for PRP treatment sites compared to control sites for each of the time points 1week ($p < .01$), and 2 weeks ($p < .05$). The PRP treatment side had a positive effect on bone density immediately following tooth extraction. Whereas, the control side when compared to its corresponding baseline bone density immediately following tooth removal (baseline density), showed a decrease in bone density for the initial week and by week 2 returned to baseline. Two-way ANOVA for the initial 2 weeks showed that treatment was significant (F = 32.16, $p < .0001$), the time elapsed following surgery was not significant (F = 2.874, $p > .05$) but there was a significant interaction between treatment and time (F =7.733, $p < .001$). For weeks 3-12, treatment was significant (F=21.97, $p < .0001$), but time was not (F=1.698, $p > .05$) and there was no significant interaction between time and treatment (F=0.1455, $p > .05$). Weeks 3, 4, 6, and 8 showed parallel density changes from their respective baseline. The two-tailed paired t test revealed at week 12 a significant difference ($p < .05$) between the density changes between the two groups as did week 20 ($p < .05$). The intervening week 16 ($p >$

.05) did not show a significant difference nor did week 25 ($p > .05$. The PRP treatment group had greater bone density changes over baseline immediately following extraction, but the differences between the groups were not significant at later time points with the exception of weeks 12 and 20. For weeks 3-25 two-way ANOVA analysis did reveal that treatment was significant (F = 15.21, $p < .0001$), time elapsed was also significant (F = 5.924, $p < .001$), but the interaction between treatment and time was not significant (F=0.07530, $p > .05$). When examining the entire 25-week period, treatment was again significant (F = 37.49, $p < .0001$), time elapsed following surgery was significant (F = 13.75, $p < .0001$) but the interaction between treatment and time was not significant (F=0.6975, $p > .05$).
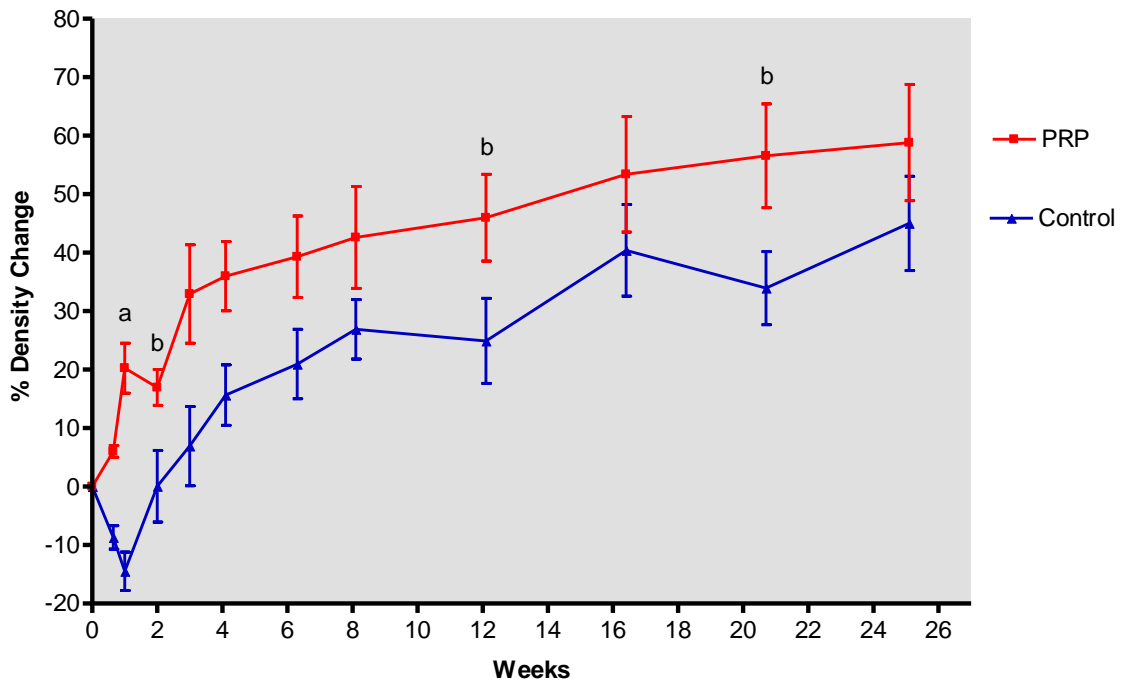
Figure 39. Percent Radiographic Density Change of Surgical ±PRP Treatment compared to Control Radiograph Taken Immediately Following Tooth Removal

All 6 patients are represented in this graph with each time point representing the average values of the patients combined. Percent bone density change on the Y-axis represents the change in bone density that has occurred at the extraction site in comparison to the extraction site immediately after tooth removal and placement of the Gelfoam® sponge ± PRP and suturing. Digital radiographs were normalized to the immediate post-operative film by comparing the unaltered adjacent tooth on the time point radiograph with the immediate post-operative radiograph's corresponding unaltered tooth. Each patient's digital radiographs were evaluated by 3-blinded evaluators. Each point on the connecting bars represents the ± S.E.M. for the six different patients and each treatment group. Analyses for each treatment site were performed in triplicate by each evaluator. Each data point was analyzed with a two-tailed paired t-test where significance was defined as $p < .05$, where $a = p < .01$; $b = p > .05$ for individual time points. For the span of time-periods, a two-way ANOVA was performed and significance was defined as $p < .05$. For the time period 0 to 2 weeks PRP-treatment was significant ($p < .0001$); time was not significant ($p > .05$); but there was a significant interaction ($p < .001$) between the benefits of PRP-treatment and time, therefore the beneficial effects of the PRP-treatment and time were related for the initial 2 week post-operative healing time period. For weeks 3 though 12 treatment was significant ($p < .0001$), but time was not ($p > .05$) and there was no significant interaction between time and treatment ($p > .05$). For the time period 0 to 25 weeks PRP-treatment was significant ($p < .0001$); time was significant ($p < .0001$); but there was not a significant interaction ($p > .05$) between the benefits of PRP-treatment and time, therefore the effect of the PRP-treatment was independent of time for the entire 25 week time period.

CT Scan Results

Sample CT scan projections for each of the 3 patients who underwent this analysis are presented in Figures 40-42. The panoramic, axial and sagital cross-sectional windows were viewed in one mm slices and sagital cross-sectional views were evaluated for each patient at their indicated time point. Three-blinded dental personal working

independently analyzed each of the CT scans. The standard error of the mean (SEM) of

these three measurements is indicated on each of the graphs. There is some subjective

interpretation in outlining areas to evaluate, as there was with the digital radiographs.

Each evaluator recorded three readings for each 1mm slice at each extraction site.

Evaluations were done for 3 criteria: 1) percent bone fill; 2) newly formed bone density

(NFBD); and 3) total bone formed density (TFBD). The three readings for each scan

slice were averaged.
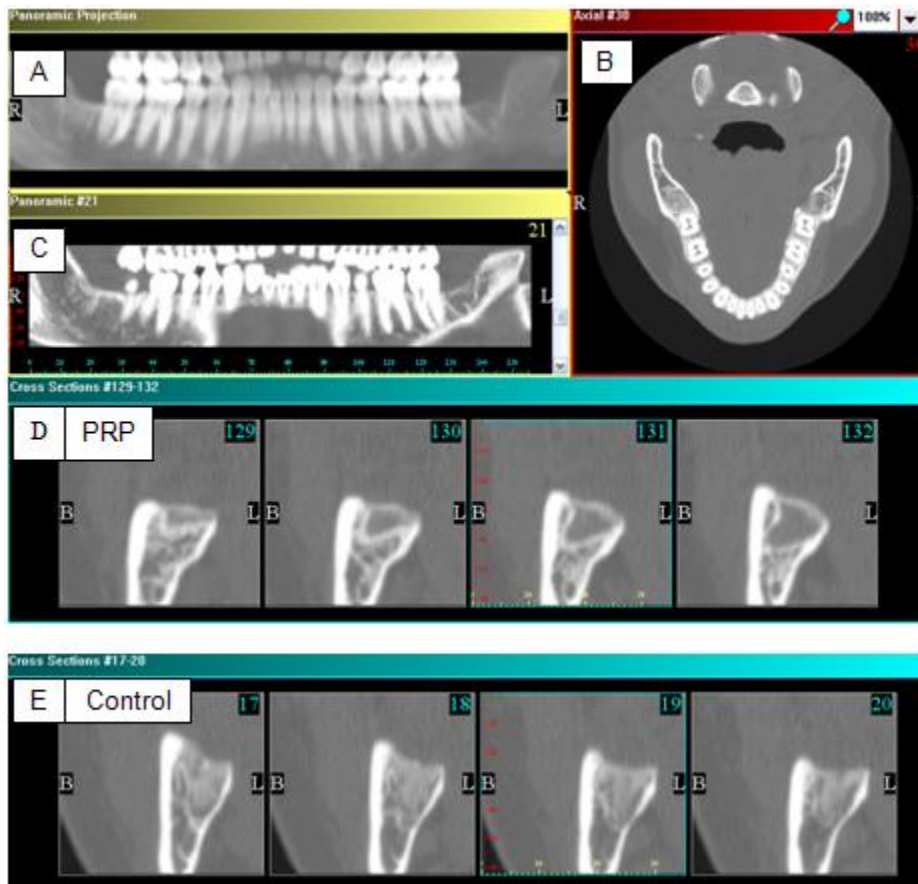
Figure 40. Patient 1 CT Scan 18 Weeks

CT scan panel for Patient 1. A. Panoramic radiographic projection (traditional x-ray);B.
Axial CT section superior to extraction sites; C. Panoramic CT section note: L (left) and
R (right) correspond to each side of the patient; D. CT scan sagittal cross-section 1mm

slices of left extraction site (PRP treated); E. CT scan sagital cross-section 1 mm slices of right extraction site (control).

Figure 41. Patient 2 CT Scan 14 Weeks

CT scan panel for Patient 2. A. Panoramic radiographic projection (traditional x-ray);B. Axial CT section superior to extraction sites; C. Panoramic CT section note: L (left) and R (right) correspond to each side of the patient; D. CT scan sagital cross-section 1mm slices of right extraction site (PRP treated); E. CT scan sagital cross-section 1mm slices of left extraction site (control).

Figure 42. Patient 3 CT Scan 10.5 Weeks

CT scan panel for Patient 3. A. Panoramic radiographic projection (traditional x-ray);B. Axial CT section superior to extraction sites; C. Panoramic CT section note: L (left) and R (right) correspond to each side of the patient; D. CT scan sagital cross-section 1mm slices of right extraction site (PRP treated); E. CT scan sagital cross-section 1 mm slices of left extraction site (control).

Three factors were evaluated for each of the CT scans. The first factor was percent

bone fill that represented the degree to which the bone had developed and filled in the

extraction socket. This was done by measuring the radiographic evidence of bone

formation in the socket from an inferior to superior manner and dividing this value by the

height of the total socket (again inferior to superior measurement). The second factor

analyzed was newly formed bone density (NFBD) which represents the density of the

bone that had actually formed in the socket. This measurement was calculated by the

computer program and was concerned only with actual new bone formation. The third

factor analyzed was Total Formed Bone Density (TFBD). This factor considered the

entire extraction socket bone density. All three factors were analyzed for each individual

patient's CT scan at a specific time with three readings (averaged) from three blinded

evaluators using the two-tailed paired t test. The data for the three patients' individual

factors were combined and analyzed with a two-way ANOVA, because three different

time points were considered.

For the first factor percent bone fill of the extraction sockets were examined and

compared. PRP treated sites were compared with non-PRP treated sites (control).

Percent bone fill for all of the patients (Patient-1 at 18 weeks, Patient-2 at 14 weeks, and

Patient-3 at 10.5 weeks) did not reveal a substantial difference in bone height between the

PRP treatment sites and control sites (Figures 43 A-C). Patient-1 (18 weeks) CT scan

(Figure 43-Panel A) indicated that bone fill for the PRP treated side was 96% in

comparison to the control side at 90%. Patient-2 CT scan (14 weeks) illustrated that the

PRP treated side bone fill was 90% in comparison to the control side at 81% (Figure 43-

Panel B). Patient-3 (Figure 43-Panel C) had the earliest CT scan (10.5 weeks) indicated

that the PRP treated side had 55% bone fill while the control side was approximately

42%. The lesser percent bone fill for the earliest CT scan and greater bone fill for the

subsequent later time point CT scan was expected. When using a two-way ANOVA to

compare all 3 patients and their respective time points together, the PRP sites did

show significant (F=19.76, $p < .05$) greater percent bone fill than the control sites

(Figure 47-Panel D); time was also significant (F=185.3, $p < .01$).
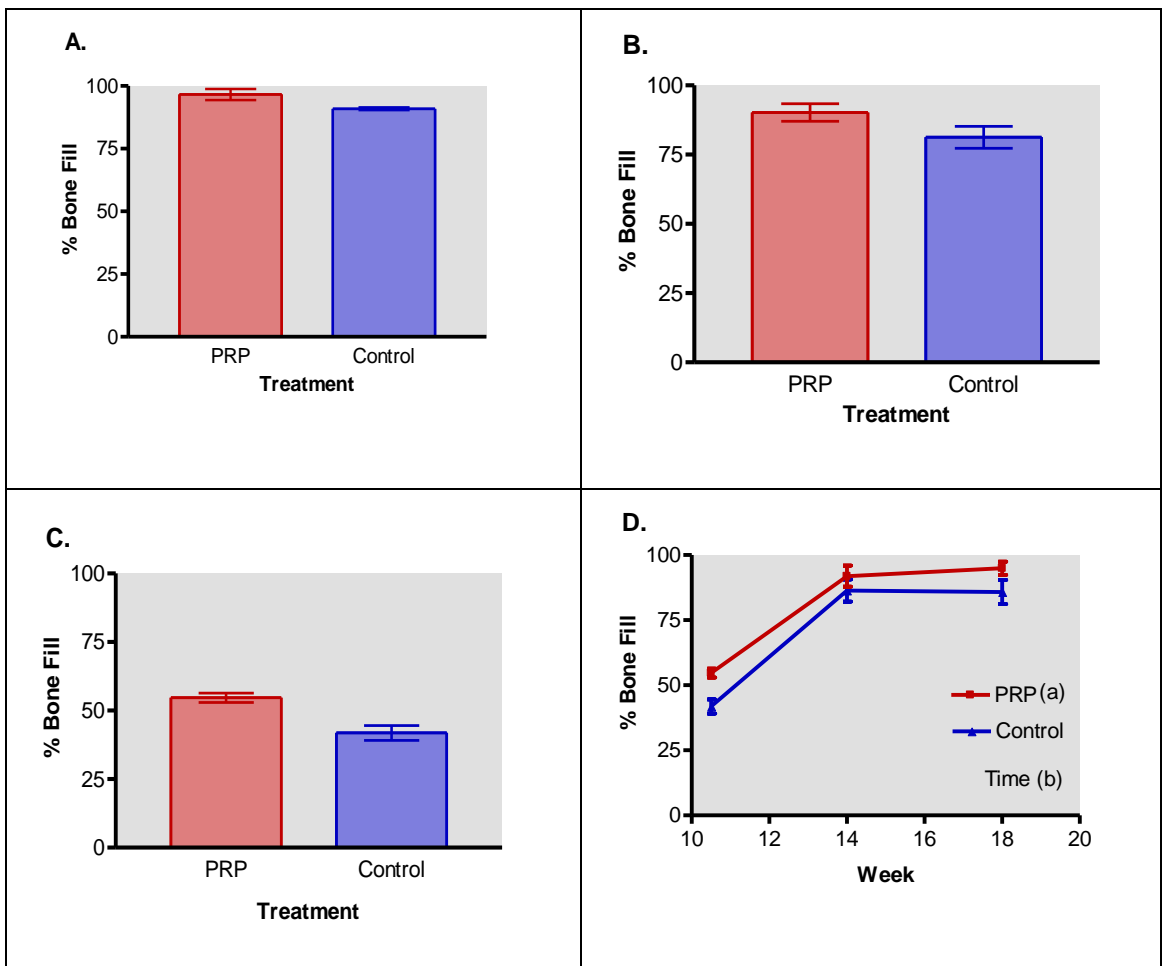
Figure 43. Percent Bone Fill of Extraction Sockets Analyzed by CT Scan

Panels A-C represents CT scan analyses of percent bone fill for the PRP-treated and control extraction sites on three different patients at a specific time point. Panel A represents a patient's percent bone fill at 18-weeks. Panel B represents a patient's percent bone fill at 14-weeks. Panel C represents a patient's percent bone fill at 10.5-weeks. Panel D represents the three patients over the three time points and analyzed by two-way ANOVA where significance was defined as $p < .05$. Where a $= p < .05$ revealed that PRP-treatment significantly enhanced the percent bone fill when compared to non-PRP-treated sites (control). For $b = p < .01$ Time elapsed since tooth removal was also found to be significant.

The second factor examined was bone that had developed since the extraction had taken place and it is referred to as newly formed bone. PRP treated sites were compared with non-PRP treated sites (control). New bone that formed was measured in HUs and illustrated in Figure 44 A-D. It is referred to as newly formed bone density (NFBD). As expected, the NFBD was greater at the later time points than the earlier 10.5-week time point. Patient -1 (18-weeks) NFBD is presented in Figure 44A. Patient-2 (Figure 44 B) had denser bone at the 14-week time point in comparison to Patient-3 (Figure 44-C)at the 18-week time point, but this may be due to individual patient variation or measurement variables. When comparing all patient treatments together (Figure 44 D) and the various time points with a two-way ANOVA, the PRP-treated and control sites did not differ significantly (F=0.01475.134, $p > .05$) in NFBD, and time was not a significant (F=13.19, p > .05) factor either.
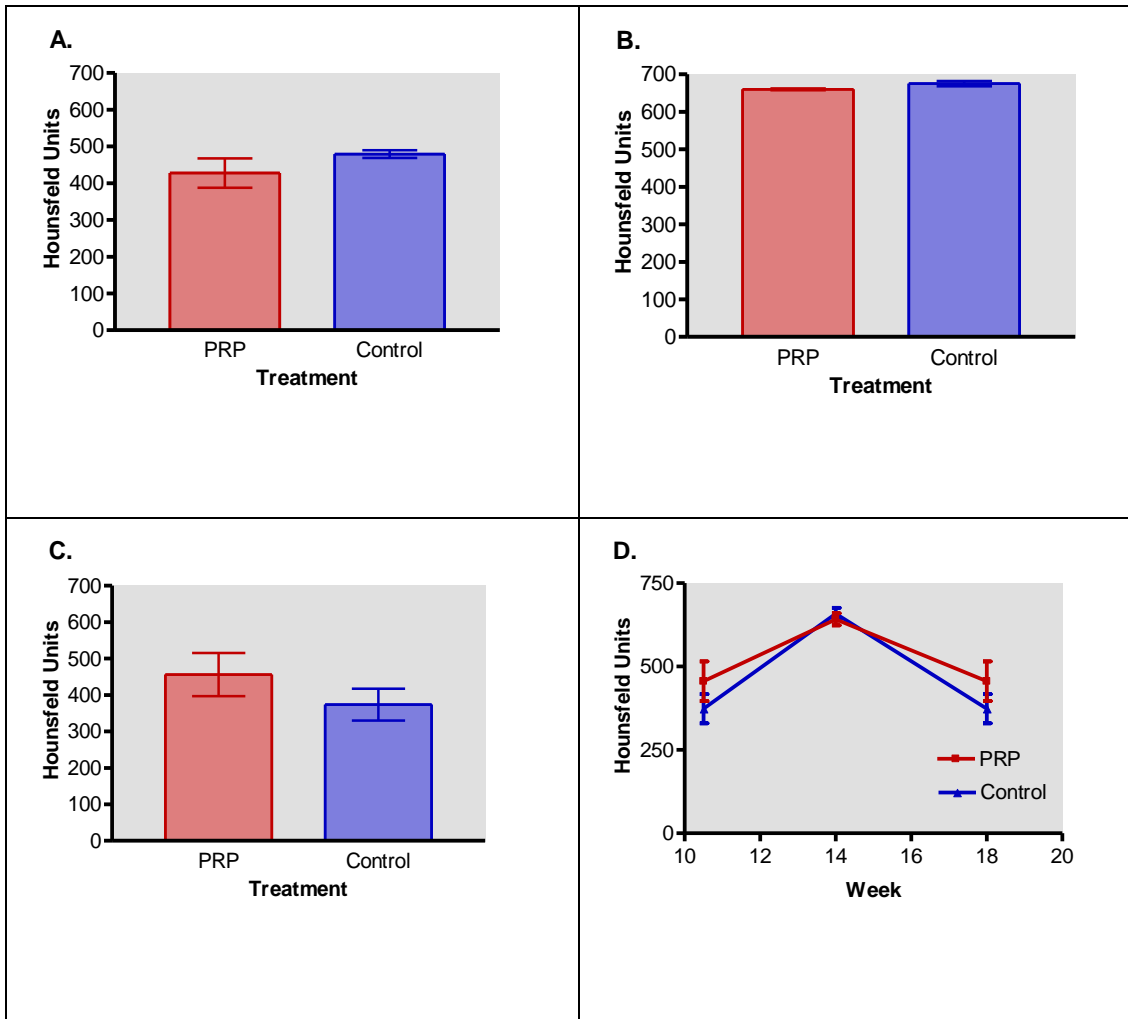
Figure 44. Newly Formed Bone Density (NFBD) of Extraction Sockets Analyzed by CT Scan

Panels A-C represents CT scan analyses of newly formed bone density (NFBD) for the PRP-treated and control extraction sites on three different patients at a specific time point. Panel A represents a patient's NFBD at 18-weeks. Panel B represents a patient's NFBD at 14-weeks. Panel C represents a patient's NFBD at 10.5-weeks. Panel D represents the three patients over the three time points and analyzed by two-way ANOVA where NFBD with PRP-treatment was not significant ($p > .05$) in comparison to the control sites. Time elapsed was found not a significant ($p > .05$) factor for NFBD.

The third factor considered was the average bone density for the entire tooth

extraction site. PRP treated sites were compared to non-PRP treated sites (control).

Total Formed Bone Density (TFBD) represents the density of the complete extraction

socket. This measurement includes new bone that had actually formed in the socket and

areas of the socket where bone had not yet developed. TFBD is measured in HUs and

illustrated in Figures 45 A-D. Again, as expected Patient-3 (10.5-weeks) (Figure 45 C)

with the earliest CT scan had the lowest TFBD, while Patient-2 (14-weeks) (Figure 45 B)

did have a slightly higher value than Patient-1 (18-weeks) (Figure 45 A). When

comparing all of the patients together (Figure 45 D) with a two-way ANOVA analysis,

the PRP-treated sites did not have a significant increase (F = 0.2557, $p > .05$) in TFBD,

but time elapsed since tooth removal was a significant (F = 96.12, $p > .0001$) factor.
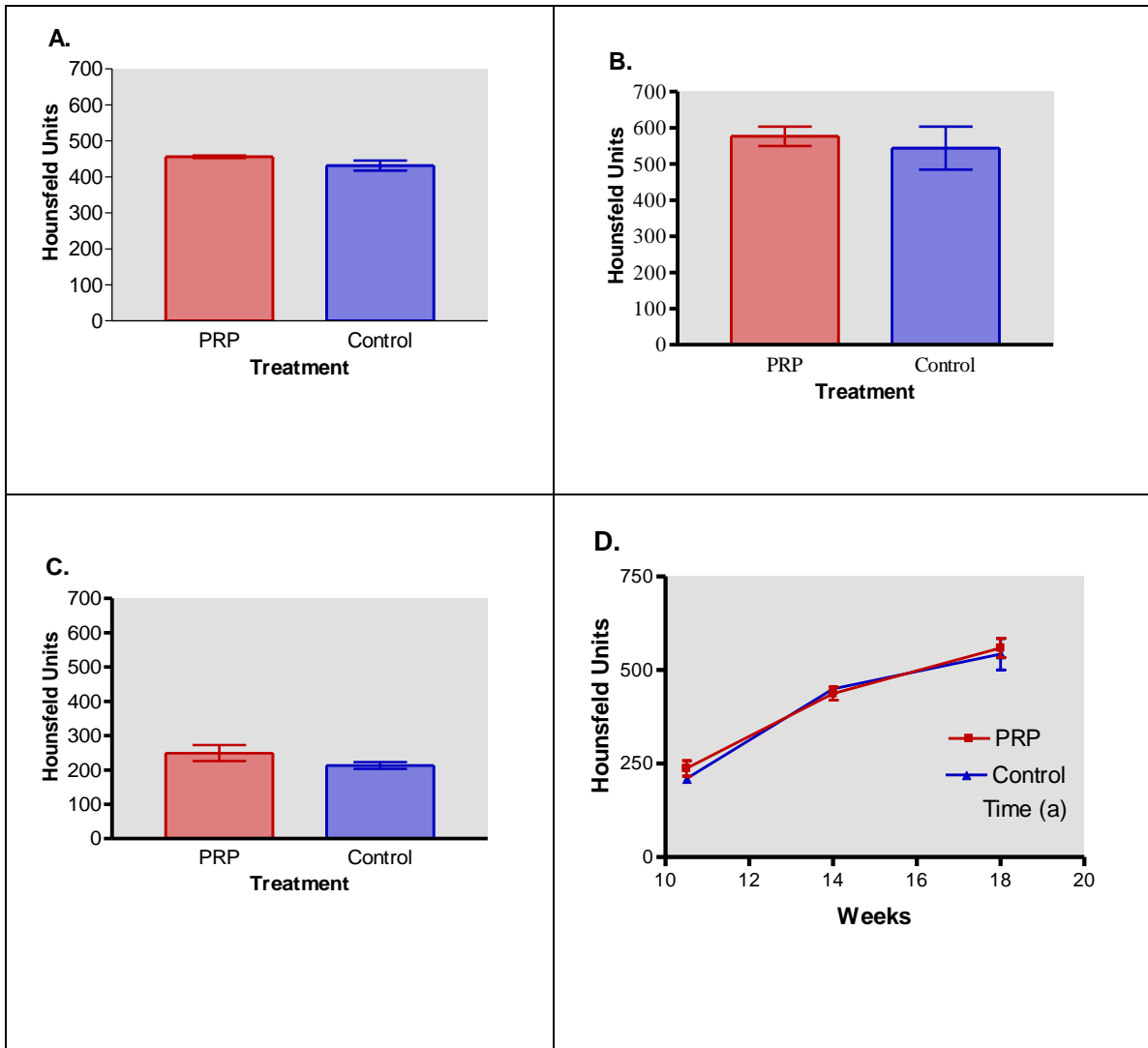
Figure 45. Total Formed Bone Density (TFBD) of Extraction Sockets Analyzed by CT Scan

Panels A-C represents CT scan analyses of total formed bone density (TFBD) for the PRP-treated and control extraction sites on three different patients at a particular time point. Panel A represents a patient's TFBD at 18-weeks. Panel B represents a patient's TFBD at 14-weeks. Panel C represents a patient's TFBD at 10.5-weeks. For each of these patients there was no substantial difference between PRP-treatment and control sites. Panel D represents the three patients over the three time points and analyzed by two-way ANOVA, where TFBD with PRP-treatment was not significant ($p > .05$) in comparison to the control sites. Time elapsed did have a significant effect ($p < .0001$) on TFBD.

Next, the TBFD values obtained from the CT scan analysis were compared to the grayscale digital radiographic analysis. The digital radiograph grayscale values were of the entire socket (as were the TBFD values) and therefore, represent similar measurements. Figure 39 shows the normalized percent change in digital radiographic bone density from the baseline value. Table 12 shows the ratio of the normalized grayscale value of the PRP treated site to the control site in each of these three patients who underwent CT scans. To minimize radiation exposure for patients the CT scans were obtained midway between two digital radiographic time points. This comparison revealed that the CT scan percent TBFD were similar, but higher than the digital radiograph grayscale values. The results for the two later time point CT scans had greater similarity to the digital radiograph grayscale values than for the CT scan taken at the earlier time point.

Patient	(A) Digital Radiograph prior to CT scan ± S.E.	(B) CT scan ± S.E.	(C) Digital Radiograph after CT scan ± S.E.
1	101.0 ± 3.377 (16 wks)	106.0± 3.99 (18 wks)	97.25 ± 0.8253 (20 wks)
2	102.7 ± 1.448 (12 wks)	107.6 ± 7.353 (14 wks)	101.2 ± 0.5452 (16 wks)
3	101.2 ± 2.247 (9.5 wks)	115.7± 5.108 (10.5 wks)	105.3 ± 2.717 (11.5 wks)

Table 12. Total Bone Formed Density (TFBD) - Percent Change Comparisons of Digital Radiographs and CT Scans

These TBFD values compare the percent radiographic density changes observed between digital radiographs and CT scans. Column A represents the digital radiograph taken 2-4 weeks prior to the CT scan (column B) and column C represents the digital radiograph taken 1-2 weeks after the CT scan. Comparison revealed that the CT scan percent TBFD were comparable, but higher than the both earlier and later digital radiograph grayscale values. The results for the two later time point CT scans had greater similarity to the digital radiograph grayscale values than for the CT scan taken at the earlier time point. It is commonly accepted that CT scan Hounsfield Unit readings are more accurate than digital radiographic grayscale values; therefore, the digital radiographic analysis may be artificially lower than reality.

Patients' Evaluation Results

Patients were asked to use a visual analogue scale (VAS) with a 1-10 rating for pain and a 1-3 rating for bleeding, numbness, facial edema and facial temperature for each time point. The patient is asked to pick a numerical score on a horizontal line that has a 1 to 10 or 1 to 3 markings to evaluate the severity of the factor being considered. The higher the numbered response represents a greater the severity of the factor. An example being a score of "8" signifies greater pain than a score of "2". Figure 46 provides illustrations for the patients' post-operative observations. Patients were blinded to which side received the PRP treatment.
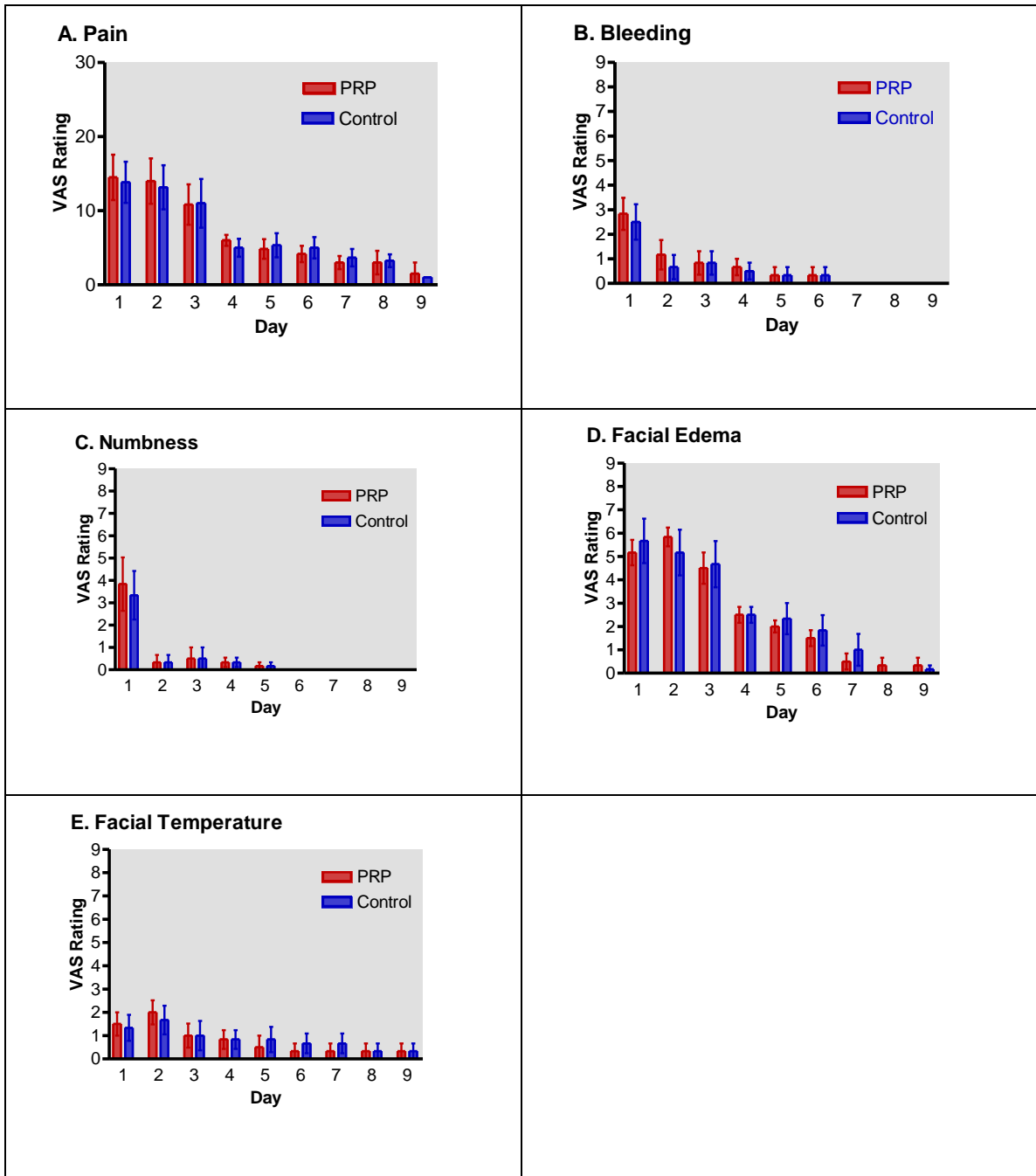
Figure 46. Patient VAS Evaluated Post-Operative Pain, Bleeding, Numbness, Facial Edema, and Facial Temperature

Visual analogue scale (VAS) ratings by patients for post-operative perceptions of pain (Panel A, 1-10 scale), bleeding (Panel B, 1-3 scale), numbness (Panel C, 1-3 scale), facial

edema (Panel D, 1-3 scale), and facial tissue temperature (Panel E, 1-3 scale). Patients provided ratings for the initial nine post-operative days. Ratings were taken every 8 hours for days 1-3 and scores are reported as a total for the entire 24-hour time period for a total possible score of 30 points for pain and 9 points for the other factors. Ratings were reported every 12 hours for days 4 -9 and scores were again reported as a total for the entire 24-hour time period for a total possible score of 20 points for pain and 6 points for the other factors. Two-tailed paired t tests revealed that there was no significant difference ($p > .05$) for any of these factors at any specific time point. For the entire nine day time two-way ANOVA analysis demonstrated that time elapsed since the surgical procedure was significant ($p < .0001$) for pain, bleeding, numbness, facial edema, and facial temperature ($p < .05$). PRP treatment did not have a significant impact on any of the factors ($p > .05$). Time and PRP treatment were independent of each other.

Patients were asked to post-operatively rate their perception of pain using a 1-10 visual analogue scale (VAS) (Figure 46 A). There was a total possible score of 30 for the first 3 days and then 20 for the subsequent days. When using a two-tailed paired t test for each specific time point there was no statistical difference ($p > .05$) between the PRP treatment side and the control side for any of the parameters. Patients were administered dexamethasone sodium phosphate IV intra-operatively; ketorolac trimethamine IV, and methylprednisolone suspension IM, and 4% bupivacaine with 1:200,000 epinephrine via an inferior alveolar block immediately following the procedure. Patients were instructed to take 600 mg ibuprofen every 6 hours for the first 3 days and thereafter, as needed. The adjuvant medications most probably reduced the post-operative pain, which may explain why the patients did not report high pain ratings. The use of bupivacaine local anesthesia would explain the higher numbness rating for the initial 24 hours. When examining the entire nine day time with a two-way ANOVA, treatment did not have a significant effect ($F = .003$, $p > .05$), time did have a significant effect ($F = 9.01$, $p < .0001$), and there was no interaction between treatment and time.

Patients reported minimal post-operative bleeding (Figure 46 B). Two-tailed paired t test analysis for each specific time point revealed no significant differences between the PRP treated sides and the control sides ($p > 05$). Two-way ANOVA analysis for the entire nine day post-operative period did show that treatment was not significant ($F = .373$, $p > .05$), time was significant ($F = 9.47$, $p < .0001$), and there was no interaction ($F = .117$, $p > .05$) between treatment and time. Therefore, PRP treatment and time were independent of each other.

Patient reports of post-operative numbness (Figure 46 C) was substantial on both treatment and control sides for the 1st day, thereafter it was very slight. The numbness on the initial post-operative day is due to the administration of the long-acting local anesthetic bupivacaine HCl 0.5% with epinephrine 1:200,000. The half-life for soft tissue anesthesia of this local anesthetic is 7 to 8 hours (470). Subsequent numbness over the remaining 8 days was minimal and most likely due to the formation of edema. The two-tailed t test analysis for each time point revealed no significant differences between the PRP treated sides and the control sides ($p > .05$). Two-way ANOVA analysis for the entire post-operative period showed that PRP treatment did not make a difference ($F = 0.72$, $p > .05$), time was significant ($F = 13.81$, $p < .0001$) and there was no interaction ($F = 0.72$, $p > .05$) between treatment and time.

Facial edema was higher on both the treatment and control sides for each of the first 3 days but the two-tailed t test revealed that there was no significant difference ($p > .05$) between sides (Figure 46 D). The administration of glucocorticosteroids and the patient's use of ice packs may also have contributed to the lower ratings for edema. When examining the entire nine day time with a two-way ANOVA, treatment did not

have a significant effect (F = .076, $p > .05$), time did have a significant effect (F = 27.71, $p < .0001$), and there was no interaction between treatment and time (F = 0.246, $p > .05$).

At no time did any of the patients report marked increases in tissue temperatures (Figure 46 E). The two-tailed paired t test for each specific time point revealed that skin temperature was not significantly different ($p > .05$) for any of the time points. Two-way ANOVA for the entire nine day post-operative period showed that tissue temperature was not affected by PRP treatment (F = .083, $p > .05$), time was significant (F = 3.176, $p < .05$), and there was no significant interaction between treatment and time (F = 1.254, $p > .05$).

The patients use of NSAIDs (ketorolac and ibuprofen) may have helped keep temperature elevations to a minimum. It has been well documented that the use of glucocorticosteroids and/or NSAIDs may interfere with new bone formation (471, 472), but this does not appear to be the case here. This is likely because the medications were administered for only a short time period. Also, the presence of PRP with constituent multiple growth factors and cytokines could have mitigated the negative effects of these medications.

A comprehensive listing of patient rated post-operative parameters are presented in Table 13.

VAS Rating Factor	Treatment			Time			Interaction		
	Significance	*p* value	F ratio	Significance	*p* value	F ratio	Significance	*p* value	F ratio
Pain	No	>.05	.003	Yes	< .0001	9.01	No	>.05	.053
Bleeding	No	>.05	.373	Yes	<.0001	9.47	No	>.05	.117
Numbness	No	>.05	.72	Yes	<.0001	27.71	No	>.05	.72
Facial Edema	No	>.05	.076	Yes	<.0001	27.71	No	.>.05	.246
Temp.	No	>.05	.083	Yes	<.05	3.176	No	>.05	1.254

Table 13. Summary Table of Two-way ANOVA Analysis of Patient Post-operative Observations

Two-way ANOVA statistics summary of the significance, F ratio, and *p*-values for each of the patient evaluated post-operative parameters. PRP treatment was not significant for any of the parameters. Elapsed post-operative time did have a significant impact on all of the parameters. Time and PRP treatment effects were independent of each other.

Observers' Evaluation Results

Blinded clinical observers evaluated the degree of tissue opening (dehiscence), bleeding, inflammation, facial edema, intra-oral edema, and perceived pain using a VAS (Figure 47 A-F).
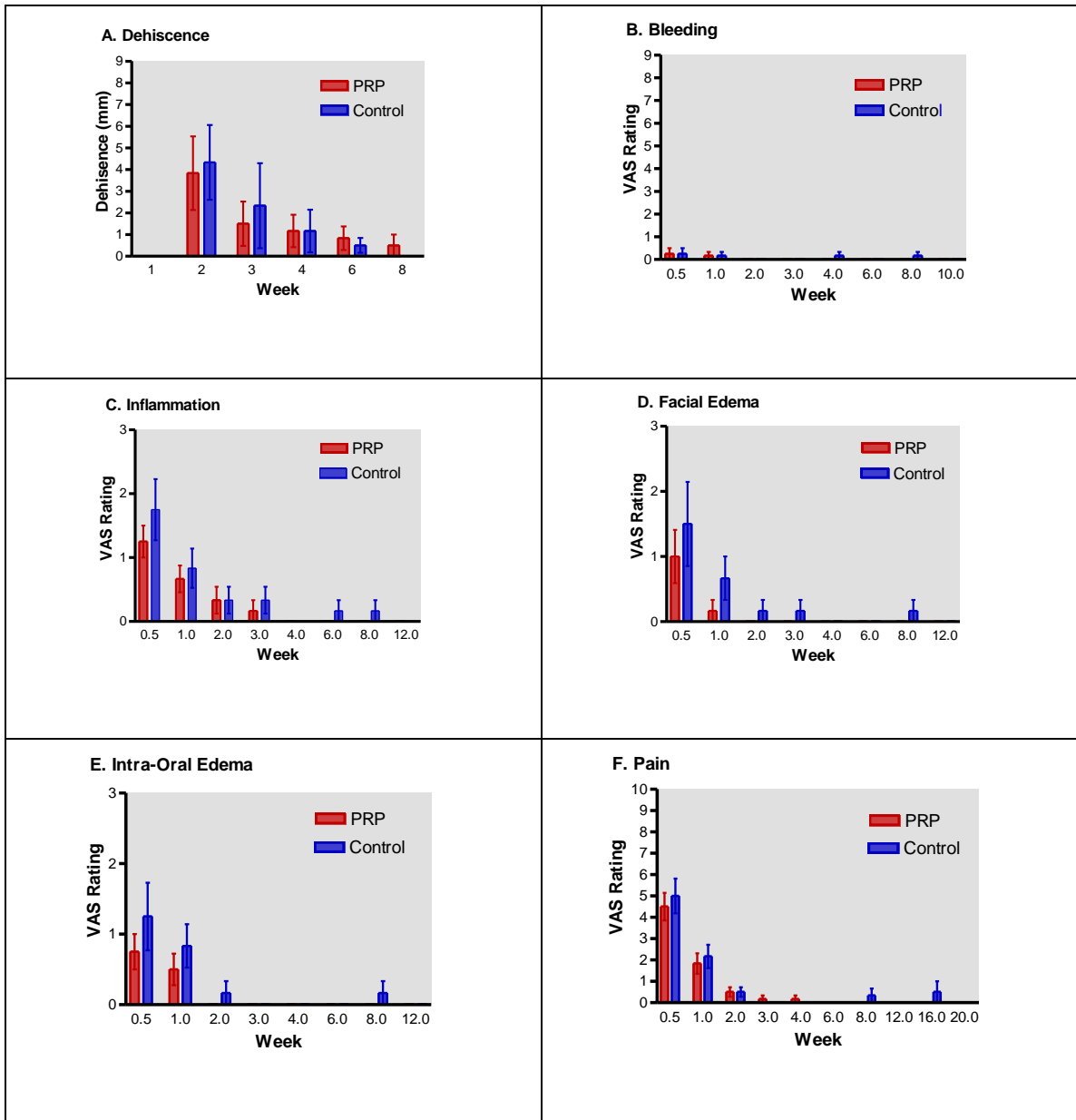
Figure 47. Observer VAS Evaluated Post-Operative Dehiscence, Bleeding, Inflammation, Facial Edema, Intra-Oral Edema, and Pain

Visual analogue scale (VAS) ratings as reported by blinded observers for post-operative perceptions of dehiscence (Panel A), bleeding (Panel B), inflammation (Panel C), facial edema (Panel D), intra-oral edema, (Panel E) and pain (Panel F). Dehiscence, bleeding, inflammation, facial edema, and intra-oral edema evaluations were done on a 1-3 scale, pain was evaluated on a 1-10 scale. Observers provided evaluations at the following post-operative time points: days 3 and 7, then weeks 2, 3, 4, 6, 8, 12, 16, 20, and 24. Two-tailed paired t tests revealed that there was no significant difference ($p > .05$) for any of the parameters at specific time points. When analyzing the entire 24-week time with a two-way ANOVA analysis PRP treatment was significant for reducing facial edema ($p < .05$). PRP treatment was not significant for any of the other parameters ($p > .05$). Two-way ANOVA analysis demonstrated that time elapsed since the surgical procedure was significant for dehiscence ($p < .01$), inflammation ($p < .0001$), facial edema ($p < .0001$), intra-oral edema ($p < .0001$), and pain ($p < .0001$). Time was not significant for bleeding ($p > .05$). Treatment and time were independent of each other ($p > .05$).

Observers found no dehiscence (Figure 47 A) on day 3 because primary closure was obtained with sutures. Subsequent ratings did reveal tissue retraction, but this does not translate to exposed bone. This was the result of the edges of the tissue rolling back, but the socket was covered initially by a blood clot and later by soft tissue. No patients experienced exposed bone. The two-tailed paired t test showed that there was no significant ($p > .05$) difference between the two treatment sites in regards to dehiscence for any of the specific time points. The two-way ANOVA did reveal the treatment was not significant (F = .019, P > .05), time was significant (F = 4.198, $p < .01$), and there was no interaction between these two factors (F = .117, $p > .05$).

Observer's perception of bleeding (Figure 47 B) was that there was minimal bleeding from all operative sites. The two-tailed paired t test analysis of the specific time points showed no significant difference between the PRP treated sides and the control sites ($p > .05$). Two-way ANOVA showed that treatment, time, and interaction were not

significant factors [treatment (F = .617, p > .05), time (F = 1.367, p > .05), and interaction (F = .277, p > .05)].

Inflammation (Figure 47 C) was not significantly different (p > .05) between PRP treated sides and the control sides for any of the specific time points when rated by the observers and analyzed by the two-tailed t test. The two-way ANOVA analysis of the 24-week post-operative period revealed that PRP treatment was not significant (F = 2.577, p > .05), time was significant (F = 13.20, p < .0001), and there was no interaction between these two factors (F = .339, p > .05).

 Observers' evaluation of facial edema (Figure 47 D) and two tailed paired t test analysis revealed that PRP treatment provided no significant differences (p > .05) between treatment and control at any of the specific time points. Two-way ANOVA of the entire post-operative period did show that treatment was significant (F = 4.416, p < .05), time was extremely significant (F = 8.986, p < .0001) and there was no interaction (F = .639, p > .05).

Intra-oral edema (Figure 47 E) was rated by the observers and two-tailed paired t test analysis revealed that treatment provided no significant differences (p > .05) for any of the specific post-operative time points. The two-way ANOVA analysis of the entire post-operative time revealed that treatment was not significant (F = 3.843, p > .05), time was significant (F = 11.4, p < .0001) and these two factors were independent of each other (F = 0.696, p > .0001).

Observers' ratings of the patients' pain (Figure 47 F) analyzed with the two-tailed paired t test showed that there was no significant difference (p > .05) at any of the

specific time points. Analysis of the entire post-operative period with two-way ANOVA revealed that treatment was not significant (F = 1.104, $p > .05$), time was significant (F = 44.5, $p < .0001$), and there was not a significant interaction between these two factors (F = 0.185, $p > .05$). There were similarities between the pain ratings provided by the patients (Figure 50-Panel A) and those provided by the observers at day 3 (Figure 51-Panel F). Observer ratings were at day 3, week 1, then weekly thereafter, while the patient ratings were on a daily basis for the initial nine post-operative days following surgery. Patients rated their pain on day 3 as 10.83 (total - maximum of 30) for the PRP side and 11.00 for the control side, representing the sum of three readings for the day. If the patient readings were divided by three to give an average reading for each 8 hour time period that the patients evaluated it would translate to 3.61 for the PRP side and 3.67 for the control side. Observers provided only one rating on day 3 resulting in a score of 4.5 for the PRP side and a score of 5 for the control side. The other reading that overlapped for the observers and patients was day 7. Patients provided an average score of 1.5 (average 12 hour reading) for the PRP side and 1.83 for the control side. Observers provided scores of 1.8 for the PRP side and 2.2 for the control side. These overlapping pain ratings were similar, but the observer always rated the pain slightly more severe than did the patients.

A summary of the statistical analysis of the post-operative parameters evaluated by the observers are listed in table 14.

VAS Rating Factor	Treatment			Time			Interaction		
	Significance	p value	F ratio	Significance	p value	F ratio	Significance	p value	F ratio
Dehiscence	No	>.05	.019	Yes	<.01	4.198	No	>.05	.117
Bleeding	No	>.05	.617	No	>.05	1.367	No	>.05	.277
Inflammation	No	>.05	2.577	Yes	<.0001	13.20	No	>.05	.339
Facial Edema	Yes	<.05	4.416	Yes	<.0001	8.986	No	>.05	.639
Intra-oral edema	No	>.05	3.843	Yes	<.0001	11.4	No	>.05	.696
Pain	No	>.05	1.104	Yes	<.0001	44.5	No	>.05	.185

Table 14. Summary Table of Two-way ANOVA Analysis of Observers Post-operative Observations

Two-way ANOVA statistical summary table of the significance, F-ratio and *p*-values for each of the observer evaluated parameters. PRP treatment over the 24-week time was significant (p < .05) for facial edema. PRP treatment was not significant for any of the other parameters. Elapsed post-operative time did have a significant impact on all of the parameters. Time and PRP treatment effects were independent of each other.

D. Discussion

This prospective blinded third molar pilot study offers insight to what is occurring clinically when BC-PRP is applied to fresh extraction sites. Third molar extractions are often used as a measurement tool for comparing treatments because they are usually performed electively on a younger population that do not present with multiple confounding factors such as systemic pathologies or multiple medications. Therefore, data analysis and interpretation from this study applies to healthy 18 to 40 year old patients.

Intra-oral digital radiographs taken of the individual surgical sites revealed that the effects of PRP were significantly beneficial ($p < .05$) for bone density determined by grayscale analysis. One can make the argument that this significant difference in bone density suggests a greater volume of new bone formation with PRP treatment. This increase in bone density (presumed as increased volume of new bone formation) was found to occur at earlier time points than the non-PRP treated control sites. Figure 48 is the same as Figure 39, except grid lines that allow for closer interpretation of the data points.
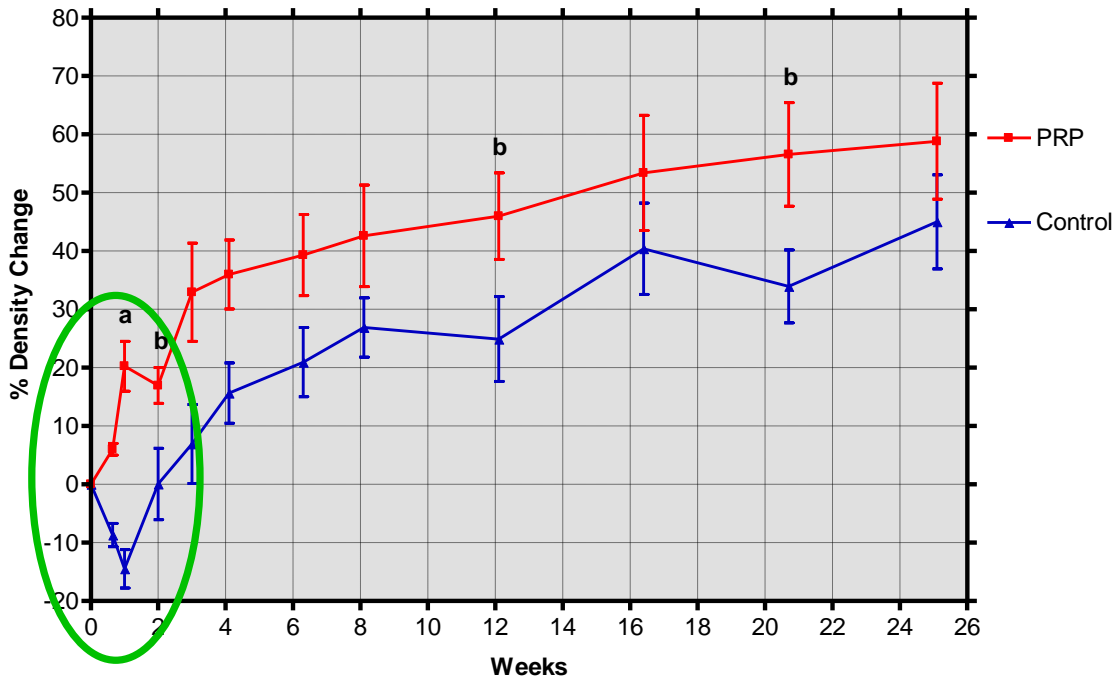
Figure 48. Percent Radiographic Density Change of Surgical ±PRP Treatment compared to Control Radiograph Taken Immediately Following Tooth Removal

This graph is the same as Figure 43 with the exception that grid lines have been added. . Grid lines allow for time comparison between PRP treated and control sides. Each data specific time point was analyzed with a two-tailed paired t-test where significance was defined as $p < .05$, where a = $p < .01$; b= $p > .05$ for individual time points. The marked difference in bone density during the initial 2 weeks post-operatively denotes the accelerated bone formation PRP treatment seems to provide. This immediate increase in bone density at the PRP treated sites indicates early bone formation in comparison to the control sites that have a decrease in bone density indicating further bone loss. Note that it takes 6 weeks to reach the same degree of bone density that the PRP treated sites had achieved at week 1.

Of note was the immediate increase in grayscale readings which represents bone density and therefore early bone formation. This finding corresponds with the results from the molecular study that demonstrated PRP treatment of hMSCs induced an early proliferation of these cell types and possibly differentiation into osteoblasts. This accelerated bone formation is in contrast to the control site that showed a drop in bone density (representing bone loss) before bone formation began to take place. It took approximately 6 weeks for the control side to reach the same degree of bone density that the PRP treated site had reached at week 1 (Figure 48). The PRP induced accelerated bone formation may be due to the presence of BMPs 2 and 6 in PRP that stimulated the hMSCs to begin the osteoblast differentiation development and subsequent calcification (473, 474). The control sites would be dependent upon osteoclast activity to initially breakdown existing bone so the bone matrix could release these two BMPs and then stimulate the hMSCs to begin bone development. These findings correspond well with the known and accepted bone-repair time-line (475). This immediate start of bone formation is of clinical relevance because, it is the initial two weeks following bone-manipulation oral surgery that is important in preventing infection, loss of the blood clot and/or AO (dry socket) formation. Moreover, there was a slight drop in grayscale density at the 1.5 to 2 week period suggesting that the initial direct impact of BC-PRP treatment might end, or at the minimum decrease, by the 1.5 – 2 week time point.

Further examination of the digital radiographic density changes shows that subsequent changes in bone density with the PRP treated sites and control sites are parallel, with no significant differences, except for the 12 and 20-week time points. The finding of the parallel lines most likely represents that normal healing is now taking place

at both sites, but the change in bone density was greater for the PRP treated site because it had the immediate bone formation, whereas the control site did not. The significant differences seen at the 12 and 20-week time points may be due to bone remodeling or inherent variations in the radiographic evaluation technique.

It should also be noted that it takes the control side 16 weeks to reach the same degree of increased radiographic grayscale for the total extraction socket as the PRP treatment achieves in 8 weeks. This is of clinical significance because it suggests decreased healing time. Therefore, patients bone recovers more rapidly to full function or is ready for the next step in dental reconstruction at an earlier date. Examples of this benefit include patients who undergo complete arch extractions and are in need of prosthesis for esthetics and function. The patient may be given an initial temporary denture that is normally utilized for 6 months prior to constructing the definitive final denture that has superior esthetics and function. This final denture could be constructed at the 2 to 3 month time point and therefore return the patient to full function in a shorter time-period. The decrease in bone healing time would also apply to the placement of dental implants that normally occurs after 4 to 6 months, unless expensive bone-grafting techniques are utilized which still require a 4-month bone healing time. With PRP treatment at the time of tooth removal, dental implants can be placed at a 2 to 4 month time, thereby decreasing the time to implant placement by 50%.

The instrumentation in this portion of the study utilized non-invasive radiographic techniques. Admittedly, bone histology studies could provide additional information with greater validity, but that analysis technique would be invasive, requiring surgical reentry. Individual site digital radiographs were taken and normalized to baseline

212

radiographs. The initial radiographs were normalized between the two surgical sites of the patient. Digital panoramic radiographs may have been a better measurement tool because the two surgical sites would be represented on one film, thereby eliminating the need for radiographic normalization between the initial surgical sites. Nonetheless, normalization between the series of radiographs and baseline radiographs would still have been necessary. The disadvantage of the digital panoramic radiograph is that these films have a 20 to 25% distortion factor incorporated into the image because it is an extra-oral film as opposed to the intra-oral individual (periapical) digital radiographs. The periapical radiograph was chosen over the panoramic radiograph because the periapical radiograph has less distortion incorporated into the images than with panoramic films. There is less distortion because the periapical film is in close proximity to the oral site being evaluated as opposed to being removed from the immediate site of interest as is the extra-oral panoramic radiograph is.

The CT scans may have shown greater differences between the PRP treated sites and the control sites, had they been obtained at earlier time points. Based on these findings and now knowing the effects of PRP-treatment are greatest during the initial 2 weeks it would be beneficial to acquire the CT scans at earlier time points. Therefore, future studies will have the CT scans taken at earlier time points to confirm the early effects of PRP treatment.

Patients in this study were exposed to medications (dexamethasone sodium phosphate, methylprednisolone suspension, ketorolac trimethamine, and ibuprofen) that interfere with inflammation and therefore may have an impact on bone healing. During the early phase of bone formation there is increased gene expression of pro-inflammatory

213

cytokines, mitogenic growth factors, and cell-differentiating factors. Inflammation, which occurs at the onset of early phase injury- or surgically-induced bone formation, is hypothesized to provide the initial signaling molecules for continuation of the healing cascade (476, 477). Cyclooxygenase-2 (COX-2) is important to the course of normal inflammation (476, 478-480). The rate-limiting step in the synthesis of prostaglandins from arachidonic acid is catalyzed by COX-2. Prostaglandins are bioactive lipids and are of significance because they possess pro-inflammatory effects plus other varied physiological effects (476, 481). COX-2 is responsible for PGE2 and PGF2 formation and is thought to have a functional role in healing (482).

Glucocorticosteroids (dexamethasone, methylprednisolone) and NSAIDs (ibuprofen, ketorolac) were used during this clinical study because of their analgesic and anti-inflammatory efficacy. The inhibition of cyclooxygenases is the mechanism by which glucocorticosteroids and NSAIDs achieve their intended effects. Following the hypothesis that inflammation is necessary for normal bone healing and formation, post-operative NSAID therapy may potentially delay bone healing. However, PRP may be a suitable agent to offset this inhibition when NSAIDs are prescribed for a short post-operative course. Figure 49 offers a possible mechanism for the beneficial effects of PRP that can offset the negative bone healing effects of NSAIDs. PRP contains platelets and monocytes. Both platelets and monocytes contain the cytokine interleukin-1α (IL-1α) (483, 484). IL-1α is involved in the local regulation of bone homoeostasis (485). It is also known that IL-1α stimulates PGE2 formation (485-489). This IL-1α-induced stimulation of PGE2 formation would counter the PGE2 inhibition induced by systemic post-operative NSAID and glucocorticoid steroid administration. Transient IL-1α has

been shown to have a potent stimulatory effect on bone formation (490, 491). PRP administration is transient in nature. The platelets in PRP also contain several growth factors (PDGF-AA, PDGF-BB, ILGF, TGFβ1, VEGF, and OPG) which work in concert in bone development and repair. Therefore, PRP use most likely would sufficiently counter any PGE2 inhibition induced by short-term use of NSAID/glucocorticoid.
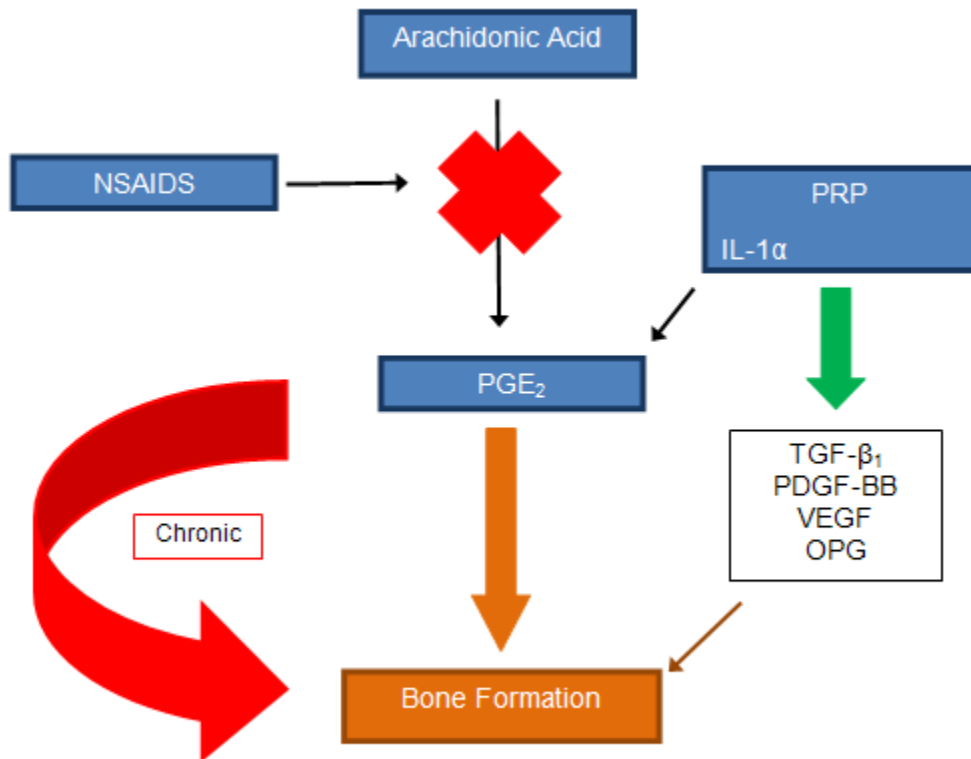
Figure 49: Effect of NSAIDs on Bone Formation

The use of NSAIDs blocks the formation of PGE_2 initiated by the release of arachidonic acid. The lack of PGE_2 formation associated with the inflammatory response interferes with bone formation. The use of PRP, which contains WBCs that release IL-1α and platelets, which release IL-1α, TGF-β$_1$, PDGF-BB, VEGF, and OPG, may potentially medicate the adverse effects that NSAID use has on bone development.

An alternative to using glucocorticosteroids and NSAIDs would be to use acetaminophen and/or narcotics for post-operative pain control. Acetaminophen does not have an anti-inflammatory effect and therefore the patients would experience greater inflammatory effects, such as edema and pain. Narcotic administration often times are fraught with unwanted side effects such as decreased mental acuity, lethargy, and GI disturbance. Therefore, these two analgesics have little advantage over NSAIDs.

When examining the data from this study it appears that PRP does accelerate bone formation and decreases the time necessary to return to full function. Other factors are present that would affect the patients' pain perception, bleeding, and numbness so it is difficult to confirm the effect PRP has on these factors. Blinded observers did report significantly less inflammation and facial edema ($p < .05$) on the sides receiving PRP. However, a larger study with fewer confounding factors would be necessary to confirm the effectiveness of PRP on inflammation and subsequent edema.

E. Conclusion

The results of this study validate the use of this simple cost-effective buffy coat (BC) PRP method with oral surgical procedures. The use of this BC system would be beneficial for the patient and clinician because it significantly increases the rate of bone formation early one (initial 2 weeks) and decrease healing time as evidenced by digital radiographic technology. However, it may not have an effect on pain perception, bleeding, and numbness. It is possible that PRP decreases inflammation and, therefore, the discomfort of edema. Having evidence-based support from this and future studies for the use of this procedure may result in expanded use of PRP with other surgical

procedures with improved clinical outcomes. Other surgical procedures requiring

enhanced and predictable bone formation that would benefit from this technology include

orthopedic joint implants, spinal surgeries, and trauma cases involving bone fractures.

General Discussion

This project contributes directly to evidence based dentistry with a possible application to orthopedics. There has been a great deal of interest in both of these disciplines regarding PRP application for enhancing outcomes by decreasing healing time in surgeries that involve osseous manipulation. A historical review of the literature reveals that PRP and its various techniques have been used with limited scientific evidence. Some authors have stated that only complex and expensive techniques for preparing PRP had clinical validity (10). This project used both *in vitro* and *in vivo* investigations to offer strong support for the use of a simple cost-effective technique for preparing PRP. Because this technique is inexpensive and simple, its use can be applied to all osseous surgical procedures, thereby improving the quality of life for more patients.

The Preparation and Characterization of PRP (Study I) confirmed that platelet recovery and enrichment of PRP using the Cliniseal™ Centrifuge was consistently optimal with a 10-minute centrifugation time (Figure 16). Moreover, platelet recovery and enrichment did not change significantly after centrifugation for up to six hours of bench set time at room temperature (Figure 18). Growth factors of interest were present at all bench set times and therefore, not affected for up to 6 hours of setting at room temperature. Platelets did aggregate and possibly undergo activation while undergoing the bench set, but the GFs that may have been released were not lost as they were most likely retained in a flexible fibrin junction (Figure 11). The aggregation and activation process is done slowly so it would most likely mimic the flexible fibrin structure of the platelet rich fibrin processing technique (page 48)   Therefore, the Buffy Coat (BC)

method of PRP preparation provides platelet concentrations and recoveries that are adequate for clinical use.

A finding not reported previously in the literature is how platelet morphology changed with bench set time over a period of six hours at room temperature (Figure 19). At two hours of bench set time, platelets in the PRP began to appear less normal and formed small-aggregates that suggest platelet activation and growth factor release. The loss of GFs with bench set time is a concern for clinicians, because the whole blood is usually collected at the start of a clinical procedure and the blood centrifuged before coagulation begins, despite the presence of trisodium citrate anticoagulant in the collection vessel. Since it is well established that TGF-β_1 stimulates osteogenesis, [7, 416, 417] a significant loss of this factor or the bioactivity of this factor by the various PRP preparation methods may account for the conflicting reports by clinicians concerning the osseous generating efficacy of PRP use. ELISA results (Table 5) suggest that PRP bench set times using our BC method of PRP preparation should not be of consequence up to a maximum of 6 hours (Table 5). Photomicrographs (Figure 19) did reveal that with the BC PRP technique platelets do begin to aggregate and possibly becoming activated after 2 hours of bench set time. The ELISA analysis in this study revealed no significant change ($p > .05$) in any of the key growth factors examined, including TGF-β_1. Researchers have reported that TGF-β_1 activity decreases when prepared using bovine thrombin. We feel that the decreased TGF-β_1 activity experienced by others may be due to: 1) natural hydrolysis, 2) degradation by proteases or 3) specific irreversible binding by molecules that may be present in various preparations of PRP. We hypothesize that bovine thrombin activates latent TGF-β1 and therefore may become subject to all of the

above. The technique examined here does not use bovine thrombin as an activator for that reason.

Growth factor levels obtained in our study were generally higher than those reported by other researchers (238). These findings may result from our analytical method for treating the platelet lysates with diluted 0.5% Triton X-100 (TX-100) prior to adding the samples to the ELISA plates. We believe that diluting the TX-100 lysates allowed for lower binding interference by the detergent and allowed a maximal TGF-β1 signal from the samples during ELISA analysis. In addition, the ELISA kit for TGF-β1 analysis utilized a monoclonal capturing antibody, whereas other researchers used kits employing Type II TGF-β_1 receptor or polyclonal anti-TGF-β_1 capturing antibodies to detect the growth factor. We believe these differences, in addition to not adding bovine thrombin, may account for the higher TGF-β_1 yields in our study.

The second investigation of this dissertation was a retrospective analysis of 904 mandibular extraction sites. The study revealed the beneficial effects of PRP in reducing the incidence of alveolar osteitis (AO). AO is believed to be due to either premature contraction of the blood clot within the socket or a localized infection. Multivariate analysis (Figure 22) revealed the odds of AO formation was 2.37 times higher for extraction sites without PRP treatment (95% CI, 1.3 to 4.4) than those with PRP treatment were. Bivariate analysis (Figure 21) demonstrated that extraction sockets treated with the immediate placement of a gelled BC PRP resulted in a significant decrease ($p < .00043$) in AO. The beneficial effects of PRP treatment that resulted in a reduced incidence of AO may be related to the variety of growth factors found in PRP that stimulate cell mitosis and differentiation [452], increased collagen production,

recruitment of leukocytes and other cells to the surgical site, and initiation of vascular in-growth (15). The presence of these growth factors in PRP promotes both soft and hard tissue healing and angiogenesis, all critical to the prevention of AO. In addition, the platelets found in PRP promote clot formation and the white blood cells found in PRP can inhibit bacterial growth. Therefore, PRP application may reduce the currently accepted causes of AO by facilitating clot and soft tissue formation and inhibiting bacterial colonization.

Multivariate analysis (Figure 22) also revealed that in addition to the absence of PRP administration, there were three other significant risk factors for AO: bruxism, oral contraceptive use, and complete impaction. Oral contraceptive use and complete impaction had been reported in the literature previously as being risk factors for AO (392, 492). Bruxism had not been reported previously as a causative factor for AO. PRP treatment reduced the incidence AO formation associated with each of these other factors by approximately 50% (Figure 22). The reduction was again most likely due to the variety of growth and other factors found in PRP that promote hard and soft tissue healing and decreased healing time. As mentioned previously in this dissertation there are PRP variants that may affect the growth factor content (234, 235, 238). Some of these variants do not contain WBCs and therefore they may not be as effective in preventing AO. In addition, if GF concentrations were to decrease below a critical concentration with some PRP variants, then that particular PRP variant may not significantly reduce AO formation. Our gelled BC PRP variant contains both WBCs and GFs; therefore, it is difficult to predict how other PRP variants would affect AO

formation. We conclude that not using gelled BC PRP following tooth extraction is the most important risk factor for AO formation.

The molecular study highlighted two important aspects of PRP- first, increased proliferation of hMSCs and second, PRP does not stop hMSC differentiation into the terminal osteoblast.

Cell count studies (Figure 25) confirmed the early proliferative effects of a 24-hour PRP exposure on hMSCs. PRP treated cells had a 3.2 fold increase in cell number over cells cultured in growth medium alone The BC-PRP technique compared favorably with (and actually surpassed in some aspects) the results of the MTT proliferation studies of Lucarrelli *et al*. (106) and Graziani *et al*. (328). The Lucarrelli and Graziani studies used bovine thrombin and calcium gluconate to activate platelets in their PRP. The results of our study brings into question whether it is in fact necessary, or beneficial, to activate the platelets through these methods. As discussed in the introduction, there are several reasons not to use bovine thrombin including: development of antibodies against thrombin, prothrombin, factor V, cross reactivity with analogous human coagulation proteins, and decreased PRP TGF-β1 concentrations. It is highly likely that *in vivo*, platelets from the BC technique are activated by collagen, thrombin, fibronectin, ADP, and thromboxane A2 present at the surgical site. Therefore, based on the results of this study and the drawbacks of bovine thrombin, the addition of bovine thrombin to PRP is a questionable clinical practice.

The significant ($p < .001$) increase in cellular total RNA production seen with PRP treated groups and not with non-PRP treated groups at day 5 (Figure 27 A) strongly

suggests that the presence of WBCs in PRP may be a confounding factor and therefore

distorting the true increase in total RNA due to increased cellular metabolism. WBCs

have RNA and vital WBCs would be making mRNA that may be inflating what is

thought to be the cellular total RNA concentration. WBCs may have accounted for over

50% of the total RNA increase observed. Further study separating the platelets and

WBCs will help discern the true effect of the platelets on total RNA production. This

could be accomplished by using a Ficoll™ separating gradient to separate the WBCs and

platelets. The project would be greatly improved by using alternate methods to determine

cell proliferation, such as the use of the CellTiter-Glo® Luminescent Cell Viability Assay

that is a homogeneous method of determining the number of viable cells in culture based

on quantification of ATP present (444, 445).

Cell differentiation was measured by two methods: 1) alkaline phosphatase assay

(ALP), an early differentiation marker and 2) examination of the expression of specific

mRNAs signifying osteoblast formation. The ALP assay (Figure 28) suggested that PRP

does not stop differentiation when differentiation signals are present *in vitro*. When

normalizing for cell number by considering percent confluence of cells (Figure 29), it

appears that PRP does not induce differentiation for hMScs in growth medium. ALP

activity did not increase at either Day 5 or 15 for cells cultured in growth + PRP medium

when compared to growth medium. However, at Day 5 differenentiation + PRP medium

did show ALP activity but it was lower than that seen with differentiation medium. At

Day 15, the ALP activity for differentiation + PRP medium was similar to that seen with

differentiation medium. Therefore, it can be suggested that PRP does not induce

differentiation, but neither does it stop differentiation when the proper differentiation

223

signals are present. This study cannot clearly state if differentiation is decreased or if the level of ALP activity with PRP-treatment of hMSCs meets that of differentiation medium at any specific time point. Day 5 ALP activity was diminished when compared to differentiation medium, yet Day 15 ALP activity was similar, it may be suggested that future studies should include several time points to determine if PRP treated cells express the same peak ALP activity seen with differentiation medium at a similar or different time point. It may be suggested that PRP induces proliferation during the initial 5 days and therefore delays differentiation when differentiation signals are present. Since proliferation and differentiation of cells cannot occur simultaneously, a question to be addressed is does the proliferation signals of PRP override the differentiation signals of differentiation medium, and if so for how long. The clinical use of PRP may be improved by following PRP treatment with an agent that further enhances differentiation and shifts it to a shorter time than normally occurs physiologically. The ALP studies may not reflect consistent findings, because ALP activity was not normalized for cell number or total protein. The cell number issue that must be corrected in future studies. Another question to be examined is what effect continuous or intermittent PRP exposure would have on differentiation.

PRP treatment increased relative mRNA expression at day 21 for two osteoblast differentiation gene markers, osteocalcin and bone sialoprotein (Table 11). Bone sialoprotein mRNA relative expression was greater than that of osteocalcin. Bone sialoprotein is expressed earlier than osteocalcin. Therefore, we may be witnessing the peak of the bone sialoprotein mRNA expression and the osteocalcin mRNA peak is yet to appear. Differentiation medium exceeded the relative expression of these two gene

224

mRNAs when compared to growth + PRP medium. However, differentiation medium did not attain the levels of relative expression that the differentiation + PRP treatments did. Therefore, this data suggests that at Day 21 (Table 11), PRP may induce differentiation when added to growth medium and it may enhance differentiation when added to differentiation medium. The expression of these mRNA markers signifies that differentiation down the osteogenic pathway has occurred, but it does not assure that functional osteoblasts have been created. We can only assume that the bone sialoprotein and osteocalcin proteins would be synthesized by these terminally differentiated cells, but we cannot be certain without doing an assay of these proteins.

The 5- and 10-day time points for evaluating differentiation gene markers (Table 11) with PRP treatment could not be determined due to the GAPDH levels being elevated, which are likely due to the WBCs providing additional housekeeper gene (GAPDH) expression. This finding was surprising and, therefore, future studies may be beneficial utilizing a gene whose expression is not affected by PRP treatment. The use of a more appropriate housekeeper gene would provide useable mRNA data. An alternative would be to use a leucodepleted PRP technique, but then we would lose the ability to confirm the effect of WBCs and its released factors on hMSC differentiation.

The molecular study confirmed that a 24-hour PRP treatment significantly increased proliferation and suggests that it does not stop differentiation. Additionally, it provided evidence that proliferation occurs at a significantly earlier time point than what is normally found for cells using growth medium (Figure 25).

The clinical prospective study utilized both digital radiographs and CT scans to determine the effect of PRP treatment on bone density. The digital radiograph analysis demonstrated that PRP treatment in mandibular third molar extraction sites did have a significant effect ($p < .001$) on changes in bone density in comparison to baseline values for the first 2 weeks following application at the time of surgery Figure 39). Two-way ANOVA showed that time and PRP treatment for the entire 25-week study were both significant and that time and treatment were independent of each other (Figures 39 and 48). Of interest is that bone density in the PRP-treated side was observed to increase during the initial 3- day post-operative digital radiographic observation, whereas the control side experienced an initial decrease in bone density before returning to baseline at the 2-week time point. The control sites did not reach the same change in bone density as the PRP treated sites at week 1 until approximately weeks 4 to 5. Additionally, in the long term, it took the control side 16 weeks to reach the same percent change in bone density that the PRP treated site had achieved by 8 weeks. Based on this result, the clinician may not have to allow for 6 months healing time prior to initiating implant placement surgeries, but rather may be able to perform implant placement after 2 to 3 months.

CT scan analyses were performed on three patients at each of the following times: 10.5, 14, and 18 weeks. Three parameters were examined, including total percent bone fill (Figure 43), newly formed bone density (NFBD) (Figure 44), and total formed bone density (TFBD) (Figure 45). When comparing averages for the three CT scans the percent bone fill for PRP-treated sites had significantly greater percent bone fill than the control sites ($p < .05$). When examining individual CT scans the total socket bone filled

bone density and newly formed bone density were not significantly different between PRP treated and control sites ($p > .05$). This is not surprising because CT scans were taken at later time points 10.5-, 14-, and 18-weeks and normal bone modeling takes approximately 16 weeks. The 10.5-week CT scan had markedly less total formed bone density and newly formed bone density than later CT scans, but when combining the three-time point scans together, there was no significant difference between sites. The results may have been different had the CT scans been obtained at earlier time points.

Therefore, the results of the digital radiographs and the CT scan analysis suggest that the BC PRP technique does enhance bone formation at an earlier time point than sites not treated with BC PRP. It can also be recommended that when deciding on time points for evaluating the effectiveness of PRP treatments that bone formation endpoints should be at earlier time points (0 to 12 weeks) and not at later time points (14 to 24 weeks).

Patients' perception of pain, bleeding, numbness, facial swelling and external skin temperature was not significantly different between PRP treated and control sites. Moreover, the observers' perception of patient pain, tissue opening, bleeding, inflammation, facial edema and intra-oral edema was similar to the patients' perception. There was no significant difference between the two treatment sites in dehiscence, bleeding, intra-oral edema, and perceived pain and there was great similarity between patients and observers pain perception values, although the observers gave slightly higher scores. The PRP treated sides did demonstrate significantly less inflammation and facial edema in comparison to the matched control side ($p < .05$). The findings that both of these items were significant are not surprising since edema is a clinical sign of inflammation.

The *in vitro* portions of this study offer a validation of the BC PRP technique and possible mechanistic explanation as to why the method significantly decreases AO formation (Figure 21) and significantly enhances radiographic bone density (Figure 39) and bone fill (Figure 43). Confirmation that platelets and WBCs are concentrated with the use of the clinical centrifuge (Figures 16 and 17), knowing that platelet morphology is not disturbed during collection and centrifugation (Figure 24) validates the use of this centrifuge for BC PRP preparation. The confirmation of the presence of growth factors (PDGF-BB, TGF-β1, EGF, and VEGF) in the BC PRP preparation (Figure 20 and Table 5) is of importance because each of these GFs are known to play an important role in healing (102, 104-106, 109-111, 116, 117, 125, 135). The prospective clinical study of the effects of PRP is consistent with the results from the cell culture study and the retrospective clinical analysis. The prospective clinical study results of increased radiographic bone density with PRP treatment at early time points (Figure 39) correlates well with the *in vitro* findings of early cell proliferation (Figure 25) followed by possible differentiation. There was also a correlation between the retrospective clinical AO study and the prospective clinical study. The increase in bone density during the first 2 weeks in the prospective study is most likely due to the presence of multiple GFs found in PRP that stimulate hMSCs to proliferate with eventual differentiation into osteoblasts. Additionally, GFs contained in PRP facilitate by the formation of soft tissue (493) that would help preserve thrombus (clot) formation thereby lessening the likelihood of AO.

The application of PRP has great clinical utility because it appears to decrease the risk of complications by closing the window of vulnerability early during post-operative healing. There are clinicians who anecdotally claim that PRP does not work and there are

those who say that it does. They may both be correct. Clinical success with PRP may be due partially to PRP processing technique and/or the temporal end-point used as a measurement tool for improved bone formation. If the temporal endpoint for measuring bone formation is beyond 12 to 14 weeks, there may not be an observable difference between PRP treatment and control.

The *in vivo* conditions cannot be duplicated in the *in vitro* environment. Therefore these studies focused on the effects of PRP on hMSCs and their differentiation into osteoblasts. Clinically, PRP may have an effect on osteoclasts in addition to osteoblasts. In the Preparation and Characterization (Study I) section of this dissertation osteoprotegerin (OPG) was found(Table 5), but it could not be quantified as it was below the detectable limits of the standard curve. OPG has been reported in murine platelets (494),but not human platelets. If OPG were present in human platelets and at effective concentrations, then PRP would effect osteoclasts as well. OPG is known to inhibit the maturation of osteoclasts (495). Therefore, an additional explanation for the early increase in bone density seen in the prospective study with PRP-treatment may be that OPG (if present) would interfere with the normal bone healing process of initial bone breakdown by osteoclasts. Osteoclasts free necessary osteoblast stimulating factors from the bone matrix, therefore beginning the bone healing process (496). This explains the initial drop in bone density observed at the non-PRP-treated sites in the prospective study. OPG would block this initial bone breakdown. Therefore, with future studies it may be determined that hMSC proliferation and possible differentiation is a partial mechanistic answer and that PRP possibly has an effect on osteoclasts as well.

Conclusion

This study confirms that a simple and cost-effective technique for concentrating platelets when performed properly will not alter platelet morphology or growth factor contents. Additionally, the BC-PRP methodology significantly decreased the formation of AO when applied immediately to tooth extraction sockets and facilitated the process of soft and hard tissue healing. This facilitation was most likely due to the enhanced proliferation and enhanced differentiation of stem cells mediated by growth factors released by PRP at the surgical site. Since PRP application facilitates healing there is less opportunity for the occurrence of complications such as AO or delayed bone formation. Based on our prospective study results the effects of PRP are optimal during the first two weeks following application. This correlates well with the proliferation of hMSC during the initial 5 days and enhanced differentiation seen at Day 21following exposure to PRP treatment. Patients and clinicians would benefit from the use of PRP in oral surgical procedures. This BC PRP technique may have applications in other types of surgery requiring bone healing.

References

1. Bielecki T, Gazdzik TS, Szczepanski T. Re: "The effects of local platelet rich plasma delivery on diabetic fracture healing". What do we use: Platelet-rich plasma or platelet-rich gel? Bone. 2006; 39:1388; author reply 1389.

2. Cieslik-Bielecka A, Bielecki T, Gazdzik TS, Cieslik T, Szczepanski T. Improved treatment of mandibular odontogenic cysts with platelet-rich gel. Oral Surg Oral Med Oral Pathol Oral Radiol Endod. 2008; 105:423-9.

3. Gandhi A, Doumas C, O'Connor JP, Parsons JR, Lin SS. The effects of local platelet rich plasma delivery on diabetic fracture healing. Bone. 2006; 38:540-6.

4. Kitoh H, Kitakoji T, Tsuchiya H, Mitsuyama H, Nakamura H, Katoh M, et al. Transplantation of marrow-derived mesenchymal stem cells and platelet-rich plasma during distraction osteogenesis--a preliminary result of three cases. Bone. 2004; 35:892-8.

5. Lowery GL, Kulkarni S, Pennisi AE. Use of autologous growth factors in lumbar spinal fusion. Bone. 1999; 25:47S-50S.

6. Lynch SE, Buser D, Hernandez RA, Weber HP, Stich H, Fox CH, et al. Effects of the platelet-derived growth factor/insulin-like growth factor-i combination on bone regeneration around titanium dental implants. Results of a pilot study in beagle dogs. J Periodontol. 1991; 62:710-6.

7. Marx RE, Carlson ER, Eichstaedt RM, Schimmele SR, Strauss JE, Georgeff KR. Platelet-rich plasma: Growth factor enhancement for bone grafts. Oral Surg Oral Med Oral Pathol Oral Radiol Endod. 1998; 85:638-46.

8. Rutkowski JL, Fennell JW, Kern JC, Madison DE, Johnson DA. Inhibition of alveolar osteitis in mandibular tooth extraction sites using platelet-rich plasma. J Oral Implantol. 2007; 33:116-21.

9. Lynch SE, de Castilla GR, Williams RC, Kiritsy CP, Howell TH, Reddy MS, et al. The effects of short-term application of a combination of platelet-derived and insulin-like growth factors on periodontal wound healing. J Periodontol. 1991; 62:458-67.

10. Marx RE. Platelet-rich plasma (prp): What is prp and what is not prp? Implant Dent. 2001; 10:225-8.

11. Bielecki TM, Gazdzik TS, Arendt J, Szczepanski T, Krol W, Wielkoszynski T. Antibacterial effect of autologous platelet gel enriched with growth factors and other active substances: An in vitro study. J Bone Joint Surg Br. 2007; 89:417-20.

12. Bhanot S, Alex JC. Current applications of platelet gels in facial plastic surgery. Facial Plast Surg. 2002; 18:27-33.

13. Martinowitz U, Spotnitz WD. Fibrin tissue adhesives. Thromb Haemost. 1997; 78:661-6.

14. Vaccaro AR, Anderson DG, Toth CA. Recombinant human osteogenic protein-1 (bone morphogenetic protein-7) as an osteoinductive agent in spinal fusion. Spine. 2002; 27:S59-65.

15. Lichtman MA, Beutler E, Kipps TJ, Seilgsohn U, Kenneth K, T. PJ. Williams hematology 7th edition. New York McGraw-Hill; 2006.

16. Rutkowski JL, Thomas JM, Bering CL, Speicher JL, Radio NM, Smith DM, et al. Analysis of a rapid, simple, and inexpensive technique used to obtain platelet-rich plasma for use in clinical practice. J Oral Implantol. 2008; 34:25-33.

17. Powell DM, Chang E, Farrior EH. Recovery from deep-plane rhytidectomy following unilateral wound treatment with autologous platelet gel: A pilot study. Arch Facial Plast Surg. 2001; 3:245-50.

18. Kajikawa Y, Morihara T, Sakamoto H, Matsuda K, Oshima Y, Yoshida A, et al. Platelet-rich plasma enhances the initial mobilization of circulation-derived cells for tendon healing. J Cell Physiol. 2008; 215:837-45.

19. Yamamiya K, Okuda K, Kawase T, Hata KI, Wolff LF, Yoshie H. Tissue-engineered cultured periosteum used with platelet-rich plasma and hydroxyapatite in treating human osseous defects. J Periodontol. 2008; 79:811-818.

20. Saratzis N, Saratzis A, Melas N, Kiskinis D. Non-activated autologous platelet-rich plasma for the prevention of inguinal wound-related complications after endovascular repair of abdominal aortic aneurysms. J Extra Corpor Technol. 2008; 40:52-6.

21. DePoi R, John V, Paez de Mendoza CY, Gossweiler MK. Development of an oro-antral fistula following sinus elevation surgery: A case report on management using platelet-rich plasma. J Indiana Dent Assoc. 2007; 86:10-6.

22. Hatakeyama M, Beletti ME, Zanetta-Barbosa D, Dechichi P. Radiographic and histomorphometric analysis of bone healing using autogenous graft associated with platelet-rich plasma obtained by 2 different methods. Oral Surg Oral Med Oral Pathol Oral Radiol Endod. 2008; 105:e13-8.

23. Schaaf H, Streckbein P, Lendeckel S, Heidinger K, Gortz B, Bein G, et al. Topical use of platelet-rich plasma to influence bone volume in maxillary augmentation: A prospective randomized trial. Vox Sang. 2008; 94:64-9.

24. Zavadil DP, Satterlee CC, Costigan JM, Holt DW, Shostrom VK. Autologous platelet gel and platelet-poor plasma reduce pain with total shoulder arthroplasty. J Extra Corpor Technol. 2007; 39:177-82.

25. Kitoh H, Kitakoji T, Tsuchiya H, Katoh M, Ishiguro N. Distraction osteogenesis of the lower extremity in patients with achondroplasia/hypochondroplasia treated with transplantation of culture-expanded bone marrow cells and platelet-rich plasma. J Pediatr Orthop. 2007; 27:629-34.

26. Creaney L, Hamilton B. Growth factor delivery methods in the management of sports injuries: The state of play. Br J Sports Med. 2008; 42:314-20.

27. Man D, Plosker H, Winland-Brown JE. The use of autologous platelet-rich plasma (platelet gel) and autologous platelet-poor plasma (fibrin glue) in cosmetic surgery. Plast Reconstr Surg. 2001; 107:229-37; discussion 238-9.

28. Eppley BL, Pietrzak WS, Blanton M. Platelet-rich plasma: A review of biology and applications in plastic surgery. Plast Reconstr Surg. 2006; 118:147e-159e.

29. Driver VR, Hanft J, Fylling CP, Beriou JM, Autologel Diabetic Foot Ulcer Study G. A prospective, randomized, controlled trial of autologous platelet-rich plasma gel for the treatment of diabetic foot ulcers. Ostomy Wound Manage. 2006; 52:68-70, 72, 74 passim.

30. Wexler MJ, Ginsburg AD, Latzina A, Aster RA, Slapak M. Twenty-four hour renal preservation and perfusion utilizing platelet-rich plasma. Ann Surg. 1971; 174:811-25.

31. Alio JL, Pastor S, Ruiz-Colecha J, Rodriguez A, Artola A. Treatment of ocular surface syndrome after lasik with autologous platelet-rich plasma. J Refract Surg. 2007; 23:617-9.

32. Italiano JE, Jr., Shivdasani RA. Megakaryocytes and beyond: The birth of platelets. J Thromb Haemost. 2003; 1:1174-82.

33. Greening DW, Glenister KM, Kapp EA, Moritz RL, Sparrow RL, Lynch GW, et al. Comparison of human platelet membrane-cytoskeletal proteins with the plasma proteome: Towards underswtanding the platelet-plasma nexus. Proteomics Clin. Appl. . 2008; 2008:63-77.

34. Michelson AD. Platelet 2nd edition. Amsterdam: Elsevier; 2007.

35. Reed GL, Fitzgerald ML, Polgar J. Molecular mechanisms of platelet exocytosis: Insights into the "Secrete" Life of thrombocytes. Blood. 2000; 96:3334-42.

36. Hartwig JH, Barkalow K, Azim A, Italiano J. The elegant platelet: Signals controlling actin assembly. Thromb Haemost. 1999; 82:392-8.

37. Peng L, Yang J, Lu X, Okada T, Kondo T, Ruan C, et al. Effects of biological variations on platelet count in healthy subjects in china. Thromb Haemost. 2004; 91:367-72.

38. Bain BJ. Ethnic and sex differences in the total and differential white cell count and platelet count. J Clin Pathol. 1996; 49:664-6.

39. Rozman P, Bolta Z. Use of platelet growth factors in treating wounds and soft-tissue injuries. Acta Dermatovenerol Alp Panonica Adriat. 2007; 16:156-65.

40. Camacho A, Dimsdale JE. Platelets and psychiatry: Lessons learned from old and new studies. Psychosom Med. 2000; 62:326-36.

41. Gresele P, ebrary Inc. Platelets in thrombotic and non-thrombotic disorders pathophysiology, pharmacology and therapeutics. Cambridge, U.K. ; New York: Cambridge University Press; 2002:xxii, 1101 p., [16] p. of plates.

42. Wagner DD, Burger PC. Platelets in inflammation and thrombosis. Arterioscler Thromb Vasc Biol. 2003; 23:2131-7.

43. Movat HZ, Weiser WJ, Glynn MF, Mustard JF. Platelet phagocytosis and aggregation. J Cell Biol. 1965; 27:531-43.

44. Weyrich AS, Zimmerman GA. Platelets: Signaling cells in the immune continuum. Trends Immunol. 2004; 25:489-95.

45. Diacovo TG, Puri KD, Warnock RA, Springer TA, von Andrian UH. Platelet-mediated lymphocyte delivery to high endothelial venules. Science. 1996; 273:252-5.

46. White. Hemostasis and thrombosis: Basic principles and clinical practice. Philadelphia: Lippincott; 1993.

47. van Joost T, van Ulsen J, Vuzevski VD, Naafs B, Tank B. Purpuric contact dermatitis to benzoyl peroxide. J Am Acad Dermatol. 1990; 22:359-61.

48. Schick. Hemostasis and thrombosis: Basic principles and clinical practice. Philadelphia: Lippencott; 1993.

49. Heemskerk JW, Bevers EM, Lindhout T. Platelet activation and blood coagulation. Thromb Haemost. 2002; 88:186-93.

50. Solum NO. Procoagulant expression in platelets and defects leading to clinical disorders. Arterioscler Thromb Vasc Biol. 1999; 19:2841-6.

51. Sims PJ, Faioni EM, Wiedmer T, Shattil SJ. Complement proteins c5b-9 cause release of membrane vesicles from the platelet surface that are enriched in the membrane receptor for coagulation factor va and express prothrombinase activity. J Biol Chem. 1988; 263:18205-12.

52. Sims PJ, Wiedmer T, Esmon CT, Weiss HJ, Shattil SJ. Assembly of the platelet prothrombinase complex is linked to vesiculation of the platelet plasma membrane. Studies in scott syndrome: An isolated defect in platelet procoagulant activity. J Biol Chem. 1989; 264:17049-57.

53. Bevers EM, Tilly RH, Senden JM, Comfurius P, Zwaal RF. Exposure of endogenous phosphatidylserine at the outer surface of stimulated platelets is reversed by restoration of aminophospholipid translocase activity. Biochemistry. 1989; 28:2382-7.

54. Tuszynski GP, Mauco GP, Koshy A, Schick PK, Walsh PN. The platelet cytoskeleton contains elements of the prothrombinase complex. J Biol Chem. 1984; 259:6947-51.

55. Comfurius P, Bevers EM, Zwaal RF. The involvement of cytoskeleton in the regulation of transbilayer movement of phospholipids in human blood platelets. Biochim Biophys Acta. 1985; 815:143-8.

56. Lopez JA. The platelet glycoprotein ib-ix complex. Blood Coagul Fibrinolysis. 1994; 5:97-119.

57. Rajagopalan V, Essex DW, Shapiro SS, Konkle BA. Tumor necrosis factor-alpha modulation of glycoprotein ib alpha expression in human endothelial and erythroleukemia cells. Blood. 1992; 80:153-61.

58. Wu G, Essex DW, Meloni FJ, Takafuta T, Fujimura K, Konkle BA, et al. Human endothelial cells in culture and in vivo express on their surface all four components of the glycoprotein ib/ix/v complex. Blood. 1997; 90:2660-9.

59. Bennett JS. Structure and function of the platelet integrin alphaiibbeta3. J Clin Invest. 2005; 115:3363-9.

60. Losonczy G, Rosenberg N, Boda Z, Vereb G, Kappelmayer J, Hauschner H, et al. Three novel mutations in the glycoprotein iib gene in a patient with type ii glanzmann thrombasthenia. Haematologica. 2007; 92:698-701.

61. Yan B, Calderwood DA, Yaspan B, Ginsberg MH. Calpain cleavage promotes talin binding to the beta 3 integrin cytoplasmic domain. J Biol Chem. 2001; 276:28164-70.

62. Woods VL, Jr., Wolff LE, Keller DM. Resting platelets contain a substantial centrally located pool of glycoprotein iib-iiia complex which may be accessible to some but not other extracellular proteins. J Biol Chem. 1986; 261:15242-51.

63. Cramer EM, Savidge GF, Vainchenker W, Berndt MC, Pidard D, Caen JP, et al. Alpha-granule pool of glycoprotein iib-iiia in normal and pathologic platelets and megakaryocytes. Blood. 1990; 75:1220-7.

64. Youssefian T, Masse JM, Rendu F, Guichard J, Cramer EM. Platelet and megakaryocyte dense granules contain glycoproteins ib and iib-iiia. Blood. 1997; 89:4047-57.

65. Plow EF, Ginsberg MH. Cellular adhesion: Gpiib-iiia as a prototypic adhesion receptor. Prog Hemost Thromb. 1989; 9:117-56.

66. Peerschke EI. The platelet fibrinogen receptor. Semin Hematol. 1985; 22:241-59.

67. Bennett JS. Platelet membranes and glycoproteins. New York: Plenum; 1985.

68. Coller BS. Platelet immunobiology: Molecular and clinical aspects. Philadelphia: Lippencott; 1989.

69. Sims PJ, Ginsberg MH, Plow EF, Shattil SJ. Effect of platelet activation on the conformation of the plasma membrane glycoprotein iib-iiia complex. J Biol Chem. 1991; 266:7345-52.

70. Wencel-Drake JD. Plasma membrane gpiib/iiia. Evidence for a cycling receptor pool. Am J Pathol. 1990; 136:61-70.

71. Coller BS, Seligsohn U, West SM, Scudder LE, Norton KJ. Platelet fibrinogen and vitronectin in glanzmann thrombasthenia: Evidence consistent with specific roles for glycoprotein iib/iiia and alpha v beta 3 integrins in platelet protein trafficking. Blood. 1991; 78:2603-10.

72. Harrison. Platelet a-granular fibrinogen. Platelets. 1992; 3:1-10.

73. Kunicki TJ, Nugent DJ, Staats SJ, Orchekowski RP, Wayner EA, Carter WG. The human fibroblast class ii extracellular matrix receptor mediates platelet adhesion to collagen and is identical to the platelet glycoprotein ia-iia complex. J Biol Chem. 1988; 263:4516-9.

74. Clemetson KJ. Platelet collagen receptors: A new target for inhibition? Haemostasis. 1999; 29:16-26.

75. Saelman EU, Nieuwenhuis HK, Hese KM, de Groot PG, Heijnen HF, Sage EH, et al. Platelet adhesion to collagen types i through viii under conditions of stasis and flow is mediated by gpia/iia (alpha 2 beta 1-integrin). Blood. 1994; 83:1244-50.

76. Coller BS, Beer JH, Scudder LE, Steinberg MH. Collagen-platelet interactions: Evidence for a direct interaction of collagen with platelet gpia/iia and an indirect interaction with platelet gpiib/iiia mediated by adhesive proteins. Blood. 1989; 74:182-92.

77. Pischel KD, Hemler ME, Huang C, Bluestein HG, Woods VL, Jr. Use of the monoclonal antibody 12f1 to characterize the differentiation antigen vla-2. J Immunol. 1987; 138:226-33.

78. Staatz WD, Rajpara SM, Wayner EA, Carter WG, Santoro SA. The membrane glycoprotein ia-iia (vla-2) complex mediates the mg++-dependent adhesion of platelets to collagen. J Cell Biol. 1989; 108:1917-24.

79. Barnes MJ, Knight CG, Farndale RW. The collagen-platelet interaction. Curr Opin Hematol. 1998; 5:314-20.

80. Kuijpers MJ, Schulte V, Bergmeier W, Lindhout T, Brakebusch C, Offermanns S, et al. Complementary roles of glycoprotein vi and alpha2beta1 integrin in collagen-induced thrombus formation in flowing whole blood ex vivo. FASEB J. 2003; 17:685-7.

81. He L, Pappan LK, Grenache DG, Li Z, Tollefsen DM, Santoro SA, et al. The contributions of the alpha 2 beta 1 integrin to vascular thrombosis in vivo. Blood. 2003; 102:3652-7.

82. Fox JE. Linkage of a membrane skeleton to integral membrane glycoproteins in human platelets. Identification of one of the glycoproteins as glycoprotein ib. J Clin Invest. 1985; 76:1673-83.

83. Pabla R, Weyrich AS, Dixon DA, Bray PF, McIntyre TM, Prescott SM, et al. Integrin-dependent control of translation: Engagement of integrin alphaiibbeta3 regulates synthesis of proteins in activated human platelets. J Cell Biol. 1999; 144:175-84.

84. Fox JE. The platelet cytoskeleton. Thromb Haemost. 1993; 70:884-93.

85. Colman RW. Hemostasis and thrombosis : Basic principles and clinical practice. 5th ed. Philadelphia, PA: Lippincott Williams & Wilkins; 2006.

86. Ulmer TS, Yaspan B, Ginsberg MH, Campbell ID. Nmr analysis of structure and dynamics of the cytosolic tails of integrin alpha iib beta 3 in aqueous solution. Biochemistry. 2001; 40:7498-508.

87. Vinogradova O, Velyvis A, Velyviene A, Hu B, Haas T, Plow E, et al. A structural mechanism of integrin alpha(iib)beta(3) "Inside-out" Activation as regulated by its cytoplasmic face. Cell. 2002; 110:587-97.

88. Tadokoro S, Shattil SJ, Eto K, Tai V, Liddington RC, de Pereda JM, et al. Talin binding to integrin beta tails: A final common step in integrin activation. Science. 2003; 302:103-6.

89. Tremuth L, Kreis S, Melchior C, Hoebeke J, Ronde P, Plancon S, et al. A fluorescence cell biology approach to map the second integrin-binding site of talin to a 130-amino acid sequence within the rod domain. J Biol Chem. 2004; 279:22258-66.

90. Nurden P, Heilmann E, Paponneau A, Nurden A. Two-way trafficking of membrane glycoproteins on thrombin-activated human platelets. Semin Hematol. 1994; 31:240-50.

91. Colman RW. Hemostasis and thrombosis : Basic principles and clinical practice. 3rd ed. Philadelphia: Lippincott; 1994.

92. Cramer EM, Norol F, Guichard J, Breton-Gorius J, Vainchenker W, Masse JM, et al. Ultrastructure of platelet formation by human megakaryocytes cultured with the mpl ligand. Blood. 1997; 89:2336-46.

93. Italiano JE, Jr., Lecine P, Shivdasani RA, Hartwig JH. Blood platelets are assembled principally at the ends of proplatelet processes produced by differentiated megakaryocytes. J Cell Biol. 1999; 147:1299-312.

94. Kenney DM, Linck RW. The cystoskeleton of unstimulated blood platelets: Structure and composition of the isolated marginal microtubular band. J Cell Sci. 1985; 78:1-22.

95. Harrison P, Cramer EM. Platelet alpha-granules. Blood Rev. 1993; 7:52-62.

96. Hayward CP, Furmaniak-Kazmierczak E, Cieutat AM, Moore JC, Bainton DF, Nesheim ME, et al. Factor v is complexed with multimerin in resting platelet lysates and colocalizes with multimerin in platelet alpha-granules. J Biol Chem. 1995; 270:19217-24.

97. Anitua E, Andia I, Ardanza B, Nurden P, Nurden AT. Autologous platelets as a source of proteins for healing and tissue regeneration. Thromb Haemost. 2004; 91:4-15.

98. George JN. Platelet immunoglobulin g: Its significance for the evaluation of thrombocytopenia and for understanding the origin of alpha-granule proteins. Blood. 1990; 76:859-70.

99. George JN. Platelet igg: Measurement, interpretation, and clinical significance. Prog Hemost Thromb. 1991; 10:97-126.

100. Maione TE, Gray GS, Petro J, Hunt AJ, Donner AL, Bauer SI, et al. Inhibition of angiogenesis by recombinant human platelet factor-4 and related peptides. Science. 1990; 247:77-9.

101. Williams LT. Signal transduction by the platelet-derived growth factor receptor. Science. 1989; 243:1564-70.

102. Phillips DR, Shuman MA. Biochemistry of platelets. Orlando: Academic Press; 1986.

103. Heldin CH, Westermark B. Platelet-derived growth factor: Three isoforms and two receptor types. Trends Genet. 1989; 5:108-11.

104. Dohan DM, Choukroun J, Diss A, Dohan SL, Dohan AJ, Mouhyi J, et al. Platelet-rich fibrin (prf): A second-generation platelet concentrate. Part ii: Platelet-related biologic features. Oral Surg Oral Med Oral Pathol Oral Radiol Endod. 2006; 101:e45-50.

105. Rosenkranz S, Kazlauskas A. Evidence for distinct signaling properties and biological responses induced by the pdgf receptor alpha and beta subtypes. Growth Factors. 1999; 16:201-16.

106. Lucarelli E, Beccheroni A, Donati D, Sangiorgi L, Cenacchi A, Del Vento AM, et al. Platelet-derived growth factors enhance proliferation of human stromal stem cells. Biomaterials. 2003; 24:3095-100.

107. Heldin CH. Simultaneous induction of stimulatory and inhibitory signals by pdgf. FEBS Lett. 1997; 410:17-21.

108. Yu J, Ustach C, Kim HR. Platelet-derived growth factor signaling and human cancer. J Biochem Mol Biol. 2003; 36:49-59.

109. Ross R. Platelet-derived growth factor. Lancet. 1989; 1:1179-82.

110. Madtes DK, Raines EW, Ross R. Modulation of local concentrations of platelet-derived growth factor. Am Rev Respir Dis. 1989; 140:1118-20.

111. Berk BC, Alexander RW. Vasoactive effects of growth factors. Biochem Pharmacol. 1989; 38:219-25.

112. Maloney JP, Silliman CC, Ambruso DR, Wang J, Tuder RM, Voelkel NF. In vitro release of vascular endothelial growth factor during platelet aggregation. Am J Physiol. 1998; 275:H1054-61.

113. Weltermann A, Wolzt M, Petersmann K, Czerni C, Graselli U, Lechner K, et al. Large amounts of vascular endothelial growth factor at the site of hemostatic plug formation in vivo. Arterioscler Thromb Vasc Biol. 1999; 19:1757-60.

114. Webb NJ, Bottomley MJ, Watson CJ, Brenchley PE. Vascular endothelial growth factor (vegf) is released from platelets during blood clotting: Implications for measurement of circulating vegf levels in clinical disease. Clin Sci (Lond). 1998; 94:395-404.

115. Katoh O, Tauchi H, Kawaishi K, Kimura A, Satow Y. Expression of the vascular endothelial growth factor (vegf) receptor gene, kdr, in hematopoietic cells and inhibitory effect of vegf on apoptotic cell death caused by ionizing radiation. Cancer Res. 1995; 55:5687-92.

116. Dohan DM, Choukroun J, Diss A, Dohan SL, Dohan AJ, Mouhyi J, et al. Platelet-rich fibrin (prf): A second-generation platelet concentrate. Part iii: Leucocyte activation: A new feature for platelet concentrates? Oral Surg Oral Med Oral Pathol Oral Radiol Endod. 2006; 101:e51-5.

117. Zachary I. Vegf signalling: Integration and multi-tasking in endothelial cell biology. Biochem Soc Trans. 2003; 31:1171-7.

118. Harry LE, Paleolog EM. From the cradle to the clinic: Vegf in developmental, physiological, and pathological angiogenesis. Birth Defects Res C Embryo Today. 2003; 69:363-74.

119. Ruhrberg C. Growing and shaping the vascular tree: Multiple roles for vegf. Bioessays. 2003; 25:1052-60.

120. Tiong A, Freedman SB. Gene therapy for cardiovascular disease: The potential of vegf. Curr Opin Mol Ther. 2004; 6:151-9.

121. Butt AJ, Firth SM, Baxter RC. The igf axis and programmed cell death. Immunol Cell Biol. 1999; 77:256-62.

122. Schilephake H. Bone growth factors in maxillofacial skeletal reconstruction. Int J Oral Maxillofac Surg. 2002; 31:469-84.

123. Giannobile WV, Hernandez RA, Finkelman RD, Ryan S, Kiritsy CP, D'Andrea M, et al. Comparative effects of platelet-derived growth factor-bb and insulin-like growth factor-i, individually and in combination, on periodontal regeneration in macaca fascicularis. J Periodontal Res. 1996; 31:301-12.

124. Border WA, Noble NA. Transforming growth factor beta in tissue fibrosis. N Engl J Med. 1994; 331:1286-92.

125. Shi Y, Massague J. Mechanisms of tgf-beta signaling from cell membrane to the nucleus. Cell. 2003; 113:685-700.

126. Sakamaki S, Hirayama Y, Matsunaga T, Kuroda H, Kusakabe T, Akiyama T, et al. Transforming growth factor-beta1 (tgf-beta1) induces thrombopoietin from bone marrow stromal cells, which stimulates the expression of tgf-beta receptor on megakaryocytes and, in turn, renders them susceptible to suppression by tgf-beta itself with high specificity. Blood. 1999; 94:1961-70.

127. Kronemann N, Bouloumi A, Bassus S, Kirchmaier CM, Busse R, Schini-Kerth VB. Aggregating human platelets stimulate expression of vascular endothelial growth factor in cultured vascular smooth muscle cells through a synergistic effect of transforming growth factor-beta(1) and platelet-derived growth factor(ab). Circulation. 1999; 100:855-60.

128. Annes JP, Munger JS, Rifkin DB. Making sense of latent tgfbeta activation. J Cell Sci. 2003; 116:217-24.

129. Schultz-Cherry S, Murphy-Ullrich JE. Thrombospondin causes activation of latent transforming growth factor-beta secreted by endothelial cells by a novel mechanism. J Cell Biol. 1993; 122:923-32.

130. Blakytny R, Ludlow A, Martin GE, Ireland G, Lund LR, Ferguson MW, et al. Latent tgf-beta1 activation by platelets. J Cell Physiol. 2004; 199:67-76.

131. Abdelouahed M, Ludlow A, Brunner G, Lawler J. Activation of platelet-transforming growth factor beta-1 in the absence of thrombospondin-1. J Biol Chem. 2000; 275:17933-6.

132. Slivka SR, Loskutoff DJ. Platelets stimulate endothelial cells to synthesize type 1 plasminogen activator inhibitor. Evaluation of the role of transforming growth factor beta. Blood. 1991; 77:1013-9.

133. Lin HY, Wang XF, Ng-Eaton E, Weinberg RA, Lodish HF. Expression cloning of the tgf-beta type ii receptor, a functional transmembrane serine/threonine kinase. Cell. 1992; 68:775-85.

134. Kiuru J, Viinikka L, Myllyla G, Pesonen K, Perheentupa J. Cytoskeleton-dependent release of human platelet epidermal growth factor. Life Sci. 1991; 49:1997-2003.

135. King GL, Buchwald S. Characterization and partial purification of an endothelial cell growth factor from human platelets. J Clin Invest. 1984; 73:392-6.

136. Ts'ao CH. Rough endoplasmic reticulum and ribosomes in blood platelets. Scand J Haematol. 1971; 8:134-40.

137. Booyse FM, Hoveke TP, Rafelson ME, Jr. Studies on human platelets. Ii. Protein synthetic activity of various platelet populations. Biochim Biophys Acta. 1968; 157:660-3.

138. Becker RC. Platelets from genome to proteome and beyond. J Thromb Thrombolysis. 2007; 23:245-8.

139. Gnatenko DV, Dunn JJ, McCorkle SR, Weissmann D, Perrotta PL, Bahou WF. Transcript profiling of human platelets using microarray and serial analysis of gene expression. Blood. 2003; 101:2285-93.

140. Weyrich AS, Dixon DA, Pabla R, Elstad MR, McIntyre TM, Prescott SM, et al. Signal-dependent translation of a regulatory protein, bcl-3, in activated human platelets. Proc Natl Acad Sci U S A. 1998; 95:5556-61.

141. Lindemann S, Tolley ND, Eyre JR, Kraiss LW, Mahoney TM, Weyrich AS. Integrins regulate the intracellular distribution of eukaryotic initiation factor 4e in platelets. A checkpoint for translational control. J Biol Chem. 2001; 276:33947-51.

142. Lindemann S, Tolley ND, Dixon DA, McIntyre TM, Prescott SM, Zimmerman GA, et al. Activated platelets mediate inflammatory signaling by regulated interleukin 1beta synthesis. J Cell Biol. 2001; 154:485-90.

143. Behnke O. The morphology of blood platelet membrane systems. Ser Haematol. 1970; 3:3-16.

144. White JG. Electron microscopic studies of platelet secretion. Prog Hemost Thromb. 1974; 2:49-98.

145. Suzuki H, Yamazaki H, Tanoue K. Immunocytochemical studies on co-localization of alpha-granule membrane alphaiibbeta3 integrin and intragranular fibrinogen of human platelets and their cell-surface expression during the thrombin-induced release reaction. J Electron Microsc (Tokyo). 2003; 52:183-95.

146. Stenberg PE, Shuman MA, Levine SP, Bainton DF. Redistribution of alpha-granules and their contents in thrombin-stimulated platelets. J Cell Biol. 1984; 98:748-60.

147. Ginsberg MH, Taylor L, Painter RG. The mechanism of thrombin-induced platelet factor 4 secretion. Blood. 1980; 55:661-8.

148. George JN, Pickett EB, Saucerman S, McEver RP, Kunicki TJ, Kieffer N, et al. Platelet surface glycoproteins. Studies on resting and activated platelets and platelet membrane microparticles in normal subjects, and observations in patients during adult respiratory distress syndrome and cardiac surgery. J Clin Invest. 1986; 78:340-8.

149. Michelson AD. Thrombin-induced down-regulation of the platelet membrane glycoprotein ib-ix complex. Semin Thromb Hemost. 1992; 18:18-27.

150. Michelson AD, Barnard MR. Plasmin-induced redistribution of platelet glycoprotein ib. Blood. 1990; 76:2005-10.

151. Suzuki H, Nakamura S, Itoh Y, Tanaka T, Yamazaki H, Tanoue K. Immunocytochemical evidence for the translocation of alpha-granule membrane glycoprotein iib/iiia (integrin alpha iib beta 3) of human platelets to the surface membrane during the release reaction. Histochemistry. 1992; 97:381-8.

152. McNicol A, Israels SJ. Platelet dense granules: Structure, function and implications for haemostasis. Thromb Res. 1999; 95:1-18.

153. Furman MI, Gardner TM, Goldschmidt-Clermont PJ. Mechanisms of cytoskeletal reorganization during platelet activation. Thromb Haemost. 1993; 70:229-32.

154. Chen D, Lemons PP, Schraw T, Whiteheart SW. Molecular mechanisms of platelet exocytosis: Role of snap-23 and syntaxin 2 and 4 in lysosome release. Blood. 2000; 96:1782-8.

155. Lemons PP, Chen D, Bernstein AM, Bennett MK, Whiteheart SW. Regulated secretion in platelets: Identification of elements of the platelet exocytosis machinery. Blood. 1997; 90:1490-500.

156. Morimoto T, Ogihara S. Atp is required in platelet serotonin exocytosis for protein phosphorylation and priming of secretory vesicles docked on the plasma membrane. J Cell Sci. 1996; 109 (Pt 1):113-8.

157. Gerrard JM, Beattie LL, Park J, Israels SJ, McNicol A, Lint D, et al. A role for protein kinase c in the membrane fusion necessary for platelet granule secretion. Blood. 1989; 74:2405-13.

158. Augustine GJ, Burns ME, DeBello WM, Pettit DL, Schweizer FE. Exocytosis: Proteins and perturbations. Annu Rev Pharmacol Toxicol. 1996; 36:659-701.

159. Reed GL, Houng AK, Fitzgerald ML. Human platelets contain snare proteins and a sec1p homologue that interacts with syntaxin 4 and is phosphorylated after thrombin activation: Implications for platelet secretion. Blood. 1999; 93:2617-26.

160. Flaumenhaft R, Croce K, Chen E, Furie B, Furie BC. Proteins of the exocytotic core complex mediate platelet alpha-granule secretion. Roles of vesicle-associated membrane protein, snap-23, and syntaxin 4. J Biol Chem. 1999; 274:2492-501.

161. Bernstein AM, Whiteheart SW. Identification of a cellubrevin/vesicle associated membrane protein 3 homologue in human platelets. Blood. 1999; 93:571-9.

162. Polgar J, Reed GL. A critical role for n-ethylmaleimide-sensitive fusion protein (nsf) in platelet granule secretion. Blood. 1999; 94:1313-8.

163. Flaumenhaft R. Molecular basis of platelet granule secretion. Arterioscler Thromb Vasc Biol. 2003; 23:1152-60.

164. Diegelmann RF, Evans MC. Wound healing: An overview of acute, fibrotic and delayed healing. Front Biosci. 2004; 9:283-9.

165. Garcia A, Zitzmann N, Watson SP. Analyzing the platelet proteome. Semin Thromb Hemost. 2004; 30:485-9.

166. Ibelgaufts H. C o p e cytokines & cells online pathfinder encyclopaedia. 2007.

167. Dinarello CA. The il-1 family and inflammatory diseases. Clin Exp Rheumatol. 2002; 20:S1-13.

168. Rosenwasser LJ. Biologic activities of il-1 and its role in human disease. J Allergy Clin Immunol. 1998; 102:344-50.

169. Dinarello CA. Therapeutic strategies to reduce il-1 activity in treating local and systemic inflammation. Curr Opin Pharmacol. 2004; 4:378-85.

170. Kwan Tat S, Padrines M, Theoleyre S, Heymann D, Fortun Y. Il-6, rankl, tnf-alpha/il-1: Interrelations in bone resorption pathophysiology. Cytokine Growth Factor Rev. 2004; 15:49-60.

171. Tiggelman AM, Boers W, Linthorst C, Brand HS, Sala M, Chamuleau RA. Interleukin-6 production by human liver (myo)fibroblasts in culture. Evidence for a regulatory role of lps, il-1 beta and tnf alpha. J Hepatol. 1995; 23:295-306.

172. Kamimura D, Ishihara K, Hirano T. Il-6 signal transduction and its physiological roles: The signal orchestration model. Rev Physiol Biochem Pharmacol. 2003; 149:1-38.

173. Heinrich PC, Behrmann I, Haan S, Hermanns HM, Muller-Newen G, Schaper F. Principles of interleukin (il)-6-type cytokine signalling and its regulation. Biochem J. 2003; 374:1-20.

174. Nishimoto N, Kishimoto T. Inhibition of il-6 for the treatment of inflammatory diseases. Curr Opin Pharmacol. 2004; 4:386-91.

175. Aggarwal BB, Shishodia S, Ashikawa K, Bharti AC. The role of tnf and its family members in inflammation and cancer: Lessons from gene deletion. Curr Drug Targets Inflamm Allergy. 2002; 1:327-41.

176. Aggarwal BB. Signalling pathways of the tnf superfamily: A double-edged sword. Nat Rev Immunol. 2003; 3:745-56.

177. Gaur U, Aggarwal BB. Regulation of proliferation, survival and apoptosis by members of the tnf superfamily. Biochem Pharmacol. 2003; 66:1403-8.

178. Zimmermann R, Jakubietz R, Jakubietz M, Strasser E, Schlegel A, Wiltfang J, et al. Different preparation methods to obtain platelet components as a source of growth factors for local application. Transfusion. 2001; 41:1217-24.

179. Keegan AD, Zamorano J. Regulation of gene expression, growth, and cell survival by il-4: Contribution of multiple signaling pathways. Cell Res. 1998; 8:1-13.

180. Kay NE, Pittner BT. Il-4 biology: Impact on normal and leukemic cll b cells. Leuk Lymphoma. 2003; 44:897-903.

181. Tiggelman AM, Boers W, Linthorst C, Sala M, Chamuleau RA. Collagen synthesis by human liver (myo)fibroblasts in culture: Evidence for a regulatory role of il-1 beta, il-4, tgf beta and ifn gamma. J Hepatol. 1995; 23:307-17.

182. Hayashi Y, Kobayashi M, Kuwata H, Atsumi G, Deguchi K, Feng Wei X, et al. Interferon-gamma and interleukin 4 inhibit interleukin 1beta-induced delayed prostaglandin e(2)generation through suppression of cyclooxygenase-2 expression in human fibroblasts. Cytokine. 2000; 12:603-12.

183. Li-Weber M, Laur O, Davydov I, Hu C, Salgame P, Krammer PH. What controls tissue-specific expression of the il-4 gene? Immunobiology. 1997; 198:170-8.

184. Brown MA, Hural J. Functions of il-4 and control of its expression. Crit Rev Immunol. 1997; 17:1-32.

185. Rosenthal AR, Harbury C, Egbert PR, Rubenstein E. Use of a platelet-fibrinogen-thrombin mixture as a corneal adhesive: Experiments with sutureless lamellar keratoplasty in the rabbit. Invest Ophthalmol. 1975; 14:872-5.

186. Witte LD, Cornicelli JA, Miller RW, Goodman DS. Effect of platelet-derived and endothelial cell-derived growth factors on the low density lipoprotein receptor pathway in cultured human fibroblasts. J Biol Chem. 1982; 257:5392-401.

187. Graves DT, Owen AJ, Antoniades HN. Evidence that a human osteosarcoma cell line which secretes a mitogen similar to platelet-derived growth factor requires growth factors present in platelet-poor plasma. Cancer Res. 1983; 43:83-7.

188. Knighton DR, Ciresi KF, Fiegel VD, Austin LL, Butler EL. Classification and treatment of chronic nonhealing wounds. Successful treatment with autologous platelet-derived wound healing factors (pdwhf). Ann Surg. 1986; 204:322-30.

189. Lynch SE, Nixon JC, Colvin RB, Antoniades HN. Role of platelet-derived growth factor in wound healing: Synergistic effects with other growth factors. Proc Natl Acad Sci U S A. 1987; 84:7696-700.

190. Gordon L, Chiu EJ. Treatment of infected non-unions and segmental defects of the tibia with staged microvascular muscle transplantation and bone-grafting. J Bone Joint Surg Am. 1988; 70:377-86.

191. Lynch SE, Williams RC, Polson AM, Howell TH, Reddy MS, Zappa UE, et al. A combination of platelet-derived and insulin-like growth factors enhances periodontal regeneration. J Clin Periodontol. 1989; 16:545-8.

192. Miyazono K, Takaku F. Platelet-derived growth factors. Blood Rev. 1989; 3:269-76.

193. Lawson JH. The clinical use and immunologic impact of thrombin in surgery. Semin Thromb Hemost. 2006; 32 Suppl 1:98-110.

194. Whitman DH, Berry RL, Green DM. Platelet gel: An autologous alternative to fibrin glue with applications in oral and maxillofacial surgery. J Oral Maxillofac Surg. 1997; 55:1294-9.

195. Krupski WC, Reilly LM, Perez S, Moss KM, Crombleholme PA, Rapp JH. A prospective randomized trial of autologous platelet-derived wound healing factors for treatment of chronic nonhealing wounds: A preliminary report. J Vasc Surg. 1991; 14:526-32; discussion 532-6.

196. Borzini P, Mazzucco L, Giampaolo A, Hassan HJ. Platelet gel - the italian way: A call for procedure standardization and quality control. Transfus Med. 2006; 16:303-4.

197. Anitua E. Plasma rich in growth factors: Preliminary results of use in the preparation of future sites for implants. Int J Oral Maxillofac Implants. 1999; 14:529-35.

198. Anitua E. The use of plasma-rich growth factors (prgf) in oral surgery. Pract Proced Aesthet Dent. 2001; 13:487-93; quiz 487-93.

199. Margolis DJ, Kantor J, Santanna J, Strom BL, Berlin JA. Effectiveness of platelet releasate for the treatment of diabetic neuropathic foot ulcers. Diabetes Care. 2001; 24:483-8.

200. Keyser JE. Diabetic wound healing and limb salvage in an outpatient wound care program. South Med J. 1993; 86:311-7.

201. Crovetti G, Martinelli G, Issi M, Barone M, Guizzardi M, Campanati B, et al. Platelet gel for healing cutaneous chronic wounds. Transfus Apher Sci. 2004; 30:145-51.

202. Valbonesi M, Giannini G, Migliori F, Dalla Costa R, Galli A. The role of autologous fibrin-platelet glue in plastic surgery: A preliminary report. Int J Artif Organs. 2002; 25:334-8.

203. Sanchez M, Anitua E, Azofra J, Andia I, Padilla S, Mujika I. Comparison of surgically repaired achilles tendon tears using platelet-rich fibrin matrices. Am J Sports Med. 2007; 35:245-51.

204. Sanchez M, Azofra J, Anitua E, Andia I, Padilla S, Santisteban J, et al. Plasma rich in growth factors to treat an articular cartilage avulsion: A case report. Med Sci Sports Exerc. 2003; 35:1648-52.

205. Mishra A, Pavelko T. Treatment of chronic elbow tendinosis with buffered platelet-rich plasma. Am J Sports Med. 2006; 34:1774-8.

206. Werner S, Grose R. Regulation of wound healing by growth factors and cytokines. Physiol Rev. 2003; 83:835-70.

207. Singer AJ, Clark RA. Cutaneous wound healing. N Engl J Med. 1999; 341:738-46.

208. McGrath MH. Peptide growth factors and wound healing. Clin Plast Surg. 1990; 17:421-32.

209. Lieberman JR, Daluiski A, Einhorn TA. The role of growth factors in the repair of bone. Biology and clinical applications. J Bone Joint Surg Am. 2002; 84-A:1032-44.

210. Brown RL, Breeden MP, Greenhalgh DG. Pdgf and tgf-alpha act synergistically to improve wound healing in the genetically diabetic mouse. J Surg Res. 1994; 56:562-70.

211. Kells AF, Coats SR, Schwartz HS, Hoover RL. Tgf-beta and pdgf act synergistically in affecting the growth of human osteoblast-enriched cultures. Connect Tissue Res. 1995; 31:117-24.

212. Liu YS, Zhou YS, Zhu SS. [effect of in vitro storage on the biological activity of human platelet-rich plasma]. Beijing Da Xue Xue Bao. 2008; 40:34-8.

213. Murphy S, Heaton WA, Rebulla P. Platelet production in the old world--and the new. Transfusion. 1996; 36:751-4.

214. Dohan DM, Choukroun J, Diss A, Dohan SL, Dohan AJ, Mouhyi J, et al. Platelet-rich fibrin (prf): A second-generation platelet concentrate. Part i: Technological concepts and evolution. Oral Surg Oral Med Oral Pathol Oral Radiol Endod. 2006; 101:e37-44.

215. Mourad N. Studies on release of certain enzymes from certain enzymes from human platelets. Transfusion. 1968; 8:363-7.

216. Froum SJ, Wallace SS, Tarnow DP, Cho SC. Effect of platelet-rich plasma on bone growth and osseointegration in human maxillary sinus grafts: Three bilateral case reports. Int J Periodontics Restorative Dent. 2002; 22:45-53.

217. Lekovic V, Camargo PM, Weinlaender M, Vasilic N, Kenney EB. Comparison of platelet-rich plasma, bovine porous bone mineral, and guided tissue regeneration versus platelet-rich plasma and bovine porous bone mineral in the treatment of intrabony defects: A reentry study. J Periodontol. 2002; 73:198-205.

218. Lekovic V, Camargo PM, Weinlaender M, Vasilic N, Aleksic Z, Kenney EB. Effectiveness of a combination of platelet-rich plasma, bovine porous bone mineral and guided tissue regeneration in the treatment of mandibular grade ii molar furcations in humans. J Clin Periodontol. 2003; 30:746-51.

219. Kassolis JD, Rosen PS, Reynolds MA. Alveolar ridge and sinus augmentation utilizing platelet-rich plasma in combination with freeze-dried bone allograft: Case series. J Periodontol. 2000; 71:1654-61.

220. Petrungaro PS. Using platelet-rich plasma to accelerate soft tissue maturation in esthetic periodontal surgery. Compend Contin Educ Dent. 2001; 22:729-32, 734, 736 passim; quiz 746.

221. Petrungaro PS. Treatment of the infected implant site using platelet-rich plasma. Compend Contin Educ Dent. 2002; 23:363-6, 368, 370 passim; quiz 378.

222. Sanchez AR, Sheridan PJ, Kupp LI. Is platelet-rich plasma the perfect enhancement factor? A current review. Int J Oral Maxillofac Implants. 2003; 18:93-103.

223. Camargo PM, Lekovic V, Weinlaender M, Vasilic N, Madzarevic M, Kenney EB. Platelet-rich plasma and bovine porous bone mineral combined with guided tissue

regeneration in the treatment of intrabony defects in humans. J Periodontal Res. 2002; 37:300-6.

224. Choi BH, Im CJ, Huh JY, Suh JJ, Lee SH. Effect of platelet-rich plasma on bone regeneration in autogenous bone graft. Int J Oral Maxillofac Surg. 2004; 33:56-9.

225. Della Valle A, Sammartino G, Marenzi G, Tia M, Espedito di Lauro A, Ferrari F, et al. Prevention of postoperative bleeding in anticoagulated patients undergoing oral surgery: Use of platelet-rich plasma gel. J Oral Maxillofac Surg. 2003; 61:1275-8.

226. Jakse N, Tangl S, Gilli R, Berghold A, Lorenzoni M, Eskici A, et al. Influence of prp on autogenous sinus grafts. An experimental study on sheep. Clin Oral Implants Res. 2003; 14:578-83.

227. Jensen TB, Rahbek O, Overgaard S, Soballe K. Platelet rich plasma and fresh frozen bone allograft as enhancement of implant fixation. An experimental study in dogs. J Orthop Res. 2004; 22:653-8.

228. Jensen TB, Rahbek O, Overgaard S, Soballe K. No effect of platelet-rich plasma with frozen or processed bone allograft around noncemented implants. Int Orthop. 2005; 29:67-72.

229. Li H, Zou X, Xue Q, Egund N, Lind M, Bunger C. Anterior lumbar interbody fusion with carbon fiber cage loaded with bioceramics and platelet-rich plasma. An experimental study on pigs. Eur Spine J. 2004; 13:354-8.

230. Schlegel KA, Donath K, Rupprecht S, Falk S, Zimmermann R, Felszeghy E, et al. De novo bone formation using bovine collagen and platelet-rich plasma. Biomaterials. 2004; 25:5387-93.

231. Weibrich G, Hansen T, Kleis W, Buch R, Hitzler WE. Effect of platelet concentration in platelet-rich plasma on peri-implant bone regeneration. Bone. 2004; 34:665-71.

232. Wiltfang J, Kloss FR, Kessler P, Nkenke E, Schultze-Mosgau S, Zimmermann R, et al. Effects of platelet-rich plasma on bone healing in combination with autogenous bone and bone substitutes in critical-size defects. An animal experiment. Clin Oral Implants Res. 2004; 15:187-93.

233. Mosesson MW, Siebenlist KR, Meh DA. The structure and biological features of fibrinogen and fibrin. Ann N Y Acad Sci. 2001; 936:11-30.

234. Fijnheer R, Pietersz RN, de Korte D, Gouwerok CW, Dekker WJ, Reesink HW, et al. Platelet activation during preparation of platelet concentrates: A comparison of the platelet-rich plasma and the buffy coat methods. Transfusion. 1990; 30:634-8.

235. Hogman CF, Eriksson L, Hedlund K, Wallvik J. The bottom and top system: A new technique for blood component preparation and storage. Vox Sang. 1988; 55:211-7.

236. Leukocyte reduction and ultraviolet b irradiation of platelets to prevent alloimmunization and refractoriness to platelet transfusions. The trial to reduce alloimmunization to platelets study group. N Engl J Med. 1997; 337:1861-9.

237. Seftel MD, Growe GH, Petraszko T, Benny WB, Le A, Lee CY, et al. Universal prestorage leukoreduction in canada decreases platelet alloimmunization and refractoriness. Blood. 2004; 103:333-9.

238. Zimmermann R, Arnold D, Strasser E, Ringwald J, Schlegel A, Wiltfang J, et al. Sample preparation technique and white cell content influence the detectable levels of growth factors in platelet concentrates. Vox Sang. 2003; 85:283-9.

239. Gibble JW, Ness PM. Fibrin glue: The perfect operative sealant? Transfusion. 1990; 30:741-7.

240. Clark RA. Fibrin and wound healing. Ann N Y Acad Sci. 2001; 936:355-67.

241. Collen A, Koolwijk P, Kroon M, van Hinsbergh VW. Influence of fibrin structure on the formation and maintenance of capillary-like tubules by human microvascular endothelial cells. Angiogenesis. 1998; 2:153-65.

242. van Hinsbergh VW, Collen A, Koolwijk P. Role of fibrin matrix in angiogenesis. Ann N Y Acad Sci. 2001; 936:426-37.

243. Tayapongsak P, O'Brien DA, Monteiro CB, Arceo-Diaz LY. Autologous fibrin adhesive in mandibular reconstruction with particulate cancellous bone and marrow. J Oral Maxillofac Surg. 1994; 52:161-5; discussion 166.

244. Saltz R, Sierra D, Feldman D, Saltz MB, Dimick A, Vasconez LO. Experimental and clinical applications of fibrin glue. Plast Reconstr Surg. 1991; 88:1005-15; discussion 1016-7.

245. Reeder SB, Widlus DM, Lazinger M. Low-dose thrombin injection to treat iatrogenic femoral artery pseudoaneurysms. AJR Am J Roentgenol. 2001; 177:595-8.

246. Ferguson JD, Whatling PJ, Martin V, Walton J, Banning AP. Ultrasound guided percutaneous thrombin injection of iatrogenic femoral artery pseudoaneurysms after coronary angiography and intervention. Heart. 2001; 85:E5.

247. Vaziri ND. Topical thrombin and control of bleeding from the fistula puncture sites in dialyzed patients. Nephron. 1979; 24:254-6.

248. Stricker RB, Lane PK, Leffert JD, Rodgers GM, Shuman MA, Corash L. Development of antithrombin antibodies following surgery in patients with prosthetic cardiac valves. Blood. 1988; 72:1375-80.

249. Flaherty MJ, Henderson R, Wener MH. Iatrogenic immunization with bovine thrombin: A mechanism for prolonged thrombin times after surgery. Ann Intern Med. 1989; 111:631-4.

250. Lawson JH, Pennell BJ, Olson JD, Mann KG. Isolation and characterization of an acquired antithrombin antibody. Blood. 1990; 76:2249-57.

251. Rapaport SI, Zivelin A, Minow RA, Hunter CS, Donnelly K. Clinical significance of antibodies to bovine and human thrombin and factor v after surgical use of bovine thrombin. Am J Clin Pathol. 1992; 97:84-91.

252. Cmolik BL, Spero JA, Magovern GJ, Clark RE. Redo cardiac surgery: Late bleeding complications from topical thrombin-induced factor v deficiency. J Thorac Cardiovasc Surg. 1993; 105:222-7; discussion 227-8.

253. Israels SJ, Leaker MT. Acquired inhibitors to factors v and x after exposure to topical thrombin: Interference with monitoring of low molecular weight heparin and warfarin. J Pediatr. 1997; 131:480-3.

254. Sands JJ, Nudo SA, Ashford RG, Moore KD, Ortel TL. Antibodies to topical bovine thrombin correlate with access thrombosis. Am J Kidney Dis. 2000; 35:796-801.

255. Kajitani M, Ozdemir A, Aguinaga M, Jazieh AR, Flick JT, Antakli T. Severe hemorrhagic complication due to acquired factor v inhibitor after single exposure to bovine thrombin product. J Card Surg. 2000; 15:378-82.

256. Ortel TL, Mercer MC, Thames EH, Moore KD, Lawson JH. Immunologic impact and clinical outcomes after surgical exposure to bovine thrombin. Ann Surg. 2001; 233:88-96.

257. Schoenecker JG, Hauck RK, Mercer MC, Parker W, Lawson JH. Exposure to topical bovine thrombin during surgery elicits a response against the xenogeneic carbohydrate galactose alpha1-3galactose. J Clin Immunol. 2000; 20:434-44.

258. Su Z, Izumi T, Thames EH, Lawson JH, Ortel TL. Antiphospholipid antibodies after surgical exposure to topical bovine thrombin. J Lab Clin Med. 2002; 139:349-56.

259. Cruickshank MK, Black J, Wall W. Development of a factor v and thrombin inhibitor following partial hepatic resection and the use of topical thrombin concentrate. Clin Lab Haematol. 1994; 16:187-90.

260. Izumi T, Kim SW, Greist A, Macedo-Ribeiro S, Fuentes-Prior P, Bode W, et al. Fine mapping of inhibitory anti-factor v antibodies using factor v c2 domain mutants. Identification of two antigenic epitopes involved in phospholipid binding. Thromb Haemost. 2001; 85:1048-54.

261. Ortel TL, Moore KD, Quinn-Allen MA, Okamura T, Sinclair AJ, Lazarchick J, et al. Inhibitory anti-factor v antibodies bind to the factor v c2 domain and are associated with hemorrhagic manifestations. Blood. 1998; 91:4188-96.

262. Ortel TL, Charles LA, Keller FG, Marcom PK, Oldham HN, Jr., Kane WH, et al. Topical thrombin and acquired coagulation factor inhibitors: Clinical spectrum and laboratory diagnosis. Am J Hematol. 1994; 45:128-35.

263. Zehnder JL, Leung LL. Development of antibodies to thrombin and factor v with recurrent bleeding in a patient exposed to topical bovine thrombin. Blood. 1990; 76:2011-6.

264. Behar SM, Porcelli SA. Mechanisms of autoimmune disease induction. The role of the immune response to microbial pathogens. Arthritis Rheum. 1995; 38:458-76.

265. Moran AP, Prendergast MM, Appelmelk BJ. Molecular mimicry of host structures by bacterial lipopolysaccharides and its contribution to disease. FEMS Immunol Med Microbiol. 1996; 16:105-15.

266. Atkinson MA. Molecular mimicry and the pathogenesis of insulin-dependent diabetes mellitus: Still just an attractive hypothesis. Ann Med. 1997; 29:393-9.

267. Karlsen AE, Dyrberg T. Molecular mimicry between non-self, modified self and self in autoimmunity. Semin Immunol. 1998; 10:25-34.

268. Albert LJ, Inman RD. Molecular mimicry and autoimmunity. N Engl J Med. 1999; 341:2068-74.

269. Grageda E, Lozada JL, Boyne PJ, Caplanis N, McMillan PJ. Bone formation in the maxillary sinus by using platelet-rich plasma: An experimental study in sheep. J Oral Implantol. 2005; 31:2-17.

270. Rodan GA, Noda M. Gene expression in osteoblastic cells. Crit Rev Eukaryot Gene Expr. 1991; 1:85-98.

271. Stains JP, Civitelli R. Genomic approaches to identifying transcriptional regulators of osteoblast differentiation. Genome Biol. 2003; 4:222.

272. Nakashima K, Zhou X, Kunkel G, Zhang Z, Deng JM, Behringer RR, et al. The novel zinc finger-containing transcription factor osterix is required for osteoblast differentiation and bone formation. Cell. 2002; 108:17-29.

273. Otto F, Thornell AP, Crompton T, Denzel A, Gilmour KC, Rosewell IR, et al. Cbfa1, a candidate gene for cleidocranial dysplasia syndrome, is essential for osteoblast differentiation and bone development. Cell. 1997; 89:765-71.

274. Komori T, Yagi H, Nomura S, Yamaguchi A, Sasaki K, Deguchi K, et al. Targeted disruption of cbfa1 results in a complete lack of bone formation owing to maturational arrest of osteoblasts. Cell. 1997; 89:755-64.

275. Chen JK, Shapiro HS, Wrana JL, Reimers S, Heersche JN, Sodek J. Localization of bone sialoprotein (bsp) expression to sites of mineralized tissue formation in fetal rat tissues by in situ hybridization. Matrix. 1991; 11:133-43.

276. Tamura M, Noda M. Identification of a DNA sequence involved in osteoblast-specific gene expression via interaction with helix-loop-helix (hlh)-type transcription factors. J Cell Biol. 1994; 126:773-82.

277. Hauschka PV. Osteocalcin: The vitamin k-dependent ca2+-binding protein of bone matrix. Haemostasis. 1986; 16:258-72.

278. Suittie. Current advances in vitamin k research. New York: Elsevier Science Publishing; 1988.

279. Noda M. Cellular and molecular biology of bone. San Diego: Academic Press; 1993.

280. Franceschi RT. The developmental control of osteoblast-specific gene expression: Role of specific transcription factors and the extracellular matrix environment. Crit Rev Oral Biol Med. 1999; 10:40-57.

281. Lamour V, Detry C, Sanchez C, Henrotin Y, Castronovo V, Bellahcene A. Runx2- and histone deacetylase 3-mediated repression is relieved in differentiating human osteoblast cells to allow high bone sialoprotein expression. J Biol Chem. 2007; 282:36240-9.

282. Bianco P, Fisher LW, Young MF, Termine JD, Robey PG. Expression of bone sialoprotein (bsp) in developing human tissues. Calcif Tissue Int. 1991; 49:421-6.

283. Fisher LW, McBride OW, Termine JD, Young MF. Human bone sialoprotein. Deduced protein sequence and chromosomal localization. J Biol Chem. 1990; 265:2347-51.

284. Fisher LW, Whitson SW, Avioli LV, Termine JD. Matrix sialoprotein of developing bone. J Biol Chem. 1983; 258:12723-7.

285. Fisher LW, Hawkins GR, Tuross N, Termine JD. Purification and partial characterization of small proteoglycans i and ii, bone sialoproteins i and ii, and osteonectin from the mineral compartment of developing human bone. J Biol Chem. 1987; 262:9702-8.

286. Kasugai S, Todescan R, Jr., Nagata T, Yao KL, Butler WT, Sodek J. Expression of bone matrix proteins associated with mineralized tissue formation by adult rat bone marrow cells in vitro: Inductive effects of dexamethasone on the osteoblastic phenotype. J Cell Physiol. 1991; 147:111-20.

287. Chen J, Shapiro HS, Sodek J. Development expression of bone sialoprotein mrna in rat mineralized connective tissues. J Bone Miner Res. 1992; 7:987-97.

288. Ganss B, Kim RH, Sodek J. Bone sialoprotein. Crit Rev Oral Biol Med. 1999; 10:79-98.

289. Yao KL, Todescan R, Jr., Sodek J. Temporal changes in matrix protein synthesis and mrna expression during mineralized tissue formation by adult rat bone marrow cells in culture. J Bone Miner Res. 1994; 9:231-40.

290. Kasugai S, Nagata T, Sodek J. Temporal studies on the tissue compartmentalization of bone sialoprotein (bsp), osteopontin (opn), and sparc protein during bone formation in vitro. J Cell Physiol. 1992; 152:467-77.

291. Slavkin HaP, P. Biology and chemistry of mineralized tissues. Amsterdam: Elsevier Science; 1992.

292. Midura RJ, McQuillan DJ, Benham KJ, Fisher LW, Hascall VC. A rat osteogenic cell line (umr 106-01) synthesizes a highly sulfated form of bone sialoprotein. J Biol Chem. 1990; 265:5285-91.

293. .

294. Mikkola HK, Orkin SH. The journey of developing hematopoietic stem cells. Development. 2006; 133:3733-44.

295. Corbel C, Salaun J. Alphaiib integrin expression during development of the murine hemopoietic system. Dev Biol. 2002; 243:301-11.

296. Corbel C, Vaigot P, Salaun J. (alpha)iib integrin, a novel marker for hemopoietic progenitor cells. Int J Dev Biol. 2005; 49:279-84.

297. Ferkowicz MJ, Starr M, Xie X, Li W, Johnson SA, Shelley WC, et al. Cd41 expression defines the onset of primitive and definitive hematopoiesis in the murine embryo. Development. 2003; 130:4393-403.

298. Mikkola HK, Fujiwara Y, Schlaeger TM, Traver D, Orkin SH. Expression of cd41 marks the initiation of definitive hematopoiesis in the mouse embryo. Blood. 2003; 101:508-16.

299. Mitjavila-Garcia MT, Cailleret M, Godin I, Nogueira MM, Cohen-Solal K, Schiavon V, et al. Expression of cd41 on hematopoietic progenitors derived from embryonic hematopoietic cells. Development. 2002; 129:2003-13.

300. Bertrand JY, Giroux S, Golub R, Klaine M, Jalil A, Boucontet L, et al. Characterization of purified intraembryonic hematopoietic stem cells as a tool to define their site of origin. Proc Natl Acad Sci U S A. 2005; 102:134-9.

301. Kiel MJ, Yilmaz OH, Iwashita T, Terhorst C, Morrison SJ. Slam family receptors distinguish hematopoietic stem and progenitor cells and reveal endothelial niches for stem cells. Cell. 2005; 121:1109-21.

302. Matsubara A, Iwama A, Yamazaki S, Furuta C, Hirasawa R, Morita Y, et al. Endomucin, a cd34-like sialomucin, marks hematopoietic stem cells throughout development. J Exp Med. 2005; 202:1483-92.

303. Noer A, Sorensen AL, Boquest AC, Collas P. Stable cpg hypomethylation of adipogenic promoters in freshly isolated, cultured, and differentiated mesenchymal stem cells from adipose tissue. Mol Biol Cell. 2006; 17:3543-56.

304. Rox JM, Bugert P, Muller J, Schorr A, Hanfland P, Madlener K, et al. Gene expression analysis in platelets from a single donor: Evaluation of a pcr-based amplification technique. Clin Chem. 2004; 50:2271-8.

305. Kawaguchi H, Yavari R, Stover ML, Rowe DW, Raisz LG, Pilbeam CC. Measurement of interleukin-1 stimulated constitutive prostaglandin g/h synthase (cyclooxygenase) mrna levels in osteoblastic mc3t3-e1 cells using competitive reverse transcriptase polymerase chain reaction. Endocr Res. 1994; 20:219-33.

306. Yang YM, Xu ZR, Wu LJ, Huang WD. Study of resistin gene expression in peripheral blood mononuclear cell and its gene polymorphism in a small range population. J Zhejiang Univ Sci B. 2007; 8:132-5.

307. Hayashi S, Yamane T, Miyamoto A, Hemmi H, Tagaya H, Tanio Y, et al. Commitment and differentiation of stem cells to the osteoclast lineage. Biochem Cell Biol. 1998; 76:911-22.

308. Fernandez-Tresguerres-Hernandez-Gil I, Alobera-Gracia MA, del-Canto-Pingarron M, Blanco-Jerez L. Physiological bases of bone regeneration ii. The remodeling process. Med Oral Patol Oral Cir Bucal. 2006; 11:E151-7.

309. Watkins BA, Lippman HE, Le Bouteiller L, Li Y, Seifert MF. Bioactive fatty acids: Role in bone biology and bone cell function. Prog Lipid Res. 2001; 40:125-48.

310. Liu F, Malaval L, Gupta AK, Aubin JE. Simultaneous detection of multiple bone-related mrnas and protein expression during osteoblast differentiation: Polymerase chain reaction and immunocytochemical studies at the single cell level. Dev Biol. 1994; 166:220-34.

311. van der Plas A, Aarden EM, Feijen JH, de Boer AH, Wiltink A, Alblas MJ, et al. Characteristics and properties of osteocytes in culture. J Bone Miner Res. 1994; 9:1697-704.

312. Martin RB. Toward a unifying theory of bone remodeling. Bone. 2000; 26:1-6.

313. Jilka RL, Weinstein RS, Bellido T, Roberson P, Parfitt AM, Manolagas SC. Increased bone formation by prevention of osteoblast apoptosis with parathyroid hormone. J Clin Invest. 1999; 104:439-46.

314. Lynch MP, Capparelli C, Stein JL, Stein GS, Lian JB. Apoptosis during bone-like tissue development in vitro. J Cell Biochem. 1998; 68:31-49.

315. Plotkin LI, Weinstein RS, Parfitt AM, Roberson PK, Manolagas SC, Bellido T. Prevention of osteocyte and osteoblast apoptosis by bisphosphonates and calcitonin. J Clin Invest. 1999; 104:1363-74.

316. Weinstein RS, Jilka RL, Parfitt AM, Manolagas SC. Inhibition of osteoblastogenesis and promotion of apoptosis of osteoblasts and osteocytes by glucocorticoids. Potential mechanisms of their deleterious effects on bone. J Clin Invest. 1998; 102:274-82.

317. Lian JB, Stein GS, Stein JL, van Wijnen AJ. Osteocalcin gene promoter: Unlocking the secrets for regulation of osteoblast growth and differentiation. J Cell Biochem Suppl. 1998; 30-31:62-72.

318. Centrella M, Horowitz MC, Wozney JM, McCarthy TL. Transforming growth factor-beta gene family members and bone. Endocr Rev. 1994; 15:27-39.

319. Canalis E, Pash J, Varghese S. Skeletal growth factors. Crit Rev Eukaryot Gene Expr. 1993; 3:155-66.

320. Goldring MB, Goldring SR. Skeletal tissue response to cytokines. Clin Orthop Relat Res. 1990:245-78.

321. Buckley MJ, Banes AJ, Jordan RD. The effects of mechanical strain on osteoblasts in vitro. J Oral Maxillofac Surg. 1990; 48:276-82; discussion 282-3.

322. Makita N, Suzuki M, Asami S, Takahata R, Kohzaki D, Kobayashi S, et al. Two of four alternatively spliced isoforms of runx2 control osteocalcin gene expression in human osteoblast cells. Gene. 2008; 413:8-17.

323. Lian JB, Stein GS, Javed A, van Wijnen AJ, Stein JL, Montecino M, et al. Networks and hubs for the transcriptional control of osteoblastogenesis. Rev Endocr Metab Disord. 2006; 7:1-16.

324. Provot S, Schipani E. Molecular mechanisms of endochondral bone development. Biochem Biophys Res Commun. 2005; 328:658-65.

325. Urist MR. Fundamental and clinical bone physiology. Philadelphia: Lippincott; 1980.

326. Ornitz DM. Fgf signaling in the developing endochondral skeleton. Cytokine Growth Factor Rev. 2005; 16:205-13.

327. Schmidmaier G, Herrmann S, Green J, Weber T, Scharfenberger A, Haas NP, et al. Quantitative assessment of growth factors in reaming aspirate, iliac crest, and platelet preparation. Bone. 2006; 39:1156-63.

328. Graziani F, Ivanovski S, Cei S, Ducci F, Tonetti M, Gabriele M. The in vitro effect of different prp concentrations on osteoblasts and fibroblasts. Clin Oral Implants Res. 2006; 17:212-9.

329. Kanno T, Takahashi T, Tsujisawa T, Ariyoshi W, Nishihara T. Platelet-rich plasma enhances human osteoblast-like cell proliferation and differentiation. J Oral Maxillofac Surg. 2005; 63:362-9.

330. ten Dijke P, Fu J, Schaap P, Roelen BA. Signal transduction of bone morphogenetic proteins in osteoblast differentiation. J Bone Joint Surg Am. 2003; 85-A Suppl 3:34-8.

331. Chen D, Zhao M, Mundy GR. Bone morphogenetic proteins. Growth Factors. 2004; 22:233-41.

332. Liu A, Niswander LA. Bone morphogenetic protein signalling and vertebrate nervous system development. Nat Rev Neurosci. 2005; 6:945-54.

333. Noth U, Tuli R, Seghatoleslami R, Howard M, Shah A, Hall DJ, et al. Activation of p38 and smads mediates bmp-2 effects on human trabecular bone-derived osteoblasts. Exp Cell Res. 2003; 291:201-11.

334. Lee KS, Hong SH, Bae SC. Both the smad and p38 mapk pathways play a crucial role in runx2 expression following induction by transforming growth factor-beta and bone morphogenetic protein. Oncogene. 2002; 21:7156-63.

335. Guicheux J, Lemonnier J, Ghayor C, Suzuki A, Palmer G, Caverzasio J. Activation of p38 mitogen-activated protein kinase and c-jun-nh2-terminal kinase by bmp-2 and their implication in the stimulation of osteoblastic cell differentiation. J Bone Miner Res. 2003; 18:2060-8.

336. Ghosh-Choudhury N, Woodruff K, Qi W, Celeste A, Abboud SL, Ghosh Choudhury G. Bone morphogenetic protein-2 blocks mda mb 231 human breast cancer cell proliferation by inhibiting cyclin-dependent kinase-mediated retinoblastoma protein phosphorylation. Biochem Biophys Res Commun. 2000; 272:705-11.

337. Celil AB, Campbell PG. Bmp-2 and insulin-like growth factor-i mediate osterix (osx) expression in human mesenchymal stem cells via the mapk and protein kinase d signaling pathways. J Biol Chem. 2005; 280:31353-9.

338. Hay E, Lemonnier J, Fromigue O, Marie PJ. Bone morphogenetic protein-2 promotes osteoblast apoptosis through a smad-independent, protein kinase c-dependent signaling pathway. J Biol Chem. 2001; 276:29028-36.

339. Lai CF, Cheng SL. Signal transductions induced by bone morphogenetic protein-2 and transforming growth factor-beta in normal human osteoblastic cells. J Biol Chem. 2002; 277:15514-22.

340. Gallea S, Lallemand F, Atfi A, Rawadi G, Ramez V, Spinella-Jaegle S, et al. Activation of mitogen-activated protein kinase cascades is involved in regulation of bone morphogenetic protein-2-induced osteoblast differentiation in pluripotent c2c12 cells. Bone. 2001; 28:491-8.

341. Pittenger MF, Mackay AM, Beck SC, Jaiswal RK, Douglas R, Mosca JD, et al. Multilineage potential of adult human mesenchymal stem cells. Science. 1999; 284:143-7.

342. Marshak DR, Gardner RL, Gottlieb D. Stem cell biology. Cold Spring Harbor, N.Y.: Cold Spring Harbor Laboratory Press; 2001.

343. Hung SC, Chen NJ, Hsieh SL, Li H, Ma HL, Lo WH. Isolation and characterization of size-sieved stem cells from human bone marrow. Stem Cells. 2002; 20:249-58.

344. Tozum TF, Demiralp B. Platelet-rich plasma: A promising innovation in dentistry. J Can Dent Assoc. 2003; 69:664.

345. Nathan S, Das De S, Thambyah A, Fen C, Goh J, Lee EH. Cell-based therapy in the repair of osteochondral defects: A novel use for adipose tissue. Tissue Eng. 2003; 9:733-44.

346. Caplan AI. Review: Mesenchymal stem cells: Cell-based reconstructive therapy in orthopedics. Tissue Eng. 2005; 11:1198-211.

347. Dugrillon A, Eichler H, Kern S, Kluter H. Autologous concentrated platelet-rich plasma (cprp) for local application in bone regeneration. Int J Oral Maxillofac Surg. 2002; 31:615-9.

348. Koveker GB. Growth factors in clinical practice. Int J Clin Pract. 2000; 54:590-3.

349. Eby BW. Platelet-rich plasma: Harvesting with a single-spin centrifuge. J Oral Implantol. 2002; 28:297-301.

350. Roussy Y, Bertrand Duchesne MP, Gagnon G. Activation of human platelet-rich plasmas: Effect on growth factors release, cell division and in vivo bone formation. Clin Oral Implants Res. 2007; 18:639-48.

351. van den Dolder J, Mooren R, Vloon AP, Stoelinga PJ, Jansen JA. Platelet-rich plasma: Quantification of growth factor levels and the effect on growth and differentiation of rat bone marrow cells. Tissue Eng. 2006; 12:3067-73.

352. Centrella M, McCarthy TL, Canalis E. Transforming growth factor beta is a bifunctional regulator of replication and collagen synthesis in osteoblast-enriched cell cultures from fetal rat bone. J Biol Chem. 1987; 262:2869-74.

353. Lee KS, Kim HJ, Li QL, Chi XZ, Ueta C, Komori T, et al. Runx2 is a common target of transforming growth factor beta1 and bone morphogenetic protein 2, and cooperation between runx2 and smad5 induces osteoblast-specific gene expression in the pluripotent mesenchymal precursor cell line c2c12. Mol Cell Biol. 2000; 20:8783-92.

354. Janssens K, ten Dijke P, Janssens S, Van Hul W. Transforming growth factor-beta1 to the bone. Endocr Rev. 2005; 26:743-74.

355. Wang M, Zhao D, Spinetti G, Zhang J, Jiang LQ, Pintus G, et al. Matrix metalloproteinase 2 activation of transforming growth factor-beta1 (tgf-beta1) and tgf-beta1-type ii receptor signaling within the aged arterial wall. Arterioscler Thromb Vasc Biol. 2006; 26:1503-9.

356. Souchelnitskiy S, Chambaz EM, Feige JJ. Thrombospondins selectively activate one of the two latent forms of transforming growth factor-beta present in adrenocortical cell-conditioned medium. Endocrinology. 1995; 136:5118-26.

357. Ben Ammar A, Mir K. [the zollinger-ellison syndrome]. Tunis Med. 1991; 69:375-80.

358. Kazes I, Elalamy I, Sraer JD, Hatmi M, Nguyen G. Platelet release of trimolecular complex components mt1-mmp/timp2/mmp2: Involvement in mmp2 activation and platelet aggregation. Blood. 2000; 96:3064-9.

359. Cavani JA, Reiner A, Cuthbertson SL, Bittencourt JC, Toledo CA. Evidence that urocortin is absent from neurons of the edinger-westphal nucleus in pigeons. Braz J Med Biol Res. 2003; 36:1695-700.

360. Hooley JR, Golden DP. The effect of polylactic acid granules on the incidence of alveolar osteitis after mandibular third molar surgery. A prospective randomized study. Oral Surg Oral Med Oral Pathol Oral Radiol Endod. 1995; 80:279-83.

361. Pedersen A. Interrelation of complaints after removal of impacted mandibular third molars. Int J Oral Surg. 1985; 14:241-4.

362. Meechan JG, Venchard GR, Rogers SN, Hobson RS, Prior I, Tavares C, et al. Local anaesthesia and dry socket. A clinical investigation of single extractions in male patients. Int J Oral Maxillofac Surg. 1987; 16:279-84.

363. Krekmanov L. Alveolitis after operative removal of third molars in the mandible. Int J Oral Surg. 1981; 10:173-9.

364. Krekmanov L, Nordenram A. Postoperative complications after surgical removal of mandibular third molars. Effects of penicillin v and chlorhexidine. Int J Oral Maxillofac Surg. 1986; 15:25-9.

365. Lilly GE, Osbon DB, Rael EM, Samuels HS, Jones JC. Alveolar osteitis associated with mandibular third molar extractions. J Am Dent Assoc. 1974; 88:802-6.

366. Berwick JE, Lessin ME. Effects of a chlorhexidine gluconate oral rinse on the incidence of alveolar osteitis in mandibular third molar surgery. J Oral Maxillofac Surg. 1990; 48:444-8; discussion 449.

367. Osborn TP, Frederickson G, Jr., Small IA, Torgerson TS. A prospective study of complications related to mandibular third molar surgery. J Oral Maxillofac Surg. 1985; 43:767-9.

368.   Goldberg MH, Nemarich AN, Marco WP, 2nd. Complications after mandibular third molar surgery: A statistical analysis of 500 consecutive procedures in private practice. J Am Dent Assoc. 1985; 111:277-9.

369.   Larsen PE. Alveolar osteitis after surgical removal of impacted mandibular third molars. Identification of the patient at risk. Oral Surg Oral Med Oral Pathol. 1992; 73:393-7.

370.   Torres-Lagares D, Serrera-Figallo MA, Romero-Ruiz MM, Infante-Cossio P, Garcia-Calderon M, Gutierrez-Perez JL. Update on dry socket: A review of the literature. Med Oral Patol Oral Cir Bucal. 2005; 10:81-5; 77-81.

371.   Houston JP, McCollum J, Pietz D, Schneck D. Alveolar osteitis: A review of its etiology, prevention, and treatment modalities. Gen Dent. 2002; 50:457-63; quiz 464-5.

372.   Blum IR. Contemporary views on dry socket (alveolar osteitis): A clinical appraisal of standardization, aetiopathogenesis and management: A critical review. Int J Oral Maxillofac Surg. 2002; 31:309-17.

373.   Larsen PE. The effect of a chlorhexidine rinse on the incidence of alveolar osteitis following the surgical removal of impacted mandibular third molars. J Oral Maxillofac Surg. 1991; 49:932-7.

374.   Brown LR, Merrill SS, Allen RE. Microbiologic study of intraoral wounds. J Oral Surg. 1970; 28:89-95.

375.   MacGregor AJ, Hart P. Bacteria of the extraction wound. J Oral Surg. 1970; 28:885-7.

376.   Catellani JE, Harvey S, Erickson SH, Cherkin D. Effect of oral contraceptive cycle on dry socket (localized alveolar osteitis). J Am Dent Assoc. 1980; 101:777-80.

377.   Cohen ME, Simecek JW. Effects of gender-related factors on the incidence of localized alveolar osteitis. Oral Surg Oral Med Oral Pathol Oral Radiol Endod. 1995; 79:416-22.

378.   Nordenram A, Grave S. Alveolitis sicca dolorosa after removal of impacted mandibular third molars. Int J Oral Surg. 1983; 12:226-31.

379.   Johnson WS, Blanton EE. An evaluation of 9-aminoacridine/gelfoam to reduce dry socket formation. Oral Surg Oral Med Oral Pathol. 1988; 66:167-70.

380. Sisk AL, Hammer WB, Shelton DW, Joy ED, Jr. Complications following removal of impacted third molars: The role of the experience of the surgeon. J Oral Maxillofac Surg. 1986; 44:855-9.

381. Schow SR. Evaluation of postoperative localized osteitis in mandibular third molar surgery. Oral Surg Oral Med Oral Pathol. 1974; 38:352-8.

382. Sweet JB, Butler DP. Increased incidence of postoperative localized osteitis in mandibular third molar surgery associated with patients using oral contraceptives. Am J Obstet Gynecol. 1977; 127:518-9.

383. de Boer MP, Raghoebar GM, Stegenga B, Schoen PJ, Boering G. Complications after mandibular third molar extraction. Quintessence Int. 1995; 26:779-84.

384. Catellani JE. Review of factors contributing to dry socket through enhanced fibrinolysis. J Oral Surg. 1979; 37:42-6.

385. Sammartino G, Tia M, Marenzi G, di Lauro AE, D'Agostino E, Claudio PP. Use of autologous platelet-rich plasma (prp) in periodontal defect treatment after extraction of impacted mandibular third molars. J Oral Maxillofac Surg. 2005; 63:766-70.

386. Sorensen LT, Jorgensen S, Petersen LJ, Hemmingsen U, Bulow J, Loft S, et al. Acute effects of nicotine and smoking on blood flow, tissue oxygen, and aerobe metabolism of the skin and subcutis. J Surg Res. 2008.

387. Hunt TK, Pai MP. The effect of varying ambient oxygen tensions on wound metabolism and collagen synthesis. Surg Gynecol Obstet. 1972; 135:561-7.

388. Allen DB, Maguire JJ, Mahdavian M, Wicke C, Marcocci L, Scheuenstuhl H, et al. Wound hypoxia and acidosis limit neutrophil bacterial killing mechanisms. Arch Surg. 1997; 132:991-6.

389. Babior BM. Oxygen-dependent microbial killing by phagocytes (first of two parts). N Engl J Med. 1978; 298:659-68.

390. Hopf HW, Hunt TK, West JM, Blomquist P, Goodson WH, 3rd, Jensen JA, et al. Wound tissue oxygen tension predicts the risk of wound infection in surgical patients. Arch Surg. 1997; 132:997-1004; discussion 1005.

391. Heng CK, Badner VM, Clemens DL, Mercer LT, Mercer DW. The relationship of cigarette smoking to postoperative complications from dental extractions among female inmates. Oral Surg Oral Med Oral Pathol Oral Radiol Endod. 2007; 104:757-62.

392. Bouloux GF, Steed MB, Perciaccante VJ. Complications of third molar surgery. Oral Maxillofac Surg Clin North Am. 2007; 19:117-28, vii.

393. Lopez-Carriches C, Gomez-Font R, Martinez-Gonzalez JM, Donado-Rodriguez M. Influence of smoking upon the postoperative course of lower third molar surgery. Med Oral Patol Oral Cir Bucal. 2006; 11:E56-60.

394. Cooke JP. Angiogenesis and the role of the endothelial nicotinic acetylcholine receptor. Life Sci. 2007; 80:2347-51.

395. Norris LA, Bonnar J. Haemostatic changes and the oral contraceptive pill. Baillieres Clin Obstet Gynaecol. 1997; 11:545-64.

396. Cei S, Kandler B, Fugl A, Gabriele M, Hollinger JO, Watzek G, et al. Bone marrow stromal cells of young and adult rats respond similarly to platelet-released supernatant and bone morphogenetic protein-6 in vitro. J Periodontol. 2006; 77:699-706.

397. Zhang H, Aronow MS, Gronowicz GA. Transforming growth factor-beta 1 (tgf-beta1) prevents the age-dependent decrease in bone formation in human osteoblast/implant cultures. J Biomed Mater Res A. 2005; 75:98-105.

398. D'Ippolito G, Schiller PC, Ricordi C, Roos BA, Howard GA. Age-related osteogenic potential of mesenchymal stromal stem cells from human vertebral bone marrow. J Bone Miner Res. 1999; 14:1115-22.

399. Beresford JN, Bennett JH, Devlin C, Leboy PS, Owen ME. Evidence for an inverse relationship between the differentiation of adipocytic and osteogenic cells in rat marrow stromal cell cultures. J Cell Sci. 1992; 102 (Pt 2):341-51.

400. Burkhardt R, Kettner G, Bohm W, Schmidmeier M, Schlag R, Frisch B, et al. Changes in trabecular bone, hematopoiesis and bone marrow vessels in aplastic anemia, primary osteoporosis, and old age: A comparative histomorphometric study. Bone. 1987; 8:157-64.

401. Meunier P, Aaron J, Edouard C, Vignon G. Osteoporosis and the replacement of cell populations of the marrow by adipose tissue. A quantitative study of 84 iliac bone biopsies. Clin Orthop Relat Res. 1971; 80:147-54.

402. Nuttall ME, Patton AJ, Olivera DL, Nadeau DP, Gowen M. Human trabecular bone cells are able to express both osteoblastic and adipocytic phenotype: Implications for osteopenic disorders. J Bone Miner Res. 1998; 13:371-82.

403. Sanchis JM, Saez U, Penarrocha M, Gay C. Tetracycline compound placement to prevent dry socket: A postoperative study of 200 impacted mandibular third molars. J Oral Maxillofac Surg. 2004; 62:587-91.

404. Eppley BL, Woodell JE, Higgins J. Platelet quantification and growth factor analysis from platelet-rich plasma: Implications for wound healing. Plast Reconstr Surg. 2004; 114:1502-8.

405. Frechette JP, Martineau I, Gagnon G. Platelet-rich plasmas: Growth factor content and roles in wound healing. J Dent Res. 2005; 84:434-9.

406. Freymiller EG, Aghaloo TL. Platelet-rich plasma: Ready or not? J Oral Maxillofac Surg. 2004; 62:484-8.

407. Reddi AH, Cunningham NS. Bone induction by osteogenin and bone morphogenetic proteins. Biomaterials. 1990; 11:33-4.

408. Beksac M. Bone marrow and stem cell transplantation. Totowa, N.J.: Humana Press; 2007.

409. Kemp KC, Hows J, Donaldson C. Bone marrow-derived mesenchymal stem cells. Leuk Lymphoma. 2005; 46:1531-44.

410. Dexter TM, Spooncer E. Growth and differentiation in the hemopoietic system. Annu Rev Cell Biol. 1987; 3:423-41.

411. Devine SM, Hoffman R. Role of mesenchymal stem cells in hematopoietic stem cell transplantation. Curr Opin Hematol. 2000; 7:358-63.

412. O'Hare S, Atterwill CK, eds. Methods in molecular biology. Totowa: Humana Press Inc.; 1995.

413. Digirolamo CM, Stokes D, Colter D, Phinney DG, Class R, Prockop DJ. Propagation and senescence of human marrow stromal cells in culture: A simple colony-forming assay identifies samples with the greatest potential to propagate and differentiate. Br J Haematol. 1999; 107:275-81.

414. Murphy JM, Dixon K, Beck S, Fabian D, Feldman A, Barry F. Reduced chondrogenic and adipogenic activity of mesenchymal stem cells from patients with advanced osteoarthritis. Arthritis Rheum. 2002; 46:704-13.

415. D'Ippolito G, Schiller PC, Perez-stable C, Balkan W, Roos BA, Howard GA. Cooperative actions of hepatocyte growth factor and 1,25-dihydroxyvitamin d3 in osteoblastic differentiation of human vertebral bone marrow stromal cells. Bone. 2002; 31:269-75.

416. Sun X, Gan Y, Tang T, Zhang X, Dai K. In vitro proliferation and differentiation of human mesenchymal stem cells cultured in autologous plasma derived from bone marrow. Tissue Eng Part A. 2008; 14:391-400.

417.   Gerlier D, Thomasset N. Use of mtt colorimetric assay to measure cell activation. J Immunol Methods. 1986; 94:57-63.

418.   Sladowski D, Steer SJ, Clothier RH, Balls M. An improved mtt assay. J Immunol Methods. 1993; 157:203-7.

419.   Iwahana H, Fujimura M, Ii S, Kondo M, Moritani M, Takahashi Y, et al. Molecular cloning of a human cdna encoding a trifunctional enzyme of carbamoyl-phosphate synthetase-aspartate transcarbamoylase-dihydroorotase in de novo pyrimidine synthesis. Biochem Biophys Res Commun. 1996; 219:249-55.

420.   Mackenzie TC, Flake AW. Human mesenchymal stem cells persist, demonstrate site-specific multipotential differentiation, and are present in sites of wound healing and tissue regeneration after transplantation into fetal sheep. Blood Cells Mol Dis. 2001; 27:601-4.

421.   Chen KF, Lai YY, Sun HS, Tsai SJ. Transcriptional repression of human cad gene by hypoxia inducible factor-1alpha. Nucleic Acids Res. 2005; 33:5190-8.

422.   Coleman PF, Suttle DP, Stark GR. Purification from hamster cells of the multifunctional protein that initiates de novo synthesis of pyrimidine nucleotides. J Biol Chem. 1977; 252:6379-85.

423.   Khoo ML, Shen B, Tao H, Ma DD. Long-term serial passage and neuronal differentiation capability of human bone marrow mesenchymal stem cells. Stem Cells Dev. 2008; 17:883-96.

424.   Disthabanchong S, Radinahamed P, Stitchantrakul W, Hongeng S, Rajatanavin R. Chronic metabolic acidosis alters osteoblast differentiation from human mesenchymal stem cells. Kidney Int. 2007; 71:201-9.

425.   Radio NM, Doctor JS, Witt-Enderby PA. Melatonin enhances alkaline phosphatase activity in differentiating human adult mesenchymal stem cells grown in osteogenic medium via mt2 melatonin receptors and the mek/erk (1/2) signaling cascade. J Pineal Res. 2006; 40:332-42.

426.   Roth JA, Kim BG, Lin WL, Cho MI. Melatonin promotes osteoblast differentiation and bone formation. J Biol Chem. 1999; 274:22041-7.

427.   Nakade O, Koyama H, Ariji H, Yajima A, Kaku T. Melatonin stimulates proliferation and type i collagen synthesis in human bone cells in vitro. J Pineal Res. 1999; 27:106-10.

428.   DoJindo. Dojindo website. 2008.

429. Helfrich MH, Ralston SH. Bone research protocols. Totowa, New Jersey: Humana Press; 2003.

430. BioAssay, Systems. Bioassay systems website. 2008.

431. Aubin JE, Liu F, Malaval L, Gupta AK. Osteoblast and chondroblast differentiation. Bone. 1995; 17:77S-83S.

432. AnaSpec. Anaspec website. 2008.

433. Ginzinger DG. Gene quantification using real-time quantitative pcr: An emerging technology hits the mainstream. Exp Hematol. 2002; 30:503-12.

434. Sila-Asna M, Bunyaratvej A, Maeda S, Kitaguchi H, Bunyaratavej N. Osteoblast differentiation and bone formation gene expression in strontium-inducing bone marrow mesenchymal stem cell. Kobe J Med Sci. 2007; 53:25-35.

435. Gordon JA, Tye CE, Sampaio AV, Underhill TM, Hunter GK, Goldberg HA. Bone sialoprotein expression enhances osteoblast differentiation and matrix mineralization in vitro. Bone. 2007; 41:462-73.

436. Catelas I, Sese N, Wu BM, Dunn JC, Helgerson S, Tawil B. Human mesenchymal stem cell proliferation and osteogenic differentiation in fibrin gels in vitro. Tissue Eng. 2006; 12:2385-96.

437. Gomperts BD, Kramer IM, Tatham PER. Signal transduction. San Diego, Calif. London: Harcourt Academic; 2002.

438. Jaiswal N, Haynesworth SE, Caplan AI, Bruder SP. Osteogenic differentiation of purified, culture-expanded human mesenchymal stem cells in vitro. J Cell Biochem. 1997; 64:295-312.

439. Parsons P, Butcher A, Hesselden K, Ellis K, Maughan J, Milner R, et al. Platelet-rich concentrate supports human mesenchymal stem cell proliferation, bone morphogenetic protein-2 messenger rna expression, alkaline phosphatase activity, and bone formation in vitro: A mode of action to enhance bone repair. J Orthop Trauma. 2008; 22:595-604.

440. Subrahmanyam YV, Yamaga S, Prashar Y, Lee HH, Hoe NP, Kluger Y, et al. Rna expression patterns change dramatically in human neutrophils exposed to bacteria. Blood. 2001; 97:2457-68.

441. Adachi S, Kubota M, Lin YW, Okuda A, Matsubara K, Wakazono Y, et al. In vivo administration of granulocyte colony-stimulating factor promotes neutrophil survival in vitro. Eur J Haematol. 1994; 53:129-34.

442. Goldsby RA, Kindt TJ, Osborne BA, Kuby J. Kuby immunology. 4th ed. New York: W.H. Freeman; 2000.

443. Sawada R, Ito T, Tsuchiya T. [safety evaluation of tissue engineered medical devices using normal human mesenchymal stem cells]. Yakugaku Zasshi. 2007; 127:851-6.

444. Crouch SP, Kozlowski R, Slater KJ, Fletcher J. The use of atp bioluminescence as a measure of cell proliferation and cytotoxicity. J Immunol Methods. 1993; 160:81-8.

445. Kangas L, Gronroos M, Nieminen AL. Bioluminescence of cellular atp: A new method for evaluating cytotoxic agents in vitro. Med Biol. 1984; 62:338-43.

446. Zhou S, Greenberger JS, Epperly MW, Goff JP, Adler C, Leboff MS, et al. Age-related intrinsic changes in human bone-marrow-derived mesenchymal stem cells and their differentiation to osteoblasts. Aging Cell. 2008; 7:335-43.

447. Owen TA, Aronow M, Shalhoub V, Barone LM, Wilming L, Tassinari MS, et al. Progressive development of the rat osteoblast phenotype in vitro: Reciprocal relationships in expression of genes associated with osteoblast proliferation and differentiation during formation of the bone extracellular matrix. J Cell Physiol. 1990; 143:420-30.

448. Radonic A, Thulke S, Mackay IM, Landt O, Siegert W, Nitsche A. Guideline to reference gene selection for quantitative real-time pcr. Biochem Biophys Res Commun. 2004; 313:856-62.

449. Sturzenbaum SR, Kille P. Control genes in quantitative molecular biological techniques: The variability of invariance. Comp Biochem Physiol B Biochem Mol Biol. 2001; 130:281-9.

450. Schropp L, Wenzel A, Kostopoulos L, Karring T. Bone healing and soft tissue contour changes following single-tooth extraction: A clinical and radiographic 12-month prospective study. Int J Periodontics Restorative Dent. 2003; 23:313-23.

451. Jahangiri L, Devlin H, Ting K, Nishimura I. Current perspectives in residual ridge remodeling and its clinical implications: A review. J Prosthet Dent. 1998; 80:224-37.

452. Guralnick WC. Textbook of oral surgery. [1st ed. Boston,: Little; 1968.

453. Atwood DA, Coy WA. Clinical, cephalometric, and densitometric study of reduction of residual ridges. J Prosthet Dent. 1971; 26:280-95.

454. Carlsson GE, Bergman B, Hedegard B. Changes in contour of the maxillary alveolar process under immediate dentures. A longitudinal clinical and x-ray cephalometric study covering 5 years. Acta Odontol Scand. 1967; 25:45-75.

455. Carlsson GE, Persson G. Morphologic changes of the mandible after extraction and wearing of dentures. A longitudinal, clinical, and x-ray cephalometric study covering 5 years. Odontol Revy. 1967; 18:27-54.

456. Hildebolt CF, Brunsden B, Yokoyama-Crothers N, Pilgram TK, Townsend KE, Vannier MW, et al. Comparison of reliability of manual and computer-intensive methods for radiodensity measures of alveolar bone loss. Dentomaxillofac Radiol. 1998; 27:245-50.

457. Bragger U, Pasquali L, Rylander H, Carnes D, Kornman KS. Computer-assisted densitometric image analysis in periodontal radiography. A methodological study. J Clin Periodontol. 1988; 15:27-37.

458. Grondahl HG, Grondahl K. Subtraction radiography for the diagnosis of periodontal bone lesions. Oral Surg Oral Med Oral Pathol. 1983; 55:208-13.

459. Webber RL, Ruttimann UE, Grondahl HG. X-ray image subtraction as a basis for assessment of periodontal changes. J Periodontal Res. 1982; 17:509-11.

460. Grondahl K, Grondahl HG, Wennstrom J, Heijl L. Examiner agreement in estimating changes in periodontal bone from conventional and subtraction radiographs. J Clin Periodontol. 1987; 14:74-9.

461. Grondahl K, Grondahl HG, Webber RL. Digital subtraction radiography for diagnosis of periodontal bone lesions with simulated high-speed systems. Oral Surg Oral Med Oral Pathol. 1983; 55:313-8.

462. Kalpakcioglu BB, Morshed S, Engelke K, Genant HK. Advanced imaging of bone macrostructure and microstructure in bone fragility and fracture repair. J Bone Joint Surg Am. 2008; 90 Suppl 1:68-78.

463. Lehmann TM, Grondahl HG, Benn DK. Computer-based registration for digital subtraction in dental radiology. Dentomaxillofac Radiol. 2000; 29:323-46.

464. Grigoryan M, Lynch JA, Fierlinger AL, Guermazi A, Fan B, MacLean DB, et al. Quantitative and qualitative assessment of closed fracture healing using computed tomography and conventional radiography. Acad Radiol. 2003; 10:1267-73.

465. Lynch JA, Grigoryan M, Fierlinger A, Guermazi A, Zaim S, MacLean DB, et al. Measurement of changes in trabecular bone at fracture sites using x-ray ct and automated image registration and processing. J Orthop Res. 2004; 22:362-7.

466. Genant HK, Engelke K, Fuerst T, Gluer CC, Grampp S, Harris ST, et al. Noninvasive assessment of bone mineral and structure: State of the art. J Bone Miner Res. 1996; 11:707-30.

467. Augat P, Merk J, Genant HK, Claes L. Quantitative assessment of experimental fracture repair by peripheral computed tomography. Calcif Tissue Int. 1997; 60:194-9.

468. Markel MD, Morin RL, Wikenheiser MA, Lewallen DG, Chao EY. Quantitative ct for the evaluation of bone healing. Calcif Tissue Int. 1991; 49:427-32.

469. Genant HK, Jiang Y. Advanced imaging assessment of bone quality. Ann N Y Acad Sci. 2006; 1068:410-28.

470. Becker D. Drug therapy in dentistry. third ed. Plymouth: Hayden-McNeil Publishing, Inc.; 1998.

471. Harder AT, An YH. The mechanisms of the inhibitory effects of nonsteroidal anti-inflammatory drugs on bone healing: A concise review. J Clin Pharmacol. 2003; 43:807-15.

472. Gerstenfeld LC, Al-Ghawas M, Alkhiary YM, Cullinane DM, Krall EA, Fitch JL, et al. Selective and nonselective cyclooxygenase-2 inhibitors and experimental fracture-healing. Reversibility of effects after short-term treatment. J Bone Joint Surg Am. 2007; 89:114-25.

473. Tomoyasu A, Higashio K, Kanomata K, Goto M, Kodaira K, Serizawa H, et al. Platelet-rich plasma stimulates osteoblastic differentiation in the presence of bmps. Biochem Biophys Res Commun. 2007; 361:62-7.

474. Lavery K, Swain P, Falb D, Alaoui-Ismaili MH. Bmp-2/4 and bmp-6/7 differentially utilize cell surface receptors to induce osteoblastic differentiation of human bone marrow-derived mesenchymal stem cells. J Biol Chem. 2008; 283:20948-58.

475. McCullough KA, Waits CA, Garimella R, Tague SE, Sipe JB, Anderson HC. Immunohistochemical localization of bone morphogenetic proteins (bmps) 2, 4, 6, and 7 during induced heterotopic bone formation. J Orthop Res. 2007; 25:465-72.

476. Simon AM, O'Connor JP. Dose and time-dependent effects of cyclooxygenase-2 inhibition on fracture-healing. J Bone Joint Surg Am. 2007; 89:500-11.

477. Champagne CM, Takebe J, Offenbacher S, Cooper LF. Macrophage cell lines produce osteoinductive signals that include bone morphogenetic protein-2. Bone. 2002; 30:26-31.

478.   Smith WL, DeWitt DL, Garavito RM. Cyclooxygenases: Structural, cellular, and molecular biology. Annu Rev Biochem. 2000; 69:145-82.

479.   Vane JR, Bakhle YS, Botting RM. Cyclooxygenases 1 and 2. Annu Rev Pharmacol Toxicol. 1998; 38:97-120.

480.   Simon LS. Role and regulation of cyclooxygenase-2 during inflammation. Am J Med. 1999; 106:37S-42S.

481.   Funk CD. Prostaglandins and leukotrienes: Advances in eicosanoid biology. Science. 2001; 294:1871-5.

482.   Dekel S, Lenthall G, Francis MJ. Release of prostaglandins from bone and muscle after tibial fracture. An experimental study in rabbits. J Bone Joint Surg Br. 1981; 63-B:185-9.

483.   Alderson MR, Armitage RJ, Tough TW, Strockbine L, Fanslow WC, Spriggs MK. Cd40 expression by human monocytes: Regulation by cytokines and activation of monocytes by the ligand for cd40. J Exp Med. 1993; 178:669-74.

484.   Sedlmayr P, Blaschitz A, Wilders-Truschnig M, Tiran A, Dohr G. Platelets contain interleukin-1 alpha and beta which are detectable on the cell surface after activation. Scand J Immunol. 1995; 42:209-14.

485.   Kinoshita O, Kawano Y, Yoshimi H, Ashida T, Yoshida K, Akabane S, et al. Acute and chronic effects of anti-endothelin-1 antibody on blood pressure in spontaneously hypertensive rats. J Cardiovasc Pharmacol. 1991; 17 Suppl 7:S511-3.

486.   Dinarello CA. Biology of interleukin 1. FASEB J. 1988; 2:108-15.

487.   Sato K, Fujii Y, Kasono K, Ozawa M, Imamura H, Kanaji Y, et al. Parathyroid hormone-related protein and interleukin-1 alpha synergistically stimulate bone resorption in vitro and increase the serum calcium concentration in mice in vivo. Endocrinology. 1989; 124:2172-8.

488.   Evans DB, Bunning RA, Russell RG. The effects of recombinant human interleukin-1 beta on cellular proliferation and the production of prostaglandin e2, plasminogen activator, osteocalcin and alkaline phosphatase by osteoblast-like cells derived from human bone. Biochem Biophys Res Commun. 1990; 166:208-16.

489.   Ikeda E, Kusaka M, Hakeda Y, Yokota K, Kumegawa M, Yamamoto S. Effect of interleukin 1 beta on osteoblastic clone mc3t3-e1 cells. Calcif Tissue Int. 1988; 43:162-6.

490. Linkhart TA, MacCharles DC. Interleukin-1 stimulates release of insulin-like growth factor-i from neonatal mouse calvaria by a prostaglandin synthesis-dependent mechanism. Endocrinology. 1992; 131:2297-305.

491. Boyce BF, Aufdemorte TB, Garrett IR, Yates AJ, Mundy GR. Effects of interleukin-1 on bone turnover in normal mice. Endocrinology. 1989; 125:1142-50.

492. Blondeau F, Daniel NG. Extraction of impacted mandibular third molars: Postoperative complications and their risk factors. J Can Dent Assoc. 2007; 73:325.

493. Wrotniak M, Bielecki T, Gazdzik TS. Current opinion about using the platelet-rich gel in orthopaedics and trauma surgery. Ortop Traumatol Rehabil. 2007; 9:227-38.

494. Chagraoui H, Sabri S, Capron C, Villeval JL, Vainchenker W, Wendling F. Expression of osteoprotegerin mrna and protein in murine megakaryocytes. Exp Hematol. 2003; 31:1081-8.

495. Boyce BF, Xing L. Functions of rankl/rank/opg in bone modeling and remodeling. Arch Biochem Biophys. 2008; 473:139-46.

496. Datta HK, Ng WF, Walker JA, Tuck SP, Varanasi SS. The cell biology of bone metabolism. J Clin Pathol. 2008; 61:577-87.

Appendix 1

Institutional Review Board Forms

A. IRB Cover letter

December 1, 2004
Institutional Review Board
403 Administration Building
Duquesne University
600 Forbes Avenue
Pittsburgh, PA 15282

Dear IRB Members:

This Investigational Review Board application is being submitted to permit us to validate a dental surgical procedure that is currently being done by some dental practitioners. This clinical research project would provide a scientific examination of the effectiveness of this procedure. In the procedure, a small quantity of blood is drawn from each subject and centrifuged to concentrate the patient's own platelets. This would be done prior to the surgical removal of bilateral mandibular (lower jaw) third molars. Platelets contain multiple growth factors that may be beneficial in the healing process. This blood drawing procedure would be exactly the same as that performed by many hospital laboratories, medical offices and a few dental practitioners today. Most dentists simply remove the tooth and do not necessarily place anything into the tooth extraction site, while some practitioners will place the concentrated platelets and the growth factors contained within them, into the extraction site to accelerate healing. It may be that post-operative complications are prevented by the addition of these concentrated platelets into the surgical site. Each patient would be his/her own control. One side would receive the concentrated platelet treatment while the contra-lateral side would not. There would not be any new or novel treatments involved in this project. The FDA currently approves the use of PRP in dental surgical procedures. This project would help provide scientific validity for providing the additional platelet treatment.

Thank you for your time and consideration with this application. If we can provide any additional information, please do not hesitate to contact us.

Respectfully,

James L. Rutkowski, D.M.D.   David A. Johnson, Ph.D. (Co-Investigator)
E-Mail: james.rutkowski@verizon.net   E-Mail: johnsond@duq.edu
Home: 814-226-8691   Office: 412-396-5952
Office: 814-226-8690

B. IRB Submission Form

Research Question:

The research question to be answered is: Does the placement of autogenous platelet rich plasma (PRP) in the surgical site enhance the soft tissue healing and radiographic density following the removal of bilateral, mandibular third molars? The radiographic density would be a measure of bone density and maturity. The purpose of the study is to verify the validity of obtaining and placing autogenous PRP in recent extraction sites to decrease post-operative complications and hasten bone formation for future dental implant placement. If a significant difference is found between a control extraction site (no treatment) on one side versus a treated PRP contra-lateral side, then it would give a scientific basis for the continual and possibly expanded use of this technique in other oral surgical procedures. Currently, extraction sites are often left untreated which may result in multiple complications such as:

1. delayed healing of the soft tissue
2. soft tissue invasion of the extraction site
3. delayed and/or decreased bone formation
4. and infection.

Many times, dental implantologists treat extraction sites with allografts (bone from cadavers), xenografts (bone from another species, such as bovine), or synthetic grafts. Barriers such as teflon sheets, collagen, or cadaver bone sheets are placed over these grafts to prevent the invasion of soft tissue into the extraction site. These procedures are costly, difficult to perform, unpredictable in the presence of an existing infection, and time consuming. Autogenous PRP is often mixed with these grafting materials. The literature is divided on the benefits of using PRP with this procedure. Some practioners have anecdotally place autogenous PRP only in extraction sites and report improved soft and hard tissue healing. If the PRP treated sites do demonstrate improved healing, then this would offer a predictable treatment protocol for all extraction sites.

Research Design and Procedures:

This research will be based on the use of a bilateral 3rd molar extraction human model. The primary investigator, in a private dental office, will perform the clinical procedures. The following criteria (protocol) will be followed on all patients:

1. Procedures will be done with intravenous (IV) sedation.

2. After sedation, but prior to administration of other medications or commencement of surgery, the researcher will perform a venous puncture in the

arm opposite the IV administration site, so that two 4.5 mL tubes of whole blood can be drawn. These tubes will be drawn via the use of a disposable Vacutainer^{TM} with a 21 gauge 1 ½ inch beveled needle. One tube will be used for a whole blood platelet count (PC) for baseline values. The other tube will be centrifuged for 10 minutes in the Clinaseal Centrifuge^{TM}. The PRP will be removed, from the centrifuged tube, and placed in only one of the extractions sites after completion of the tooth removal. The contra-lateral extraction site will be treated by a traditional procedure that does not include the use of PRP.

3. Patients will be administered either Ancef^{TM} 2.0 gram or Clindamycin 600 mg. immediately pre-operative via IV.

4. Adequate local anesthesia will be obtained by the use of mandibular blocks and local infiltration. This is normally achieved with the use of three to four 1.8 mL. carpules of the lidocaine 2% with epinephrine 1:100,000 for each surgical site.

5. To help prevent excessive post-operative inflammation, patients will be administered dexamethasone 4-8 mg. IV pre-operatively and methyprednisolone acetate suspension 40 mg. IM immediately post-op.

6. Patients will be given Toradol^{TM} 30 mg. IV immediately post-op.

7. Immediate post-operative bilateral Gow-Gates mandibular block injection using 1.8 ml. of bupivacaine 0.5% with 1:200,000 epinephrine will be administered to prevent immediate post-op pain.

8. Bilateral 3rd molars of a similar eruptive state and angulation will be removed (both sides must be either impacted or erupted).

9. After removal of the teeth, a periapical (small) digital radiograph (Dentsply Gendex^{TM}) will be taken of each side, using an XCP mount with documented KVP and time settings to determine a baseline gray scale at each extraction site. Digital radiographs will be used for two reasons: 1. the technique will allow for consistent radiograph opacity and evaluation and 2. it exposes patients to only 25% of the radiation used with conventional radiography. A correlation of bone density will be confirmed during the study with computerized axial tomography scanning technology (CAT scan) and computer reformatting for bone density determination via Hounsfield units (HU) on 3 patients. Because of the need to evaluate the post-operative bone healing, participants in this study will be exposed to 22 digital peri-apical radiographs, and some participants will also be required to get a limited CAT scan analysis of the extraction sites. Patients not involved in this study would not normally receive these radiographs. The radiation exposure of these 22 digital radiographs is equivalent to that received with 6 traditional peri-apical dental radiographs.

10. The control side will be treated immediately post-extaction as follows:
    a. Digital radiograph
    b. Place Gelfoam^{TM} only
    c. Primary closure with 3-O chromic gut suture material.

11. The contra-lateral side will be treated immediately post-extraction as follows:
    a. Digital radiograph
    b. Injection of 200 μL of PRP into the extraction site.
    c. Placement of Gelfoam^{TM} moistened with 100 μL PRP.
    d. Primary closure with 3-O chromic gut suture material.

12. Dismiss patient with a grade card for notations every 8-hours for 3 days, then notations every 12 hours for the following 4 days. Each side will be graded for:
    a. Visual analogue scale (VAS) for pain
    b. Number of and type of analgesic tablets taken
    c. Temperature (external feeling of warmth)
    d. Facial swelling
    e. Bleeding
    f. Numbness or altered sensation of tongue, face, lip or chin.

13. Patient will return in 3 days for a post-op grading scale evaluation for each side by a licensed dental hygienist that is blinded to the study. The PI (who would not be blinded) will also examine the patient, but will not be involved in the grading process. The following will be graded:
    a. Dehiscence (degree of opening)
    b. Inflammation
    c. Bleeding
    d. Pain
    e. Swelling intra-oral and extra-oral

14. Patient will return 7 days post-op for the above evaluations plus digital radiographs (same protocol as immediate post-op)

15. The above will be repeated at weeks 2, 3, 4, 6, 8, 12, 16, 20, and 24.

16. Starting at 6 weeks post-op periodontal probe readings will be recorded for the bilateral mandibular 2nd molars.

17. Three of the patients will have mandibular CAT scans performed at a local hospital at post-op week 12. This would allow for verification of the gray scale from digital radiography with the bone density HU of the CAT scan.

Sample Selection and Size:

All patients will be between ages 18-40 and with a negative medical history and non-smokers. Six patients will be included in the study.

Recruitment of subjects:

Subjects will be recruited from the PI's private practice. Patients who meet sample selection criteria and in need of the removal of mandibular third molars, will be asked if they would like to enroll in the study. After the completion of their radiographic examinations, subjects will receive a $250.00 remuneration. Risks/benefits will be explained in detail to all patients. Patients will be given the opportunity to have questions answered prior to surgery. Attached is a recruitment hand-out that will be given to potential candidates.

Informed Consent Procedures:

Standard intravenous sedation consent and surgical third molar removal consent forms will be used (see attached forms). HIPAA acknowledgement consent forms will be used (see attached form). Subjects will also be informed of the need to have two 4.5 mL tubes of whole blood drawn prior to surgery. They will also be informed for the need to:

1. complete post-operative questioners
2. permit post-operative digital radiographs and a possible limited CAT scan of the mandible
3. report for follow up evaluations.

Please see the attached post-operative evaluation forms for the study participants. A certified dental assistant will explain the sedation and surgical procedures to be performed. This same dental assistant will go thru the consent forms line by line, as is normally done with non-study patients. The researcher (Dr. Rutkowski) will be present and available to clarify any terms and answer questions that subjects may have.

Collection of Data and Method of Data Analysis:

Data will be collected for the following items:

1. Patient self-evaluation for:
   a. Visual analogue scale (VAS) for pain
   b. Number of and type of analgesic tablets taken
   c. Temperature (external feeling of warmth)
   d. Facial swelling
   e. Bleeding
   f. Numbness or altered sensation of tongue, face, lip or chin.

2. Investigator evaluation of:
   a. Dehiscence (degree of opening)

     b. Inflammation
     c. Bleeding
     d. Pain
     e. Swelling intra- and extra-orally.
     f. Post-operative digital radiographs at 1, 2, 3, 4, 6, 8, 12, 16, 20, and 24.
     g. CAT scans on 3 of the subjects at week 12.

Data will be analyzed by a paired T-test or Mann-Witney U test. Data will be kept in a locked cabinet for 5 years, and then destroyed.

Issues relating to interactions with subjects and subjects' rights:

Subjects will have the opportunity to ask questions prior to surgery and then decide to participate or not. Subjects' needs for pain control, post-operative examinations, further treatment, and referrals will be the same as those extended to all non-research patients. If subjects do not wish to partake in the study, they will be given the opportunity to be treated as routine (non-research) patients. All records or data with names associated will be stored in a locked cabinet, which only the researcher has access. No name identity will be made in the data analysis.

C. Wisdom Tooth Study Announcement

LOWER WISDOM TOOTH SUDY

If you are between the ages of 18 and 40 and need your lower wisdom teeth removed, you may be eligible to participate in a study that involves the removal of lower wisdom teeth. The study compares two techniques currently used by dentists when removing these teeth. Both techniques remove the teeth by the same surgical principles, but upon closure of the extraction sites one technique utilizes a self-dissolving surgical plug and sutures, while the other technique utilizes concentrated blood products (platelets and growth factors) taken from the patient via a standard blood drawing technique. The method that utilizes the blood drawing technique is believed to enhance the healing process and decrease post-operative complications. Retrospective studies appear to support this believe. This project would compare the two techniques in the patient. One side from the removal of the wisdom teeth would receive the traditionally used technique of a self-dissolving surgical plug and sutures. The other side would receive the blood products that had been concentrated, the self-dissolving surgical plug and sutures. We must emphasize that the blood products are taken from the subject's own blood. Two small tubes of blood would be drawn from the patient's arm just prior to starting the extractions. The blood would be centrifuged and a layer of concentrated platelets would be removed and placed in the surgical site. To be eligible for this study you must be:

1. in need of the removal of two lower wisdom teeth
2. willing to participate in the study under your own free will
3. between the ages of 18 and 40
4. in good health
5. not taking any medications prior to the removal of the teeth
6. willing to have 2 small tubes of blood drawn from your arm
7. willing to be sedated for the tooth removal
8. willing to have a series of 10 digital radiographs taken over a 6 month period of time after the surgery
9. the possibility of having a CAT scan at a local hospital 3 months after the surgery
10. complete a post-surgical evaluation form for pain, swelling, and other complications for 4 days after the removal of the teeth
11. present for routine post-surgical in-office evaluations by our staff over a 6 month time period.

You would be free to leave the study at any time if you should so desire. If you complete the study you would receive a $250.00 remuneration at the conclusion of the final 6 month radiograph and post-op evaluation.

If you are interested in learning more about the possibility of your involvement in this research project, please contact: James L. Rutkowski D.M.D.

    35 South Second Ave.
    Clarion, Pa. 16214
    Phone: 814-226-8690

D. Third Molar Consent Form

THIRD MOLAR/PRP RESEARCH PROJECT

CONSENT FORM

This consent form consists of four (4) parts:

1. Third molar removal consent form that includes possible surgical and post-operative complications.

2. Intravenous conscious sedation consent form that includes possible sedation risks.

3. Intravenous conscious sedation patient information sheet.

4. Health Insurance Portability and Accountability Act (HIPAA) acknowledgment form.

All forms are to be completed and signed by a patient or legal guardian, prior to participation in the study.

Appendix 2

Patients' Post-Surgical Evaluation Form

PARTICIPANTS POST-SURGICAL EVALUATION FORM

Post-surgical grade card for participants of the research project titled: "Effects of Growth Factors on Cell Proliferation and Differentiation with Radiographic Analysis of Tooth Extraction Socket Fill Utilizing Autogenous Growth Factors"

(**To be completed by the participant. A new form should be completed every 8 hours for the 1st 3 days, then every 12 hours for the next 4 days.**)

Patient ID: _____ (Do not use your name only use the ID # assigned to you)

Date:_____

Time:_____

A. Visual analogue scale for pain

(Please place circle the number that represents your perception of the pain you are currently experiencing. 0 = no pain; 10 = severe pain)

0…….1…….2…….3……4…….5…….6…….7…….8…….9…….10

B. Please check analgesic tablets and number taken since surgery (if this is your first

report) or since your last report

Check if any of the following were taken	Analagesic	Strength (dose)	Quantity
	Advil	200 mg	
	Alleve	200 mg	
	Darvocet-N 100	100 mg	
	Ibuprofen	200 mg	
	Nuprin	200 mg	
	Percocet		
	Percodan		
	Tylenol regular strength	325 mg	
	Tylenol extra strength	500 mg	
	Tylenol with Codeine ½ grain	325/30	
	Viocodin	500/5	
	Vicodin ES	750/7.5	
	Vicodin HP	660/10	

Check if any of the following were taken	Analagesic	Strength (dose)	Quantity
Other please specify			

C. Left: Temperature   _____°F   Right: Temperature   _____°F

D. Swelling (Please circle the best description)

  Left: Slight……..Moderate………Severe   Right:
Slight……..Moderate………Severe

E. Bleeding (Please circle the best description)

  Left: Slight……..Moderate………Severe   Right:
Slight……..Moderate………Severe

F. Numbness or altered sensation of tongue, face, lip or chin. (Please give location
    and circle the best description(s)

    Location_____   Slight……..Moderate………Severe

    Location_____   Slight……..Moderate………Severe

Appendix 3

Observers' Post-Surgical Evaluation Form

OBSERVERS POST-OP EVALUATION FORM

Post-surgical evaluation sheet for participants of the research project titled; "Effects of Growth Factors on Cell Proliferation and Differentiation with Radiographic Analysis of Tooth Extraction Socket Fill Utilizing Autogenous Growth Factors"

(To be completed by the blinded Dental Hygienist on post-op days 3 & 7, plus weeks 2,3,4,6,8,12,16,20 & 24.)

Patient ID:_____(Do not use patient's name)

Date:_____

Time:_____

Dental Hygienist ID:_____

    A. Dehiscence (degree of opening): Site #17___mm opening; Site #32____mm

    B. Inflammation: (degree of)   Circle the best description.

        Left side: Slight….Moderate....Severe;   Right side: Slight….Moderate....Severe

    C. Bleeding: (degree of)   Circle the best description.

        Left side: Slight….Moderate....Severe;   Right side: Slight….Moderate....Severe

C. Pain (Observers perception of pain at the time of visit)
    Circle the number that best describes the observed pain (0 = no pain; 10= severe pain)

    Left side: 0….. 1…..2…….3…….4…….5…….6……..7…….8…….9…….10

    Right side: 0…..1…..2…….3…….4…….5…….6……..7…….8…….9…….10

D. Swelling (extra-oral)   Circle the best description.

   Left side: Slight….Moderate....Severe;   Right side: Slight….Moderate....Severe

E. Swelling (intra-oral)   Circle the best description.

    Left side: Slight….Moderate....Severe;   Right side: Slight….Moderate....Severe

Appendix 4

Percent Radiographic Density Changes of Surgical ±PRP Treatment Compared to Control Radiograph Taken Immediately Following Tooth Removal in Six Trial Patients

In all graphs, percent bone density change on the Y-axis represents the change in bone density that has occurred at the extraction site in comparison to the extraction site immediately after tooth removal and placement of the Gelfoam® sponge ± PRP and suturing. Digital radiographs were normalized to the immediate post-operative film by comparing the unaltered adjacent tooth on the time point radiograph with the immediate post-operative radiograph's corresponding unaltered tooth. Each digital radiograph was evaluated by 3-blinded evaluators. Patients are coded as Patients 1,2, 5,6, 9, and A.
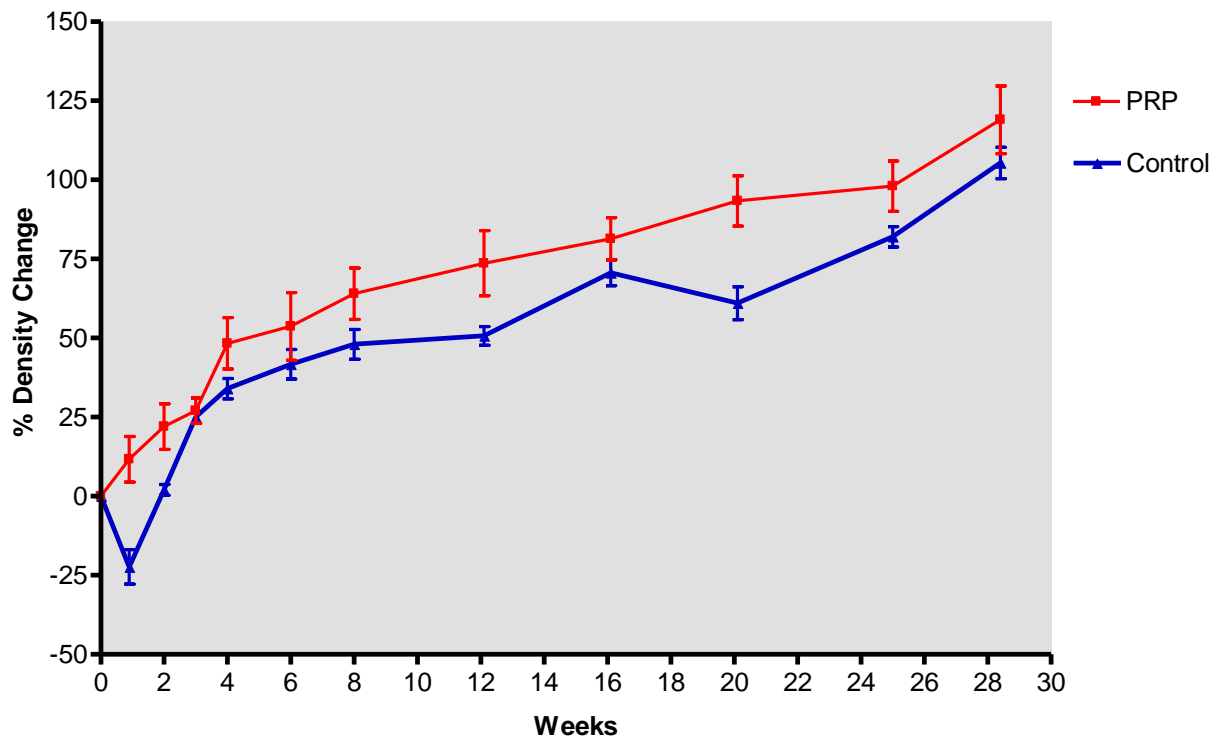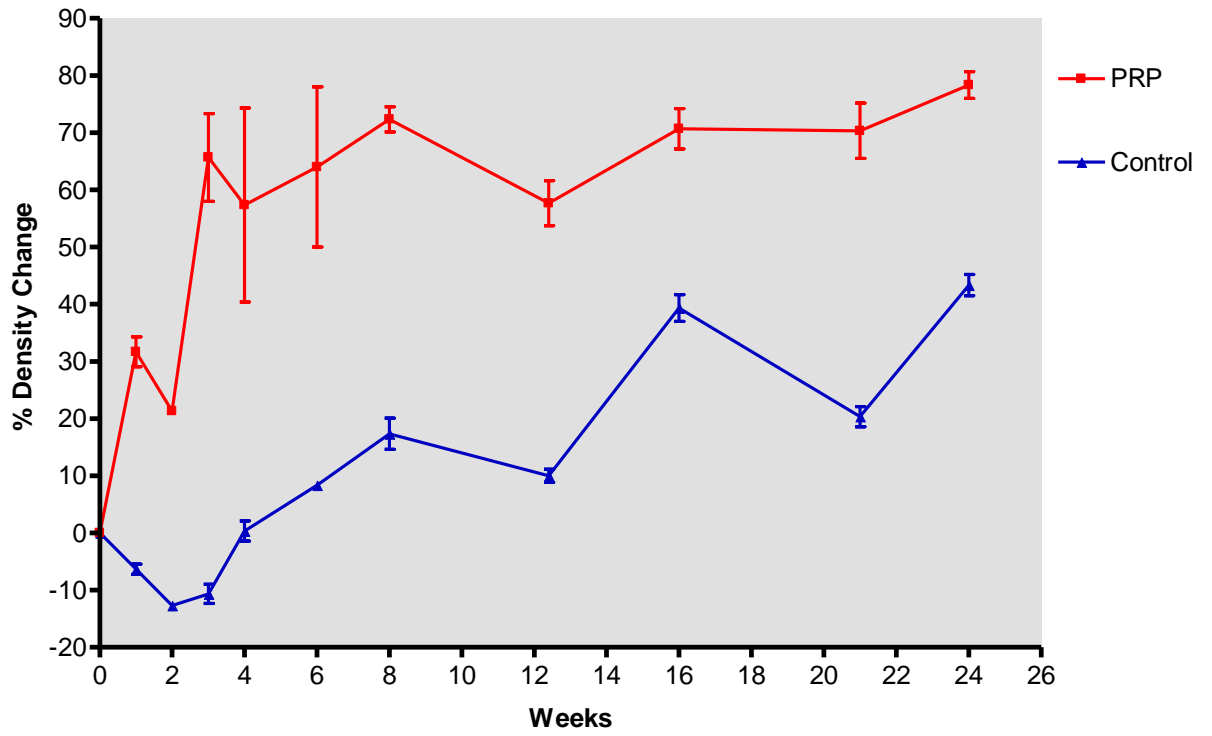
Patient 1
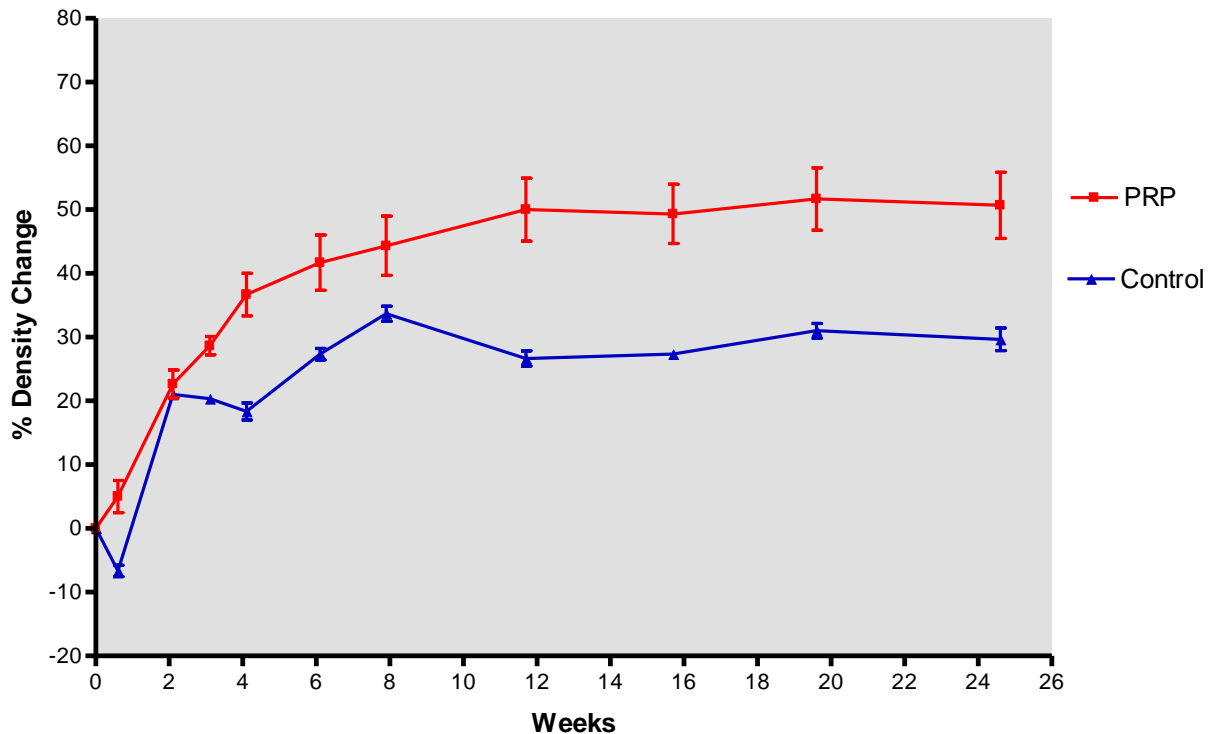
Patient 2
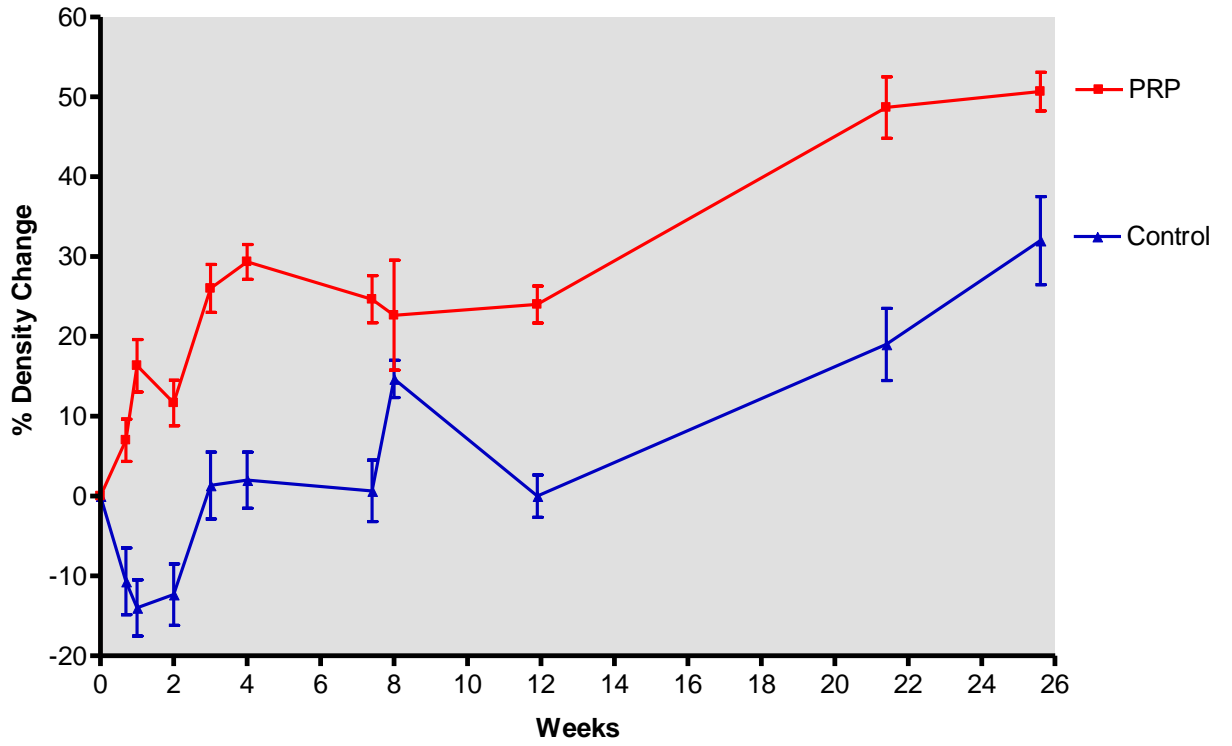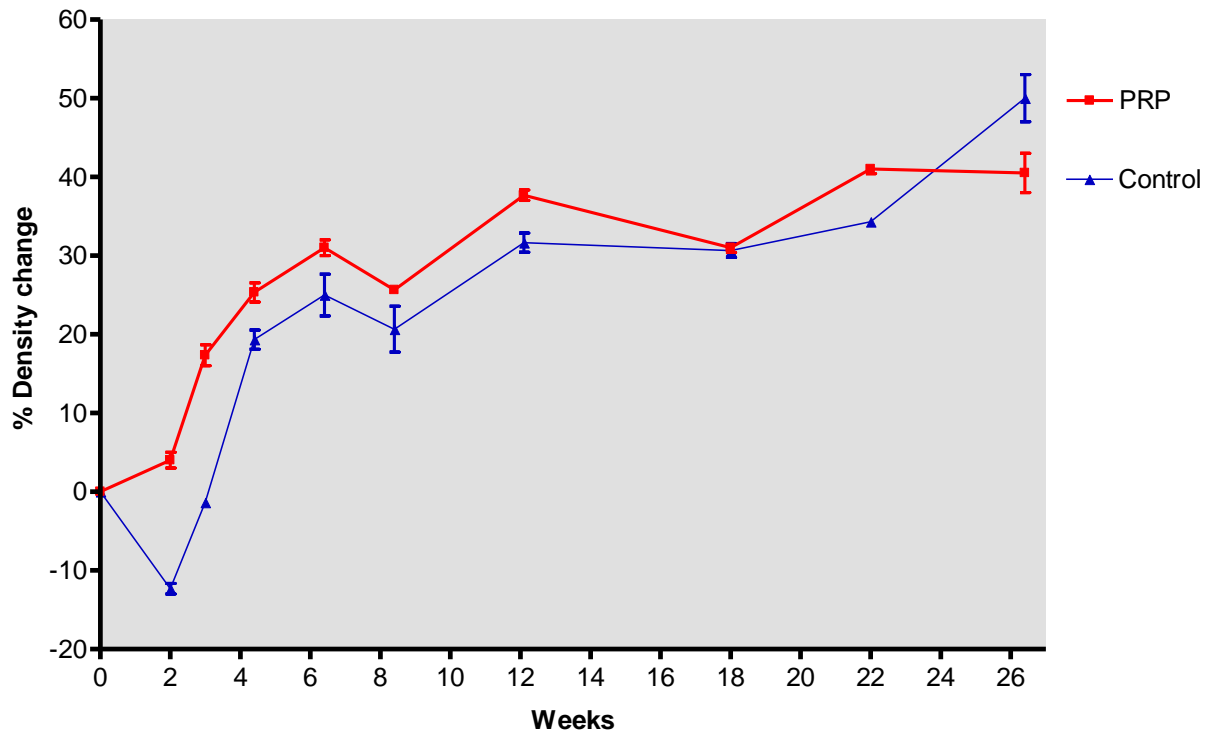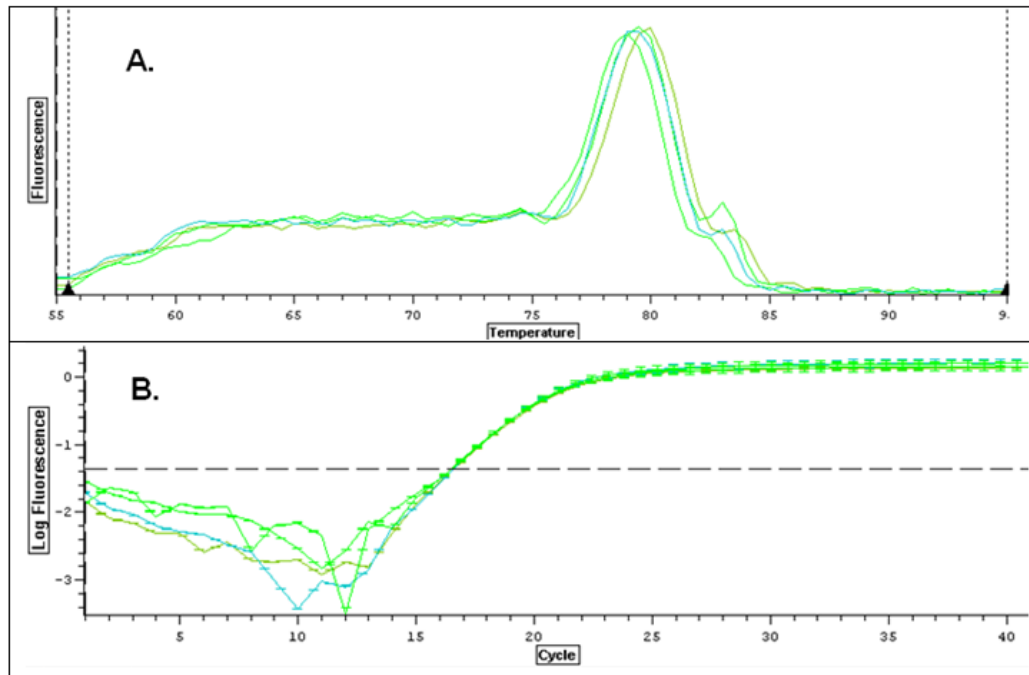
Patient 5
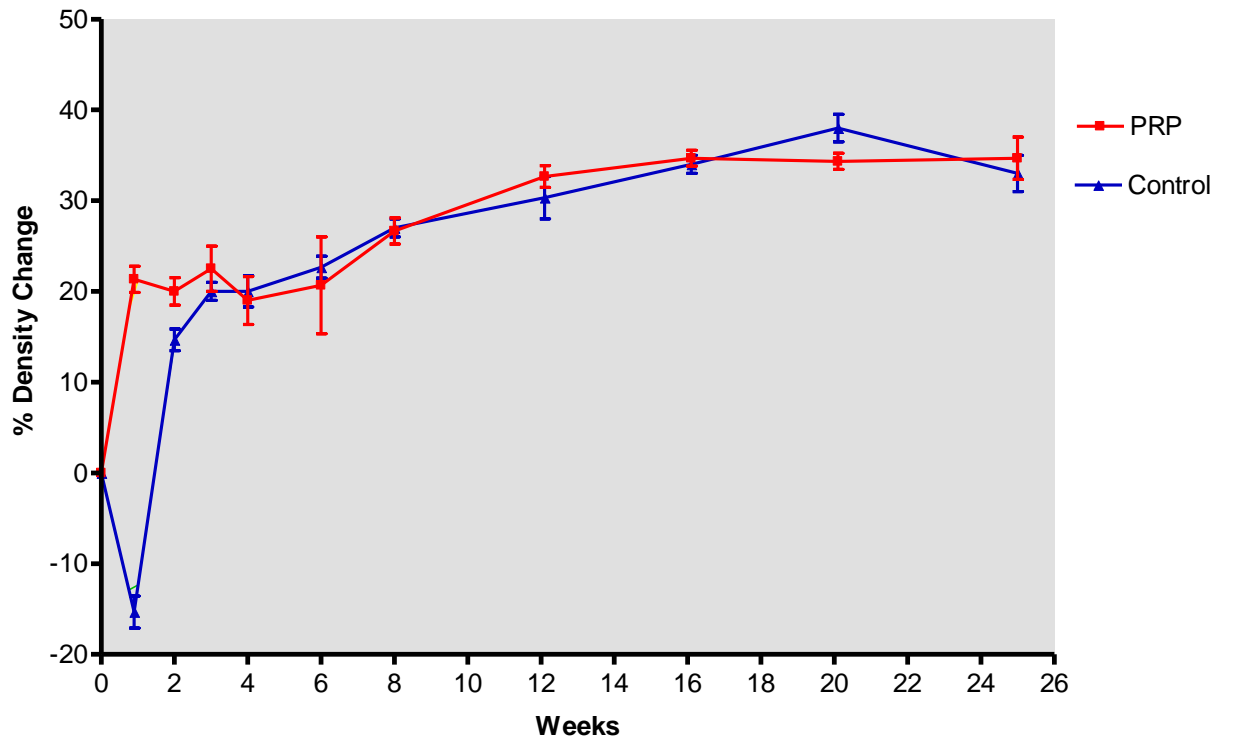
Patient 6

Patient 9

Patient A

Appendix 5

Representative Real Time RT-PCR Results for Day 21 Bone

Sialoprotein Gene (IBSP) Expression in Growth, Growth + PRP,

Differentiation, and Differentiation + PRP media

The reaction protocol was completed in a Bio-Rad Chromo4 Real Time Detection System® using the iScript One-Step RT-PCR Kit® (Bio-Rad, Hercules, CA). Each reaction mixture contained 100 nM RNA. The 50 μL reaction mixture was placed in the thermal cycler and incubated at 55°C for 10 minutes, 5 minutes at 95°C for cDNA synthesis and reverse transcriptase inactivation. The PCR cycling was completed after 45 cycles; 10 seconds at 95°C, 30 seconds at 57°C. A melt curve analysis was completed; 1 minute at 95°C, 1 minute at 55°C, and 10 seconds at 55°C for 80 cycles, increasing 0.5°C each cycle. Data were analyzed using MC Opticon® software. Panel A represents the melt curve for bone sialoprotein gene (IBSP) in growth medium, growth + PRP medium, differentiation medium, and differentiation + PRP medium. The peaks are all relatively close over a specific high temperature range indicating amplification of one specific product in the PCR reaction. The specific, thermodynamically stable product is represented by the single peak followed by the sharp decrease in fluorescence at the higher temperature range. Panel B represents cycle expression (C_T) for the same gene in the same media. The C_T cycle was defined automatically by the iCycler software.